Metabolically induced neuronal differentiation

Dissertation

zur Erlangung des Doktorgrades

der Naturwissenschaften

vorgelegt beim Fachbereich 15

Biowissenschaften

der Johann Wolfgang Goethe-Universität

in Frankfurt am Main

von

Sandy Maurer

aus Bad Soden am Taunus

Frankfurt am Main 2021

D30

Vom Fachbereich 15 der

Johann Wolfgang Goethe-Universität als Dissertation angenommen.

Dekan: Prof. Dr. Sven Klimpel

Gutachter: Prof. Dr. Virginie Lecaudey; Prof. Dr. Amparo Acker-Palmer

Datum der Disputation:

Table of contents

I Summary

In recent years, several neuronal differentiation protocols were published that circumvent the requirement of embryoid body (EB) formation under serum-deprivation and simplified medium conditions. But a neuronal default model to establish an approach that works efficiently for all pluripotent cells and neuronal precursors is still lacking. Whether such a default neural mechanism exist and how this is implemented across a broad spectrum of cell source, is addressed in several studies and still controversially discussed. It was proposed that the default neuronal fate is initiated in the absence of extrinsic signals and is achieved by eliminating extracellular inhibitors of neuroectodermal fate and suppressing cell-cell signalling through limited cell density. Previous studies reported that ESC and ECC grown at low density and in absence of exogenous factors or feeder layers die within 24 h but acquire a neural identity as indicated by expression of the neural marker Nestin. Thus, this application is not suitable for generating neural cultures. Furthermore, it was reported that P19 cells survive and express neuroectodermal marker genes in serum-free DMEM/F12 medium containing transferrin, insulin, and selenite, although no neurites were identified.

Based on this background, in this study, a novel approach to induce neuronal differentiation *in vitro* was developed that implements a nutrient-poor environment, which, in contrast to previous studies, ensures the survival of neuronally differentiated cells over a long period of time and allows normal formation of neurites. Neither the formation of free-floating aggregates nor supplementation of growth factors or known inducers was required to establish a reliable neuronal differentiation protocol. A simple medium, consisting of DMEM/F12+N2 that was highly diluted in salt solution, was sufficient to drive a fast neuronal differentiation in monolayer cultures. Serum deprivation and strong dilution of DMEM/F12+N2 medium cause a nutrient-poor environment in which the influence of growth factors and inducers is minimized. This medium creates a metabolically defined environment that is presumably free of extrinsic signals that prevent the decision of neuronal fate. Analysis of the medium components discovered no actual inducer. Hence, it was suggested that the metabolic composition of the medium exclusively covers specific cell requirements of neurons, therefore ensures their survival, and drives the switch from pluripotent cells to neurons. The self-developed method was established by usage of the murine embryonal carcinoma cell line P19 and could be transferred to murine ESC. Consequently, the method could provide a feasible protocol for a generally valid neuronal default model.

The established protocol provides several advantages such as the possibility to generate stable pure neuronal cultures by a fast, simple, and highly reproducible one-step induction under defined medium conditions with a minimum of exogen effectors. The method is characterised by clear and steady medium conditions that makes the investigation of specific cell requirements during differentiation accessible. It is therefore expected to be a useful tool to investigate the molecular basis of neuronal differentiation as well as for high throughput screenings. The phenotype of mature postmitotic neurons was arising within one week and cultures were shown to stay stable

at least for three weeks. The neuronal identity was confirmed by expression of neuronal markers through immunofluorescence staining and mass spectrometry analysis. Furthermore, increased levels of axon markers were detected in early neuronal differentiation and functionality of the synapses of the P19-derived neurons was ascertained by detection of calcium activity. Axonal laser ablation, immediately followed by fast regrowth of connections in the neuronal network, revealed a strong regeneration potential under the given conditions. Furthermore, the generated neurons showed a morphologically distinct phenotype and the formation of neural rosettes. Immunofluorescence staining demonstrated the generation of pure and homogeneous neuronal cultures, free of glial cells.

Retinoic acid (RA) plays an essential role in cell signalling during embryogenesis and efficiently induces neuronal differentiation *in vitro* in a concentration dependent manner. Neither retinol nor retinoic acid was included in any of the components of the self-prepared medium in this work. However, I observed, dependence on RARβ- and/or RARγ-regulated RA signalling in serum-free monolayer cultures. Nevertheless, neuronal differentiation in serum-free monolayer cultures was assumed to be RARα-independent because (i) RARα was slightly downregulated after neuronal induction, (ii) the truncated RARα of the RAC65 mutant had no effect on induction efficiency, and (iii) a pan-RAR inhibitor suppressed neuronal differentiation. In contrast to serum-free monolayer cultures, the truncated RARα prevented neuronal differentiation by application of the conventional protocol where cells are grown in free floating cell aggregates in serum-containing medium. Proteome analysis of P19 cells, treated by the self-developed differentiation protocol over five days showed increased levels of cellular RA binding proteins that mediate the cellular RA transport and are involved in canonical as well as non-canonical RA signalling. In turn, the RA synthesising enzyme ALDH1B1 and RARα were downregulated. In total, this work suggests that supplementation of high RA concentrations is only required to supress signals from added components like serum or DMSO (> 0.1 %). In absence of these components, subnanomolar RA concentrations was sufficient for neuronal induction

By application of the established protocol to induce neuronal differentiation the regulation of signalling pathways that are involved in mediating the switch from pluripotent to neuronal cells was investigated. The proteomic analysis indicated that Wnt and Notch signalling were downregulated in the early neuronal differentiation, while SMAD and BMP inhibition showed mixed results. Further inhibition of Wnt, Notch or BMP by supplementation of inhibitors that were applied in several protocols to promote differentiation, had no effect on neuronal differentiation. Since the proteomic data indicated that these signalling pathways are already downregulated without the addition of effectors, these inhibitors appeared to be redundant for the established method. In contrast, proteome analysis suggests an activation of the Hh pathway. The requirement for activated Hh signalling was enhanced by the suppressive effect of an Hh inhibitor upon neuronal induction in this study. Altogether, these results show that the regulation of diverse signalling pathways, required to mediate the switch from

pluripotent cells to neurons, occurred independently of exogenous factors besides the likelihood of residual RA.

Furthermore, the influence of altering ROS levels and the antioxidant defence after neuronal induction was investigated. ROS are known to be critical in the mediation of autophagy, apoptosis and diverse pathways that are involved in the switch from pluripotent proliferating cells to postmitotic neurons. In this study, a decreased ROS levels through antioxidant treatment attenuated axonal growth and the potential to induce neuronal differentiation, while an increased ROS level through *Nrf2* knockdown negatively affected the survival of mature neurons. NRF2 is a transcription factor that controls expression of several antioxidant and detoxifying genes, containing an antioxidant response element (ARE) in their promoter sequence. At the proteome level, it was shown that the NRF2-regulated enzymes studied are differentially regulated after neuronal induction. While the analysed glutathione modifying enzymes were downregulated, SOD2 and APOE were upregulated during early neuronal differentiation. Thus, these mediators were suggested to be involved in the weak intrinsic antioxidant defence that provide a tight regulation of redox-sensitive signalling pathways during early neuronal differentiation. Analysis of a generated P19 Δ*Becl1* knockout mutant showed that downregulation of p62, APOE, GCLc, and GSR, which are involved in antioxidant defence, is dependent on autophagy level after neuronal induction.

The mTOR/PI3K/AKT signalling pathway is a key player of autophagy and during neuronal development. In previous studies, the regulation of the PI3K/AKT pathway, and thus regulation of autophagy during neuronal differentiation, yielded conflicting results. In this study, manipulation of autophagy regulation was performed by interfering with the PI3K/AKT pathway or by direct targeting of autophagy related proteins. Remarkably, autophagy inhibition with 3-MA, LY294002, A-674563, chloroquine, or STF-62247 as well as the knockout of *Becl1*, *p62*, *Atg7*, or *Atg9a* that address autophagy at different stages, demonstrated to cause a similar morphological phenotype during the neuronal differentiation process, indicating that this effect is caused by a lack of autophagy in general. Inhibition of autophagy showed to cause an axonal overgrowth during early neuronal differentiation and premature cell death of mature neurons. Accordingly, the mTOR inhibitors rapamycin and torin2 demonstrated the opposing effect and caused a shortening of the neurites.

Proteomic analysis of a generated P19 Δ*Becl1* knockout mutant during early neuronal differentiation provided evidence that axonal overgrowth, limited to early differentiation, was induced by a lack of degradation of the axon marker NCAM1. The NCAM1 level appeared to be highly increased in the Δ*Becl1* mutant during early neuronal differentiation. This suggest that downregulation of NCAM1 levels is mediated by autophagy, possibly even by direct degradation. Increased NCAM1 levels resulting from the lack of autophagy could cause axonal overgrowth during early differentiation that likely disappears with the redistribution of NCAM1 from the growth cone to the cell soma and would consequently explain why the effect of axonal overgrowth is limited to

early neuronal development. Moreover, the regulation of ASCL2, MYC, Gli3 and some factors involved in the antioxidant defence and RA signalling during early neuronal differentiation were affected by the *Becl1* knockout. Nevertheless, successful neuronal differentiation of the Δ*Becl1* mutant could be clearly verified morphologically, by an increase of neuronal and axonal markers and a similar signalling pathway regulation as shown for differentiating wildtype (WT) cells, such as the necessary Notch downregulation. Therefore, autophagy was suggested to be upregulated but not essential for neuronal differentiation but demonstrated to be crucial for axonal development and the survival of mature neurons.

On the other hand, to examine the effects of an increased autophagic flux, *BirC6* was depleted in P19 cells by generating a gene knockout. The phenotype of the *BirC6* knockout mutant was completely different from that of the rapamycin treated WT during neuronal induction. Therefore, it was hypothesized that the lack of ability of the Δ*BirC6* mutant to differentiate into neurons under the given conditions was caused either by a higher effectiveness to increase the autophagic flux than mediated by rapamycin treatment or by the loss of other *BirC6* functions. From the proteomic profile, no clear conclusion could be drawn about the effect of the *BirC6* knockout on autophagic flux. Neuronal marker stayed downregulated also the different regulation of signalling pathways indicated a non-neuronal cell fate. Moreover, downregulation of the Notch pathway, crucial for neuronal differentiation, failed. Furthermore, in contrast to WT and Δ*Becl1* cells, neither the PI3K/AKT survival pathway nor pro-apoptotic factors or KIF proteins indicated an upregulation through induction of differentiation in Δ*BirC6* cells. Proteins, involved in the execution or prevention of apoptosis, showed a clear separation of the Δ*BirC6* mutant to WT and Δ*Becl1* cells in differentiation medium. The Δ*BirC6* cells showed no (up)regulation of pro-apoptotic proteins, while anti-apoptotic effectors were downregulated simultaneous to WT cells. Thus, this suggested a decreased responsiveness to apoptotic signals in the Δ*BirC6* mutant. Only the anti-apoptotic BCL2L1 (BCL-X) was upregulated in the Δ*BirC6* mutant in both analysed conditions. Therefore, BCL-X was a potential candidate that compensate for the loss of the anti-apoptotic BIRC6 function, independently of the medium conditions. The differences in the regulation of apoptotic factors, in WT and Δ*Becl1* compared to Δ*BirC6*, by switching from growth to differentiation medium was suggested to be attributed to the different cell fate decisions.

Additionally, the increased level of cell death during early neuronal differentiation was addressed. In this study, early neuronal differentiation was characterized by a period of highly increased cell death due to apoptosis rather than autophagic cell death. It was shown that blocked autophagy only had an impact on the survival of mature neurons since dysfunctional proteins probably accumulated in the cell. An increased level of several pro-apoptotic proteins was detected in differentiating P19 WT and Δ*Becl1* mutant cells. In turn, except for the anti-apoptotic BCL-X, other anti-apoptotic proteins were downregulated after neuronal differentiation was induced. The data highly suggested an increased responsiveness to apoptotic signals during early neuronal differentiation. The increased BCL-X level and the implied upregulation of the PI3K/AKT

and MAPK/ERK pathway was assumed to restrict the apoptotic pathway and protect cells from cell death during early neuronal differentiation. Hence, the proteomic profile suggests tight regulation of cell death adapted by neuronal differentiation with a reduced threshold to induce apoptosis.

In conclusion, in this work, I established a method to differentiate pluripotent cells into neurons in a one-step induction under metabolically defined medium conditions. I have shown that neuronal differentiation in the generated monolayer culture was driven by subnanomolar RA concentrations. The developed method was used to analyse the regulation and control of cellular processes such as autophagy, apoptosis, antioxidant-defence, and other signalling pathways in the neuronal differentiation process. The results of proteome analysis provide evidence for autophagic regulation of several proteins during early neuronal differentiation and serves as an important starting point for further studies.

II Zusammenfassung

In den letzten Jahren wurden einige neuronale Differenzierungsprotokolle entwickelt, welche sich durch vereinfachte Medienbedingungen auszeichnen und weder Serum zugegeben noch Embryoidkörper (EB) gebildet werden müssen. Ein neuronales Default-Modell, das für alle pluripotenten Zellen und neuronalen Vorläufer effizient genutzt werden kann, konnte bisweilen noch nicht etabliert werden. Ob ein solcher vorgegebener neuronaler Zellschicksalsmechanismus existiert und wie dieser über ein breites Spektrum von Zellen verschiedenen Ursprungs Anwendung finden kann, wird in mehreren Studien kontrovers diskutiert. Es wird angenommen, dass das standardmäßige neuronale Schicksal in Abwesenheit von extrinsischen Signalen und somit durch die Eliminierung extrazellulärer neuroektodermaler Inhibitoren und die Unterdrückung interzellulärer Signalübertragung, durch begrenzte Zelldichte, initiiert wird. In früheren Studien wurde berichtet, dass ESC und ECC, die in geringer Dichte und ohne exogene Faktoren oder Fütterungsschichten gezüchtet wurden, innerhalb von 24 Stunden absterben, aber eine neurale Identität erlangen, wie die Expression des neuralen Markers Nestin zeigt. Somit erwies sich diese Anwendungen als ungeeignet um neuronale Kulturen zu generieren. Zudem wurde berichtet, dass P19 Zellen in serumfreiem DMEM/F12 Medium, das Transferrin, Insulin und Selenit enthält, überleben und neuroektodermale Markergene exprimieren, obwohl keine Neurite identifiziert wurden.

Vor diesem Hintergrund wurde in dieser Studie ein neuartiger *in vitro* Ansatz zur Induktion der neuronalen Differenzierung entwickelt, der eine nährstoffarme Umgebung implementiert, die im Gegensatz zu früheren Studien das Überleben neuronal differenzierter Zellen über einen langen Zeitraum sicherstellt und eine normale Ausbildung von Neuriten ermöglicht. Weder die Bildung von freischwebenden Aggregaten noch die Supplementierung von Wachstumsfaktoren oder bekannten Induktoren war erforderlich, um ein zuverlässiges neuronales Differenzierungsprotokoll zu etablieren. Ein einfaches Medium, bestehend aus DMEM/F12+N2, das stark mit Salzlösung verdünnt war, reichte aus, um eine schnelle neuronale Differenzierung in Einzelzellschicht-Kulturen zu erreichen. Der Serumentzug und die starke Verdünnung des DMEM/F12+N2 Mediums führen zu einer nährstoffarmen Umgebung, in welcher der Einfluss von Wachstumsfaktoren und Induktoren minimiert wird. Da bei der Analyse der Medienbestandteile kein Induktor identifiziert werden konnte, wird vermutet, dass die metabolische Zusammensetzung des Mediums ausschließlich die spezifischen Zellbedürfnisse neuronal differenzierter Zellen abdeckt, somit deren Überleben sichert und den Wechsel von pluripotenten Zellen zu Neuronen antreibt. Die selbstentwickelte Methode wurde unter Verwendung der murinen embryonalen Karzinom-Zelllinie P19 etabliert und konnte auf murine ESC übertragen werden. Somit könnte es sich bei der entwickelten Methode um einen realisierbaren Ansatz für ein allgemeingültiges neuronales Standardmodell handeln.

Das etablierte Protokoll bietet mehrere Vorteile, wie z. B. die Möglichkeit stabile neuronale Reinkulturen durch eine schnelle, einfache und hoch reproduzierbare Ein-

Schritt-Induktion unter metabolisch definierten Mediumbedingungen mit einem Minimum an exogenen Signalen zu erzeugen. Die Methode zeichnet sich durch klare und konstante Mediumbedingungen aus, welche die Analyse spezifischer Zellanforderungen während der Differenzierung zugänglich macht. Daher eignet sich diese Anwendung zur Untersuchung molekularer Grundlagen des neuronalen Differenzierungsprozesses sowie für Hochdurchsatz-Screenings. Der Phänotyp reifer post-mitotischer Neuronen bildete sich innerhalb einer Woche aus und blieb für mindestens drei Wochen stabil. Die neuronale Identität wurde durch die Expression neuronaler Marker mittels Immunfluoreszenzfärbung und Massenspektrometrie-Analyse verifiziert. Darüber hinaus wurden erhöhte Konzentrationen verschiedener Axonmarker in der frühen neuronalen Differenzierung gemessen und die Funktionalität der Synapsen P19 abgeleiteter Neuronen wurde durch den Nachweis von Kalziumaktivitäten sichergestellt. Die axonale Laserablation, unmittelbar gefolgt von einem schnellen Nachwachsen der Verbindungen im neuronalen Netzwerk, demonstrierte ein starkes Regenerationspotential unter den gegebenen Bedingungen. Darüber hinaus zeigten die generierten Neuronen einen morphologisch ausgeprägten Phänotyp und die Bildung von neuronalen Rosetten. Mit Immunfluoreszenzfärbungen wurde die Erzeugung von reinen und homogenen neuronalen Kulturen, frei von Gliazellen, nachgewiesen.

Retinsäure (RA) spielt eine essentielle Rolle in der Zellsignalisierung während der Embryogenese und induziert effizient die neuronale Differenzierung *in vitro* in Abhängigkeit der RA Konzentration. In dieser Arbeit war in keiner der verwendeten Medienkomponenten Retinol oder Retinsäure enthalten. Die vorliegende Studie legt jedoch eine Abhängigkeit von RARβ- und/oder RARγ-regulierter RA-Signalisierung in serumfreien Einzelzellschicht-Kulturen nahe. Eine Unabhängigkeit hingegen von RARα unter den gegebenen Bedingungen wurde durch die Beobachtung belegt, dass sich (i) die RARα Konzentration nach der neuronalen Induktion als leicht herunterreguliert erwies, (ii) der verkürzte RARα der RAC65 Mutante keinen Einfluss auf die Induktionseffizienz hervorrief und (iii) ein pan-RAR Inhibitor die neuronale Differenzierung unterdrückte. Im Gegensatz zu serumfreien Einzelzellschicht-Kulturen wurde die neuronale Differenzierung durch den verkürzten RARα, bei Durchführung des konventionellen Protokolls, bei dem die Zellen in freischwimmenden Zellaggregaten in serumhaltigem Medium gezüchtet werden, unterdrückt.

Proteom Analysen der P19 Zellen, welche mit dem selbstentwickelten Differenzierungsprotokoll über fünf Tage behandelt wurden, zeigten einen erhöhten Spiegel zellulärer RA-Bindungsproteine, welche den zellulären RA Transport vermitteln und sowohl an der kanonischen als auch an der nicht-kanonischen RA Signalisierung beteiligt sind. Im Gegenzug waren das RA synthetisierende Enzym ALDH1B1 und RARα, nach dem Austausch des Wachstumsmediums mit RA-freiem Differenzierungsmedium, herunterreguliert. Diese Studie deutet darauf hin, dass die Zugabe hoher RA Konzentrationen nur erforderlich ist, um Signale von supplementierten Komponenten wie Serum oder DMSO (> 0,1 %) zu unterdrücken. Ohne diese Komponenten im Differenzierungsmedium waren subnanomolare RA Konzentrationen ausreichend, um die neuronale Induktion anzutreiben.

Unter Anwendung des etablierten Protokolls wurde die Regulation von beteiligten Signalwegen untersucht. Bei dem etablierten Ansatz wurde der Einfluss von Wachstumsfaktoren und Induktoren minimiert. Daher wurde angenommen, dass diese Signalwege durch die Abwesenheit von Induktoren und geringen Mengen von RA reguliert werden. Die Erstellung eines Proteom Profils zeigte, dass die Wnt- und Notch-Signalwege in der frühen neuronalen Differenzierung herunterreguliert wurden, während die Regulation von SMAD und BMP Signalen gemischte Ergebnisse zeigte. Eine weitere Hemmung von Wnt, Notch oder BMP durch Zugabe von Inhibitoren, die in verschiedenen Protokollen zur Förderung der neuronalen Differenzierung eingesetzt wurden, hatte keinen Effekt. Da die Daten der Proteom Analyse darauf hindeuten, dass diese Signalwege bereits ohne die Zugabe von Effektoren herunterreguliert wurden, schienen somit diese Inhibitoren für die etablierte Methode redundant zu sein. Die Proteom Analyse wiederum deutet auf eine Aktivierung des Hh-Signalweges hin. Dies wird bestärkt durch den negativen Effekt eines Hh-Inhibitors auf die neuronale Induktion.

Darüber hinaus wurde in dieser Studie der Einfluss eines veränderten ROS-Spiegels und der antioxidativen Abwehr nach neuronaler Induktion untersucht. ROS spielen eine entscheidende Rolle bei der Vermittlung von Autophagie, Apoptose und verschiedenen Wegen, die am Übergang von pluripotenten proliferierenden Zellen zu postmitotischen Neuronen beteiligt sind. In dieser Studie wurde gezeigt, dass die Zugabe von Antioxidantien das axonale Wachstum und das Potenzial der neuronalen Differenzierung verringert, während ein ROS Anstieg, ausgelöst durch ein *Nrf2*-Knockdown, das Überleben reifer Neuronen negativ beeinflusste. Auf Proteom Ebene konnte gezeigt werden, dass die untersuchten NRF2-regulierten Enzyme nach neuronaler Induktion eine vielfältige Regulation aufwiesen. Während die analysierten Glutathion-modifizierenden Enzyme herunterreguliert waren, wurden SOD2 und APOE während der frühen neuronalen Differenzierung hochreguliert. Somit wird vermutet, dass diese Mediatoren an der schwachen intrinsischen antioxidativen Abwehr beteiligt sind, die für eine strenge Regulierung redox-sensitiver Signalwege während der frühen neuronalen Differenzierung sorgen. Die Analyse einer generierten P19 Δ*Becl1*-Knockout-Mutante zeigte, dass die Herabregulierung von p62, APOE, GCLc und GSR, die an der antioxidativen Abwehr beteiligt sind, vom Autophagie-Niveau nach der neuronalen Induktion abhängig ist.

In dieser Studie wurde der Einfluss eines veränderten Autophagie-Niveaus auf die neuronale Differenzierung und Entwicklung untersucht. Die Manipulation der Autophagie-Regulation wurde durch Eingriffe in den PI3K/AKT-Signalweg oder durch direktes Deletieren von Autophagie-bezogenen Proteinen durchgeführt. Bemerkenswert ist, dass obwohl Autophagie durch die Zugabe von 3-MA, LY294002, A-674563, Chloroquin oder STF-62247 sowie durch den Knockout von *Becl1*, *p62*, *Atg7* oder *Atg9a* in verschiedenen Stadien inhibiert wird, in allen Ansätzen ein ähnlicher morphologischer Phänotyp während des neuronalen Differenzierungsprozesses hervorgerufen wurde. Die Inhibierung des autophagischen Prozesses verursachte axonales Überwachstum während der frühen neuronalen Differenzierung und einen

vorzeitigen Zelltod reifer Neuronen. Dementsprechend zeigten in dieser Studie die mTOR-Inhibitoren Rapamycin und Torin2, welche Autophagie induzieren, den gegenteiligen Effekt zu den Autophagie-Inhibitoren und verursachten eine Verkürzung der Neurite.

Die Erstellung eines Proteom Profils für eine generierte Δ*Becl1*-Knockout-Mutante während der frühen neuronalen Differenzierung, lieferte Hinweise darauf, dass das auf die frühe Differenzierung beschränkte axonale Überwachstum durch einen fehlenden Abbau des Axonmarkers NCAM1 induziert wurde. Der NCAM1-Spiegel erschien in der Δ*Becl1*-Mutante während der frühen neuronalen Differenzierung stark erhöht. Dies legt nahe, dass die Reduktion des NCAM1-Spiegels durch Autophagie, möglicherweise sogar durch den direkten Abbau, vermittelt wird.

Weiterhin wurde gezeigt, dass die Regulation von ASCL2, MYC und GLI3 sowie einiger Faktoren, die an der antioxidativen Abwehr und der RA-Signalisierung während der frühen neuronalen Differenzierung beteiligt sind, durch den *Becl1*-Knockout beeinträchtigt werden. Dennoch konnte eine erfolgreiche neuronale Differenzierung der Δ*Becl1*-Mutante morphologisch, durch einen Anstieg neuronaler und axonaler Marker und eine ähnliche Signalwegregulation, wie sie für differenzierende WT-Zellen gezeigt wurde, wie die notwendige Runterregulierung von Notch Signalen, eindeutig nachgewiesen werden. Daher wurde angenommen, dass die Autophagie zwar hochreguliert, aber nicht essentiell für die neuronale Differenzierung ist, sondern sich als entscheidend für die axonale Entwicklung und das Überleben reifer Neuronen erweist.

Um andererseits die Auswirkungen eines erhöhten autophagischen Flusses zu untersuchen, wurde ebenfalls ein *BirC6* Gen-Knockout in P19-Zellen durchgeführt. Der Phänotyp der *BirC6*-Knockout-Mutante unterschied sich während der neuronalen Induktion vollständig von dem, des mit Rapamycin behandelten WT. Daher wurde die Hypothese aufgestellt, dass die fehlende Fähigkeit der Δ*BirC6*-Mutante, unter den gegebenen Bedingungen zu Neuronen zu differenzieren, entweder durch eine höhere Effektivität zur Steigerung des autophagischen Flusses oder durch den Verlust anderer *BirC6*-Funktionen verursacht wurde. Aus dem Proteom Profil konnte keine eindeutige Aussage über den Effekt des *BirC6*-Knockouts auf den autophagischen Fluss getroffen werden. Neuronale Marker blieben herunterreguliert und auch die abweichende Regulation von Signalwegen deutete auf ein nicht-neuronales Zellschicksal hin. Außerdem blieb die Herunterregulierung des Notch-Signalwegs, der für die neuronale Differenzierung entscheidend ist, aus. Weiterhin zeigten sich im Gegensatz zu WT- und Δ*Becl1*-Zellen, weder Proteine des PI3K/AKT-Signalwegs noch pro-apoptotische Faktoren oder KIF-Proteine in Δ*BirC6*-Zellen hochreguliert.

Die analysierten Proteine, die an der Ausführung oder Verhinderung der Apoptose beteiligt sind, wiesen eine deutliche Abgrenzung der Δ*BirC6*-Mutante zu WT- und Δ*Becl1*-Zellen im Differenzierungsmedium auf. Die Δ*BirC6*-Zellen zeigten keine (Hoch-) Regulation der pro-apoptotischen Proteine CASP3, CASP6, APAF1 und SEPT4, während die anti-apoptotischen Proteine MCL-1, BIRC5 und AMBRA1 simultan zu den WT-Zellen

herunterreguliert wurden. Dies deutet auf eine verminderte Ansprechbarkeit auf apoptotische Signale in der Δ*BirC6*-Mutante hin. Das anti-apoptotische Protein BCL2L1 (BCL-X) erwies sich in der Δ*BirC6*-Mutante in beiden untersuchten Bedingungen als hochreguliert. Somit wurde vermutet, dass BCL-X möglicherweise den Verlust der anti-apoptotischen BIRC6-Funktion, unabhängig von den Medium-Bedingungen, kompensiert. Die Unterschiede in der Regulation der apoptotischen Faktoren in WT und Δ*Becl1* im Vergleich zu Δ*BirC6* beim Wechsel von Wachstums- zu Differenzierungsmedium wurde auf die unterschiedlichen Zellschicksalentscheidungen zurückgeführt.

Außerdem wurde das erhöhte Ausmaß des Zelltods während der frühen neuronalen Differenzierung untersucht. In dieser Studie wurde die frühe neuronale Differenzierung durch eine Periode mit stark erhöhtem apoptotischem Zelltod geprägt. Autophagie scheint sich ausschließlich auf das Überleben reifen Neuronen auszuwirken, da sich wahrscheinlich mit der Zeit dysfunktionale Proteine in der Zelle anreichern. In differenzierenden P19 WT- und Δ*Becl1*-Mutanten-Zellen wurde ein erhöhtes Niveau mehrerer pro-apoptotischer Proteine nachgewiesen. Im Gegenzug wurden, mit Ausnahme des anti-apoptotischen BCL-X, die untersuchten anti-apoptotische Proteine herunterreguliert, nachdem die neuronale Differenzierung induziert wurde. Es wird angenommen, dass das molare Verhältnis zwischen pro-apoptotischen und anti-apoptotischen Proteinen Auskunft über die Reaktionsfähigkeit auf apoptotische Signale gibt. Daher deuten die Daten stark auf eine erhöhte Empfänglichkeit für apoptotische Signale während der frühen neuronalen Differenzierung hin. Es wird angenommen, dass der erhöhte BCL-X-Spiegel und die angedeutete Hochregulierung des PI3K/AKT- und MAPK/ERK-Signalwegs den apoptotischen Signalweg einschränkt und die Zellen während der frühen neuronalen Differenzierung vor dem Zelltod schützt.

1. Introduction

1.1 Neurogenesis

1.1.1 From the discovery of the brain to *in vitro* cultures of cerebral organoids

Neuroscience covers all research areas related to nervous system, from behavioural observations to molecular approaches. Hippocrates, the fore father of neurology, first made the associations between brain and mind (Breitenfeld *et al*., 2014). About 2500 years of investigation brought us to our presently wide range of knowledge about function, structure, and development of the central and peripheral nervous system. The rapid gain of knowledge in recent decades is due to greatly improved application possibilities and technological advances. The approach on cellular and molecular level enabled a deeper understanding of multitude processes involved in neuroscience. Despite the enormous gain of knowledge, many processes remain still encrypted. This gives society the motivation to push the field forward to improve approaches and implementation of innovative neurotechnology. For example, Altimus *et al.* (2020) predict a significant acceleration of knowledge about nervous system in the next decades, moving development of new therapeutic strategies forward. To implement *in vivo* experiments, rats and mice have been the leading model organisms during last century, while studies with mice became more popular in the last decades (Ellenbroek and Youn, 2016). But although other animals, such as non-human primates, zebrafish, fruit flies and roundworms are established model organisms. A fundamental step in neuroscience was the ability to generate *in vitro* cultures of neurons, glia, and astrocytes (Gordon *et al.,* 2013).

In the early 20th century, neuroscience was revolutionised by establishment of *in vitro* cultures by cultivating of nerve fibres from a frog in hanging drops (Harrison *et al.,* 1907). In the following decades tissue culture techniques were strongly expanded, and *in vitro* cell-based models became increasingly important. Neuronal cell culture provides an enhanced access to multitude areas of neuroscience like for instance investigation of neurogenesis, neurotoxicology assays or drug development. The possibility to reduce the ethically questionable *in vivo* experiments and to enable high throughput screenings on cell or molecular based levels turns it to an attractive alternative. But *in vitro* experiments will even in future probably never replace *in vivo* experiments completely because it is not possible to fully mimic conditions in the body, but it offers a great source to reveal complex mechanism in a simplified system. Certain applications require conditions closer to the *in vivo* situation. For this purpose, 3D culture systems started to be developed to complement culture of cell monolayers. This process started with the first neurosphere culture (Reynolds and Weiss, 1992) followed by protocols based on neural aggregates (Zhang *et al.*, 2001) up to cortical spheroids (Eiraku *et al.,* 2008; Kadoshima *et al.,* 2013). In 2013, Lancaster *et al*. established a method to grow cerebral organoids with various brain regions from human stem cells. This three-dimensional model offers a great possibility to access questions about brain development and causes for neuronal disorders or neurodegenerative disease, even if cerebral organoids are still far away from being identical to the human brain. To exploit the full research potential

several groups are currently working on the refinement of this model (Gonzalez *et al*., 2018; Karzbrun and Reiner, 2019; Sloan *et al*., 2017).

1.1.2 *In vitro* models of neurogenesis

Most common cell lines for studying neurogenesis are from human or mouse origin. Neurodevelopment, brain architecture and cell types of humans and rodent share multitude similarities but also differ in numerous points (Hodge *et al.,* 2019; Semple *et al.,* 2013). Choice of an appropriate model is therefore always dependent on the aim of the study. Different approaches offer various advantages and disadvantages. Primary cells are isolated directly from the tissue and established for growth *in vitro*. Thus, characteristics are rather like *in vivo* conditions. But primary cells are quite sensitive and show a strongly diminished potential of self-renewal. Accordingly, material for experiments is very limited. Another adverse point is that primary neurons require demanding culture conditions (Gordon *et al.,* 2013). One way to overcome this is the establishment of immortalised and proliferating cell lines for *in vitro* analysis (Fig. 1).

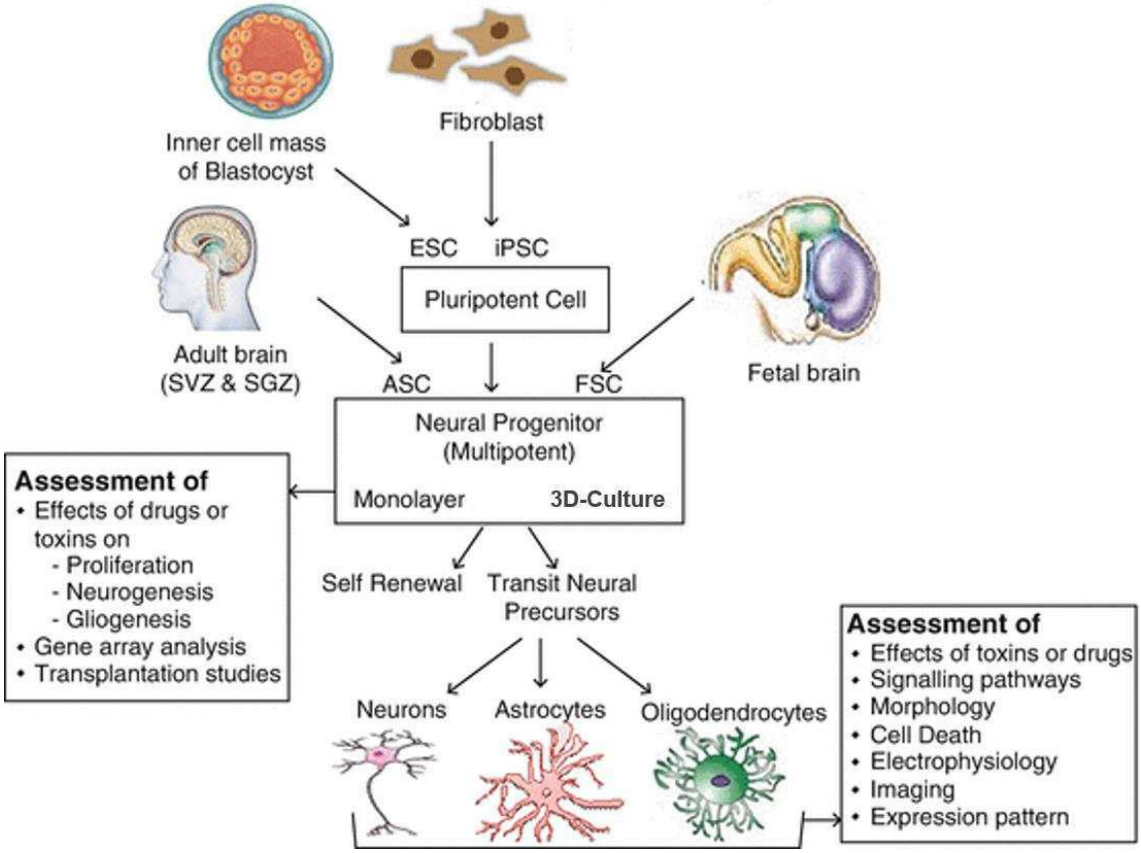

Figure 1: Sources of cell-based *in vitro* cultures with neuroectodermal fate. Need of pluripotent stem cells is either covered by embryonal stem cells (ESC), isolated from a blastocyst, or induced pluripotent stem cells (iPSC), reprogrammed from somatic cells, in general fibroblasts. The adult stem cells (ASC) or fetal stem cells (FSC) are extracted from brain and serve as multipotent neural stem cells. Neurons, astrocyte, and oligodendrocytes can be derived from progenitor cells and cultivated as monolayers or in three-dimensional cultures. (Adapted from Tewari *et al.,* 2017)

Progenitor cells like the multipotent neural stem cells (NCS) have the potential to generate neurons, astrocytes, and oligodendrocytes, while it is limited to specific neuron types (Elkabetz and Studer, 2009). Adult stem cells (ASC) and fetal stem cells (FSC) are

neural progenitor cells that are utilized as model for adult neurogenesis, while studies of embryonic neurogenesis are mainly based on pluripotent stem cells (Azari and Reynolds, 2020). Pluripotent stem cells, like embryonal stem cells (ESC) have the potential to differentiate to all three germ layers and therefore to all neuronal subtypes depending on media conditions. Therefore, it provides a great source for studies of embryonal development and neural specification (Germain *et al.,* 2010; Zhang *et al.,* 2001). ESCs are isolated from the inner cell mass (ICM) of a blastocyst (Evans and Kaufman, 1981). Since investigations of human ESCs are facing several ethical issues (Robertson, 2001), induced pluripotent stem cells (iPSCs) became an attractive alternative (Lu *et al*. 2013; Compagnucci *et al.,* 2014; Velasco *et al.*, 2014). iPSCs are epigenetically reprogrammed somatic cells (predominantly fibroblasts) from a patient (Park *et al.,* 2008) or healthy donor (Yu *et al.,* 2007). For analysis of neuronal dysfunction, derivation of iPSCs that already contain specific mutations was a huge benefit before genome editing of ESC became facilitated by CRISPR/Cas9 system (Jinek *et al.,* 2012; Mali *et al.,* 2013). Unfortunately, iPSC demonstrate an incomplete reprogramming of somatic cells (Chin *et al.,* 2009; Marchetto *et al.,* 2009; Ohi *et al.,* 2011). Recently, a direct reprogramming from fibroblasts to mature neurons of many different subtypes by usage of transcription factors or microRNAs became possible (Tsunemoto *et al.,* 2015). Embryonal carcinoma cells (ECCs), derived from teratocarcinomas, provide a further source of pluripotent cells (Andrews *et al.,* 1984; Martin, 1980).

ECCs are immortal cells, characterised by a high proliferation without apparent limit in culture. Therefore, ECC lines are easy to maintain in undifferentiated state, while differentiation is induced very efficiently (Michael and McBurney, 1993; Rosenthal *et al.,* 1970). But different ECC lines reveal varied characteristics and differentiation potential (Andrews *et al.,* 1980; Sennerstam and Strömberg, 1984). Even if ECCs show plenty overlapping characteristics with ESCs (Dawud *et al.,* 2012), different ECC lines feature varied capacities to differentiate (Andrews *et al.,* 1984; Pera *et al.,* 1989, Thompson *et al.,* 1984). The two murine ECC lines P19 and F9 were isolated a couple of decades ago and became popular models for studies of neurogenesis (Datta, 2013; Kuff and Fewell, 1980; McBurney and Roggers, 1982).

1.1.3 P19 cells as model of neuronal differentiation

P19 is a murine embryonal carcinoma cell line, expressing several embryonic markers. This cell line was established in the early eighties, when a 7.5-day old embryo from a female *mus musculus* was grafted into testes of a male mouse (C3H/He strain), resulting in tumour growth. P19 cells were derived from this tumour and established in *in vitro* culture showing a stable euploid male karyotype (40:XY) (McBurney and Roggers, 1982). Besides the benefit of simple culture conditions without feeder layer, P19 cells have a high efficiency in transfection and genetic manipulations (McPherson and McBurney 1995). Cells are easy to maintain in undifferentiated state whereas a reproducible differentiation to ectodermal or mesodermal derivates can be induced in culture (McBurney, 1993). P19 cells present a phenotype close to the primitive ectoderm (Jones-Villeneuve *et al.,* 1982). Differentiation of this cell line resemble many of the molecular and morphological events occurring during early embryonic development *in vivo*

(McBurney *et al.,* 1982). For *in vitro* induction, cell aggregation and supplementation of chemical inducer are common tools (see chapter 1.1.5). Dimethyl sulfoxide (DMSO) induces mesodermal differentiation in P19 cells aggregates (McBurney *et al.,* 1982) while retinoic acid (RA) act as an efficient inducer of differentiation along the neuroectodermal lineage (Jones-Villeneuve *et al.,* 1982). Therefore, the P19 cell line became a popular model for studies of cardiac muscle (van der Heydena and Defizeb, 2003) and neuroectodermal differentiation (Marikawa *et al.*, 2009; McBurney, 1993). P19 derived neurons express several of the most characteristic and functionally relevant genes and phenotypes of neurons (Bain *et al.*, 1994; Resende *et al.,* 2007; Wu and Chow, 2005;). Hence, RA induced neurons demonstrate functional synapses expressing predominantly GABA and glutamic acid decarboxylase, the most prevalent neurotransmitter of the central nervous system (CNS) (McPherson *et al.,* 1994; Reynolds *et al.,* 1996; Staines *et al.,* 1994). Other neuropeptides like acetylcholine, NMDA (N-methyl-d-aspartate), somatostatin, serotonin, neuropeptide Y and others are also expressed but in significantly smaller amount (Resende *et al.,* 2017; Stains *et al.,* 1994). The observed distribution of neurotransmitter is reminiscent of mammalian forebrain and besides some exceptions, this is unique under ECC lines (Bain *et al.,* 1994; Stains *et al.,* 1994). P19 derived neurons are even able to mature *in vivo* after implantation to rat brain (Magnuson *et al.,* 1995; Morassutti *et al.,* 1994). Besides the generation of neurons, RA treatment of P19 culture results in differentiation to glia and fibroblast-like cells (Jones-Villeneuve *et al.,* 1983). The multitude of benefits of P19 cells makes it, even in these days, to a suitable model to study the complex processes of embryonal neurogenesis in a strongly simplified system. Investigations over decades resulted in a big pool of methods and recorded insights in neuronal differentiation process of this cell line with the hope to transfer majority of the knowledge on processes occurring in the developing human CNS.

1.1.4 Embryonic development of the neural ectoderm

Ectoderm is one of the three germ layers, which arise during early embryogenesis. Cells derived from this germ layer differentiate into surface and neural ectoderm. Neuroectoderm is the origin of the central and peripheral nervous system (Tam and Loebel, 2007). Differentiation from the primitive stem cells to a whole nervous system is a highly complex process, here described in simplified form (Fig. 2). Embryonic development starts with cleavage of a fertilized egg, the zygote. In a 16-32 cell stage, designated as morula, first differentiation process starts, resulting in an outer cell layer, known as trophoblast, and the inner cell mass (ICM), located on one side of the generated blastocyst (Shahbazi, 2020). Pluripotent cells of the ICM differentiate to epiblast (“primitive ectoderm”) and hypoblast (“primitive endoderm”), the two layers of the bilaminar disc. The primitive streak forms in the epiblast and cells from the epiblast start to migrate through the bilaminar disc. In this process, called gastrulation, cells differentiate and form three germ layers, referred as ectoderm, mesoderm, and endoderm (Gossler, 1992).

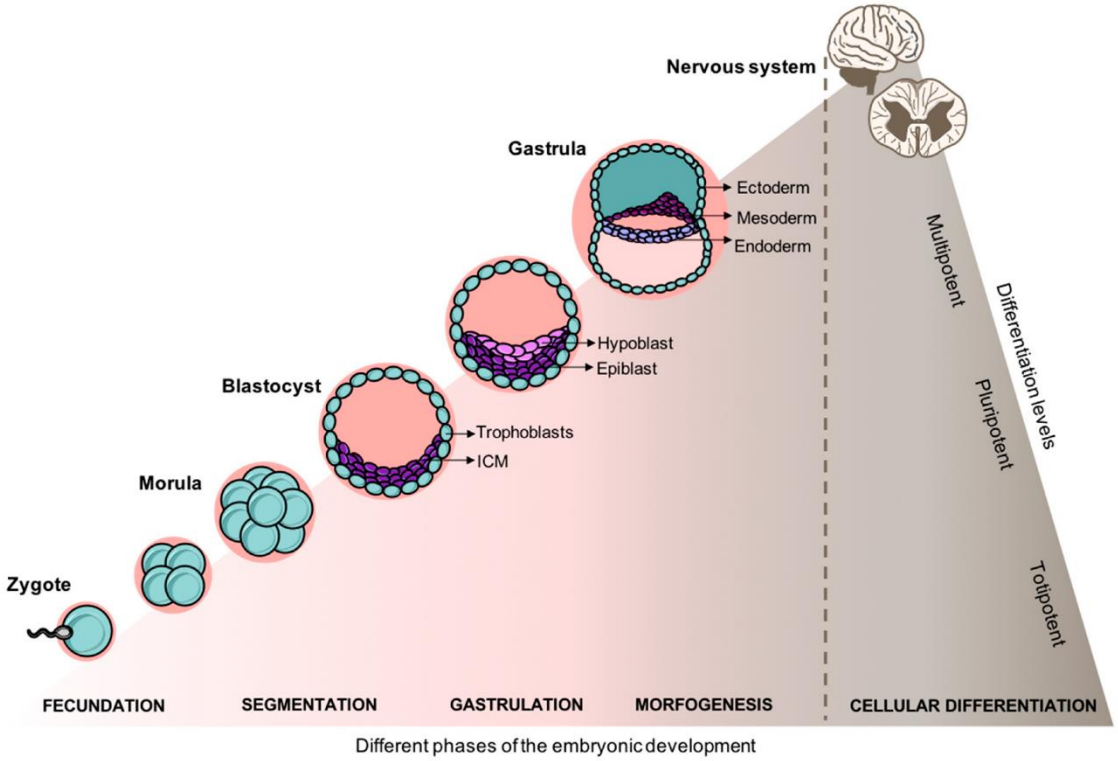

Figure 2: Differentiation levels during embryogenesis. Embryogenesis starts with a fertilized egg, the zygote in a totipotent differentiation level. Differentiation potential decreases through development on the way over establishment of the three germ layers in the gastrula to fully mature neurons in the CNS. (Adapted from Pereira *et al.,* 2019)

Further differentiation of mesodermal cells (central germ layer) leads to a chord structure beneath the primitive streak, called notochord (Fig. 3). Neurulation starts by ectodermal differentiation to a neural plate, induced by the notochord located underneath. The neural plate extends the length of the rostral-caudal axis and the edges to the remaining ectoderm thickened (Smith and Schoenwolf, 1989; Keller *et al.,* 1992). Subsequently, the neural plate invaginate along the central axis during the process of neurulation. The ends of this bended neural plate finally fuse together to form the neural tube (Smith and Schoenwolf, 1997). Cells located on the interface between neural plate and the surface or non-neural ectoderm, delaminate from the ectoderm as the neural tube is forming. These so-called neural crest cells migrate away and differentiate to form most of the peripheral nervous system, while the neural tube ultimately forms the spinal cord and the brain (Wilde *et al.,* 2014). The neuroepithelial cells, building the neural tube, undergo massive proliferation and differentiate to neuroblasts, glioblasts and precursors that can generate both, neurons and glial cells (Davis and Temple, 1994; Kilpatrick *et al.,* 1994). The time course of neuron and glial cell development is still not fully understood. However, some evidence suggests that neurogenesis largely precedes gliogenesis (Quian *et al.,* 2000). In invertebrates like *Drosophila melanogaster*, neuroblasts divide asymmetrically to produce another neuroblast and a precursor, called a ganglion mother cell that divides to give two differentiated daughter cells (Udolph *et al.,* 1993). In vertebrates, the pattern of the lineage tree is still not clear yet but an asymmetric cell division in the ventricular zone during neurogenesis has been observed (Caviness *et al.,* 1995; Rakic, 1995). The two daughter cells appear to have

different cell fates (Chenn and McConnell, 1995). The progenitors of different neuronal and glia subtype are arranged along the dorsoventral axis of the neural tube. The whole spatiotemporal pattern of neuronal cell fate determination in vertebrates is still not clear and raises numerous questions (Guerrero *et al.,* 2019). The neurons and glia cells migrate from the ventricular proliferative zone into the mantle zone of the neural tube. The mantle layer becomes most of the substance of the spinal cord and brain (gray matter), containing nerve cell bodies and dendrites, unmyelinated axons, and glial cells. The growing axons move out of mantle zone with the differentiating neurons and build the marginal zone. Myelinated axons of the marginal zone finally built the white matter of the spinal cord and brain. The posterior part of the neural tube finally forms the spinal cord, while the anterior part forms the brain (Swenson, 2006).

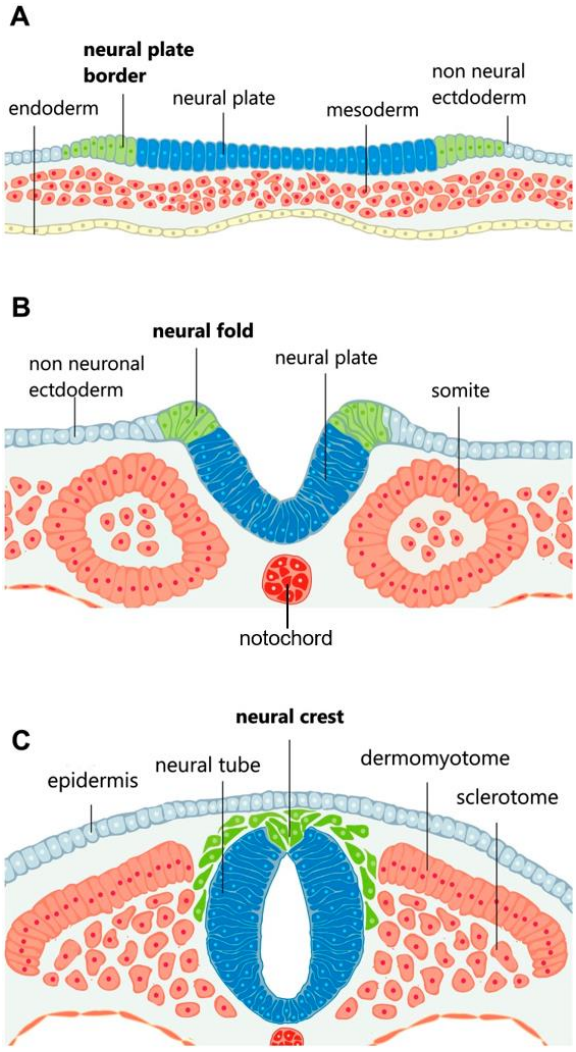

Figure 3: Neurulation. Embryonic development from neural plate to neural tube. **A:** The neural plate, derived by the ectoderm, is separated by the neural plate border from non-neural ectoderm. **B:** The neural plates folds and invaginates into the underlying mesoderm, induced by the mesodermal notochord. **C:** Closure of the neural tube and delamination of the neural crest cells. (Adapted from Simões-Costa and Bronner, 2013)

Regulation of cellular organisation and differentiation during embryogenesis is an extremely complex and spatiotemporal controlled process. Because *in vivo* studies of embryogenesis are difficult to implement, *in vitro* differentiation of mouse embryonic

stem cells became a popular model to investigate some aspects of the complex *in vivo* development in human. The drawback of this approach is that human and rodent neurodevelopment share many similarities, but also differ in many ways that complicate these studies (Shahbazi and Zernicka-Goetz, 2018). *In vitro* studies are very simplified and quite far away from *in vivo* conditions but provide a good source to make these complex studies accessible. Moreover, several insights supplied by ESC differentiation could be verified *in vivo* (Cazillis *et al.,* 2006).

1.1.5 Classification and morphological appearance of neurons and neuroglia

The central nervous system, including the brain and the spinal cord is made up of neurons and glia cells. The human brain contains around hundred billion neurons and even more glial cells (Herculano-Houzel and Dos Santos, 2018). The numerous phenotypes of neuronal populations display a vast diversity while fairly limited for the glia cells (Fig. 4). There are large numbers of neurons that differ from each other, for example molecularly, functionally, in electrophysiological properties, synapse type and morphologically. Observation of new neuronal subtypes is still ongoing, therefore making classification challenging (Fishell and Heintz, 2013; Zeng and Sanes, 2017). Three major neuron types, called motor, sensory, and interneurons, are divided by their function. Motor neurons transfer signals from brain or spinal cord to the muscle and sensory neurons sense stimuli like the name already says. Interneurons are the most abundant neuron type of the CNS and transfers signals between sensory and motor neuron or communicate among each other. Neurons are also categorized by their cell morphology into uni/bipolar, pseudo-unipolar and multipolar neurons.

Multipolar neurons are the most abundant cell type in vertebrate CNS. Diversity in size and shape is furthermore adapted to specific tasks of neuronal subtypes and varies in one and the same category to cover the tremendous complexity of the nervous system (Sathyamurthy *et al.,* 2018). For instance, multipolar purkinje cells in cerebellum are characterised by a very complex dendritic tree, able to receive and process a high number of signals. Classification as excitatory, inhibitory, or modulatory neurons based on their neurotransmitter phenotypes was implemented. But several studies observed also multiple combinations of excitatory, inhibitory, or modulatory transmitters (Granger *et al.,* 2016; Vaaga *et al.,* 2014). Glutamate is the main excitatory neurotransmitter in mammalian cortex and immediate precursor of the inhibitory neurotransmitter γ-aminobutyric acid (GABA) (Bak *et al.,* 2006; Meldrum, 2000). In the nervous system exist a multiplicity of neurotransmitters like for instance acetylcholine, glycine, N-acetylaspartylglutamate (NAAG), dopamine, serotonin, norepinephrine, adenosine and so on. Several neurotransmitters co-exist in the same areas and some are partially limited to distinct brain areas (Butt *et al.,* 2014).

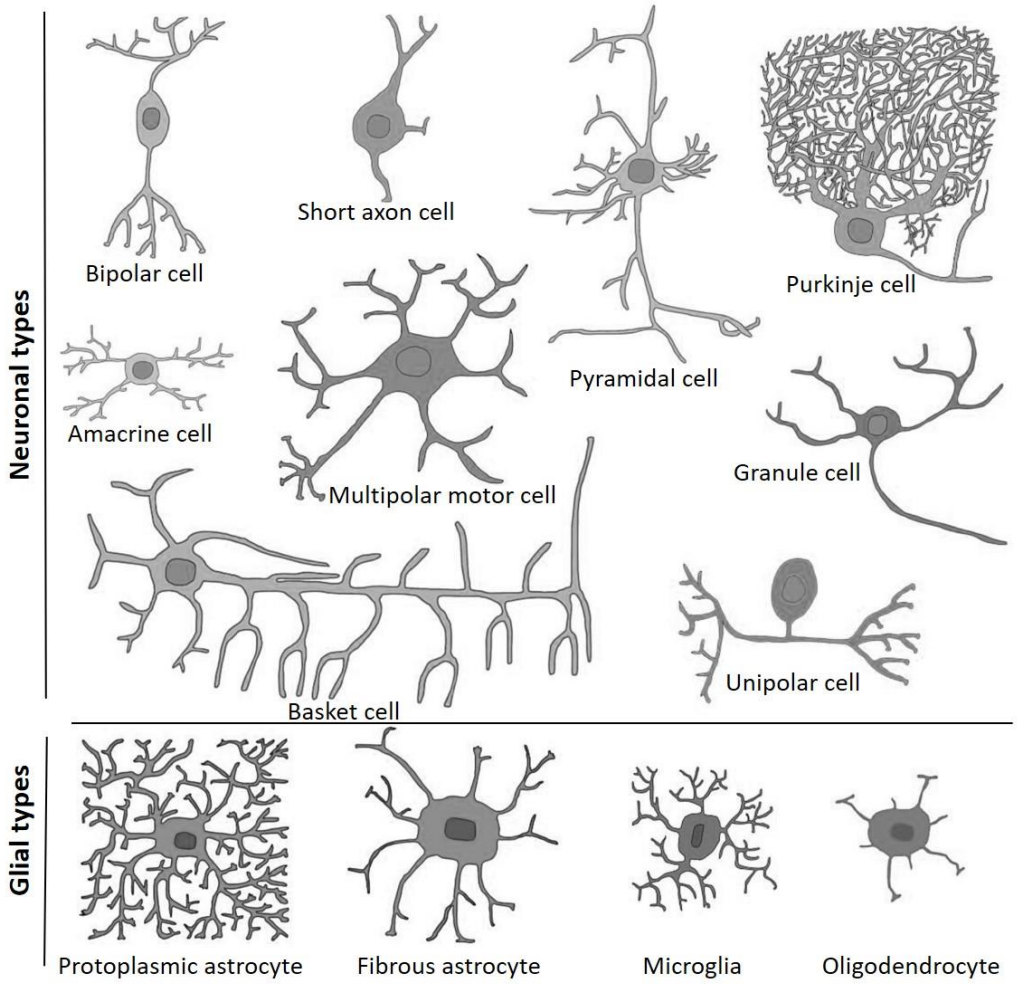

Figure 4: Morphological phenotypes of neurons and glia cells. Overview over a selection of morphological distinct neurons and phenotypes of the glial cells, displaying a very limited morphological diversity. (Adapted from Herculano-Houzel and Dos Santos, 2018)

Neuroglia, the non-neuronal cells of CNS, show, compared to neurons, a very limited morphological diversity. Glia cells appear smaller and with only local branches. Compared to neurons, glial cells of different types are much more homogeneously distributed in nervous tissue and limited on generation of local signals (Wang *et al.,* 2006). Transcriptome analysis of neurons and glia cells demonstrate a restricted number of glial phenotypes and a reduced RNA content (Von Bartheld *et al.,* 2016; Zeisel *et al.,* 2015). Glial cells play an essential role in many aspects of CNS formation and function regulation. Neuroglia are divided into astrocytes, oligodendrocytes, microglia, and ependymal cells. The astrocytes represent the most abundant glia type (Kettenmann and Ransom, 2005). Protoplasmic astrocytes are star-shaped cells characterised by multiple branches that interact with synapses, blood vessels, and other cells and are found in the gray matter. Fibrous astrocytes, located in the white matter, exhibit a morphology of many long fiber-like processes (Sofroniew and Vinters, 2010). Astrocytes fulfil several tasks in the CNS such as regulation of synapse formation, mediation between neurons, aid homeostasis and they are capable to proliferate in the mature brain (Madhusudanan *et al.,* 2017). Oligodendrocytes show smaller cell size, fewer, and shorter branches compared to astrocytes. Myelin sheaths around the axons speed up

nerve impulse conduction. These myelin sheets are built in the CNS by oligodendrocytes while neurons of the PNS are myelinated by Schwann cells. Besides this function, oligodendrocytes are involved, among others, in axonal integrity and health as well as nerve conduction and neurotransmitter metabolism (Bradl and Lassmann, 2010). Microglia are the smallest glial cell but becomes enlarged, mobile, and phagocytic if the CNS is injured. Microglia are specialised macrophages of the brain that are responsible for phagocytotic clearance of damaged brain cells (Madhusudanan *et al.,* 2017). Proliferation capacity and marker expression of microglial cells in neurogenic and non-neurogenic regions differ (Goings *et al.,* 2006). Ependymal cells are simple cuboidal glial cells that plays a central role in many aspects of central nervous system as well. These cells line ventricles in the brain and the central canal of the spinal cord. Therefore, ependymal cells act as physical barrier between ventricular cerebrospinal fluid and brain parenchyma (Jimenez *et al.,* 2014).

1.1.6 Induction of neuronal differentiation *in vitro*

Differentiation of pluripotent cells to neuroectodermal cell fate *in vitro* can be implemented by supplementation of epigenetic and growth factors, overexpression of transcription factors, embryoid body (EB) formation, and altered culture conditions. Various protocols give rise to different efficiency of neuronal differentiation and thus the purity of neuronal culture. Ratio of neurons to glial cells and generation of distinct neuronal subtypes is highly influenced by the chosen differentiation protocol. Different culture surface substrates or media compositions play a reinforcing role for efficiency of differentiation to neuroectodermal fate. Without a culture substrate to which cells can adhere, a three-dimensional formation can be built up, the EB. EB formation mimics embryogenesis of different tissues deriving from all three germ layers including primitive neural tissue (Leahy *et al.,* 1999; Robertson, 1987). In this multicellular aggregate, cells differentiate spontaneously into different cell lineages, complicating achievement of pure neuronal cultures (Azari and Reynolds, 2016).

To enhance differentiation to neuroectodermal fate, RA act as the most common inducer. It plays an essential role in cell signalling during embryogenesis (Blumberg, 1997, Ross *et al.,* 2000) and efficiently induces neuronal differentiation *in vitro* in a concentration dependent manner (Bain *et al.,* 1996; Okada *et al.,* 2004). Induction of the differentiation process by RA supplementation in combination with EB formation in serum-containing media is the classic neuronal differentiation protocol that was first applied, although handling and culture conditions vary between different research groups (Jones-Villeneuve *et al.,* 1982; McBurney *et al.,* 1982; Okabe *et al.,* 1996; Stewart *et al.,* 2003, Yang *et al.,* 2017). RA promotes neuroectodermal and represses mesodermal gene expression and accordingly significantly increase the neuronal population (Bain *et al.,* 1996; Boudjelal *et al.,* 1997). Pluripotent cells, treated by a version of the conventional protocol, derive to functional neurons, glial and fibroblast-like cells (Bain *et al.,* 1994; Fraichard *et al.,* 1995; Strübing *et al.,* 1995). Nevertheless, the classical approach was shaped by the lack of lineage specific subtypes generation and a reduced neuronal differentiation efficiency compared to modern methodologies. Therefore, an optimization process ran over several decades resulting in a huge variety

of controlled differentiation conditions due to enrichment of neuronal population and derivation of distinct subtypes. To enhance purity of neuronal cultures, for example mitotic inhibitor like cytosine arabinosine (AraC), fluorodeoxyuridine, or uridine are supplemented during the differentiation procedure to achieve selection of postmitotic neurons (Monzo *et al.,* 2012; Stewart *et al.,* 2003). Serum, supplemented to media, faces the problem to be undefined and to vary in composition, preventing regulated and steady conditions. It contains several factors presumably influencing differentiation process but investigation of specific cell requirements during differentiation stayed under this condition inaccessible (Cai and Grabel, 2007). Furthermore, promotion of neural stem cell differentiation into glial cells and thus inhibition of differentiation into neurons was observed to be caused by FBS supplementation in a concentration dependent manner (Liu *et al.,* 2018). The supplementation of RA as well as the EB formation is essential to induce efficient neural differentiation of pluripotent cells in serum-containing cultures (Bain *et al.,* 1995, 1996; Jones-Villeneuve *et al.,* 1982; Glaser and Brüstle, 2005; Rohwedel *et al.,* 1999).

Modern protocols mostly renounce the usage of serum like FBS or FCS, implemented in the initial protocols, because serum-free cultures benefit from a chemically defined media composition and therefore gives the possibility to investigate single factors involved in neurogenesis. In consequence, several approaches under serum-free growth conditions developed (Bouhon *et al.,* 2005; Finley *et al.,* 1999; Okabe *et al.,* 1996; Tropepe *et al.,* 2001; Wiles and Johansson, 1999; Ying *et al.,* 2003;). Serum was replaced by defined nutrition mixture adjusted on neuronal demands like the N2 supplement that is based on Bottenstein's prominent N1-formulation, developed to maintain neuroblastoma in culture (Bottenstein and Sato, 1979). Serum-deprivation offers several new induction approaches since nutrition mixtures like the knockout serum replacement can lead to neuronal differentiation without need of any further inductor (Verma and Seshagiri, 2018). The increasing knowledge about epigenetic and endogenous cellular signals during cell fate decision (detailed description in chapter 1.2) offers a reliable source of several approaches to induce neural induction *in vitro* without EB formation and/or RA supplementation. In monolayer cultures, the neural differentiation process is only induced when complex signalling from serum factors is avoided (Pacherník *et al.,* 2005).

Circumvention of EB formation by the establishment of serum-free monolayer cultures shortens the length of the neuralization process considerably (Azari and Reynolds, 2020). Induction in this system can be implemented by co-cultures with stromal cells or usage of their conditioned medium. Neural differentiation process is then induced by factors secreted by stromal cells and cell-surface-anchored molecules (Kawasaki *et al.,* 2000; Vazin *et al.,* 2008). These are factors like for instance Sonic hedgehog (Shh), that facilitate a dopaminergic phenotype in generated neurons (Swistowska *et al.,* 2010). Neuronal induction during embryogenesis is, among others, regulated by the coordinated action of bone morphogenic proteins (BMP), fibroblast growth factors (FGF), and the wingless-related integration site (Wnt) signalling pathways (Linker and Stern, 2004). The inhibition of mesoderm and endoderm-promoting signals, such as

Wnts (via Dkk1), Nodal (via cerberus and lefty), BMPs (via chordin, noggin, and follistatin), and Notch (via DAPT) offers an opportunity to enhance or induce neuronal fate decision *in vitro* (Azari and Reynolds, 2020; Crawford and Roelink, 2007; Levine and Brivanlou, 2007).

In addition to protocols that generate a broad range of neuronal subtypes, approaches have been developed that promote the generation of certain neuronal cell fates such as glutamatergic, dopaminergic, serotonergic, GABAergic neurons, motor neurons, cerebellar neurons, astroglia, or oligodendroglia (e.g. protocols listed in Compagnucci *et al.,* 2014). Furthermore, many cell fate-specific transcription factors are capable of positively regulating cell fate decision, while suppressing other cell fates (Anderson, 1993; Sun *et al.,* 2001). Overexpression of specific transcription factors provide a rapid generation of homogenous populations of functional neurons. Recently, many combinations of transcription factors have been identified that cause mouse fibroblasts to differentiate into neurons of a particular subtype (Tsunemoto *et al.,* 2015; 2018). For instance, the transcription factor neurogenin promotes neurogenesis while supressing glial differentiation (Sun *et al.,* 2001). And overexpression of neurogenin 2 (NGN2) is widely used to induce neuronal differentiation into a homogeneous glutamatergic neuronal population in pluripotent stem cells (Busskamp *et al.,* 2014, Zhang *et al.,* 2013). Established neuronal differentiation protocols for different cell sources like the pluripotent ESC, ECC, iPSC or the multipotent neural stem cells (NSC) partially differ due to adaptation of diverse demands or because of various handling strategies of different labs. Even cell lines with close characteristics can vary in their culture standards. For example, the two murine embryonic carcinoma cell lines F9 and P19, both popular ECC lines to study cell proliferation, differentiation and self-renewal, show differences in their expression profiles and thus partly different requirements for the conditions (Kelly and Gatie *et al.,* 2017). Thus, unlike P19 cells, F9 cells require cAMP in addition to RA under serum deprivation to generate a neuronal phenotype (Datta, 2013; Murtomäki *et al.,* 1999).

A neuronal default model to establish an approach that works efficiently for all pluripotent cells and neuronal precursors is still lacking but is currently in focus of research (Kelly and Gatie *et al.,* 2017; Tropepe *et al.,* 2001). It was reported that ESC, grown at low density and in absence of exogenous factors or feeder layers, either die or acquire a neural identity as indicated by expression of the neural marker Nestin (Smukler *et al.,* 2006; Tropepe *et al.,* 2001). This default cell fate is thought to be achieved by eliminating extracellular inhibitors of neuroectodermal fate and suppressing cell-cell signalling through limited cell density. Studies in different vertebrate species suggest that the neuronal default mechanism occurs through a lack of BMP signalling that prevents neuronal tissue formation (Levine and Brivanlou, 2007; Muñoz-Sanjuán and Brivanlou, 2002). Thus, it is proposed that a neuronal default model is achieved through inhibition of BMP realized by the factors noggin and chordin, which can be isolated from mesendodermal tissue (Levine and Brivanlou, 2007; Muñoz-Sanjuán and Brivanlou, 2002). Meanwhile, the field is swamped with neuronal differentiation protocols, continuously trying to improve conditions to promote neuronal enrichment during long-

term cultures and to establish cell fate decision into different subclasses *in vitro*. Many factors and their regulatory system involved in neurogenesis remain obscure. Further insights in the mechanisms of cell fate decisions will give rise to further improvements and might lead to the establishment of a general default model of neuronal differentiation and to clarify molecular mechanisms underlying neuronal development.

1.1.7 Classical versus modern approach of neural induction *in vitro*

The classical approach to induce neuronal differentiation in vitro includes supplementation of RA as well as EB formation in serum-containing cultures (Bain *et al.,* 1995, 1996; Jones-Villeneuve *et al.,* 1982; Glaser and Brüstle, 2005; Rohwedel *et al.,* 1999). Modern protocols mostly renounce the usage of serum because serum-free cultures benefit from a chemically defined media composition and therefore gives the possibility to investigate single factors involved in neurogenesis. Another advantage of modern protocols is that circumvention of EB formation by establishing serum-free monolayer cultures significantly shortens the duration of the neuralization process (Azari and Reynolds, 2020). A part of this work was the development of an approach to induce neuronal differentiation in mouse ECC and ESC independently of EB formation, RA, or serum supplementation. For comparative purposes, both the conventional method of McBurney *et al.* (1988) and a modern approach of Nakayama *et al.* (2014), were performed in this work. Both protocols are developed for the implementation of neuronal differentiation in P19 ECCs (Fig. 5). The first step of the classical protocol implicates the formation of multicellular aggregates in α-MEM media supplemented with 5 % FBS and 500 nM RA over four days. Subsequently, EBs are plated on a poly-L-lysine coated surface, cultured with media containing 10 % FBS. First evidence of neurons and glial cells appear five days after RA exposure (McBurney *et al.,* 1988). The generated culture is extremely inhomogeneous, containing patches with neurons growing on top of glial cells, spread in a culture, more and more dominated by the growth of non-neuronal fibroblast-like cells.

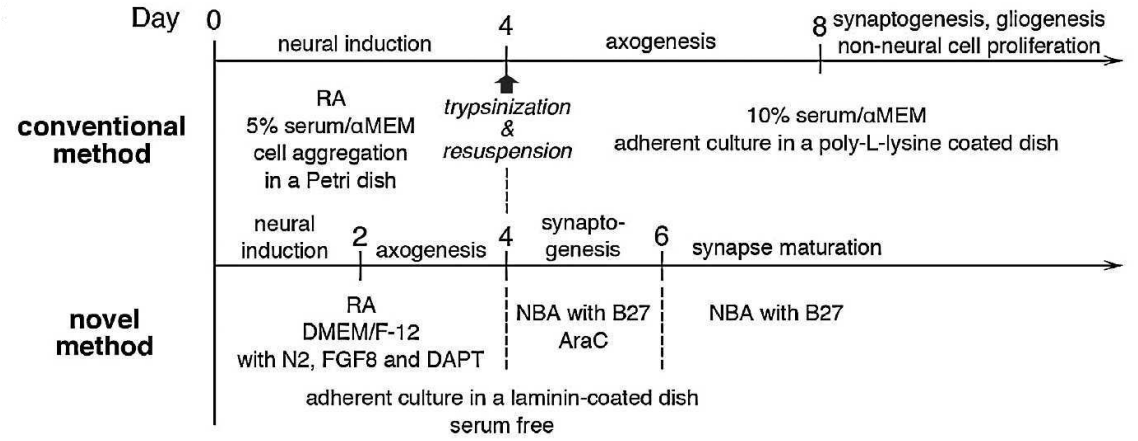

Figure 5: Comparison of the conventional and a novel approach to induce neuronal differentiation in P19. The convenient approach is based on the protocol of McBurney *et al.* (1988) while the novel strategy, displayed here, was established by Nakayama *et al.* (2014). Conditions and steps of neurogenesis are listed in a timeline, starting at day 0 with neuronal induction. (Adapted from Nakayama *et al.,* 2014)

On the contrary, Nakayama *et al.* (2014) claim the development of a rapid and efficient method to generate mature neurons within six days. Differentiation is induced in a monolayer culture, adhered to laminin substrate. Development to neuronal fate is likewise induced by supplementation of 500 nM RA but in serum-free DMEM/F12 media, supplemented with further enhancer like N2-supplement, FGF8 (fibroblast growth factor 8) and DAPT (N-[N-(3,5-difluorophenacetyl)-l-alanyl]-S-phenylglycine t-butyl ester). DMEM with the nutrition mixture F12 was proven to be suitable for differentiation of P19 cells under serum-free condition (Pacherník *et al.,* 2005). N2 is based on Bottenstein's N1 formulation (Bottenstein and Sato, 1979) and was originally developed for neuronal *in vitro* cultures under serum-deprivation and without feeder culture. The N1 and N2 supplements contain the proteins insulin and transferrin as well as the components progesterone, putrescine, and sodium selenite in different concentrations. FGF8 overexpression results in neural induction of P19 monolayer cultures (Wang *et al.,* 2006). FGF8 supplementation proved to be essential in this protocol, since a withdrawal resulted in cell detachment before differentiation process is completed (Nakayama *et al.,* 2014). DAPT is a γ-secretase inhibitor, supressing Notch signalling, resulting in enhanced neurogenesis while supressing gliogenesis (Crawford and Roelink, 2007; Taylor *et al.,* 2007). Nakayama *et al.,* reported that DAPT is essential under this condition for neurite development. And besides supplementation of multiple effectors, the inductor RA asserted to be indispensable in this novel protocol. Abolishment of this morphogen led to overgrowth of undifferentiated cells. After four days, conditions are switched and cells are incubated with Neurobasal medium, supplemented with B27 and AraC (for 2 days). B27 supplemented Neurobasal medium was originally designed for culturing primary neurons, containing vitamin A, a RA precursor (Brewer *et al.,* 1993). AraC is a mitotic inhibitor. Therefore, AraC inhibit the proliferation of non-neuronal cells and supresses derivation to GFAP-positive glial cells (Monzo *et al.,* 2012, Nakayama *et al.,* 2014). Nakayama *et al.* claimed that this developed method is highly effective and that derived neurons survive at least three weeks without the proliferation of non-neural cells. But neither are these data shown nor are experiments done or data presented with neurons from a culture older than six days.

1.2 Effectors and signalling pathways involved in neuronal fate decision

1.2.1 Retinoic acid signalling in neuronal development

RA, a common inducer of neuronal differentiation *in vitro*, is a small lipophilic molecule, derived from Vitamin A (retinol). Several isomeric forms of RA like all-trans-RA, 9-cis-RA and 13-cis-RA exist but all-trans-RA is the primary ligand during development (Cunningham and Duester, 2015). RA signalling has been lost in a variety of lineages, like for instance in *Drosophila melanogaster* but is highly conserved in vertebrates (Albalat, 2009; Rhinn and Dollé, 2012). Vitamin A deficiency causes several abnormalities during embryogenesis resulting in neurological symptoms. This observation revealed a critical role of RA in the early development (White *et al.,* 2000; Wilson *et al.,* 1953). The ability to inhibit cell proliferation and induce neuronal differentiation *in vitro* by RA was discovered by early experiments with ECC lines and got soon after verified in various

stem cells (Jones-Villeneuve *et al.,* 1982; Maden, 2007; Strickland and Mahdavi, 1978). Besides the essential function during embryonal development, RA is also indispensable postnatally, for survival, growth, reproduction, epithelial differentiation, and neuronal plasticity (Ghyselinck and Duester, 2019; Maden, 2007). The capability to induce a switch between proliferation and differentiation served as an early evidence of the *in vivo* function of RA signalling. Meanwhile RA was shown to be essential for embryonic development of many chordate animal organs such as hindbrain, spinal cord, and eyes (Clagett-Dame and DeLuca, 2002; Marlétaz *et al.,* 2006). RA is involved in the regulation of several events related to mesodermal segmentation and neurogenesis in caudal neural tube (future spinal cord) during elongation of embryonic body axis (Rhinn and Dollé, 2012). The number of primary neurons depends critically on level and spatial distribution of RA during embryogenesis (Diez del Corral *et al.,* 2003; Janesick *et al.,* 2013). Specific synthesising and metabolising enzymes enable a tight control of RA distribution within embryonic cell populations (Rhinn and Dollé, 2012). RA is synthesised by paraxial/somitic mesoderm of the developing embryo and diffuse to the adjacent neural plate to promote differentiation and control specification of neuronal cell types in the caudal neural tube (Diez del Corral *et al.,* 2003; Molotkova *et al.,* 2005; Novitch *et al.*, 2003; Wilson *et al.,* 2004).

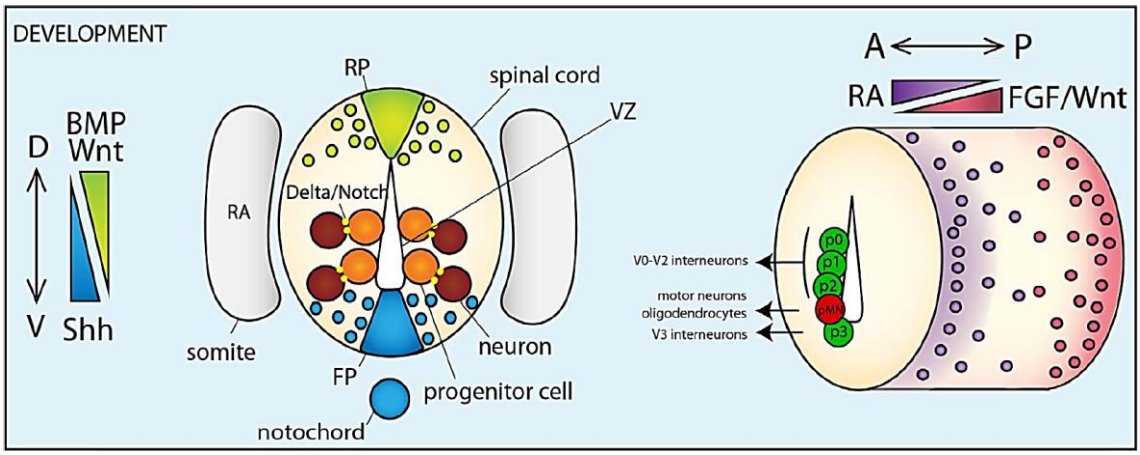

Figure 6: Signalling pathway-dependent patterning of the neural tube. Shh diffuses in a ventral-high, dorsal-low gradient, while BMP and Wnt establish a dorsal-high, ventral-low gradient. In the ventricular zone (VZ) high notch expressing cells remain in proliferative state (orange), while cells that present higher Delta/Serrate level differentiate into mature neurons (brown). FGF/Wnt and RA gradients mediate embryonal anterior-posterior patterning of the neuroectoderm and establish distinct ventral progenitor zones p0-p3 and pMN. (Adapted from Cardozo *et al.,* 2017)

A study in zebrafish showed that posteriorly expressed genes require a short period of high RA levels for induction, while anteriorly expressed genes display induction later by a lower RA level (Maves and Kimmel, 2005). The spatiotemporal distribution is regulated by a gradient of RA that supports anteroposterior and dorsoventral patterning of the neural plate and neural tube (Kudoh *et al.,* 2002). Along the dorsoventral axis, patterning of the neural tube is primarily controlled by Shh, Wnt and BMP signal gradients (Le Dreau and Marti, 2012). Whereas FGF, Wnt, and RA signalling mediate the embryonal anterior-posterior patterning of neuroectoderm (Kudoh *et al.,* 2002; Lara-Ramírez *et al.,* 2013).

FGF signalling represses differentiation and act as functional antagonist of RA signalling. The transition from FGF to RA signalling during axis elongation is mediated by canonical Wnt signalling (Olivera-Martinez and Storey, 2007). Specification during development is dependent on a caudal to rostral Wnt/FGF gradient and an opposing RA gradient (Aulehla and Pourquie, 2010; Diez del Corral *et al.,* 2003). Within the telencephalon RA acts in combination with SHH to constitute ventral identities and with Wnt/FGF signalling to generate a dorsal pattern (Marklund *et al.,* 2004). Mouse and human ESC, exposed to RA and SHH at specific timepoints, generate i*n vitro* motor neurons at high efficiency (Wichterle *et al.,* 2002). Exposure of RA to different cell sources (*in vivo* or *in vitro*) show sometimes diverse or opposite effects depending on the concentration, stage, or duration of exposure (Rhinn and Dollé, 2012). This effect and the complex network of RA signalling and interaction with other signalling pathways, partially limited on distinct areas and timepoints, impede studies of common regulatory networks and left many unsolved questions behind. Duester (2017) even proposed that this field is currently in a reproducibility crisis for RA signalling because several previously observed functions for RA could not be proven by *in vivo* genetic loss-of-function studies

1.2.2 RA metabolism and signalling pathways

RA is a derivate of retinol (Vitamin A). Retinol, transferred in the blood stream, is bound to transthyretin (TTR) and a retinol binding protein (RBP) (Fex *et al.,* 1979; Yamauchi and Ishihara, 2009). For the cellular uptake of retinol, the RBP binds to the transmembrane receptor STRA6 (Kawaguchi *et al.,*2007; D'Ambrosio *et al.,* 2011). RA synthesised by adjacent cells acts non cell autonomously and diffuses through cell membranes (Roberts, 2020). In the cytoplasm, retinol is reversibly oxidised to retinal (retinaldehyde) by either alcohol or retinol dehydrogenases (ADH/RDH). Retinal is further irreversibly oxidised by retinaldehyde dehydrogenases (RALDH) to all-trans RA (Duester, 1996). Both oxidation steps are NAD-dependent and catalysed by several enzymes that control the endogenous RA level (Lara-Ramírez *et al.,* 2013). Regulation also occurs through degradation by enzymes of the cytochrome p450 subfamily 26 (CYP26), able to oxidize RA to various inactive metabolites (White *et al.,* 1997; Niederreither *et al.,* 2002). Rapid RA degradation results in a short half-life of about one hour (Pennimpede *et al.,* 2010). During gastrulation, the expression of CYP26A1 is controlled by complex feedback and feedforward loops, involving the RA and FGF signalling pathways (Abu-Abed *et al.,* 2001; White *et al.,* 2007). Along dorsoventral axis, patterning of the neural tube is primarily controlled by Sonic Hedgehog (Shh), Wnt and BMP signal gradients (Le Dreau and Marti, 2012). Whereas FGF, Wnt and RA signalling act as the main posteriorizing signals that regulate cell specification of neuroectoderm (Lara-Ramírez *et al.,* 2013). CYP26 has an important role to regulate the FGF, Wnt, and RA signals to mediate the embryonal anterior-posterior patterning of the neural ectoderm (Kudoh *et al.,* 2002).

Additionally, the RA level presumably depends on the activity of carrier proteins like cellular retinol binding proteins (CRBPs) and cellular retinoic acid binding proteins (CRABPs) that ensure the solubility of the hydrophobic retinoids in the cytosol. CRBPs can bind retinol as well as RA and is assumed to prevent oxidation (Lara-Ramírez *et al.,* 2013; Rhinn and Dollé, 2012). CRAPBs regulate signalling by delivering RA either into the

nucleus or to CYP26 enzymes for degradation (Cai *et al.*, 2012). In the nucleus, RA binds to heterodimers build of the retinoic acid receptor (RAR) and the retinoid X receptor (RXR) (Mark *et al.,* 2009). These heterodimers bind in conserved regulatory regions of RA target genes, called retinoic acid response elements (RAREs) (Chambon, 1996). Over 14,000 RAREs are identified in the human genome while assignment to distinct developmental processes is still largely receivable (Lalevée *et al.,* 2011; Moutier *et al.,* 2012). Binding of the RA to the ligand-dependent transcription factors results in release of co-repressors, recruitment of transcriptional co-activators, and finally in initiation of transcription (Germain *et al.,* 2002; Rhinn and Dollé, 2012).

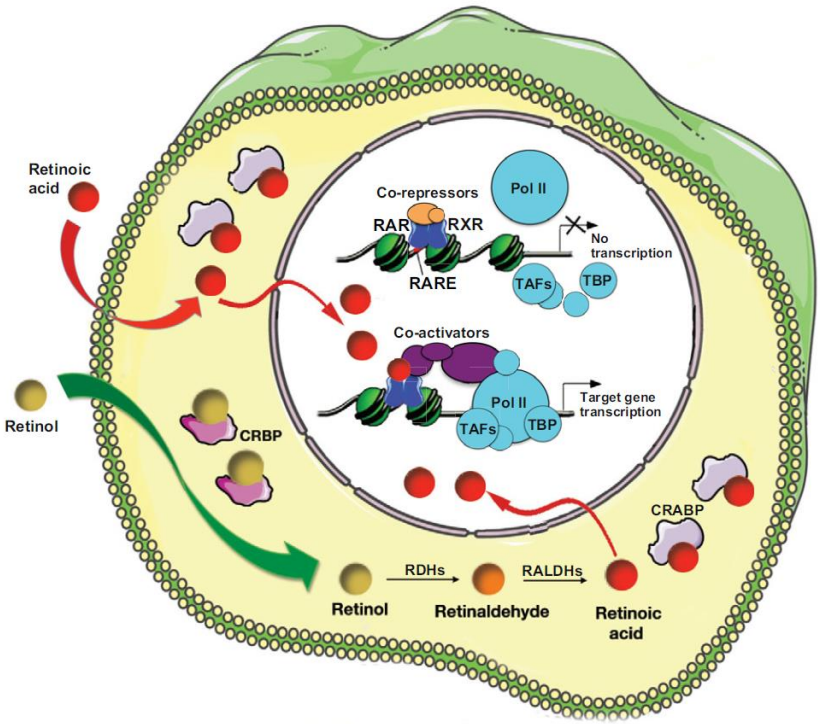

Figure 7: The classical RA signalling pathway. The canonical RA signalling pathway is characterised by retinol (or RA) uptake, RA synthesis, transfer to the nucleus and transcription initiation. (Adapted from Rhinn and Dollé, 2012)

RA induces the expression of numerous pro-neural factors like transcription factors, structural proteins, neurotransmitters, neuropeptide hormones, growth factors, neuro-specific enzymes and cell surface receptors and arrest cells in the G1-phase of cell cycle (Maden and Hind, 2003; Melino *et al.,* 1997). The classical retinoic acid signalling pathways was described above. Besides this pathway, certain non-canonical retinoic acid signalling pathways were recently discovered that are less well understood so far (Wei, 2013). It was shown that RARs can be localized in the membrane of dendrites, where RA activation mediates translation (Chen and Napoli, 2008; Poon and Chen, 2008). Besides this, a non-canonical, cytoplasmic, but RAR independent way was revealed. RA activates extracellular signal-regulated kinase 1/2 (ERK1/2) (Gupta *et al.,* 2008; Persaud *et al.,* 2013). CRABP1 was reported to be involved in this mechanism (Persaud *et al.,* 2013). The non-canonical pathway proved to be a rapid mechanism that like the canonical pathway results in the disrupting pluripotency and proliferation by for

instance Oct4 repression and blocking cell cycle G1 to S phase transition (Gupta *et al.,* 2008; Orford and Scadden, 2008; Wei, 2013). RA mediated, phosphorylation-based activation of ERK1/2 was shown to be essential for survival of ESCs and early neural differentiation (Li *et al.,* 2006). Future studies are needed to identify transcriptional mechanisms and spatiotemporal regulation of key genes by RA signalling and to fully discover and understand the non-canonical and RAR dependent pathways (Ghyselinck and Duester, 2019; Wei, 2013).

1.2.3 Retinoic acid receptors and their downstream effectors

Retinoic acid receptors (RARs) are members of the nuclear receptor superfamily that regulates transcription in a ligand dependent manner. Three subtypes have been described in mammals, referred as RARα, RARβ, and RARγ (Roberts, 2020). These receptors bind to one of the three subtypes of the retinoid X receptor, RXRα, RXRβ, and RXRγ, building heterodimers (Kastner *et al.,* 1997). Furthermore, RAR as well as the RXR subtypes contain several isoforms such as the well-studied RARβ2 or recently discovered forms like RARα1ΔB (Parrado *et al.,* 2001; Zelent *et al.,* 1991; Kastner *et al.,* 1990). The activity of RAR-RXR heterodimers is dependent on RA binding (Mic *et al.,* 2003). RARs are conserved in vertebrates and primarily bind all-trans-RA, while 9-cis-RA binds to RXRs (Rhinn and Dollé, 2012). But 9-cis-RA could not be detected endogenously in embryos or adult tissues (Mic *et al.,* 2003). This led to the assumption that RXRs act mainly as scaffolding proteins to facilitate binding of RAR-RXR heterodimers to DNA (Chawla *et al.,* 2001). Involvement of RARα in the neuronal differentiation process, was studied in the P19 mutant RAC65 that was supposed to be RA-resistant, provoked by a truncated RARα (Jones-Villeneuve *et al.,* 1982; Pratt *et al.,* 1990). Binding of RA to RARα was shown to be inhibited in this mutant, while the DNA binding site is still intact (Pratt *et al.,* 1990). Consequently, activation of the transcription factor by binding of RA is repressed and the truncated RARα acts as a dominant repressor (Bain *et al.,* 1994). The RAC65 mutant revealed to be incapable to differentiate in response to RA treatment and keeps the undifferentiated phenotype (Jones-Villeneuve *et al.,* 1982). This fact strongly suggested that RARα is crucial for RA-induced neuronal differentiation. Nevertheless, it was discovered that the expression of the truncated RARα in normal P19 cells is not capable to block the RA responsiveness completely (Pratt *et al.,* 1990). The discrepancy could be explained by the identification of additional mutations in RAC65 (Pratt *et al.,* 1990).

The retinoid receptors RARα, RXRα and RXRβ revealed widespread expression patterns, while the RARβ, RARγ and RXRγ show a complex, tissue-specific expression (Dollé, 2009). For instance, RARα and RARγ are expressed in the neural plate and neural tube during neurula stage to regulate primary neurogenesis (Janesick *et al.,* 2013). The RAR and RXR subtypes can build different heterodimer combinations that transduce the RA signal in various tissues, revealing a high degree of functional redundancy (Roberts, 2020). Accordingly, except for RXRα, usually at least two receptors must be inactivated in concert to observe developmental defects in mice (Mark *et al.,* 2009). Several studies suggest that depletion of one RAR subtype results in the upregulated expression of the other RARs (Koide *et al.,* 2001; Mark *et al.* 1999; Taneja *et al.,* 1995). Therefore, it was

assumed that the redundancy of the receptors enables a functional substitution. No response to RA on the transcriptional level was observed after a simultaneous knockout of all RAR subtypes, revealing their crucial function in RA induced neuronal differentiation (Laursen and Gudas, 2018). Analysis of the RAR pattern in P19 cells showed that low levels of RARα and RARγ mRNA are expressed and no RARβ mRNA is present in undifferentiated state (Jonk *et al.,* 1992). While RA induced neuronal differentiation in P19 cell aggregates resulted in a rapid increase of RARα and RARβ mRNA, RARγ appeared to be strongly repressed (Bain *et al.,* 1994; Jonk *et al.,* 1992). In contrast, culturing cells in monolayers lead to a higher maximal RARα level, while the RARγ mRNA remains constant (Bain *et al.,* 1994). In P19 cells, the RARβ transcript was strongly expressed during RA induced neuronal differentiation as well as by DMSO induced mesoderm and muscle differentiation, resulting in an increased sensitivity to RA (Pratt *et al.,* 2000; Pozzi *et al.,* 2006). This indicates that besides activation through a consensus RA-response element in the RARβ promoter, RA-independent induction of RARβ2 expression is possible (Pratt *et al.,* 2000).

While the mechanism of RA-induced initiation of transcription is well understood, RA mediated repression of pluripotency genes such as Nanog, Oct4, and Klf4 remains largely elusive (Kashyap *et al.,* 2013; Laursen *et al.,* 2012). The possibility of ligand-dependent transcriptional corepressors recruitment was not excluded (White *et al.,* 2004). But it is suggested that the repression can be indirectly regulated because RARs showed no association to regulatory elements of these stem cell markers (Laursen and Gudas, 2018; Mendoza-Parra *et al.,* 2011). Thus, this could be probably implemented by activation of a nongenomic signalling cascade that is independent of the direct transcriptional regulation by RA (Rochette-Egly and Germain 2009). Contradictory observations regarding RAR involvement in gene repression cause the mechanism to remain controversial (Laursen and Gudas, 2018). Anyway, most of the direct target genes are upregulated through RA binding to the heterodimer complex. Despite the identification of thousands of genes characterised by a RARE sequence in the promotor region, direct targets of RA that are definitively involved in the switch to neuronal differentiation have been barely identified yet (Lalevée *et al.,* 2011; Janesick *et al.,* 2015). For instance, RAREs are located in the regulatory regions of many Hox genes (Deschamps and van Nes, 2005; Maconochie *et al.,* 1996). During neuronal differentiation, induced by RA treatment, several Hox genes such as Hoxa1 and Hoxb1 have been found to be strongly upregulated, crucial for differentiation of ESC or neuronal progenitors to neurons (Gouti and Gavalas, 2008; Martinez-Ceballos and Gudas, 2008; Shahhoseini *et al.,* 2013). Furthermore, pro-neural genes like Ascl1 (Mash1) and Numb that are involved in the Notch pathway, are identified as direct downstream effectors of RA (Janesick *et al.,* 2015). Ascl1 was reported to regulate proliferation and differentiation in a spatiotemporally restricted manner (Castro *et al.,* 2011). Numb can promote proliferation or differentiation, depending on which isoform is expressed (Verdi *et al.,* 1999).

Additionally, it is known that RA directly and indirectly regulates the expression of several genes that regulate the cell cycle exit to facilitate neuronal differentiation

(Janesick *et al.,* 2015). The pro-neural and neurogenic transcription factors that control the exit of neural progenitors from cell cycle were partially discovered. RA was shown to increase expression of cyclin-dependent kinase (CDK) inhibitors that promote cell cycle exit of G1 phase cells (Galderisi *et al.,* 2003; Herrup and Yang, 2007). Furthermore, it was demonstrated that activation of the PI3K/AKT pathway is required for RA induced differentiation of neuroblastoma cells (Lopez-Carballo *et al.,* 2002). This finding was recently complemented by the observation that RA induced neuronal differentiation of F9 cells follows a biphasic regulation of the PI3K/AKT pathway, with an early activation followed by an inhibition (Bastien *et al.,* 2006). The activation of the PI3K/AKT pathway found to be dependent on RARγ/RXRα heterodimers, while the followed inhibition is less well understood (Bastien *et al.,* 2006). The RA signalling system is highly complex. To completely discover the involvement of nuclear receptors and their downstream effectors in the process of neuronal differentiation, much effort must be spent in future.

1.2.4 Signalling pathways involved in neuronal induction

Multiple signalling pathways and effectors are involved in neuronal cell fate decision, partially regulating each other in a complex interplay. It is suggested that RA could mediate the crosstalk of diverse signalling pathways such as the Wnt/β-catenin, FGF, and the ERK pathways, to induce neural differentiation (Chuang *et al.,* 2015). As already mentioned above, the patterning of neuroectoderm during embryogenesis is mainly controlled by Shh, Wnt, BMP, FGF, and RA gradients (Kudoh *et al.,* 2002; Lara-Ramírez *et al.,* 2013; Le Dreau and Marti, 2012). The Hedgehog (Hh) signalling pathway was shown to mediate regulators of cell cycle in neural progenitors during spinal cord development (Cayuso *et al.,* 2006). In ESC, it was revealed to be crucial to generate neuronal and glial progenitors and especially to differentiate into V3 interneurons (Maye *et al.,* 2004). Simultaneous activation of the Shh pathway and inhibition of the Notch pathway induce neural differentiation during neural tube development *in vivo*, while the absence of Shh is associated with an increased number of interneurons (Cardozo *et al.,* 2017). The Notch signalling pathway was shown to promotes glial differentiation while it supresses neuronal differentiation (Artavanis-Tsakonas *et al.,* 1999; Lutolf *et al.,* 2002). Several evidences indicate that Notch is downstream of BMP signalling (Beck *et al.,* 2003). The BMP signalling pathway is critical for CNS development as well (Hegarty *et al.,* 2013). During gastrulation, neuronal induction is promoted by inhibition of BMP signalling, while it revealed to be essential in a later stage to generate mature neurons as well as for synapse formation and gliogenesis (Le Dreau and Marti, 2013). Therefore, dual SMAD inhibition proved to be sufficient to induce neuronal differentiation in ESCs (Chambers *et al.,* 2009). Canonical Wnt/β-catenin signalling, is required for maintenance and proliferation of neuronal progenitors in the spinal cord (Zechner *et al.,* 2003). It is involved in neuronal differentiation by control of cell cycle (Niehrs and Acebron). RA induced neurogenesis of ESC was shown to be promoted by inhibition of the canonical Wnt pathway through e.g. Dickkopf-related protein 1 (Dkk-1) overexpression (Verani *et al.,* 2007).

FGF signalling pathway was shown to play diverse roles during different stages of neuronal differentiation of ESCs (Kunath *et al.,* 2007). Some evidence indicate that FGF

has a key role in early neural differentiation (Stern, 2005). Several FGF family members have been shown to enhance the neurogenesis of mESCs (Chen *et al.,* 2010). Depending on the ligand concentration, FGF promotes proliferation and survival of neuroepithelial cells and differentiation into mature neurons and glia cells, *in vitro* (Qian *et al.,* 1997). For instance, FGF4 regulates neural progenitor cell proliferation and neuronal differentiation by activation of ERK1/2 that leads to the release of ESC from the self-renewal program (Kosaka *et al.,* 2006; Kunath *et al.,* 2007). The ERK1/2 signalling pathway already demonstrated to promote neuronal differentiation in murine ESCs (Li *et al.,* 2006). During embryogenesis, RA and FGF represent opposing signals, promoting either neuronal differentiation by RA signalling or proliferation by FGF signalling (Lara-Ramírez *et al.,* 2013). Dependency on FGF signalling to induce neuronal differentiation is still highly controversial (Cohen *et al.,* 2010; Dorey and Amaya, 2010). Several of the pathways and effectors, involved in neuronal fate decision, have already been discovered. But spatial and temporal coordination and regulation of signalling pathways involved in neurogenesis, cell fate decision and other complex mechanism are still far from being completely understood. Multitude *in vitro* and *in vivo* studies attempt to clarify this complex interaction network.

1.2.5 Redox signalling in neuronal development

Homeostasis of reactive oxygen species (ROS), generated during cell metabolism at several cellular compartments, revealed to be critical for cell survival and function (Freeman and Crapo, 1982; Monticone *et al.,* 2014). High cellular ROS level can cause damages in the DNA, proteins, and lipids, leading to cellular dysfunction and apoptosis (Trachootham *et al.,* 2008). Nevertheless, ROS are involved in cell signalling and act as second messenger, involved in regulation of several cellular processes like e.g. proliferation and cell survival (Bae *et al.,* 2009). A physiological ROS level is required to maintain the self-renewal in stem cells (Le Belle *et al.,* 2011; Kobayashi and Suda, 2012; Pérez Estrada *et al.,* 2014). The cellular redox homeostasis is provided by the balance between ROS production and destruction (Hu *et al.,* 2017). A strong decrease of intracellular ROS was reported to impair proliferation or survival of several cell types, while the same effect is also observed from a strongly increased ROS level by affecting cell cycle checkpoint functions mediated by DNA damage response (Martin *et al.,* 2007; Monticone *et al.,* 2014; Shackelford *et al.,* 2000). To prevent intracellular damages caused by cellular oxidative stress, detoxification is implemented by several antioxidants (Halliwell, 1996). Cellular protection against oxidative stress is controlled enzymatically by for example superoxide dismutase, catalase, glutathione peroxidase, and glutathione reductase, or non-enzymatically by e.g. vitamin A, C, and E (Velusamy *et al.,* 2017). The KEAP1 (Kelch-like ECH-associated protein 1)/ nuclear factor erythroid 2–related factor 2 (NRF2) complex functions as a key sensor of oxidative stress (Hu *et al.,* 2017). NRF2 is a transcription factor that controls expression of several antioxidant and detoxifying genes and stimulates the PI3K/AKT survival signalling pathway (Ma, 2013; Surh *et al.,* 2009). NRF2 is targeted for ubiquitin-mediated degradation by its inhibitor KEAP1 in the cytoplasm. In response to oxidative stress, KEAP1 becomes inactivated and NRF2 accumulates and is translocated to the nucleus, activating the expression of genes,

containing an antioxidant response element (ARE) in their promoter sequence (Element, 2004; Itoh *et al.,* 1999; Liu *et al.,* 2007). NRF2-ARE signalling pathway is also reported to be regulated by a direct interaction of RXRα with the Neh7 domain of NRF2 (Wang *et al.,* 2013).

p62 functions as cargo receptor for autophagic degradation of ubiquitinated targets and is upregulated ins response to oxidative stress (Mathew *et al.,* 2009; Zaffagnini and Martens, 2016). The promotor of p62 contains an ARE and therefore, the expression of p62 is also induce by NRF2 (Jain *et al.,* 2010). p62 itself stimulates the NRF2 activity by binding to the NRF2 inhibitor KEAP1, resulting in an autophagic degradation of the repressor, creating a feedback-loop in the KEAP1/NRF2-pathway (Jain *et al.,* 2010). Direct reprogramming of fibroblasts into target cells like neurons as well as the reprogramming to iPSC and finally to target cells, is known to result in oxidative stress and is therefore supported by antioxidants (Suzuki and Shults, 2019). Oxidative stress, induced through paraquat or by Nrf2 knockdown was reported to promote exit from the stem cell state and spontaneous neuronal differentiation of hESC (Hu *et al.,* 2017). The expression of stemness marker genes, including Nanog and Oct4 are supressed while expression of neuronal differentiation marker, like Pax6 and NeuroD1, for example, is enhanced.

Moreover, it is known that excessive oxidative stress can lead to synapse overgrowth (Milton *et al.,* 2011). On the other hand, forced Nrf2 expression revealed to retard early neuronal development (Bell *et al.,* 2015). Recently, a steady decrease of Nrf2 expression during the neuronal differentiation process was reported (Olguín-Albuerne and Morán, 2018). Suppression of this pathway is thought to provides a more flexible redox environment, which is critical for redox-sensitive signalling pathways that mediate early neuronal development (Bell *et al.,* 2015). The MAPK-ERK1/2 signalling pathway is suspected to be involved in induction of neuronal differentiation by oxidative stress (Hu *et al.,* 2017). Wnt signalling and several pathways, important for dendritic and synaptic development, proved to be enhanced by mild ROS exposure (Budnik *et al.,* 2011; Rharass *et al.,* 2014; Rosso *et al.,* 2005). Even mature neurons exhibit a weakened antioxidant defence in contrast to glial cells, whereas neurons generate more ROS than most cell types because of a high metabolic activity (Oswald *et al.,* 2018). The weak intrinsic antioxidant defence of neurons is caused by an inactivation of the NRF2 pathway by epigenetic repression of the Nrf2 gene promoter early in development (Bell *et al.,* 2015). The protection of neurons by oxidative stress is mediated by glial cells in a non-autonomous manner (Dringen *et al.,* 1999; Oswald *et al.,* 2018). Forebrain neurons, for instance, were reported to receive antioxidant support from surrounding astrocytes by glutathione release (Shih *et al.,* 2003). Recently, neuronal activity was shown to increase NRF2 protein accumulation in astrocytes (Habas *et al.,* 2013). By identification of additional NRF2 target genes, involvement in the regulation of processes like inflammation, autophagy, and proteostasis was discovered (He *et al.,* 2020). The NRF2 pathway is still not fully understood and thus it remains possible that NRF2 may control the expression of genes that directly affect neuronal differentiation (Bell *et al.,* 2015). Because tumour cells (unlike cancer stem cells) and neurons with distinct

dysfunctionalities present high ROS level, the understanding of the regulation of NRF2 is of interest (Bittinger *et al.,* 1998; Monticone *et al.,* 2014).

1.3 Cell death in neurons and during neurogenesis

1.3.1. Forms of neuronal cell death

Programmed cell death is a highly regulated mechanism that is required to maintain tissues, organ size, and function. Therefore, removal of excessive neurons in development of the nervous system is a crucial process (Fricker *et al.,* 2018). While postmitotic neurons are characterized by a long lifespan, both, mature postmitotic and mitotic neuronal precursor die during development (Buss *et al.,* 2006; Kuan *et al.,* 2000; Sadoul, 1998). It was reported that half of the produced neurons are degraded by neuronal death through development of the nervous system (Oppenheim, 1991). This is not due to a major cell death event, but rather restricted to distinct sites and developmental stages (Kuan *et al.,* 2000). Neuronal death can be regulated cell autonomously or by interactions with neighbouring cells or extrinsic influences (Fricker *et al.,* 2018). As with other cell types, neurons undergo various forms of cell death. Currently, several forms of cell death are distinguished, although definition is not always clear and uniform, and other forms of programmed cell death may yet be discovered (Elmore, 2007; Sperandio *et al.,* 2007). The so far known cell death mechanisms include a highly diverse range of phenotypes and molecular mechanisms. The main forms are necrosis, apoptosis, or autophagy mediated cell death. Crosstalk and overlap occur between the different mechanisms, between some forms of cell death and with other cellular processes, complicating the study of the regulation and interplay of these forms in neuronal development (Kuan *et al.,* 2000). Dysfunctional neuronal cell death regulation is one of the principal causes of acute and chronic neurodegenerative disease (Fricker *et al.,* 2018). Therefore, investigations of mechanisms to control and regulation neuronal cell death are of great interest.

1.3.2 Necrosis

Necrosis initially involved the rupture of the plasma membrane and release of intracellular contents triggering an inflammatory response (Kerr *et al.,* 1972). But this is the fatal result for almost all forms of cell death, including apoptosis in pure cell cultures and *in vivo* when cells fail to be cleared by phagocytosis. Nowadays, unregulated and various forms of programmed (genetically controlled) necrosis are discovered (Fricker *et al.,* 2018). Necrosis is characterised as pro-inflammatory process because loss of cell membrane integrity results in the release of cytoplasmic contents and causes damage of the surrounding tissue (Edinger and Thompson, 2004). Cells respond from a sudden shock and usually start to swell and rupture (D'Arcy, 2019). Major morphological changes observed for necrotic cells are swelling of mitochondria, ER, lysosomes, and finally the whole cell as well as the formation of cytoplasmic vacuoles and cytoplasmic blebs, disaggregation and detachment of ribosomes and the disruption of organelle membranes and eventually of the cell membrane (Kerr *et al.,* 1972; Trump *et al.,* 1997). The regulated necrosis is subdivided in different forms like necroptosis, parthanatos, ferroptosis, pyroptosis, autolysis, and mitochondrial permeability transition (Fricker *et*

al., 2018). In contrast to apoptosis and autophagy, necrosis is an energy independent mechanism. It is defined as passive process that usually affects large fields of cells whereas apoptosis can affect individual or clusters of cells. Although the mechanisms and morphologies of apoptosis and necrosis differ, there is an overlap between these two processes (Elmore, 2007). Evidence indicates that necrosis and apoptosis represent a shared biochemical network described as the "apoptosis-necrosis continuum" (Zeiss, 2003). Whether a cell dies by necrosis or apoptosis depends in part on the nature of cell death signal, tissue type, developmental stage of the tissue, and the physiologic milieu (Fricker *et al.,* 2018; Zeiss, 2003). Neuronal necrosis widely happens in devastating neurodegenerative diseases, such as brain injury, stroke, and Alzheimer's disease (Liu *et al.,* 2015).

1.3.3 Apoptotic cell death

Apoptosis is a highly conserved and regulated mechanism within multi-cellular organisms (Lockshin and Zakeri, 2004). It is an essential process to remove defective or aberrant cells. Apoptotic cell death is triggered, for instance, by a lack of pro-survival signals such as growth factors, hormones, or cytokines and, on the other hand, by harmful factors such as ROS, toxins, or radiation (Brenner and Mak, 2009). It was reported that oxidative stress plays a primary role in the pathophysiology of age-induced apoptosis (Ozawa, 1995). Induction of this programmed cell death is dependent on the activation of a series of caspases (D'Arcy, 2019). Caspases activation initiates a cascade of events that results in chromatin condensation, destruction of nuclear proteins and cytoskeleton, crosslinking of proteins, expression of ligands for phagocytic cells, and formation of apoptotic bodies (Martinvalet *et al.,* 2005; Poon *et al.,* 2014). Apoptotic bodies contain the intracellular content and can be quickly phagocytosed by adjacent cells or macrophages (Elmore, 2007). Because apoptotic cells do not release their cellular constituents into the surrounding tissue and apoptotic bodies are quickly removed, apoptosis is principally not causing an inflammatory reaction (Kurosaka *et al.,* 2003). Therefore, secondary necrosis is prevented even if engulfing cells do not produce anti-inflammatory cytokines (Savill and Fadok, 2000). Morphological changes are characterised by cell shrinking during early apoptosis resulting in smaller cell size with dense cytoplasm (appears dark) and tightly packed organelles (Hacker, 2000; Kerr *et al.,* 1972). This process is followed by chromatin condensation, karyorrhexis and the formation of apoptotic bodies, including cell fragments such as cytoplasm and tightly packed organelles (Elmore, 2007). Activation of the caspase cascade that results in apoptotic cell death can be initiated by an intrinsic or extrinsic pathway (D'Arcy, 2019). The intrinsic pathway is induced when intracellular sensors detect cell damage, while the extrinsic pathway is stimulated by an interaction of the damaged cell with an immune cell (Sica *et al.,* 1990; Oppenheim *et al.,* 2001). Because it depends on factors released from mitochondria, the intrinsic pathway is also called the mitochondrial pathway.

Several stressors activate stimulus-specific signalling events such as reduced protein kinase B/AKT signalling, activation of c-Jun N-terminal kinase (JNK) by trophic factor deprivation, or activation of p53 with DNA damage (Hollville *et al.,* 2019; Schuler and

Green, 2001). These stressors-induced signalling events activate pro-apoptotic Bcl-2 family proteins. Bcl-2 family proteins can be either anti-apoptotic such as MCL-1, BCL-2, BCL-w or pro-apoptotic e.g., BAX, BAK, BIM (Fig. 8). Pro- and antiapoptotic Bcl-2 family proteins regulate the release of mitochondrial proteins by inducing or preventing permeabilization of the outer mitochondrial membrane (Cory and Adams, 2002). BH3-only proteins represent a subset of pro-apoptotic members of the Bcl-2 family that activate pro-apoptotic Bcl-2 family proteins and inactivate anti-apoptotic Bcl-2 family proteins (Hollville *et al.,* 2019). Anti-apoptotic Bcl-2 proteins inhibit apoptosis either by direct binding to activated BAX and BAK or by binding and sequestering BH3-only proteins (Chipuk *et al.,* 2010; Happo *et al.,* 2012; Shamas-Din *et al.,* 2011). When the pro-apoptotic factors BAX and BAK are activated, oligomers are built that insert in the mitochondrial outer membrane, creating pores that result in mitochondrial outer membrane permeabilization (MOMP) (Hollville *et al.,* 2019). MOMP causes a release of pro-apoptotic factors such as cytochrome c, from the mitochondrial intermembrane space into the cytosol (Saelens *et al.,* 2004). Cytosolic binding of cytochrome c to the apoptotic protease-activating factor 1 (APAF-1) leads to the formation of an apoptosome which in turn activates the initiator caspase-9 (CASP9) and consequently the caspase cascade (Cory and Adams, 2002). Altogether, cellular apoptotic stimuli result in the activation of BH3-family proteins and finally in the release of mitochondrial proteins that initiate the caspase cascade, causing the apoptotic death of the cell (Taylor *et al.,* 2008). The extrinsic pathway is described as death receptor pathway. Death receptors are members of the tumour necrosis factor (TNF) receptor gene superfamily (Locksley *et al.,* 2001). Natural killer cells or macrophages that produce the corresponding death ligand bind to the extracellular domain of the death receptor and induce the extrinsic pathway by activation of the caspase cascade (Kim *et al.,* 2004).

1.3.4 Apoptosis in neuronal development

The development of the nervous system is defined by an overproduction of cells, followed by a period where neuronal progenitors and neurons are selectively eliminated by apoptosis (Nijhawan *et al.,* 2000; Opferman and Korsmeyer, 2003). To ensure long-term survival of post-mitotic neurons in the mature nervous system, the threshold required to induce apoptosis is increased during neuronal differentiation and maturation (Polster *et al.,* 2003). Mature post-mitotic neurons that are fully integrated in the neuronal network restrict the apoptosis pathway (Kole *et al.,* 2013). Control and regulation of apoptosis during development, maintenance and aging of the nervous system is highly critical. Abnormal levels of apoptosis can have tremendous effects on health of a multicellular organism. It can cause neurodegenerative diseases such as Alzheimer's or Parkinson's disease (Dickson, 2004; Tatton *et al.,* 2003) as well as uncontrolled growth and division of cells that is observed in cancer (King and Cidlowski, 1998). Regarding the regulation of the apoptotic signalling pathway, neurons show some specific features. The apoptotic pathway becomes increasingly restricted during neuronal differentiation and maturation (Kole *et al.,* 2013). Multiple mechanisms at the transcriptional and posttranscriptional level repress the expression of BH3-only genes in

neurons, while the level of anti-apoptotic proteins increases in neuronal development (Fig. 8).

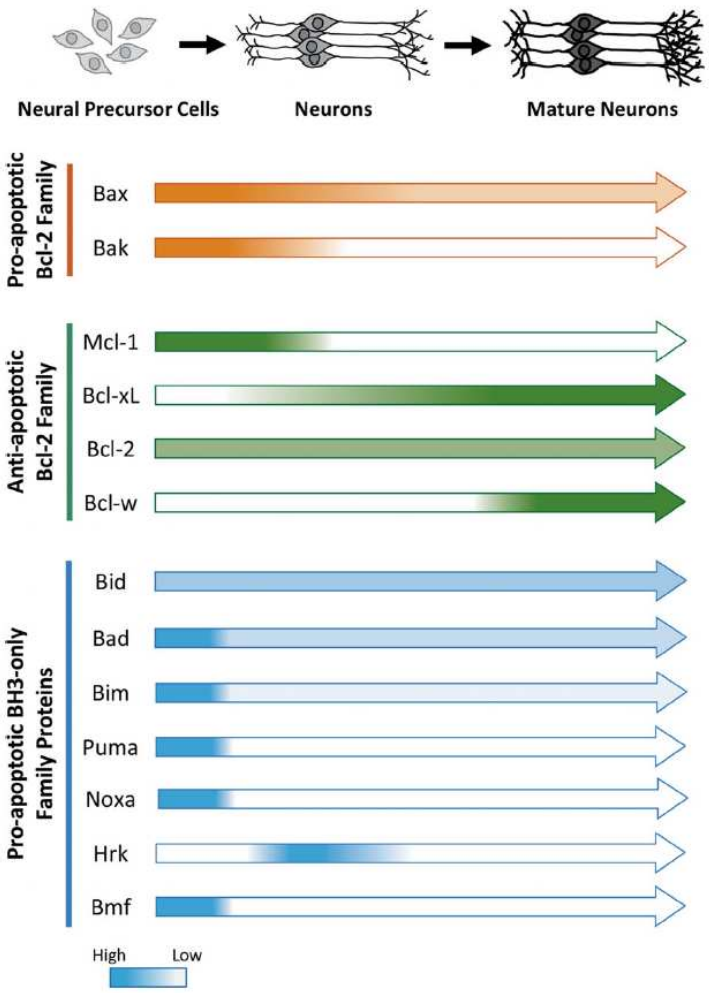

Figure 8: Regulation of neuronal Bcl-2 family proteins during neuronal differentiation. Expression of pro- and anti-apoptotic proteins is regulated from neuronal precursor cells to mature neuron to provide a tight regulation of neuronal cell death and ensure survival of postmitotic neurons. (Adapted from Hollville *et al.,* 2019)

The level of the pro-apoptotic Bcl-2 family protein BAX decrease in the brain postnatally but is maintained at low levels (Krajewska *et al.,* 2002; Vekrellis *et al.,* 1997). While neuronal progenitor cells still express BAK, post-mitotic neurons only express an alternatively spliced form of BAK (N-BAK) (Deckwerth *et al.,* 1996). A pro-apoptotic or neuroprotective function of this form is still controversial (Fannjiang *et al.,* 2003; Sun *et al.,* 2001; Uo *et al.,* 2005). However, this likely provides neurons with the ability to tightly control apoptosis without BAK, solely through the regulation of BAX. Many pro-apoptotic BH3-only genes, that control the initiation of apoptosis, are expressed in the embryonic brain while their expression is significantly reduced in neurons of the postnatal brain (Krajewska *et al.,* 2002, Shimohama *et al.,* 1998). At the same time, the levels of the anti-apoptotic factors BCL-xL and BCL-w increase during development to post-mitotic neurons, while BCL-2 is constantly expressed throughout the developing

and mature brain (Fogarty *et al.,* 2019; Merry *et al.,* 1994). MCL-1, on the other hand, is responsible for neuronal survival at an early stage of development (Fogarty *et al.,* 2019).

The PI3K/AKT and the MEK/ERK survival pathway are reported to be involved in the restriction of the apoptotic pathway in neurons (Hollville *et al.,* 2019). A pro-apoptotic c-Jun N-terminal kinases (JNK) pathway was discovered, that is strictly limited to neurons and play an essential role in activating the intrinsic apoptosis pathway (Ghosh *et al.,* 2011; Putcha *et al.,* 2003). JNK activation, causing neuronal cell death in response to a wide variety of stimuli, is tightly regulated in neurons (Hollville *et al.,* 2019). Activated JNK promotes neuronal death by phosphorylation or transcriptional activation of several pro-apoptotic BH3-only family proteins (Harris and Johnson, 2001). The AKT-pathway has an anti-apoptotic function and represses the JNK pathway, inactivates the BH3-only protein BAD and is preventing transcriptional upregulation of the BH3-only proteins BIM and PUMA (Kamada *et al.,* 2007; Sanphui and Biswas, 2013; Wang *et al.,* 2007). Neuronal AKT activation is mediated by PI3K signalling and activated by pro-survival signals. Active suppression of AKT pro-survival signalling, is required for apoptosis in response to neurotoxic stimuli (Saleem and Biswas, 2017). Whereas the pro-survival MEK/ERK signalling pathway promotes the proteasomal degradation of BIM and downregulate BAD expression in the maturing and adult brain (Biswas and Greene, 2002; Finegan *et al.,* 2009; Ordonez *et al.,* 2010). The level of APAF-1, the main scaffold protein of the apoptosome complex, decreases during neuronal differentiation until expression is completely shut down in mature neurons (Wright *et al.,* 2007; Yakovlev *et al.,* 2001). Also, expression of several caspase genes, including effector caspase-7 and caspase-3 (CASP7 and CASP3) are downregulated in neurons (Kumar *et al.,* 1992). Besides involvement in apoptosis, CASP3 demonstrates non-apoptotic functions during early neuronal development as regulatory molecule in neurogenesis and synaptic activity, facilitating neurogenesis of neuronal progenitors (D'Amelio *et al.,* 2010). Altogether, mature neurons become extremely resistant to triggers of apoptotic cell death (Putcha *et al.,* 2000). But in the context of injury and disease, apoptotic cell death becomes facilitated by, for example re-expression of APAF-1 or CASP3 (de Bilbao *et al.,* 1999; Fortin *et al.,* 2001). Overall, the increased threshold for apoptosis in mature neurons is realised by restricting the apoptotic machinery through repression of sensors and effectors of the mitochondrial apoptotic pathway at several levels (Kole *et al.,* 2013).

1.3.5 Autophagy

Autophagy is the primary intracellular multistep catabolic mechanism for degrading and recycling long-lived proteins and organelles and occurs as cellular response to stress conditions such as nutrient starvation, damaged organelles, or accumulation of protein aggregates (Levine and Klionsky, 2004). After substrate degradation, free amino acids, fatty acids, and adenosine triphosphate (ATP) are recycled back for biomolecule synthesis. Autophagy is described as conserved process that is involved in cellular homeostasis and is required to maintain cellular physiology under stressful conditions (Cooper, 2018). This mechanism is involved in several cellular processes like cell growth, survival, development, and death. Therefore, control and regulation of autophagy level is critical, as indicated by the fact that dysregulated autophagy has been linked to many

human pathophysiologies (Chen and Klionsky, 2011). Defective autophagy is associated with degeneration, premature aging, and cancer whereas increased autophagy contributes to longevity in several model organisms (Mizushima and Levine, 2010; Rubinsztein *et al.,* 2011). While this mechanism improves the cellular function, extends lifespan and avoids cell death, it also represents another mechanism for programmed cell death. Normally, this mechanism functions to prevent cell death, but excessive autophagy can cause cell death by "self-eating" (Fricker *et al.,* 2018).

Besides microautophagy and chaperone-mediated autophagy, macroautophagy is the main type of autophagy, hereafter referred to as autophagy. Initiation of autophagy is mediated by a variety of stressors, most notably nutrient deprivation as result of signals that occur during cellular differentiation and embryogenesis and on the surface of damaged organelles (Mizushima *et al.,* 2008). Autophagy is an evolutionarily conserved process of bulk degradation by sequestration of cytoplasmic components within a double membrane structure and subsequent delivery to lysosomes for degradation and recycling (Levine and Klionsky, 2004). Thereby, cellular components such as macroproteins or even whole organelles are sequestered into lysosomes for degradation (Shintani and Klionsky, 2004, Mizushima *et al.,* 2008). Subsequently, the digested substrate can be recycled and used for anabolic processes or as energy source (D'Arcy, 2019). Autophagy is controlled by a core group of about twenty conserved autophagy-related genes (Atg) (Klionsky *et al.*, 2003). Initiation starts with the activation of the ULK1 (unc-51-like kinase 1) complex (Fig. 9).

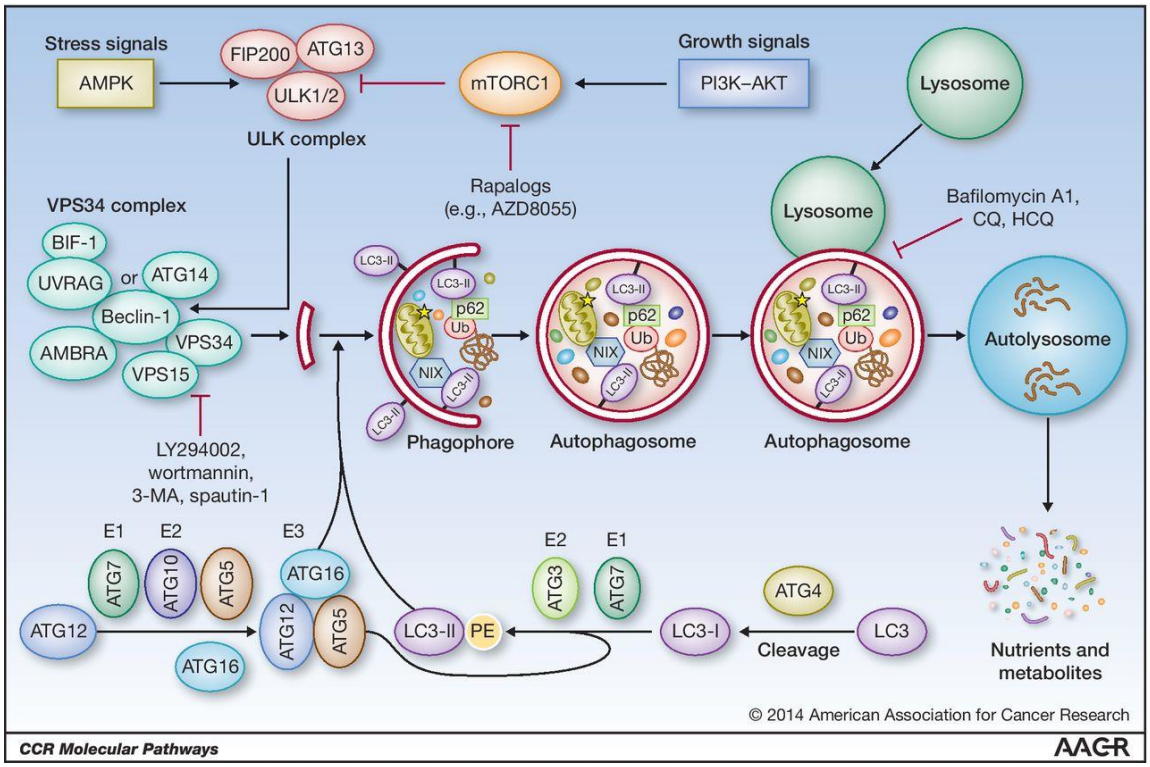

Figure 9: Overview of the autophagic process. Initiation, formation of the autophagosome, fusion with the lysosome, followed by digestion of the cargo and nutrition recycling, are covered by autophagy. This process is regulated by a variety of factors like about twenty ATG proteins, implemented in this process. (Adapted from Cicchini *et al.,* 2015)

This autophagy-specific complex is activated by cellular stress via the mechanistic target of rapamycin (mTOR) inhibition and/or AMP-activated protein kinase (AMPK) activation (Alers *et al.,* 2012). The kinase mTOR is found in two distinct protein complexes, named as mTORC1 and mTORC2, but only mTORC1 is assumed to directly regulate autophagy (Bar-Peled and Sabatini, 2014). mTORC2 is defined as rapamycin-insensitive complex, that is activated directly by AMPK (Jacinto *et al.,* 2004; Kazyken *et al.,* 2019). Recently, it was reported that AMPK, mTORC2, and AKT suppress apoptosis to promote cell survival during acute energetic stress (Kazyken *et al.,* 2019). In high-nutrient conditions, ATG13 and ULK1 are bound and phosphorylated by mTORC1, whereas starvation caused an activation of these factors by dephosphorylation and dissociation from the mTORC1 complex (Hosokawa *et al.,* 2009; Jung *et al.,* 2009). ULK1 activation promotes recruitment of a multiprotein complex that is required for initiation of phagophore formation (Itakura and Mizushima, 2010). Upon autophagy induction, an ULK1/2 complex is formed, consisting of ULK1 itself, ATG13, FIP200 (focal adhesion kinase family interacting protein of 200 kDa), and ATG101 (Zachari and Ganley, 2017). This complex is referred to as VPS34 and requires activity of the class-III phosphoinositide 3-kinase (PI3K) and is with VPS15, BECLIN1 (BECL1), and ATG14 for complex I, or UVRAG part of a large macromolecular complex (Itakura *et al.,* 2008). BECL1 acts as a regulator of autophagy since it is inhibited by the anti-apoptotic protein BCL-2, inactivated by AKT and EGFR (epidermal growth factor receptor) and activated by ULK1, AMPK and DAPK (death- associated protein kinase) (Dikic and Elazar, 2018; Pattingre *et al.,* 2005). VPS34 produces phosphatidylinositol 3-phosphate (PI3P) on the membrane destinated to become a phagophore, and PI3P recruits proteins required for phagophore elongation (Cicchini *et al.,* 2015). Additionally, ULK1 regulates trafficking of the transmembrane proteins ATG9a and ATG9b (Zachari and Ganley, 2000). Phosphorylation of ATG9 proteins promote the translocation of ATG9-positive vesicles to the autophagy initiation sites (Zhou *et al.,* 2017). In mammalian cells, ATG9A is reported to cycle mainly between the trans-Golgi network (TGN) and the endosomal system (Imai *et al.,* 2016). Upon autophagy induction, ATG9A partially localizes transiently to autophagic membranes (Young *et al.,* 2006). The two isoforms, ATG9a and ATG9b, may have similar functions in the autophagosome formation, but this is not yet clear (Zhang *et al.,* 2020). The exact functions of ATG9 in the cell, and how the ULK1 complex regulates ATG9 trafficking, are poorly understood so far (Parzych and Klionsky, 2014).

Expansion of the phagophore involves the recruitment of two ubiquitin-like protein conjugation systems composed of multiple other ATG proteins such as ATG5, ATG7, ATG12 etc. (Klionsky and Schulman, 2014). Both these systems involve the E1-like ATG7 that initiates the conjugation of light chain 3 (LC3) with phosphatidylethanolamine (LC3/PE) and ATG5 with ATG12 (Cooper, 2018; Mizushima and Levine, 2010). These systems are reported to catalyse the formation of phosphatidylethanolamine (PE)-lipidated LC3-II and direct it into the phagophore membrane (Cicchini *et al.,* 2015). The membrane lipids can be derived from multiple sources, including the endoplasmic reticulum (ER) (Axe *et al.,* 2008). The phagophore expands until its membranes fuse to form an autophagosome, which eventually fuses with the lysosome to form an autolysosome where cargo is degraded, and nutrients are recycled. LC3 is involved in

cargo recognition, autophagosome closure and fusion with lysosomes. The p62/SQSTM1 (sequestosome 1) protein functions as a cargo receptor for autophagic degradation of ubiquitinated targets and is upregulated by various stressors (Jain *et al.,* 2010). For instance, induction of the p62 gene by oxidative stress is mediated by NRF2 (Ishii *et al.,* 2000). The specific interaction between p62 and LC3 was shown to be essential for the formation and degradation of polyubiquitin-containing bodies by autophagy (Pankiv *et al.,* 2007). The least understood step of autophagy depends on molecules that regulate maturation of autophagosomes, including their fusion with endosomes and lysosomes, as well as acidification of the autophagic compartments, and recycling of metabolites from lysosomal compartment (Parzych and Klionsky, 2014).

1.3.6 Crosstalk between autophagy and apoptosis

Autophagy represents besides apoptosis another type of energy-dependent programmed cell death with important roles in developmental processes, human diseases, and cellular responses to nutrient deprivation (Debnath *et al.,* 2005; Gozuacik and Kimchi, 2004; Schwartz *et al.,* 1993). Therefore, apoptosis and autophagy represent two processes through which redundant, damaged, or aged cells are eliminated. In addition to this function, autophagy plays an essential role in adapting cellular metabolism to avoid cell death, e.g., due to cellular stress such as starvation. Additionally, autophagy represents an alternative cell-death pathway under certain circumstances (Maiuri *et al.,* 2007). Between both cell death mechanisms, described as “self-eating” (autophagic death) and “self-killing” (apoptosis), exists an extensive crosstalk since both pathways share some common signals and regulatory components (Denton *et al.,* 2015; Maiuri *et al.,* 2007). Because autophagy and apoptosis are partially triggered by common signals such as ROS, which arise predominantly from defective mitochondria, it sometimes results in combined autophagy and apoptosis (Marino *et al.,* 2014). On the other hand, both pathways can inhibit each other. A molecular switch between these two processes has been reported that is mediated by a complex crosstalk that is not completely elucidated (Wu *et al.,* 2014; Piacentini *et al.,* 2003). Autophagy that arises from the inhibition of apoptosis is able to protect cells from death. Removal or inhibition of essential apoptotic proteins can switch a cellular stress response from the apoptotic default pathway to a state of massively increased autophagy (Maiuri *et al.,* 2007). Mitochondria function as central regulators of apoptosis and autophagy (Elmore *et al.,* 2007). For instance, autophagy decreases the possibility of apoptosis by removal of damaged mitochondria by mitophagy, and through the specific targeting and degradation of pro-apoptotic proteins (Marino *et al.,* 2014). In case of a failure to restore cellular homeostasis, cells can switch to regulated cell death response (Cooper, 2018; Elmore *et al.,* 2007).

It should be noted that inhibition of autophagy does not always induce cell death by apoptosis, and that other types of cell death may also result from autophagy inhibition (Golstein and Kroemer, 2007; Maiuri *et al.,* 2007). At the same time, activation of apoptosis inhibits autophagy through caspases mediated cleavage and inactivation of essential autophagy proteins (Marino *et al.,* 2014). For instance, BECL1, ATG5 and ATG4D can be cleaved by caspases thereby destroying the pro-autophagic activity

(Djavaheri-Mergny *et al.,* 2010; Kang *et al.,* 2011; Luo and Rubinsztein, 2010). The cleavage of BECL1 is mediated by the caspase-3-, 7- and 8 and generates a N- and C-terminal fragment that lost the ability to induce autophagy. The C-terminal fragment translocate to mitochondria, where it sensitizes cells to apoptotic signals (Djavaheri-Mergny *et al.,* 2010). The N-terminal fragment that is generated during the cleavage of ATG5, translocate likewise to the mitochondria, where it acts as pro-apoptotic factor and causes release of cytochrome c by interacting with BCL-xL (Yousefi and Simon, 2007). The CASP3 mediated cleavage of ATG4D creates a fragment with increased autophagic activity (Kang *et al.,* 2011). In turn, CASP8 can be degraded by autophagy to inhibit the apoptotic cell death (Hou *et al.,* 2010). BCL-2 and BCL-xL are anti-apoptotic as well as being blockers of autophagy (Ravikumar *et al.,* 2009). The autophagy-inducing activity of BECL1 is inhibited by an interaction with these anti-apoptotic multidomain proteins (Kang *et al.,* 2011). This was reported to be spatially limited since only ER and not mitochondrial localized interaction between BECL1 with BCL-2 or BCL-xL inhibits starvation-induced autophagy (Maiuri *et al.,* 2007; Pattingre *et al.,* 2005). The BH3-only protein BAD competitively disrupt the interaction between BECL1 and BCL-2 or BCL-xL and facilitates BECL1 stimulated autophagy (Maiuri *et al.,* 2007). A further dependence on each other is shown by clearance of dead cells during EB cavitation, since autophagy revealed to be essential to create a critical “eat-me” signal for apoptotic cell engulfment (Qu *et al.,* 2007). Despite the findings so far, there are still many uncertainties regarding the crosstalk, and it is not yet clear how the switch occurs.

1.3.7 Autophagy in neuronal development

Evidence suggests that autophagy plays a crucial role in neuronal development and the axonal outgrowth of neurons (Ban *et al.,* 2013; Fimia *et al.,* 2007). Autophagy presents to interact with crucial developmental pathways like Wnt, SHH, transforming growth factor β (TGFβ) and FGF (Zhang *et al.,* 2012; Jimenez-Sanchez *et al.,* 2012; Gao *et al.,* 2010; Kiyono *et al.,* 2009). Therefore, it is assumed that the switch between proliferation and differentiation could be regulated by autophagy, but the mechanism is poorly understood. It is known that basal autophagy regulates Wnt and Notch signalling during development. Regulation of Wnt and Notch signalling is required for appropriate neuronal differentiation (Casares-Crespo *et al.,* 2018; Wu *et al.,* 2016). It is assumed that the downregulation of the β-catenin/Wnt and Notch pathways limits the expansion of NSC (Casares-Crespo *et al.,* 2018). An upregulation of the expression of Atg9a, Atg7, Becl1, Ambra1 and the LC3-II/LC3-I ratio was described during neurogenesis of olfactory bulb derived NSCs and in the mouse cerebral cortex during the initial period of neuronal differentiation (Lv *et al.,* 2014; Morgado *et al.,* 2015, Vázquez *et al.,* 2012). In turn, suppression of autophagy by PI3K inhibitors was reported to impair neuronal differentiation (Morgado *et al.,* 2015). Studies of N2a mouse neuroblastoma cells revealed that autophagic activity and a precise control of mTOR signalling are critical in the neuronal differentiation process (Zeng and Zhou, 2008). RA induced differentiation of N2a cells was shown to increase the autophagy level, while the AKT/mTOR signalling is downregulated. Further inhibition of mTOR activity as well as the suppression of

autophagy impairs neuronal differentiation while the process is delayed by knocking down Becl1 (Zeng and Zhou, 2008).

Furthermore, observations suggest that autophagy participates in neuronal development by regulation of ROS levels through mitophagy (Boya *et al.,* 2018). Moreover, it was reported that NRF2, a master transcription factor for cellular defence of oxidative stress, plays a critical role in self-renewal and differentiation (Jang *et al.,* 2014). An increased ciliation in neuroectodermal precursor cells induce autophagy that results in the inactivation of NRF2 and thereby lead to the transcriptional inactivation of Oct4 and Nanog, directing ESCs towards a neuroectodermal fate (Boya *et al.,* 2018; Jang *et al.,* 2016). Anyway, the knowledge about the involvement of autophagy in neuronal differentiation is still fragmented. Much effort must be spent to discover more connections between involved pathways and the role of autophagy in this complex process. Beside the importance of autophagy in neuronal development, it has a crucial function in mature neurons by providing a continuous turnover of cytoplasmic contents, a process that prevents axon degeneration and is essential for neuronal survival (Hara *et al.,* 2006; Komatsu *et al.,* 2006). A constitutive basal autophagy level works in part as quality-control mechanism and especially postmitotic cells such as neurons are dependent on proper cellular homeostasis (Yin *et al.,* 2016). Interestingly, compared to liver, proteins in the brain present a two to five-fold longer half-time, consistent to a lower autophagic turnover in neurons (Price *et al.,* 2010). Dysregulation of autophagy in neurons results in detrimental neurodegenerative disorders that are characterized by the accumulation of protein aggregates such as in Alzheimer's, Parkinson's and Huntington's disease, while a loss of autophagy is reported to be sufficient to induce neuronal death (Hara *et al.,* 2006; Komatsu *et al.,* 2006; Nishiyama *et al.,* 2007). Accumulation of dysfunctional organelles in the axon is leading to oxidative damage and finally to apoptotic cascades (Maday, 2016). Unlike other cells, autophagy in neurons is not induced by starvation in either the axonal or somatodendritic compartments (Ariosa and Klionsky, 2016). Nutrient-starved neuronal cells show considerably lower levels of LC3 conjugated to PE (LC3-II) and although mTOR signalling is decreased (Yu *et al.,* 2004). Additionally, pharmacological mTOR inhibition by rapamycin or torin1 revealed to be insufficient to upregulate autophagy in neurons (Maday and Holzbaur, 2016). Recently, depletion of Baculoviral IAP repeat-containing protein 6 (BIRC6, also known as BRUCE) was shown to enhance autophagy in non-neuronal cells as well as in neurons (Jia and Bonifacino, 2019). BIRC6 functions as Ub-conjugating enzyme (E2/E3) that negatively regulate autophagy. It is involved in monoubiquitination of LC3β, marking it for degradation by the proteasome. The knockout of BirC6 demonstrated to facilitate clearance of protein aggregates by increasing the level of cytosolic LC3β-I (Jia and Bonifacino, 2019).

Neuron-specific knockout of Atg5 or Atg7, coding for protein that are required for autophagosome formation, result in axonal degeneration and neuronal death in mice (Hara *et al.,* 2006; Komatsu *et al.,* 2006; Nishiyama *et al.,* 2007). The loss of Purkinje cells in the cerebellum is shown to be dramatic, while degeneration of pyramidal cells in the cerebral cortex occur to a lesser degree (Hara *et al.,* 2006; Komatsu *et al.,* 2006).

Accordingly, it remains unclear why different neuronal populations respond differently to a lack of autophagy (Maday, 2016). A basal autophagy level is critical for axonal homeostasis and regulation of the presynaptic function (Maday, 2016). It was shown that autophagy is enhanced within presynaptic and postsynaptic terminals to regulate neuronal activity and synaptic transmission (Hernandez *et al.,* 2012; Shehata *et al.,* 2012). Blocked autophagy caused axon terminal swelling before it comes to retraction followed by neuronal death (Maday, 2016). Increased neurotransmitter release and presynaptic recovery, specifically in dopaminergic neurons in mice, was reported to result from an Atg7 knockout (Hernandez *et al.,*2012). In turn, the number of synaptic vesicles is decreased by autophagy induction (Hernandez *et al.,* 2012). This leads to the assumption that autophagy modulates neurotransmission by sequestering synaptic vesicles (Maday, 2016). In contrast to the observation that autophagy disruption causes axonal retraction, it was demonstrated that depletion of ATG7 in murine neurons caused growth of longer axons, while activation of the autophagy pathway with rapamycin results in shorter neurites (Ban *et al.,* 2013; Chen *et al.,* 2013). The autophagosomes generated at tips of actively elongating axons contain membrane and cytoskeletal components (Hollenbeck and Bray, 1987; Maday *et al.,* 2012). Induction of autophagy results in degradation of cytoskeletal components and consequently to an inhibition of neurite outgrowth (Chen *et al.,* 2013; Stavoe *et al.,* 2016). Information must cross a large distance in the extended axonal and dendritic processes of polarised neurons with a length up to one meter in humans. Accordingly, autophagy is spatially compartmentalized in neurons, and autophagosome biogenesis and maturation is spatiotemporally regulated along the axon (Ariosa and Klionsky, 2016). Autophagosome biogenesis occurs in the distal axons (Maday and Holzbaur, 2014). The smooth ER in axons may provide the membrane for the autophagosome formation, according to the production of autophagosomes in axons (Yue, 2007). Autophagosomes are transported from the distal axon towards the cell body driven by the microtubule-based molecular motor dynein (Lee *et al.,* 2011; Maday and Holzbaur, 2014; Wang *et al.,* 2015). Recently, it was shown that the fusion event itself likely triggers the transport of autophagosomes to the cell body by recruiting dynein (Cheng *et al.,* 2015). Along the way, autophagosomes fuse with lysosomes and mature into degradative organelles (Lee *et al.,* 2011; Wang *et al.,* 2015). Hence, a gradient of lysosome function is generated along the axonal processes, with proteolytic activity concentrated in the soma of the neurons (Gowrishankar *et al.,* 2015; Lee *et al.,* 2011; Xie *et al.,* 2015). The soma probably facilitates the degradation and recycling because it is also the primary site of protein synthesis in neurons (Maday, 2016). In the aging human brain, efficiency of the autophagic pathway declines (Cuervo, 2008; Labbadia and Morimoto, 2014). Thus, autophagy related genes, essential for autophagosome formation such as Atg5 and Atg7, are downregulated with age (Lipinski *et al.,* 2010). Anyway, we are only at the beginning of understanding the mechanisms of autophagy in neuronal development and neurons. Further investigations will provide a deeper insight into cross reactions of several pathways with the autophagy machinery.

2. Material and methods

2.1. Material

Table 1: Mammalian cell lines and bacterial strain

Strain	Description	Reference
P19	Murine embryonal teratocarcinoma cells isolated from male C3H/He *Mus musculus*	ATCC® CRL-1825™
P19 Rac65	P19 cells with a truncated RARα	Gift from the lab of Pierre Chambon, Institut de Génétique et de Biologie Moléculaire et Cellulaire, Strasbourg
129S2/C57Bl6J, F1(G4)	Embryonal stem cells from *Mus musculus*, wildtype	Gift from Phillip Grote, Institute of Cardiovascular Regeneration, Frankfurt
Hek239	Human embryonic kidney cells	Gift from Anja Bremm, Buchmann Institute of Molecular Life Science, Frankfurt
XL1-Blue	Competent *E. coli* cells	Agilent Technologies

Table 2: Oligonucleotides. All guide sequences contain a BsmBI overhang on 5'-endings. Reverse Primer (rev) additionally contain a Cytosine (C) at the 3'-endings (illustrated in grey). All oligonucleotides were ordered from Sigma-Aldrich.

Name	Sequence	Usage
***Becl1*_gRNA1_1**	CACCGGGCGAGTTTCAATAAATGGC	Guide sequence beclin-1 gRNA1, forward
***Becl1*_gRNA1_2**	AAACGCCATTTATTGAAACTCGCCC	Guide sequence beclin-1 gRNA1, reverse
***Becl1*_gRNA2_1**	CACCGATCTTCGAGAGACACCATCC	Guide sequence beclin-1 gRNA2, forward
***Becl1*_gRNA2_2**	AAACGGATGGTGTCTCTCGAAGATC	Guide sequence beclin-1 gRNA2, reverse
***Becl1*_gRNA3_1**	CACCGGGCCCGACATGATGTCAAAC	Guide sequence beclin-1 gRNA3, forward
***Becl1*_gRNA3_2**	AAACGTTTGACATCATGTCGGGCCC	Guide sequence beclin-1 gRNA3, reverse
***Becl1*_PCR_fw**	CTCACTGTCATCCTCATTCATCTGC	Amplification and sequencing of DNA

***Becl1*_PCR_rev**	GTGACTTCCAGGACAGCCAG	fragments complementary to area coding for all three beclin-1 guide sequences
***Atg7*_gRNA1.2_1**	CACCGGACCTTCGCGGTAAGTAAAT	Guide sequence Atg7 gRNA1, forward
***Atg7*_gRNA1.2_2**	AAACATTTACTTACCGCGAAGGTCC	Guide sequence Atg7 gRNA1, reverse
***Atg7*_gRNA1.2_ fw**	GAGATATCAGCAGCCCAAC	Amplification and sequencing of DNA fragments complementary to area coding atg7 guide sequence 1
***Atg7*_PCR1_rev**	GCTGGGTACTTGCTTGC	
***Atg7*_gRNA2_1**	CACCGCAGTGGATGTATGGACCCCA	Guide sequence Atg7 gRNA2, forward
***Atg7*_gRNA2_2**	AAACTGGGGTCCATACATCCACTGC	Guide sequence Atg7 gRNA2, reverse
***Atg7*_PCR2_fw**	GCTGTCTGGCTAGAGAGGTG	Amplification and sequencing of DNA fragments complementary to area coding atg7 guide sequence 2
***Atg7*_gRNA2_rev**	CGCTCAGCTACGCAGGA	
***Atg7*_gRNA3_1**	CACCGTGGTAAGAACAGTAGCCATG	Guide sequence Atg7 gRNA3, forward
***Atg7*_gRNA3_2**	AAACCATGGCTACTGTTCTTACCAC	Guide sequence Atg7 gRNA3, reverse
***Atg7*_gRNA3_fw**	ACCCAGTCCTCTGTAAGAG	Amplification and sequencing of DNA fragments complementary to area coding *Atg7* guide sequence 3
***Atg7*_PCR3_rev**	GACTTGAGAAGCTGTGTCTAG	
***Atg9a*_gRNA1_1**	CACCGAGATAAACTTGATAAGCCGG	Guide sequence *Atg9a* gRNA1, forward
***Atg9a*_gRNA1_2**	AAACCCGGCTTATCAAGTTTATCTC	Guide sequence *Atg9a* gRNA1, reverse
***Atg9a*_gRNA2_1**	CACCGCCACGTTTGTACTCGGCCTT	Guide sequence *Atg9a* gRNA2, forward
***Atg9a*_gRNA2_2**	AAACAAGGCCGAGTACAAACGTGGC	Guide sequence *Atg9a* gRNA2, reverse

***Atg9a*_gRNA2_ fw**	GGAAGTTGGCGATGCCAATC	Amplification and sequencing of DNA fragments complementary to area coding *Atg9a* guide sequence 1and 2
***Atg9a*_gRNA1_ rev**	GGGACCCTACTTTATCTCC	
***Atg9a*_gRNA3_1**	CACCGCTCGGCTTGCTGGTACACTG	Guide sequence Atg9a gRNA3, forward
***Atg9a*_gRNA3_2**	AAACCAGTGTACCAGCAAGCCAGC	Guide sequence *Atg9a* gRNA3, reverse
***Atg9a*_gRNA3_ fw**	GAAAGCTGTGCTCTCACG	Amplification and sequencing of DNA fragments complementary to area coding *Atg9a* guide sequence 3
***Atg9a*_PCR3_rev**	GGCCATCCTCAGGTACTG	
***Nrf2*_gRNA1_1**	CACCGGCGAGGAGATCGATGAGTAA	Guide sequence *Nrf2* gRNA1, forward
***Nrf2*_gRNA1_2**	AAACTTACTCATCGATCTCCTCGCC	Guide sequence *Nrf2* gRNA1, reverse
***Nrf2*_gRNA2_1**	CACCGAGCCTTCAATAGTCCCGTCC	Guide sequence *Nrf2* gRNA2, forward
***Nrf2*_gRNA2_2**	AAACGGACGGGACTATTGAAGGCTC	Guide sequence *Nrf2* gRNA2, reverse
***Nrf2*_gRNA2_ fw**	ATTGTGCCTTCAGCGTGC	Amplification and sequencing of DNA fragments complementary to area coding *Nrf2* guide sequence 1 and 2
***Nrf2*_PCR1/2_ rev**	CTCATGAGAGCTTCCCAGACTC	
***Nrf2*_gRNA3_1**	CACCGATGTGCTGGGCCGGCTGAAT	Guide sequence *Nrf2* gRNA3, forward
***Nrf2*_gRNA3_2**	AAACATTCAGCCGGCCCAGCACATC	Guide sequence *Nrf2* gRNA3, reverse
***Nrf2*_gRNA3_ fw**	CTAAGCACAGGGTCACAAC	Amplification and sequencing of DNA fragments complementary to area coding *Nrf2* guide sequence 3
***Nrf2*_gRNA3_ rev**	GAAGGAACAGGAGAAGGC	
***BirC6*_gRNA1_1**	CACCGTAGCTGCTGCAACCAAACGT	Guide sequence *BirC6* gRNA1, forward

***BirC6*_gRNA1_2**	AAACACGTTTGGTTGCAGCAGCTAC	Guide sequence *BirC6* gRNA1, reverse
***BirC6*_gRNA1_fw**	GATGGAGCTGACAGAATAGC	Amplification and sequencing of DNA fragments complementary to area coding *BirC6* guide sequence 1
***BirC6*_PCR1_rev**	GTG TAT TTA ACA CAC AGT GGC	
***BirC6*_gRNA2_1**	CACCGCTCAGGGAGGATACGTGAAA	Guide sequence *BirC6* gRNA2, forward
***BirC6*_gRNA2_2**	AAACTTTCACGTATCCTCCCTGAGC	Guide sequence *BirC6* gRNA2, reverse
***BirC6*_gRNA2_fw**	TGCTGAGGAAATGCAGTTAGC	Amplification and sequencing of DNA fragments complementary to area coding *BirC6* guide sequence 2
***BirC6*_PCR2_rev**	GCC TCA AAC TCA TGA CCC TAG	
***BirC6*_gRNA3_1**	CACCGTGTGCATTAGGTTGGTGTGT	Guide sequence *BirC6* gRNA3, forward
***BirC6*_gRNA3_2**	AAACACACACCAACCTAATGCACAC	Guide sequence *BirC6* gRNA3, reverse
***BirC6*_PCR3_fw**	CAGGTCACAGAGCACGC	Amplification and sequencing of DNA fragments complementary to area coding *BirC6* guide sequence 3
***BirC6*_gRNA3_ rev**	GTC AGG GCT CCA CTC ATC	
***p62*_gRNA1_1**	CACCGGGGCGGCCATCCCCTGCACG	Guide sequence *p62* gRNA1, forward
***p62*_gRNA1_2**	AAACCGTGCAGGGGATGGCCGCCCC	Guide sequence *p62* gRNA1, reverse
***p62*_gRNA2_1**	CACCGCGCACACGCTGCACAGGTCG	Guide sequence *p62* gRNA2, forward
***p62*_gRNA2_2**	AAACCGACCTGTGCAGCGTGTGCGC	Guide sequence *p62* gRNA2, reverse
***p62*_gRNA3_1**	CACCGTTATAGCGAGTTCCCACCAC	Guide sequence *p62* gRNA3, forward
***p62*_gRNA3_2**	AAACGTGGTGGGAACTCGCTATAAC	Guide sequence *p62* gRNA3, reverse
***p62*_gRNA1_ fw**	GCTGGCTACTTAAGACACC	Amplification and sequencing of DNA fragments
***p62*_gRNA3_ rev**	GTC CTG GCC TCC TAA GC	

		complementary to area coding for all three *p62* guide sequences
U6_fw	GGGCCTATTTCCCATGATTCCTTCATATTTGC	Verification of guide sequence integration in lentiCRISPRv2

Table 3: Plasmids

Name	Description	Reference
psPAX2	2nd generation lentiviral packing plasmid, mammalian expression plasmid	Gift from Anja Bremm, Buchmann Institute of Molecular Life Science, Frankfurt
pMD2.G	VSV-G lentiviral envelope expressing plasmid, mammalian expression plasmid	Gift from Anja Bremm, Buchmann Institute of Molecular Life Science, Frankfurt
lentiCRISPRv2	lentiviral CRISPR/Cas9-knockout plasmid, mammalian expression plasmid, ampicillin and puromycin resistance gene	Gift from Anja Bremm, Buchmann Institute of Molecular Life Science, Frankfurt
plenti*Becl1*_1	*Becl1*_gRNA1 guide sequence inserted into lentiCRISPv2	Constructed in this study
plenti*Becl1*_2	*Becl1*_gRNA2 guide sequence inserted into lentiCRISPv2	Constructed in this study
plenti*Becl1*_3	*Becl1*_gRNA3 guide sequence inserted into lentiCRISPv2	Constructed in this study
plenti*Atg7*_1	*Atg7*_gRNA1 guide sequence inserted into lentiCRISPv2	Constructed in this study
plenti*Atg7*_2	*Atg7*_gRNA2 guide sequence inserted into lentiCRISPv2	Constructed in this study
plenti*Atg7*_3	*Atg7*_gRNA3 guide sequence inserted into lentiCRISPv2	Constructed in this study
plenti*Atg9a*_1	*Atg9a*_gRNA1 guide sequence inserted into lentiCRISPv2	Constructed in this study
plenti*Atg9a*_2	*Atg9a*_gRNA2 guide sequence inserted into lentiCRISPv2	Constructed in this study
plenti*Atg9a*_3	*Atg9a*_gRNA3 guide sequence inserted into lentiCRISPv2	Constructed in this study
plenti*Nrf2*_1	*Nrf2*_gRNA1 guide sequence inserted into lentiCRISPv2	Constructed in this study

plenti*Nrf2*_1	*Nrf2*_gRNA2 guide sequence inserted into lentiCRISPv2	Constructed in this study
plenti*Nrf2*_3	*Nrf2*_gRNA3 guide sequence inserted into lentiCRISPv2	Constructed in this study
plenti*BirC6*_1	*BirC6*_gRNA1 guide sequence inserted into lentiCRISPv2	Constructed in this study
plenti*BirC6*_2	*BirC6*_gRNA2 guide sequence inserted into lentiCRISPv2	Constructed in this study
plenti*BirC6*_3	*BirC6*_gRNA3 guide sequence inserted into lentiCRISPv2	Constructed in this study
plentip*62*_1	*p62*_gRNA1 guide sequence inserted into lentiCRISPv2	Constructed in this study
plentip*62*_2	*p62*_gRNA2 guide sequence inserted into lentiCRISPv2	Constructed in this study
plentip*62*_3	*p62*_gRNA3 guide sequence inserted into lentiCRISPv2	Constructed in this study

Table 4: Antibodies for immunoblotting and immunofluorescence. Application of antibodies used in this study are classified in either western blotting (WB) or immunofluorescence (IF).

Name	Description	Dilution/ Application	Item number, Provider
Anti-Acetylated α-Tubulin	IgG Mouse, monoclonal	1:100/IF	6-11B-1, Santa Cruz
Anti-ASCL1	IgG Mouse, monoclonal	1:100/IF	D7, Santa Cruz
Anti-GFAP	IgG Mouse, monoclonal	1:100/IF	2E1, Santa Cruz
Anti-Map LC3β	IgG Rabbit, polyclonal	1:100/IF	Santa Cruz
Anti-NeuroD	IgG Goat, polyclonal	1:100/IF	N-19, Santa Cruz
Anti-Neurogenin2	IgG Goat, polyclonal	1:100/IF	C-16, Santa Cruz
Anti-Nestin	IgG Mouse, monoclonal	1:100/IF	10c2, Santa Cruz
Anti-Goat	Rhodamin (TRITC)-conjugated IgG Donkey	1:50/IF	Jackson ImmunoResearch
Anti-Mouse	Rhodamin (TRITC)-conjugated IgG Donkey	1:50/IF	Jackson ImmunoResearch
Anti-Rabbit	Rhodamin (TRITC)-conjugated IgG Goat	1:50/IF	Jackson ImmunoResearch

Anti-Rabbit	Fluorescine (FITC)-conjugated IgG Goat	1:100/IF	Jackson ImmunoResearch
Anti-Goat	Alexa Fluor® 488 conjugated IgG Donkey	1:100/IF	Jackson ImmunoResearch
Anti-ATG7	IgG Rabbit, monoclonal	1:1000/WB	D12B11, Cell Signaling
Anti-ATG9a	IgG Rabbit, monoclonal	1:1000/WB	D409D, Cell Signaling
Anti-BECLIN1	IgG Rabbit, monoclonal	1:1000/WB	D40C5, Cell Signaling
Anti-BIRC6	IgG Rabbit, monoclonal	1:1000/WB	D8B5, Cell Signaling
Anti-GAPDH	IgG Rabbit, monoclonal	1:1000/WB	14C10, Cell Signaling
Anti-NRF2	IgG Rabbit, polyclonal	1:1000/WB	PA5-27882, Thermo Scientific
Anti-SQSTM1/p62	IgG Rabbit, monoclonal	1:100/WB	D6M5X, Cell Signaling
Anti-Rabbit HRP	IgG Goat, Anti-Rabbit, HRP-conjugated	1:10,000-1:20,000/WB	AP156P, Merck Millipore

Table 5: List of used compounds

Compound	Function	Provider
4-Diethylaminobenz-aldehyde (DEAB)	Aldehyd-dehydrogenase inhibitor	Sigma-Aldrich
BMS 493	Invers pan-RAR (retinoic acid receptor) inhibitor	Sigma-Aldrich
SB-431542	Inhibition of TGF-β-mediated activation of SMAD proteins	Cayman Chemical
Cyclopamine	Hedgehog pathway antagonist	Sigma-Aldrich
4-Hydroxy-Tempo (Tempol)	Antioxidant	Sigma-Aldrich
4,5-Dihydroxy-1,3-benzenedisulfonic acid disodium salt monohydrate (Tiron)	Antioxidant	Sigma-Aldrich

STF-62247	Trans-Golgi-network (TGN) inhibitor	Chemcruz
Chloroquine diphosphate	Lysomotropic agent	Sigma-Aldrich
A-674563	Akt1 (Protein Kinase B) inhibitor	Cayman Chemical
LY294002	PI3K inhibitor	Sigma-Aldrich
3-Methyladenin (3-MA)	Class III PI3K inhibitor	Sigma-Aldrich
Rapamycin	mTORC1 inhibitor	Cayman Chemical
Torin2	mTORC1 and PI3K inhibitor	Cayman Chemical

2.2. Methods

2.2.1. Mammalian cell culture

2.2.1.1 Maintenance of cells in culture

All cells were cultivated in an incubator at 37 °C, 5 % CO_2 and a humidity of approximately 80 %. P19 and HEK-293 cells were cultured in Dulbecco's Modified Eagle's Medium (DMEM-high glucose) with 10 % Fetal Bovine Serum (FBS; non USA origin), 4 mM glutamine, penicillin (100 Units/mL), and streptomycin (100 µg/mL). 75 or 25 cm^2 Flasks and 10 cm plates were used. Every 1-3 day, cells were subdivided in a ratio of 1:5-1:20, depending on confluency. Media was aspirated, cells were washed with 1x Dulbecco's Phosphate Buffered Saline (DPBS without calcium and magnesium), treated with 0.25 % Trypsin-EDTA solution, and transferred to a fresh culture vessel after the enzymatic reaction was stopped by the admixture of growth medium. All reagents were provided by Sigma-Aldrich.

Murine ESC were grown in self-prepared (feeder and serum free) 2i-media (Tab. 6) on dishes coated with truncated recombinant human vitronectin (rhVTN). Subdivision was implemented by usage of TrpLE™ Express (Gibco™).

Table 6: Formulation of self-prepared 2i media. F12/DMEM (Sigma-Aldrich) media was mixed with Neuro-BS Basal media with L-glutamin (Bio&Sell) 1:1 and following listed supplements were added to prepare 2i media. Media contained already standard antibiotics penicillin and streptomycin. Selective GSK3β & Mek 1/2 inhibitors as well as Leukemia Inhibitory Factor (LIF) were elements of the ESGRO®-2i Supplement Kit (1000x).

Name	Final concentration	Provider
N2-supplement	1x	Gibco™
B27-supplement	1x	Gibco™
β-mercaptoethanol	100 µM	Sigma-Aldrich
BSA solution	0,05 %	Gibco™
Glutamax	1x	Gibco™
NEAA	1x	Gibco™
Na-Pyruvat	1x	Gibco™
Lif	1000 U/mL	Merck Millipore
GSK3β & Mek 1/2 inhibitors	1x	Merck Millipore

2.2.1.2 Freezing and thawing cells from cryo culture

Cells of a 70-80 % confluent 75 cm^2 flask or 10 cm plate were treated with 0.25 % Trypsin-EDTA solution. Reaction was stopped by adding growth medium. Finally, cells were centrifuged (34x g, 3 min) and resuspended in 1 mL freezing media (90 % FBS, 10 % DMSO). Suspension was transferred to a cryovial before frozen in a cryobox at -80 °C. For thawing cells, frozen cryovial was swivelled in 37 °C warm water bath until suspension was almost defrosted. Suspension has been transferred to a tube with 10 mL prewarmed media followed by a centrifugation step (34x g, 3 min). After aspiration of the medium, cells got resuspended in fresh medium and were transferred on a culture vessel.

2.2.1.3 Counting cells

10 µL cell suspension was mixed 1:1 with trypan blue in a 96-well plate. 10 µL were transferred on a Neubauer improved counting chamber (0.1 mm depth, 0,0025mm^2). Death cells were dyed in blue. Vital cells of two large corner squares were counted by usage of 10x objective at the microscope (2.2.3.1). The counted cell number was multiplied with 10^4 to calculate the ration of cells per mL.

2.2.2 Neuronal differentiation

2.2.2.1 Methods of neuronal differentiation

Neuronal differentiation was either done by a modified version of the classical protocol (McBurney *et al.,* 1988), after the novel method of Nakayama *et al*. (2014) or by the protocol developed in this study. The self-developed method was designated as Starvation-Differentiation (SD) method. For SD protocol, dish had to be coated with a 0.005 % Poly-L-Lysine solution for P19 cells and with 0.5 µg/cm^2 rhVTN for ESC (2.2.2.2). 10^5-20^5 cells were seeded in one well of a 6-well plate or an Ibidi µ-dish (Ibidi, 35 mm, high). 40^5-80^5 cells were transferred to 10 cm cell culture dishes. Cells were cultivated with self-developed SD-media. To prepare this media, 1x N2-supplement (Gibco™) and 1x glutamax (Gibco™) were added to DMEM/F12 medium (Sigma-Aldrich). 67 mL of this medium was mixed into 505 mL Earls Balanced Salt Solution (EBSS, containing 5 ml of a penicillin/streptomycin mixture). For ESC, 0.05 % Bovine Albumin Fraction V, 1x NEAA and 100 µM of 2-Mercaptoethanol were added to F12/DMEM medium (including N2 and Glutamax). Medium was changed very gently on a daily base. For inhibitor studies, inhibitors were appropriated diluted and mixed with SD-media before adding to neuronal culture. The concentration of the solvent DMSO was always kept below the critical level of 0.1 %.

2.2.2.2 Coating with PLL, rhVTN and laminin

PLL (mol wt 150,000-300,000; 0.01 %) was 1:1 diluted with sterile water. 0.5 mL of the dilution was used for coating of one Ibidi µ-dish, 1 mL for a well of a 6-well plate and 3 mL for a 10 cm plate. Dishes were incubated 1 h at 37 °C and subsequently washed three times

with sterile water while preventing desiccation of the vessel surface in between the washing steps. Coated dishes were operationally after 1 h drying at RT.

A 5 µL aliquot of a truncated recombinant human vitronectin (rhVTN) provided from Gibco™ (0.5 mg/mL) was thawed and mixed with 500 µL 1x PBS. Solution was transferred on the glass bottom of an Ibidi µ-dish and incubated at 37 °C for 1 h. Solution was removed immediately before seeding cells to avoid desiccation of the surface.

A frozen aliquot of 1 mg/mL laminin from mouse engelbreth-holm-swarm tumor (Sigma-Aldrich) was thawed at 4 °C and gently mixed 1:400 with 1x PBS. The surface of 10 cm dishes was covered with each 4 mL of 2.5 µg/mL laminin solution and incubated 4 h at 37 °C. Solution was removed immediately before seeding cells to avoid desiccation of the surface.

2.2.2.3 Replacement of N2-supplement by single compounds

N2 supplement (Gibco^{TM}) was deployed as a serum-free additive of F12/DMEM medium (2.2.2.1). Single components of N2 were analysed in this work according to the concentration of the provider (Tab.7).

Table 7: Formulation of 100x N2-supplement. Composition of 100x N2 supplement from GibcoTM, provided by Thermo Fisher Scientific. Transferrin and insulin represent the protein components of this supplement. All components were provided by Sigma-Aldrich for analysis of single N2 ingredients.

Name	Concentration	Molarity
Transferrin, human, holo	10 mg/mL	1 mM
Insulin, recombinant, full chain	0.5 mg/mL	86 µM
Progesterone	0.63 µg/mL	2 µM
Putrescine	1.611 mg/mL	10 mM
Selenite	0.52 µg/mL	3 µM

Despite selenite, all components of N2 were analysed individually and in combination. For each component was a working solution prepared according to N2 formulation (Tab. 6) and mixed 1:100 in F12/DMEM medium. If one or more components were left out, volume was replaced by sterile water. 794 µl of the modified F12 was finally mixed into 6 mL EBSS to generate several SD medium variations. Modified medium was applied in neuronal differentiation by usage of SD method (2.2.2.1).

2.2.3 Imaging and staining of mammalian cells

2.2.3.1 Brightfield imaging of living cells

Cells in 10 cm dishes or 6-well plates were visualised by a Nikon ECLIPSE TS 100 microscope by usage of a Nikon Plan Fluor 10x/0,30 objective. Images were taken by a Moticam 3.0 MP (Nikon) and processed with Motic Images Plus 2.0 ML.

2.2.3.2 Long term imaging of living cells

To image neuronal differentiation with a tight frame rate, cells were seeded on Ibidi µ-dishes and incubated in an Ibid incubation chamber that was connected to an Ibidi gas mixer CO_2 and temperature controller. Incubation chamber was installed on a Zeiss Observer Z1 microscope. Every 3 min, a picture was taken by usage of Axiocam 504 mono (Zeiss) and 5x or 10x objective (see below). Process was controlled by the Zen pro 2.3 software. The dish had to be removed from the chamber for daily medium change. The imaged spots were tried retrieve after every interruption. Subsequently, Fiji (ImageJ) was used to wrap up daily videos, fused and converted by Free Video Joiner to one video that was covering the complete imaged period. Same microscope, camera and software was also used for all fluorescence images by usage of a Zeiss N-achroplan 5x/015, Plan-Neofluar 10x/0,30, Plan-Neofluar 20x/0,5 or Plan Neofluar Oil 40x/1,3 oil dic objective.

2.2.3.3 Trypan Blue staining

The medium from a three-week-old neuronal culture was aspirated and 2 mL of a trypan blue dye solution was rinsed for approximately 30 s over the cells that adhered on a 10 cm dish. Cells were washed carefully two times with 1x DPBS before brightfield imaging by usage of the Nikon ECLIPSE TS 100 microscope (2.2.3.1).

2.2.3.4 Ca2+-indication

50 µg Fluo-4 (AM) from Thermo Fisher Scientific was solved in DMSO to prepare a 1 mM working solution. By adding Fluo-4 to media, the concentration was decreased to 2.3 µM. Cells were incubated with the dye for 2 h and washed twice with SD medium before imaging at 506 nM by usage of the Zeiss Observer Z1 microscope (2.2.3.2).

2.2.3.5 Imaging of apoptotic and necrotic cells

Neurons were stained by Abacam's Apoptosis/Necrosis Detection Kit (ab176750). Experiment was implemented according to the microscopy assay protocol from Abacam by usage of living cells in glass bottom dishes (Ibidi) at different time points of differentiation.

2.2.3.6 Cell fixation

Cells were cultured on a glass bottom dish (Ibidi µ-dish, 35 mm, high). The medium was completely aspirated, and cells were washed twice with 1x PBS (5 mM Tris, 150 mM NaCl). 4 % paraformaldehyde solution was added and incubated for 20 minutes at 4 °C. Afterwards cells were washed three times with 1x PBS of each 5 minutes. In case of storage, 1x PBS was replaced by 1x PBST (5 mM Tris, 150 mM NaCl, 0.05 % Tween 20) and samples were stored at the 4 °C.

2.2.3.7 Immunofluorescence staining

1x PBS/T was removed from the fixed cells and replaced by blocking buffer (1x PBS, 5 %FBS, 0.05 % Tween 20). Cells were incubated for 1 h at RT. Blocking buffer was replaced by the first antibody, diluted (1:50-1:200) in antibody dilution buffer (1x PBS, 1% BSA, 0.05 % Tween 20). After incubation overnight at 4 °C, cells were washed three times with 1x PBS.

Incubation of the diluted secondary antibody (1:50-1:100) for 1-2 h at RT in a dark place. After washing three times with 1x PBS, cells were imaged or stored at 4 °C in the dark.

2.2.4 CRISPR/Cas9 gene knockout

2.2.4.1 Cloning of CRISPR/Cas9-knockout plasmids

Three gRNAs were designed for each target gene. Sequence was chosen from the Mouse_GeCKOv2_Library (*Beclin1*, *Nrf2*, *p62*) or by recommendation of Manuel Kaulich (Atg7, Atg9a, BirC6). Two oligonucleotides (forward and reverse) had to be designed for each gRNA. The designed sequences contain overhangs that are complementary to the BsmBI digested vector (oligonucleotide sequences are shown in Tab. 2). 1.5 µg of the plasmid lentiCRISPRv2 was digested by BsmBI. 100 µM of the forward and reverse oligonucleotides were annealed by decreasing temperature from 95 °C to 10 °C in steps of 5 °C per minute in a thermal cycler. Oligonucleotides were diluted to 0.5 µM with water. 0.5 µM of the annealed oligos were ligated each with 100 ng of the digested backbone by adding 2.5 U of T4 DNA ligase (Biolabs) and incubated 10 min at RT. For redigestion of the non-ligated backbone was the ligation mix incubated for further 40 min at 55°C. 10 µL were used for transformation of ligated plasmids in *E. coli* (2.2.5.2). Ampicillin resistant colonies were picked to inoculate LB-media for plasmid isolation (2.2.5.3). Plasmids of each 1-2 clones were sequenced (2.2.5.8) for verification by using the U6 primer.

2.2.4.2 Generation of lentiviral supernatant

1.5x 10^6 HEK239 cells were seeded per well of a 6-well plate and cultivated in 2 mL DMEM medium, respectively with all supplements. After 30 h, cells were transferred to S2 laboratory and subsequently transfected with lentiviral plasmids by Lipofectamine™ 3000 Transfection Reagent (Invitrogen™). Plasmids for packing and envelop expression (pPAX2, pMD2.G) were combined with three modified lentiCRISPRv2 plasmids to produce high titer lentivirus. Consequently, all three plasmids that code for guide sequences on one and the same gene were supposed to be transferred all together. For each transfection, two vials were prepared with each 250 µL OptiMEM medium. In one vial, 7 µl Lipofectamine 3000 was added, while 6 µL P3000 enhancer and the required plasmid DNA (1 µg pMD2.G, 2.7 µg pPAX2, each 1.1 µg of plenti*gene*_1-3) were mixed in the other one. Freshly prepared solutions of both vials were mixed and incubated 15 min at RT. 1 mL of media was aspirated from each well and partially replaced by carefully adding transfection mix (pipetting against dish wall). Plate was slightly moved to distribute the mixture in media before returning to incubator. After 12 h, medium was carefully changed. After further 24 h, 1.9 mL viral supernatant was harvested in a tube. The removed supernatant was replaced by medium. 24 h later, supernatant was harvested again in the same tube as the day before. Hek239 cells got discarded. To avoid transfer of HEK239 cells, supernatant was centrifuged (10 min, 170x g) before subdivision into four cryo vials and freezing at -80 °C.

2.2.4.3 Transduction of P19 cells with generated lentiviruses

50,000 P19 cells were seeded in each well of a 6-well plate. Next day, 500 µL of thawed lentiviral supernatant (2.2.4.2) and 8 µg/mL propylene was added dropwise to each well with 2 mL DMEM (full) from day before. Two days later, the old media was completely removed, and adherent cells were washed once with 1x PBS before adding fresh media containing puromycin (3 µg/mL). Cells were passaged in selection media every second day for two weeks in total before transfer to S1 laboratory.

2.2.5 Cloning and mutant identification tools

2.2.5.1 Determination of DNA concentration

Concentration of plasmid or gDNA was determined by usage of a Nanodrop 1000 Spectrophotometer (Thermo Scientific) according to manufacturer's construction. Solvent was used as blank.

2.2.5.2 Transformation of competent *E. coli*

Competent *E. coli* XL1-Blue cells were thawed for 10 min on ice. 50 ng plasmid DNA or 10 µL of ligation mix was added to 10 µL of cell suspension and incubated 30 min on ice. In every process, one aliquot of cells was carried along without adding DNA, as a negative control. Heat shock was implemented by 90 sec at 42 °C followed by 2 min incubation on ice. 100 µL prewarmed LB-medium was added and cell suspension was shaken 45-60 min at 37 °C before seeding on LB-agar plates containing ampicillin (100 µg/mL). Plates were incubated over night at 37 °C. Single clones were picked to be separated on a fresh plate and to inoculate a liquid culture for plasmid isolation.

2.2.5.3 Plasmid Isolation

Nucleospin® Plasmid Kit from Macherey-Nagel has been used according to manufacturer's instruction.

2.2.5.4 gDNA Isolation

gDNA from P19 cells was isolated by usage of Nucleospin® Tissue Kit from Macherey-Nagel. Half of a 60-80 % confluent 10 cm dish was used for isolation of gDNA. Pre-lysis of cells was implemented by adding 200 µL T1 buffer and 25 µL Proteinase K and incubation at 56 °C for 3,5 h. Further steps had been done by following manufacturer's instruction for animal cells.

2.2.5.5. Polymerase-Chain-Reaction (PCR)

For verification of gene knockouts, the 500-600 bp comprising area around this sequence was amplified for sequencing. Isolated gDNA (2.2.5.4) was used as DNA template. For each clone was a 100-200 µL PCR-reaction mix (1x Red HS Master Mix from Biozym, 0.2 µM forward/reverse primer, 1,6 ng/µL gDNA) prepared. To ensure an optimized temperature distribution, reaction mix was proportioned on several PCR tubes to achieve a volume of 20 µL in each tube. Amplification occurred in a thermal cycler through running the following temperature protocol.

Table 8: PCR Temperature protocol. Before running the protocol, the lid of the thermal cycler was heated up to avoid condensation. After running, samples were cooled down to 4 °C. Annealing temperature was chosen according to melting temperature of oligonucleotides and was approved previously in temperature gradient PCRs.

Temperature	Time	Number of cycles
95 °C	2 min	x 1
95 °C	15 s	x 35
X °C	15 s	
72 °C	20 s(15s/kb)	
72 °C	5 min	x 1

2.2.5.6 PCR clean up

Amplified PCR products (2.2.5.6) were purified before sequencing (2.2.5.8) by usage of Nucleospin® Gel and PCR clean up Kit from Macherey-Nagel according to manufacturer's instruction.

2.2.5.7 Agarose gel electrophorese

Due to expected DNA size, 0.8-1.2 % agarose gels were prepared. Agarose was boiled in 1x TAE (40 mM Tris [pH 7,4], 20 mM Acetic acid, 1 mM EDTA) to bring it into solution. Solution was cooled down to approximately 45 °C and supplemented with 2.5 µl Roti® GelStain (Carl Roth) per 50 mL gel before transferring to a chamber. The cured gel was transferred to electrophoresis chamber of the Biometra Compact Multi-Wide System (Analytik Jena). 5 µl of 1 kb DNA Ladder (Carl Roth) or an appropriate sample volume that was mixed with 6x loading dye, was loaded in a gel pocket. DNA was separated by constant 80 V. Signal was detected by ChemiDoc™ MP Imaging System (BioRad).

2.2.5.8 Sequencing

Isolated plasmids (2.2.5.3) or purified PCR products (2.2.5.6) were sequenced by Eurofins (formally GATC) and samples were prepared in beforehand due to the predefined protocol of the provider. Sequences were compared by usage of NCBI blast.

2.2.6 Immunoblot

2.2.6.1 Protein isolation

Cells from an approximately 80 % confluent 75 cm^2 flask were enzymatically separated by usage of trypsin. Reaction was stopped by addition of serum containing medium. Half of the cell suspension was used for protein isolation. Cells were washed twice in cold 1x DPBS and resuspended with 100-200 µl cold IP buffer (50 mM HEPES [pH 7.3], 150 mM NaCl, 2 mM EDTA, 1 % NP-40) with 1 mM freshly added PMSF (Roche). Cell suspension was incubated 30 min on ice and shook several times in between. Cell debris was removed by centrifugation (16,000x g, 4 °C, 10 min). Supernatant of cell lysate was transferred to a fresh tube and was ready to use for SDS-Page.

2.2.6.2 SDS-Page

Acrylamide concentration was similar in all stacking gels (5 % Acrylamide, 125 mM Tris [pH 6.8], 0.1 % SDS, 0.1 % APS, 0.01 %TEMED), while it varied between 8-12 % in the separation-gels (8-15 % Acrylamide, 370 mM Tris pH 8.8, 0.1 % SDS, 0.1 % APS, 0.01 % TEMED) according to molecular weight of the proteins. VWR® Mini Vertical Page System was used to prepare the gels and run protein electrophoresis. Chamber was filled with 1x SDS running buffer (25 mM Tris, 192 mM Glycine, 0.1 % SDS) after placing gels. Before loading samples, pockets of the gels had to be flushed carefully with a syringe filled with running buffer to remove plugging leftovers from gel. 4x LDS sample buffer (Invitrogen) was freshly mixed with 1/5 β-mercaptoethanol. 12 µL of the cell lysate was mixed with 4 µL of sample buffer and boiled 5 min at 95 °C. Cooled off samples were short spun before loading on to SDS-gel. One pocket was set loose between every sample. Finally, 5 µL of the protein standard Roti®-Mark TRICOLOR was loaded on each gel. Electrophoresis was running with constant 60 V in stacking and 80-110 V in the separation gel.

2.2.6.3 Immunoblotting

After protein separation on SDS-Page, gel was equilibrated in transfer buffer (25 mM Tris, 192 mM Glycine, 10 % Methanol). An Amersham™ Hybond™ P0.45 PVDF Blotting membrane (GE Healthcare Life Science) was equilibrated first in methanol and subsequently in transfer buffer. Proteins were transferred onto membrane by blotting in a Hoefer TE22 tank transfer unit (3h, 300 mA const.) over night in a 4 °C room while slightly stirring the transfer buffer to avoid temperature variations.

2.2.6.4 Immunodetection

After immunoblotting, membrane was washed 5 min in 1x TBST. The washed membrane was slightly shaken with blocking buffer (1x TBST, 5 % BSA) at RT for 1h. To detect proteins of a housekeeping gene as loading control additionally to the proteins of choice, membrane was cut apart due to protein size of the visible marker protein. Accordingly, membrane was washed three times in 1x TBST before incubation with first antibody (1:1000 in blocking buffer) over night at 4 °C. Next day, membrane was washed again three times in 1x TBST and incubated with second antibody (1:5000 resp. 1:10000 for GAPDH) for 1-2 h at RT. Finally, membrane was washed three times with 1x TBST and rinsed several times with 1 mL freshly mixed (1:1) Amersham™ ECL™ Western Blotting Detection Reagents (GE Healthcare Life Science). Signal was detected by ChemiDoc™ MP Imaging System (BioRad) using Image Lab 5.2 software.

2.2.7 Mass spectrometry

Native and neuronal differentiated P19 cells (wildtype and knockout mutants) were analysed by tandem mass tag (TMT) spectrometry. Each condition was analysed in triplicates. The analysed samples were divided on two mass spectrometry runs. For a comparative purpose, WT was included in both runs:

1st run	**2nd run**	
*Becl1*_WT_CTRL	*BirC6*_WT_CTRL	ND= neuronal differentiation
*Becl1*_WT_ND	*BirC6*_WT_ND	(SD method)
*Becl1*_WT_3MA	*BirC6*_WT_Rap	CTRL= control (native cells)
*Becl1*_KO_CTRL	*BirC6*_KO_CTRL	WT= wildtype
*Becl1*_KO_ND	*BirC6*_KO_ND	KO= knockout mutant (Δ*Becl1*, Δ*BirC6*)

For sample preparation, native P19 cells were cultured in growth medium on an uncoated 10 cm^2 cell culture dish until confluency of 70-80 % was achieved. Neuronal differentiation was implemented by seeding 10^5 cells in each well of a PLL coated 6-well plate and culturing for five days with SD medium. Before cells were harvested, adherent cells were washed three times with PBS. The cells of three wells were collected for one sample after five days of the SD differentiation protocol. Each sample was generated in triplicates, grown in independent cultures. All cells were lysed directly on the plate by adding 200-300 µL lysis buffer (2 % SDS, 150 mM NaCl, 50 mM Tris [pH 8], Protease Inhibitor Cocktail P8340 (Sigma, EDTA-free)). Lysate was gently collected by a cell scraper and transferred to a tube. After 10 min at 95 °C, the samples were stored at -20 °C. Further sample preparation, the mass spectrometry analysis itself and the row data generation were realised in cooperation with Christian Münch group (Institute of Biochemistry II, Goethe University) by Martin Adrian-Allgood and Dr. Georg Tascher. The provided data were analysed by usage of the software Perseus (version 1.6.15.0). Data were log2 transformed, categorial annotated and a multi-sample test was implemented that included analysis of variance (ANOVA), Benjamini–Hochberg correction with a false discovery rate (FDR) of 0.05 and log10 transformation. Z-score was calculated to generate heatmaps and Euclidean distance was applied to indicate the row tree clustering. The number of clusters was limited to 20 with maximal 10 iterations. Triplicates were composited to average groups, based on the median, for the heatmaps of specific protein groups and the multi scatter plot. Specific groups were generated by manual selection of distinct regulated proteins of interest. Principal component analysis was based on Benjamini–Hochberg correction (FDR= 0.05). Multi scatter plot analysis was implemented by the comparison of the generated average groups and denoted by Pearson correlation.

3. Results

3.1 Neuronal differentiation of P19 cells by self-developed SD method

In recent years, several neuronal differentiation protocols were developed, that circumvent the requirement of EB formation under serum-deprivation and simplified medium conditions (Morii *et al.,* 2020; Nakayama *et al*., 2014; Pauly *et al.,* 2018; Yamazoe *et al.,* 2006). Referring to the proposed default neuronal fate, initiated in the absence of extrinsic signals (Smukler *et al.,* 2006; Tropepe *et al.,* 2001), application of growth factors and inducers was kept down to a minimum in this study. Achieved was the establishment of a rapid, stable, and simple method to generate pure cultures of mature neurons under defined medium conditions, applicable to several cell lines. Previous *in vivo* studies indicate that fasting in *C. elegans* induces neuronal differentiation within a tumour and enhances neurogenesis in mice (Gomes *et al*., 2016; Lee *et al.,* 2002). Based on this background, a novel approach to induce neuronal differentiation *in vitro* under starved conditions, was established in this work. Neither the formation of free-floating aggregates nor supplementation of growth factors or known inducers was required to establish a reliable neuronal differentiation protocol. The development of this method was implemented by the usage of the P19 ECC line.

3.1.1 P19 cells differentiate through self-developed SD method

Since it is known that ESC and ECC die within 24 h in pure starvation medium (Li *et al.,* 2010; Smukler *et al.,* 2006; Tropepe *et al.,* 2001), DMEM/F12 media, supplemented with N2, was mixed to starvation medium (Earles Balanced Salt Solution - EBSS), to keep a appropriate number of cells alive. DMEM/F12 is commonly used as basis media to cultivate neurons or for neuronal differentiation under serum deprivation (Nakayama *et al.*, 2014; Pacherník *et al.,* 2005; Yamazoe *et al.,* 2006). In this study, the P19 cells were seeded on PLL coated 10 cm dish, treated for a couple of days with this enriched starvation medium (EBSS+DMEM/F12+N2) until first signs of neuronal differentiation were discovered. This observation was followed by a long process to optimize conditions. Therethrough, it was figured out that the efficiency of neuronal differentiation in this approach was highly dependent on several settings like cell density, cell substrate, the ratio of DMEM/F12 to pure starvation medium, frequency, velocity of media changes, and even culture conditions of the pluripotent cells before seeding. After optimization of all these conditions and parameters, a quite pure neuronal culture could be generated in one step and in only one week through the treatment with a simple, serum-free, and nutrition-poor media mixture, without the requirement of EB formation or supplementation of further factors (Fig. 10). Because of the former expectation that the neuronal differentiation was implemented by starvation, the developed method was named “Starvation-Differentiation” (SD).

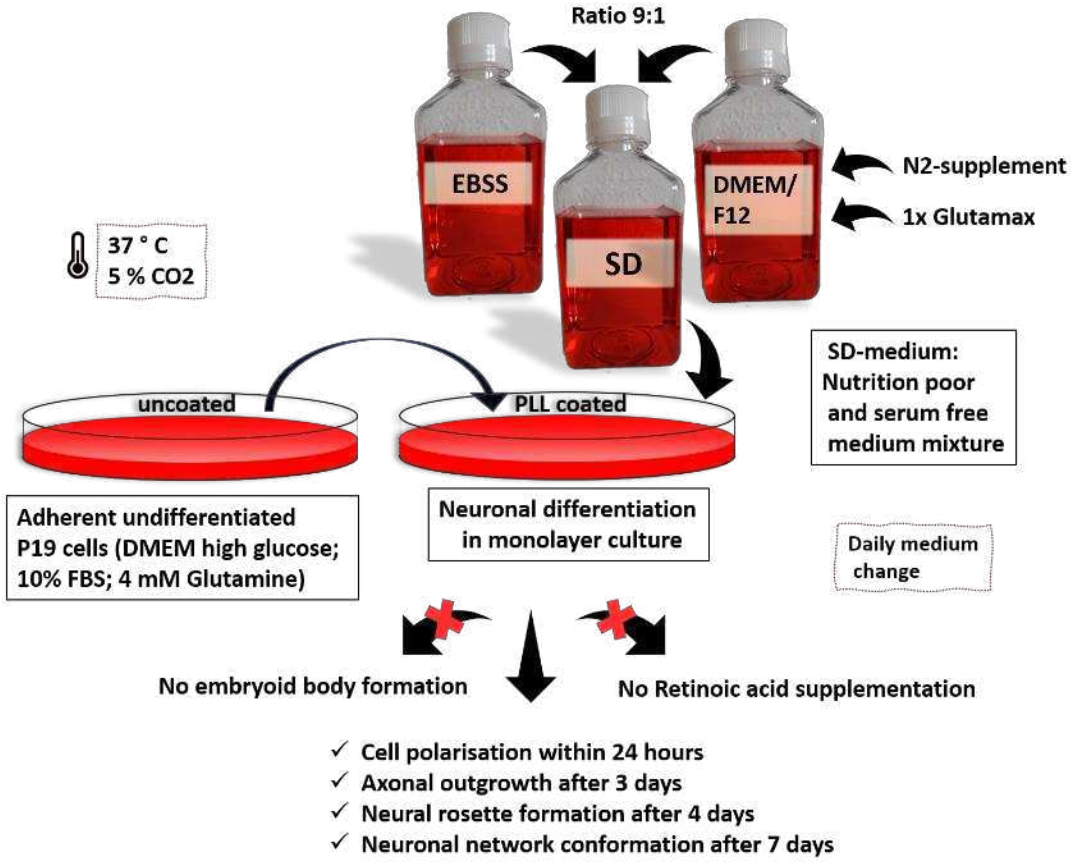

Figure 10: Schematic overview of SD method. Prior to induction of neuronal differentiation, P19 cells were grown on an uncoated cell culture dish in DMEM medium supplemented with 10 % FBS and 4 mM glutamine. Cells were harvested in exponential growth phase and subsequently transferred to a Poly-L-lysine (PLL) coated cell culture dish and grown in SD medium. To prepare the SD medium, initially, DMEM/F12 medium was supplemented with 1x N2 and 1x Glutamax. This enriched DMEM/F12 medium was mixed with EBSS in a ratio of 1:9 to generate a nutrition-poor and serum-free medium mixture. SD medium was gently changed daily. In comparison to the most common *in vitro* neuronal differentiation methods, neither embryoid body formation nor RA addition was required.

By imaging P19 cells during the neuronal differentiation process using the SD method, changes in cell organisation and morphology were traced by microscopy (Fig. 11). After seeded cells adhered to substrate, cells proliferated in a morphologically undifferentiated state for the first approximately 24 hours. Subsequently, cells moved together and built small clusters. From the second to the third day, cluster rounded up, which made it difficult to recognizing individual cells. This step was reminiscent of embryoid body formation but the cells at the lower end of this formations still adhered on the surface. Many cells started to degenerate in this phase, and media was full of debris, partially sticking on the clusters themselves. Just some small cluster remained after this period of high degradation level. These clusters flattened on the surface, generating neural rosettes formations. Observation of rosette-like formations started at day four of this differentiation protocol, partially hidden by the deposits, created by cell debris of degenerated cells. Neural rosettes, also observed by *in vitro* differentiation of hESCs, were reminiscent of secondary neurulation during neural tube formation (Fedorova *et al.,* 2019). The molecular process of this formation is barely understood

but it was discovered that cells of the neural rosettes have the potential to differentiate into distinct region-specific neurons and glial cells (Harding *et al.,* 2014; Li *et al.,* 2011). In the following days, the cellular clusters increased in size, driven by proliferation of polarised neuronal precursor cells. Cells of this cluster formation appeared polarised and started to organize their outgrowth. While the first outgrowth was detected at day three, some clusters got already connected with each other from next day on. Branches of adjacent neurons wired together and developed connections to nearby clusters. Scale and number of connections rapidly increased over time, while axonal connections became thicker. A neuronal network with morphologically mature neurons was built within one week after starting the experiment. After day ten, clusters manifested more of a clear round shape. Many adjacent clusters fused together during next couple of days. Within the next two weeks, connections got strengthened and multiplied while still some clusters fused together, consequently gaining length and height. Whereas the neuronal network got after over three weeks quite dense (Fig. 11- 25 d), occasional neuronal cluster started to show slight signs of degeneration. After 50 d, the neuronal network became partially so dense, that it was hard to distinguish between single clusters while other parts totally degenerated.

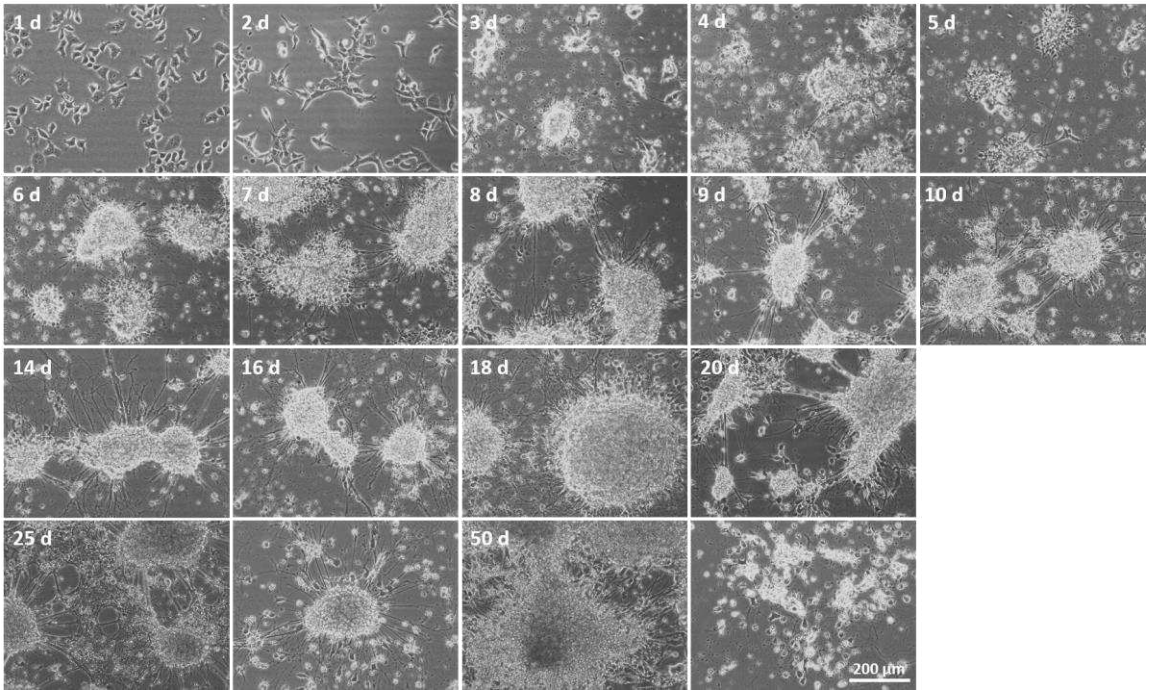

Figure 11: Pluripotent P19 cells differentiate to neurons by applying the SD method. Development of P19 cells, treated by SD method to generate neurons *in vitro* was imaged by confocal microscopy (10x objective) over 50 days. The first image was taken 24 h after the start of treatment with the SD protocol (1 d). Scale bar, 200 µm.

Additionally, differentiation process was monitored by cultivating cells under the microscope for two weeks, while generating a picture every three minutes. Subsequently, the snapshots were compiled to movies (supplemental DVD with movies attached). Two of the generated movies in various magnifications (5x and 10x objective) were chosen to be presented in this work (supplemental movie S1 and S2). Short interruptions in the movie were caused by media exchanges. Velocity of cell movement

and organisation during differentiation process could be easily retraced in these movies. As soon as cells started to generate clusters and polarised, first outgrowth was recognizable. Single neurons constantly moved in and out of the rosette formations and seemed to organise neuronal networking by moving quite fast up and down along the neurites. In addition to the neuronal cells, small particles were constantly taken up and released from the clusters. Extracellular vesicles like microvesicles, apoptotic blebs or exosomes were observed, that were released by cells into the extracellular space (Caruso Bavisotto *et al.,* 2019). Several *in vitro* studies demonstrated an inter-neuronal communication by released exosomes, retaken by other neurons to provide an activity-dependent synaptic growth (Korkut *et al.,* 2013). However, identification and function of the particles, observed in this setting, remained obscure. Due to the movies, it was even more distinctly recognizable that many cells died during the differentiation process, primary at day three to six. Dead cells could be only removed partially by media exchange but inclusion of a washing step, to remove more cell debris, ended up in detaching neuronal clusters. Debris accumulated on the neuronal cluster formations that became so dense that it partially turned dark for massive, aging clusters. Tracing of cell debris leads to the assumption that the debris of dead cells may have sticked on these neuronal cluster formations. This thesis was proven below (see chapter 3.3). To sum up, by usage of the developed SD method, P19 cells polarised and differentiated to morphologically distinct neurons, presenting a phenotype identical to P19-derived neurons of related protocols (e. g. Morii *et al.,* 2020; Nakayama *et al.,* 2014). Optically pure cultures of mature neurons were rapidly generated by the differentiation to neural rosettes followed by development of strong axonal branching patterns. The derived neurons appeared stable for at least three weeks until first signs of degeneration were observed. In addition to the morphological identification of a neural phenotype, the derived P19 cells were later proven to be neurons at the molecular level.

3.1.2 Branching pattern of neurites generated by P19-derived neurons

Some branches in the developed neuronal networks appeared free swinging on different levels, while others seemed to adhere on the substrate. Clusters, predominantly generated by the cell bodies of the neurons, were attached to the dish but still mobile. Side experiments done by laser ablation of these junctions gave a hint about the strong tension (supplemental movie S3). In the moment of ablation, connections snapped back, suggesting that there was probably a strong pulling force that let clusters move and fuse together. The ablated junctions were rapidly rebuilt in the given conditions. Tracing the neuronal differentiation process over weeks demonstrated that the fusion events got slightly reduced after approximately two weeks and the branching pattern condensed by building up an uncountable number of connections between clusters. The branching pattern was illustrated by immunofluorescence staining of acetylated α-tubulin, highly detected in the axons (Fig. 12). Acetylation of α-tubulin was reported to be much more pronounced in the microtubules of axons compared to dendrites of the neuron, while distribution of acetylation along the length of the microtubules is quite heterogene (Baas *et al.*, 1991). Here, we revealed a characteristic acetylated α-tubulin cytoskeletal arrangement of rosette formations (Curchoe *et al.,* 2013).

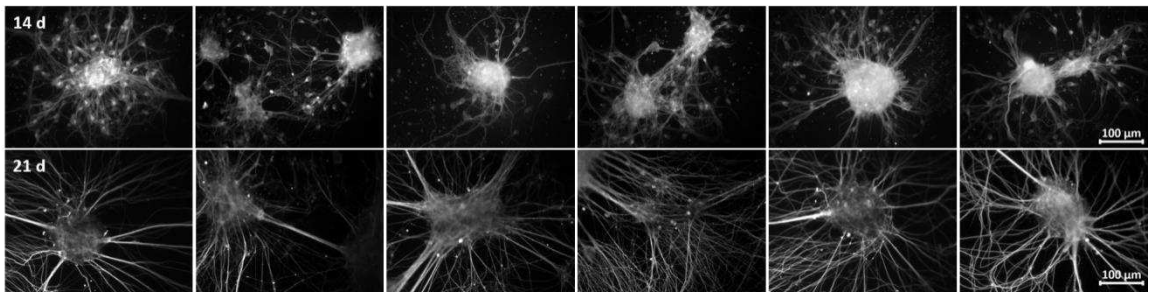

Figure 12: Immunofluorescence staining of acetylated α-tubulin in P19-derived neurons. Acetylated α-tubulin was highly expressed in the axons. Detection of acetylated α-tubulin by immunofluorescence staining (20x objective) underlined the branching pattern of P19-derived neurons by SD method. Neurons illustrated in the upper series were imaged 14 days after seeding, while neurons shown in the bottom row were imaged after 21 days. Scale bar, 100 µm.

A local shift of the immunofluorescence signals between the second and third week of differentiation was observed (Fig. 12). While the signal in the core of a neuronal cluster appeared quite high, signals were more concentrated on the outgrowing branches in a three-week-old neuronal culture. If this was caused by a translocation of the neurites or by a decrease of the acetylation level of α-tubulin remains unclear. Molecular mechanism of axon branching is not completely revealed so far but acetylated α-tubulin is discussed to play a crucial role by preventing an overgrowth of neuronal branches (Wei *et al*., 2017). Number and strength of these branches dramatically increased during this further week of neuronal development and clusters appeared more three-dimensional while still being attached to a plane surface. Interestingly, no cell body beyond the core was detected in the older culture. It is possible that they all migrated to the clusters after the network structure was established.

The neuronal differentiation protocol, published by Nakayama *et al*. (2014), was partially used as comparative value in this study due to some protocol similarities (see chapter 1.1.6). After one week, connections between neuronal clusters, generated by the method of Nakayama *et al.,* exhibited to be way stronger than that generated by the SD method (Fig. 13). But even if they looked more robust, after ten days, networks mostly teared of. It worked just once in multiple trials that the neuronal network was partially not detached until day 13 of their differentiation protocol. But in this case, strong indications of degeneration were detected. Connections thinned significantly down, and cluster formations were losing integrity. This was probably the reason that the clusters became unstable. Also, the authors of this protocol did not present any images or experiments with neuronal cultures older than six days.

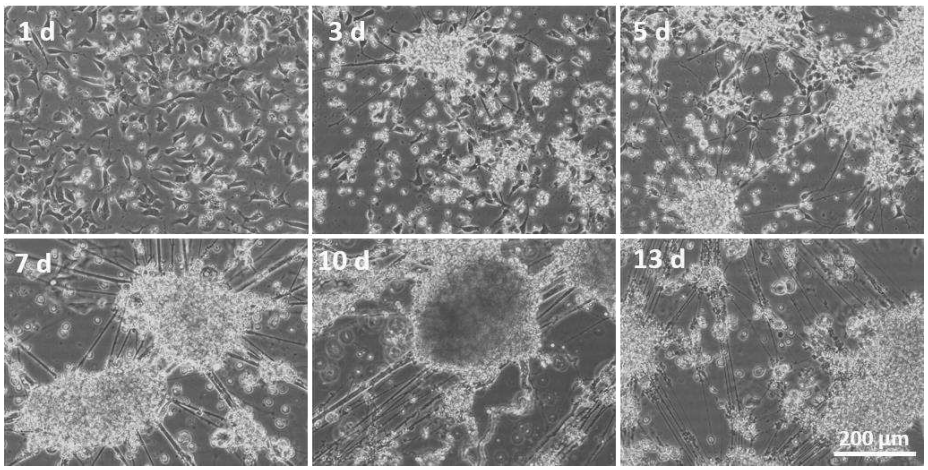

Figure 13: Neuronal differentiation of P19 cells by a modern and comparable method. P19 cells were differentiated, following the protocol of Nakayama *et al.* 2014. Scale bar, 200 µm.

In summary, by following the protocol published by Nakayama *et al*. (2014), cells differentiated at the beginning in the same way regarding cluster formation and establishment of connections to build a neuronal network. Despite, or perhaps because of, the improved medium conditions that allow a rapid differentiation process, the network easily detached or began to degenerate, whereas the neurons produced by the simple SD method proved stable for at least another two weeks.

3.1.3 Immunofluorescence staining of neuronal marker in P19-derived neurons

Neurons, generated in this work, were clearly identified by their morphology so far. To verify their expected cell fate decision, pro-neuronal molecular markers were detected by immunofluorescence staining of P19-derived neurons after application of the SD protocol over two weeks (Fig. 14). Nestin, an intermediate filament protein, and the basic helix–loop–helix (bHLH) transcription factors Neurogenin2, Achaete-scute homolog 1 (ASCL1) and the neurogenic differentiation factor (NeuroD) were strongly expressed in neuronal progenitor cells and during neurogenesis. Glutamatergic marker genes were described to be induced by Neurogenin2, while Ascl1 induces the expression of GABAergic marker genes (Huang *et al.,* 2014). Nevertheless, these pro-neuronal markers are applicable to verify cells that undergo the neuronal fate but are inappropriate to distinguish between cholinergic, dopaminergic, serotonergic, GABAergic or glutamatergic neurons. While NeuroD, Neurogenin2, ASCL1, and Nestin were strongly detected inside the neuronal cluster formations and thus especially in cell bodies, acetylated α-tubulin showed an impressive overview of the branching between the clusters (Fig. 14 A and Fig. 12).

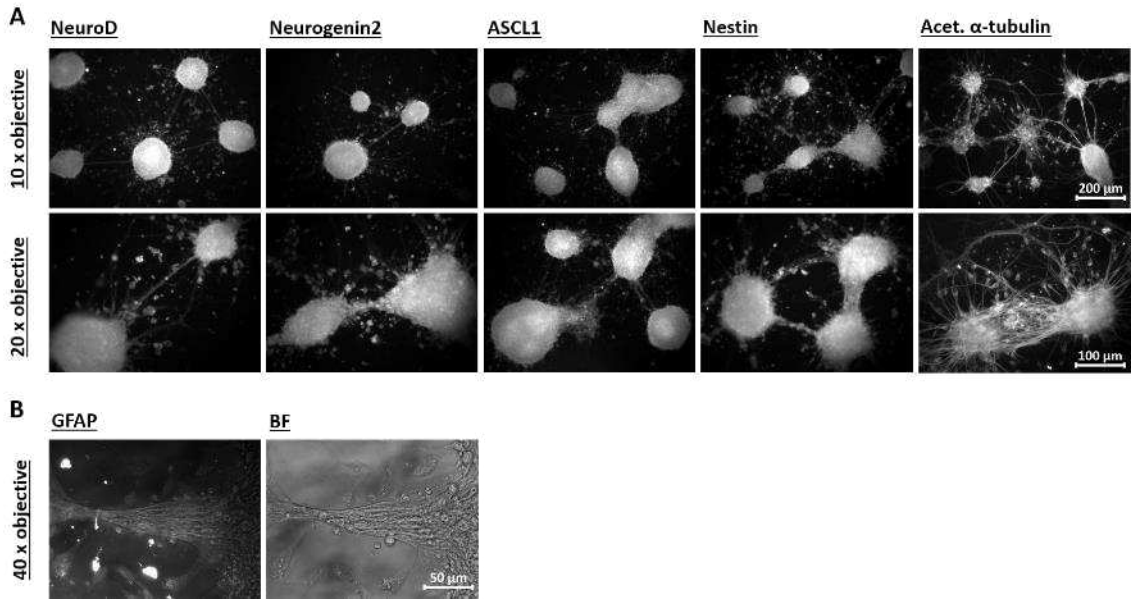

Figure 14: Immunofluorescence staining of P19-derived neurons. A: The expressed neuronal markers NeuroD, Neurogenin2, ASCL1, Nestin and acetylated α-tubulin were stained and imaged (10x and 20x objective). Scale bar, 100-200 µm. **B:** GFAP is an astrocyte marker. In comparison to brightfield (BF) view, spots stained with immunofluorescence emerged as dye accumulation (40x objective). Scale bar, 50 µm.

Nearly 100 % of all P19 cells that passed the process of neuronal differentiation by usage of SD method showed an equal morphology. This suggested a pure neuronal culture, manifested by detection of neuronal markers in all imaged cells. Several differentiation protocols result in the generation of mixed neuronal populations, including glial cells. The glial fibrillary acidic protein (GFAP) served as astrocyte marker. In the generated culture, no astrocytes could be detected with GFAP. A closer look at the single illuminating spots in comparison with the related brightfield shot, exposed to be an accumulation of the fluorescence dye (Fig. 14 B). Even if no astrocytes were detected, generation of astrocytes or other glial cells was not totally excluded but seems to not occur or to be at least a very rare event. Recapitulated, the P19-derived neurons could be verified and the SD method displayed to be capable to generate very pure cultures of neurons without astrocytes.

3.1.4 Monitoring of calcium activity in P19-derived neurons

Functionality of the synapses of the generated neurons was proven by detection of calcium activity. Fluo-4 dye, a fluorescence labelled indicator of Ca^{2+}-ions, was applied. Comparison of fluorescence signals of P19-derived neurons (by SD method) with undifferentiated P19 cells resulted in an unambiguous difference (Fig. 15). While there was no signal at all detected in the culture of undifferentiated cells, high fluorescence signals were detected from the generated neurons. The high intracellular calcium concentration strongly indicated that the neurons were active, constantly generating action potentials.

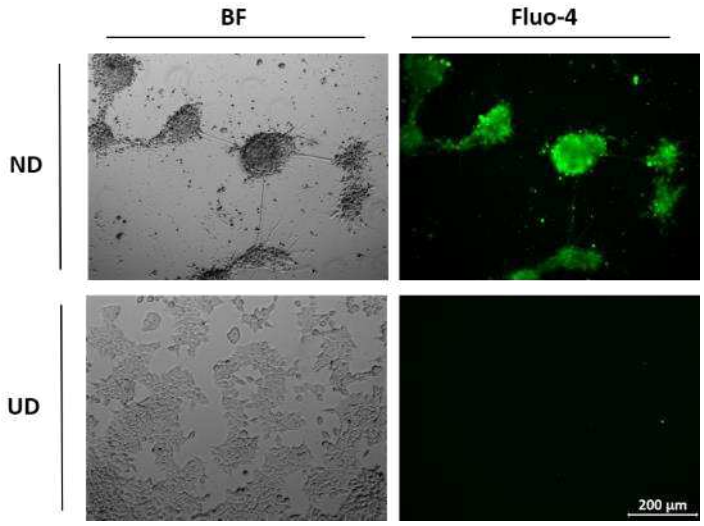

Figure 15: Calcium activity in P19-derived neurons. Calcium activity was detected in P19-derived neurons (ND) in comparison to undifferentiated (UD) cells by usage of Fluo-4. Neurons were generated by usage of the SD method and imaged after 10 days. All cells of the differentiated culture showed clear fluorescence signals. Native P19 cells, shown additionally in brightfield (below left), did not manifest any distinct signal over 24 hours, after exposure to Fluo-4. Scale bar, 200 µm.

Thus, after several hours, the dye was mostly pumped out of the neurons and mixed up with the surrounded medium, leading to an evenly spread fluorescence signal. Undifferentiated cells did not show this effect because Fluo-4 was not taken up by these cells and thus directly washed out before imaging. Several previous studies demonstrated the expression of functional voltage-gated calcium channels in P19-derived neurons by the usage of a calcium indicator (Canzoniero *et al.,* 1996; Lin *et al.,* 1996; Nakayama *et al.,* 2014). Generation of neurons with functional synapses was likewise verified for the developed SD method.

3.1.5 Analysis of the influence of SD medium components on neuronal differentiation

SD medium was developed, driven by the idea that pluripotent cells undergo neuronal cell fate decision under starved conditions. In comparison to serum-rich growth media the serum-free SD medium provided a strongly reduced nutrition supply and a defined medium composition. It was not clear so far which condition and media components appeared to be essential for neuronal induction. To test this, composition of SD medium was modified. First, cells were treated with pure DMEM/F12 medium with and without supplementation of N2. Without N2, all cells died within three days. Compared to EBSS, where cells die within 24 hours, lifespan was slightly extended. In pure DMEM/F12 medium, supplemented with N2, neuronal differentiation was partially induced but the non-polarised proliferating cells that did not undergo neuronal cell fate decision, expanded so fast that cells overgrew, and died within one week (Fig. 16 A). This suggested that N2 acted as an essential component under these conditions and that the dilution of DMEM/F12 + N2 was necessary to increase the ratio of postmitotic neurons.

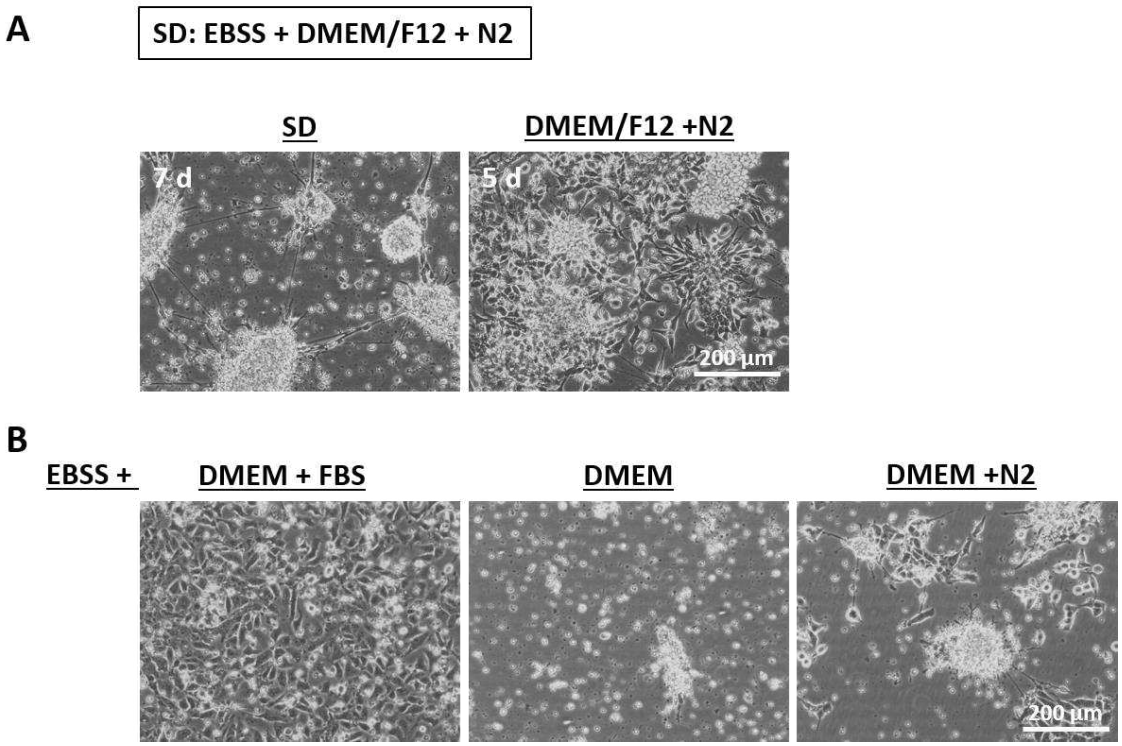

Figure 16: Variations of SD medium composition. A: SD medium was a mixture of nine parts EBSS and one part DMEM/F12, supplemented with 1x N2. Phenotypically mature neurons appeared within seven days in SD medium. In pure DMEM/F12 + N2 the potential of neuronal cell fate decision was decreased and the culture was rapidly overgrown, resulting in full degeneration after seven days. **B:** DMEM/F12 + N2 of the SD medium was replaced by serum-free DMEM as well as DMEM with 10 % FBS. Differentiation totally failed with this composition. A declined neuronal differentiation took place by usage of DMEM supplemented with 1x N2 in mixture with EBSS. Scale bar,200 µm.

Furthermore, the DMEM/F12 medium, supplemented with N2, was replaced by pure DMEM or DMEM supplemented with 10 % FBS, to check whether just the ratio of starvation medium to nutrition-rich medium matters or if also the composition was critical (Fig. 16 B). Neuronal differentiation failed under both chosen conditions. The serum withdrawal caused an almost complete degeneration after one week, while cells treated with serum (FBS) just overgrow without any sign of cell differentiation. Finally, DMEM medium was supplemented with N2 instead of being mixed with EBSS. Neuronal differentiation occurred partially, even if cell survival and therefore cluster size was significantly decreased. Purity of the neuronal culture appeared to be decreased but cells that did not present a neuronal phenotype, demonstrated slow proliferation rates, and did not threaten to overgrow postmitotic neurons within this week. To summarise, dilution of DMEM/F12 + N2 and thus a strong nutrition reduction seems necessary to diminish proliferation of non-neuronal cells. Thus, it was shown that, contrary to the previous assumption, starvation does not induce neuronal differentiation but only allows neuronal cells to survive under certain minimum conditions. The F12 nutrition mixture supports the survival of neuronally differentiated cells, whereas differentiation was induced by the addition of N2 only.

3.1.6 Analysis of the impact of N2 supplement components in SD medium

After the N2 supplement was identified to be an essential component of the neuronal differentiation process, in the SD method, the influence of single components of this supplement was examined. N2 is a mixture composed of selenite, progesterone, and putrescine together with the two proteins transferrin and insulin. All components except selenite were available for analysis in this study. Thus, the N2 in SD medium was replaced by a mixture of transferrin, insulin, progesterone, and putrescine, at the same concentrations as the N2 formulation (see Tab. 7). At the second and third day of the differentiation protocol, the cell clusters that were treated by the component mixture dragged slightly behind the N2 control, likely due to the lack of selenite (Fig. 17). But the potential and efficiency of differentiation into neurons as well as the neuronal pattern after five days were not affected. After testing all possible combinations of these four components, the most meaningful results were pooled for a broad view Even a brief look on it revealed that none of the other combination resulted in an induction of the neuronal differentiation process or even provided viable conditions. As already mentioned before, N2 withdrawal in SD medium caused the degeneration of cultured P19 cells within three days. Usage of various combinations of one to three components revealed to be insufficient to prevent complete degeneration of all cells. The lifespan was partially affected but induction of neuronal differentiation failed in all these combinations. Consequently, all cells degenerated rapidly.

The most characteristic differences to the control cells were discovered on third day of the SD differentiation protocol. Progesterone and putrescine as single factor demonstrated similar effects. The cell morphology at the third day had completely changed. Compared to control, cells appeared much smaller in size and unipolar in shape. Transferrin, chosen as the only component of N2, led to a quick degeneration like observed for complete N2 withdrawal. Transferrin in combination with progesterone and putrescine resulted in the generation of small clusters, partially with tiny outgrowth. Despite the promising start at day three, all cells degenerate in the following 24 hours. Insulin showed the strongest effect on life span extension but was also not sufficient to induce neuronal differentiation under these conditions. In comparison to transferrin, supplementation of progesterone and putrescine additionally to insulin did not cause significant differences. Taken together, except for selenite, all components of the N2 supplement were necessary to facilitate neuronal induction or at least ensure survival of differentiating cells in the SD method.

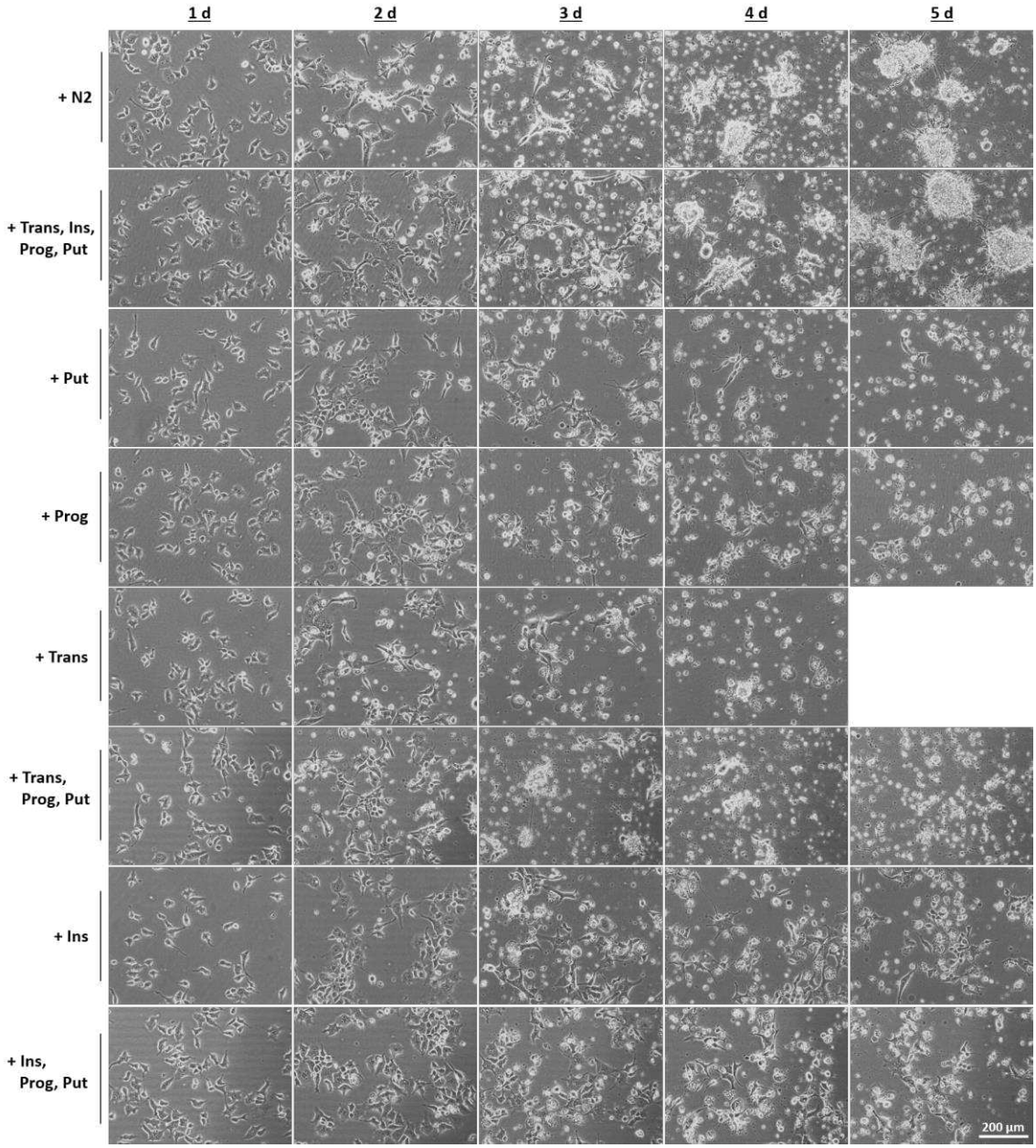

Figure 17: SD medium with varied N2 components. N2 supplement is a mixture of transferrin (Trans), insulin (Ins), progesterone (Prog), putrescine (Put), and selenite. Besides selenite was the N2 supplement in the SD medium replaced by varied combinations or by the single components. The potential to induce neuronal differentiation was reported over five days. Scale bar, 200 µm.

3.1.7 Screen of RA and RAR dependency by application of the SD method

In none of the components of self-prepared SD medium, retinol or retinoic acid was included. Nevertheless, effects of residual RA or endogenous synthesis could not be completely excluded, as RA has been reported to be able to induce neuronal differentiation at subnanomolar levels (Engberg *et al.,* 2010). Engberg *et al.* claimed that RA signalling is required to differentiate to neuroectodermal fate in serum-free, adherent monocultures. Therefore, RA synthesis and signalling was investigated with three different approaches in this study. The group of Pierre Chambon of the university

of Strasbourg kindly provided the P19 RAC65 mutant to proof whether the retinoic acid receptor α (RARα)-dependent RA signalling was involved into neuronal induction by implementation of the SD method. The RAC65 mutant is supposed to be RA resistant due to a truncated RARα (Pratt *et al.,* 1990). The dependency of RA regulated transcription initiation was proven by treatment of the provided RAC65 mutant with distinct differentiation protocols.

First, the P19 wildtype and RAC65 mutant were treated with the conventional neuronal differentiation protocol (McBurney *et al.,* 1988). In this case, cells were cultured in full medium with serum. Differentiation was induced by RA treatment of three-dimensional organised EBs. Like reported before, a heterogenic culture was generated, probably including neurons, glial and fibroblast-like cells (Bain *et al.,* 1994; Fraichard *et al.,* 1995; Strübing *et al.,* 1995). While several cell clusters, derived from the wildtype cells, showed a certain neuronal phenotype, the RAC65 mutant totally failed to differentiate by application of the classical protocol (Fig. 18). The mutant cells demonstrated no change in their morphology, proliferated, and overgrew fast without any evidence of differentiation. Subsequently, wildtype and mutant were both successfully differentiated by SD protocol, without sensing any differences. Thus, the SD method demonstrated to be independent of transcription activation by RARα.

Both cell types were also differentiated by the protocol established by Nakayama *et al*. (2014). In this method, differentiation is also induced by RA, but compared to the conventional approach, the process in this protocol is additionally greatly enhanced by several enhancers. The RAC65 mutant showed slight differences from the wildtype, but not as drastic as expected, although RA was used as the actual inducer. Only the branching pattern proved to be slightly reduced in the mutant. Nevertheless, neuronal induction was strongly induced under the given conditions.

A crosscheck using the same protocol but without RA supplementation showed that all supplemented enhancers and the perfectly matched medium compositions were also likely sufficient to trigger neuronal differentiation, but axonal growth and the integrity of cell clusters were significantly impaired. And it is noted that the phenotype of WT and mutant cells was affected by skipping RA under this condition in the same way. Therefore, RA was shown to affect the differentiation potential of the mutant in this serum-free monolayer culture and thus in this case likely independent of RARα activation by RA.

In conclusion, neuronal induction by the SD method is independent of RARα activation by RA. The new method of Nakayama *et al.* also proves to be RARα-independent, reinforced by the observation that here the effect of RA on the WT and the RAC65 mutant was identical. In contrast to these serum-free monolayer cultures, induction by the classical protocol in serum-containing medium with EB formations failed.

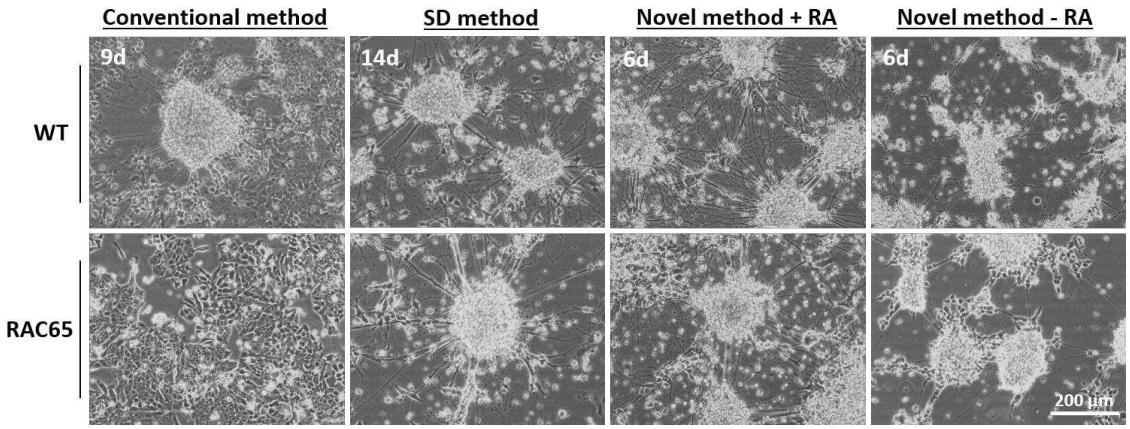

Figure 18: Neuronal differentiation of P19 WT and RAC65 mutant by usage of various protocols. Ability of P19 WT and RAC65 mutant cells to differentiate to neurons by usage of the conventional protocol established by McBurney *et al.* (1988), the developed SD method, and a novel protocol set up by Nakayama *et al.* (2014) with and without RA supplementation. Only significant differences between WT and RAC65 mutant were discovered by application of the classical differentiation protocol. Scale bar, 200 µm.

The observations, made by differentiating the RAC65 mutant, raised the question of whether induction by the SD method might be affected by RA signalling in a RARα-independent manner. To eliminate this uncertainty, diethylamino benzaldehyde (DEAB) was used. DEAB acts as non-specific inhibitor of aldehyde dehydrogenases (ALDHs). ALDHs include the RALDH subfamily that catalyse oxidation of retinal to RA in the cytoplasm (Duester, 1996). DEAB performs as competitive, reversible inhibitor antagonist that acts as substrate of several retinaldehyde dehydrogenases and irreversibly inhibits the RALDHs ALDH1A2, ALDH2 and ALDH7A1 (Begemann *et al.,* 2004; Morgan *et al.,* 2015). To analyse in which concentration range DEAB creates a toxic effect on the pluripotent P19 cells, native P19 cells were cultured in full medium (DMEM with 10 % FBS) with 1-20 µM DEAB over ten days (Fig. 19). Below a concentration of 20 µM DEAB, cells were not affected (no change in proliferation rate or shape). Even with 20 µM, cells just slightly started to partially round up and degenerated after seven days. Consequently, for the analysis of cells driven to neuronal fate, a concentration up to 10 µM revealed to be uncritical.

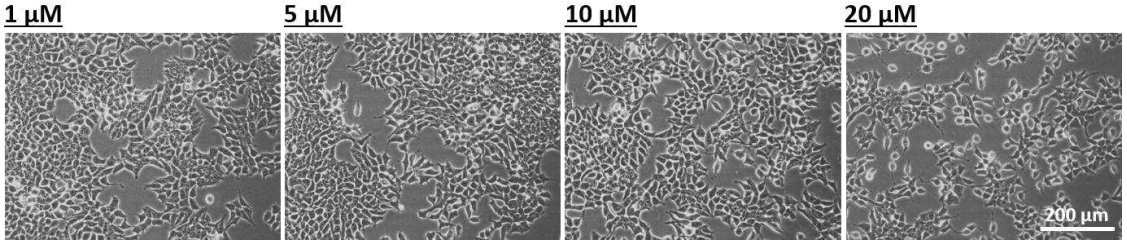

Figure 19: Definition of non-toxic DEAB concentrations on native P19 cells. Native P19 cells were grown in uncoated cell culture dishes with DMEM supplemented with 10 % FBS and 1-20 µM DEAB over ten days. Here shown at day seven, when the first evidence of toxicity appeared by supplementation of 20 µM DEAB. Cells were subdivided every second day and media was changed on a daily base. Scale bar, 200 µm.

An effect on cell fate decision was investigated by supplementation of 1-10 µM DEAB to SD medium during the whole differentiation process (Fig. 20). During differentiation, cells reacted way more sensitive compared to the undifferentiated state. At the second day of differentiation protocol, 10 µM DEAB showed already a strong effect, followed by 1-5 µM, with first indications at day three and four. Beside a strong reduction of the cell number, finally leading to complete degeneration in higher inhibitor concentration, the neuronal phenotype was not affected. Thereby, cluster formations and axonal outgrowth were also detected through the whole tested concentration range.

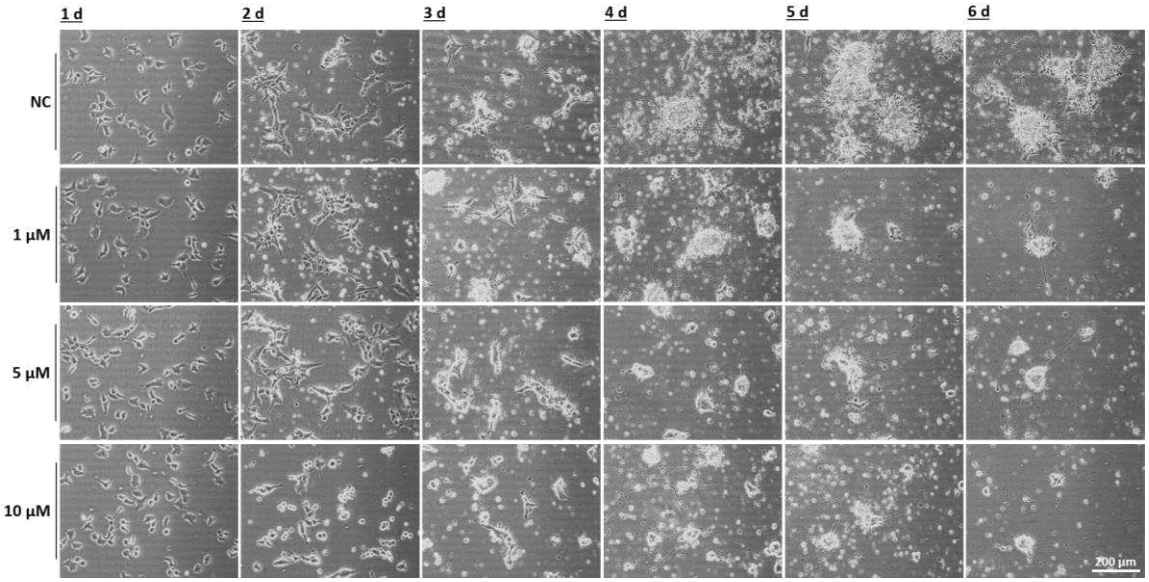

Figure 20: Effect of DEAB on neuronal differentiation of P19 by SD method. P19 cells were grown in SD medium supplemented with 1-10 µM DEAB in comparison to negative control (NC) with DMSO. Media was changed daily. Scale bar, 200 µm.

Additionally, influence of DEAB on neuronal induction by the protocol established by Nakayama *et al.* (2014) was analysed (Fig. 21). In comparison to SD method, DEAB evoked the same effect. Neuronal induction was not impaired, but the survival was massively diminished. This observation led to the assumption that cells which passed the differentiation process might be more sensitive to this toxic inhibitor or that RA was not essential for the induction but for survival of neuronal cells in serum-free monolayer cultures.

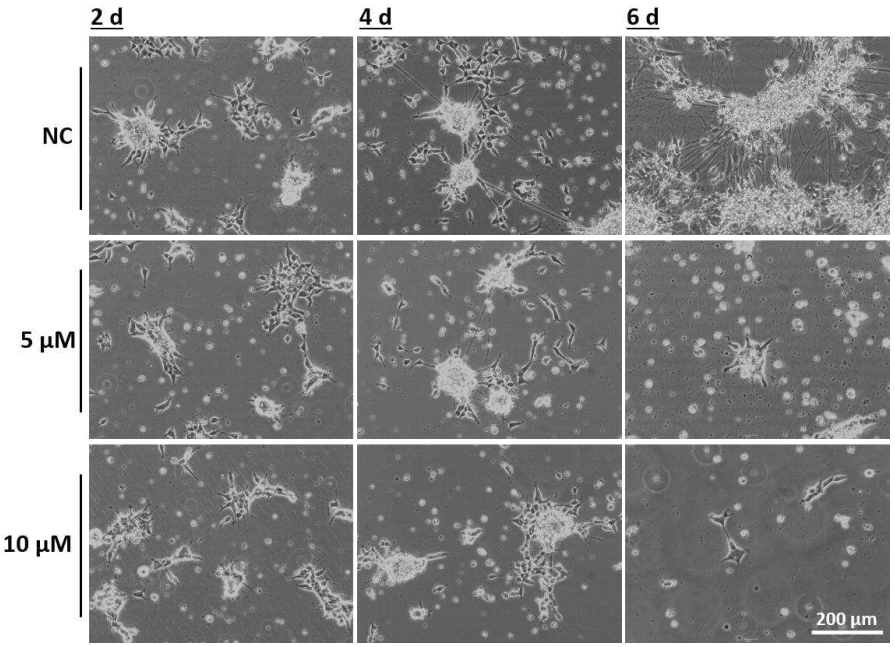

Figure 21: Effect of DEAB on neuronal induction of P19 cell by the protocol of Nakayama *et al*. P19 cells were differentiated after the protocol established by Nakayama *et al.* (2014). The medium was supplemented with 5 and 10 µM DEAB, respectively or with DMSO in negative control (NC). Medium was gently changed every day. Scale bar, 200 µm.

BMS493 is an inverse pan-retinoic acid receptor (pan-RAR) agonist. Thus, it is a ligand-dependent transcription factor that is supposed to act on all isoforms of the RAR through an enhancement of the co-repressor binding to RARs (Germain *et al.,* 2002). Treatment of P19 cells with BMS493 during neuronal differentiation by application of the SD method as well as the protocol of Nakayama *et al*. (2014), highly prevent the neuronal cell differentiation process and ended up in cell degeneration under the given circumstances (Fig. 22 A). In contrast to this strong effect, detected through differentiation conditions, native cells cultured in growth medium stayed totally unaffected by BMS493 (Fig. 22 B).

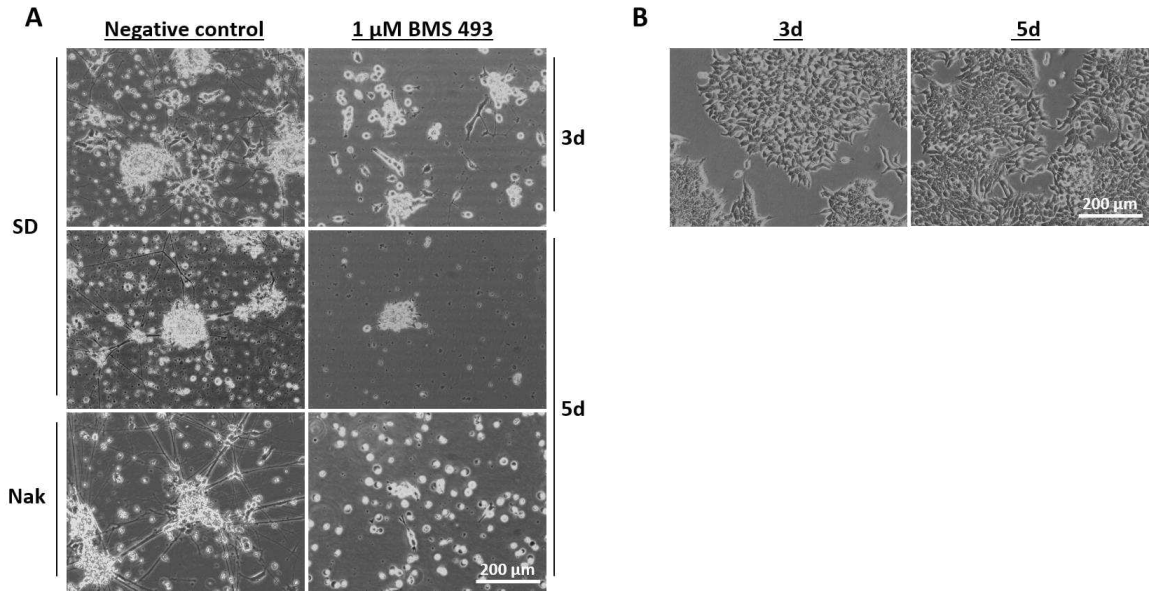

Figure 22: Effect of a pan-RAR antagonist on P19 cells. A: P19 cells were neuronal differentiated by the protocol of Nakayama *et al.,* 2014 (Nak) or the SD method w/o (negative control) or with 1 µM of the pan-RAR agonist BMS493. **B:** Undifferentiated P19 cells, cultured in growth medium, were treated with 1 µM of BMS493. Scale bar, 200 µm.

In summary, the truncated RARα of the RAC65 mutant displayed no effect on the potential to induce neuronal differentiation by application of the SD method and only a slight effect when the novel approach by Nakayama *et al*. was used. Therefore, induction in both cases might be regulated in a RARα-independent manner. Blocking RA synthesis by DEAB resulted in strong reduction of the cell number that survived the differentiation process, but this inhibitor appeared to be unable to prevent neuronal induction. The pan-RAR antagonist BMS493 silenced the activity of all RAR isoforms and caused complete cell degeneration without showing any evidence of neuronal differentiation. These observations led to the assumption that neuronal differentiation by both analysed serum-free approaches might be dependent on RA signalling, probably regulated by RARβ or RARγ.

3.1.8 Influence on neuronal differentiation by signalling pathway inhibitors

To provide an insight into the pathways and factors involved in neuronal induction by implementation of the SD method, the influence of several inhibitors was probed. Several lipophilic compounds are poorly soluble in water and had to be solved in dimethyl sulfoxide (DMSO). Beside the function as potent organic solvent, DMSO is an efficient inducer of differentiation in ESC and ECC (Jacob and Herschler, 1986). Starting at a concentration of 0.125 % DMSO for ESC and 0.25 % for ECC, gene expression of pluripotency factors like Oct-4 are downregulated (Adler *et al.,* 2006). Exposure to 1 % DMSO is usually used for induction of mesodermal differentiation in P19 cells (Jasmin *et al.,* 2010; McBurney *et al.,* 1982). But RA that is supplemented to induce neuroectodermal differentiation is commonly solved in DMSO. A high RA level combined with the treatment of 1 % DMSO was reported to prevent mesodermal differentiation, while a low RA level enhances skeletal myogenesis (Kennedy *et al.,* 2009; Pratt *et al.,*

1998). The SD protocol did not include RA supplementation, resulting in the expectation that the RA level was not exceeding the subnanomolar range. Consequently, the influence on the neuronal differentiation potency by supplementation of DMSO as solvent had to be proven under these conditions (Fig. 23).

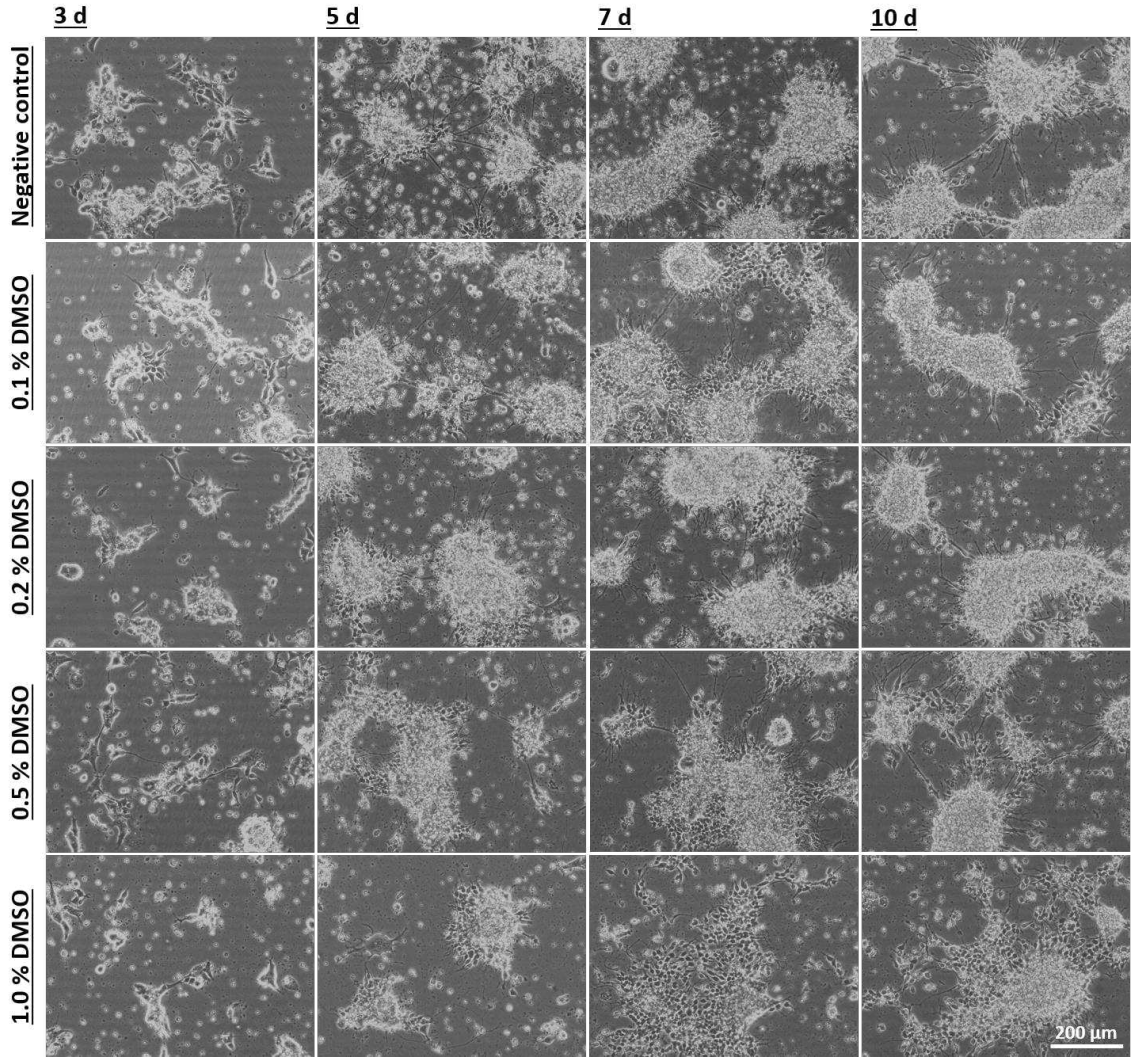

Figure 23: Effect of DMSO on neuronal differentiation by SD method. P19 cells were differentiated by SD method over ten days while treated with 0.1- 1 % DMSO. The SD medium with or w/o DMSO (negative control) was daily changed. Scale bar, 200 µm.

A concentration range of 0.1-1 % DMSO was added over ten days to the SD medium. During the first days of differentiation, no significant effect was detected up to 0.5 % DMSO (Fig. 23). Even with 0.5-1 % DMSO, just a slight difference was observed. Morphological changes caused by DMSO supplementation became clearly noticeable on the third day of treatment. With increasing DMSO concentration, the number of axons decreased dramatically while integrity of the cluster formations got lost. Polarised cells formed just loose clusters that demonstrated a lack of organisation. Neural rosettes formation appeared to be perturbed. Axons were randomly arranged and did not build up merged connections between clusters. Even the settled debris on top of cluster formations decreased. After five days treatment with 0.2 % and 1 % DMSO, cells with the morphology reminiscent on astrocyte phenotype were detected. Neuronal

differentiation did not appear to be inhibited by higher DMSO content, but rather delayed and disrupted. Treatment with 0.1 % DMSO displayed no morphological effect. To exclude an effect of the solvent, the critical concentration of 0.1 % was never exceeded in all implemented SD experiments.

Subsequently, the influence of several signalling pathway inhibitors was analysed. SB431542 is a potent inhibitor of TGF-β1 receptor ALK4, ALK5, and ALK7 (Du *et al.,* 2014). Thus, TGF-β-mediated activation of SMAD proteins was suppressed. SB431542 in combination with a BMP inhibitor is included in protocols of dual SMAD inhibition that induces or promotes neuronal differentiation of human pluripotent stem cells (Kim *et al.,* 2010; Pauly *et al.,* 2018). On the other hand, SB431542 was recently reported to partially inhibit RA response to neuronal differentiation of mESC (Du *et al.,* 2014). In this study, differentiation of P19 cells combined to treatment with SB431542 resulted in a reduced cell number at the beginning of the SD protocol (Fig. 24 A). While first connections between cell clusters were established in the negative control after three days, no evidence of neural induction was detected. Surprisingly, this culture caught up to the negative control within another three days. Hence, neuronal differentiation was only shortly impaired in the early SD protocol and not completely prevented by SMAD inhibition. In addition, SB431542 was added to the growth medium to analyse the response of undifferentiated P19 cells (Fig. 24 B). Compared to differentiating cells, the opposite effect was observed. While the cell number was only slightly reduced by day three, the negative influence increased over time.

Cyclopamine is a hedgehog (Hh) pathway antagonist. Hh signalling is required for the differentiation of ES cells into neurectoderm (Maye *et al.,* 2004). Inhibition was reported to prevent response to RA treatment and results in the arrest at primitive ectoderm stage (Maye *et al.,* 2004). The ability to induce neuronal differentiation by the SD method appeared to be abolished by cyclopamine treatment (Fig. 24 A). Supplementation of cyclopamine caused small cluster formations that partially detached and degenerated. Only a small number survived under these circumstances. Afterwards, the remaining cluster dissolved and only a few suffering single cells remain. Consequently, induction of neuronal differentiation was prevented by cyclopamine mediated Hh inhibition. Native cells were shown to be not affected by cyclopamine treatment (Fig. 24B).

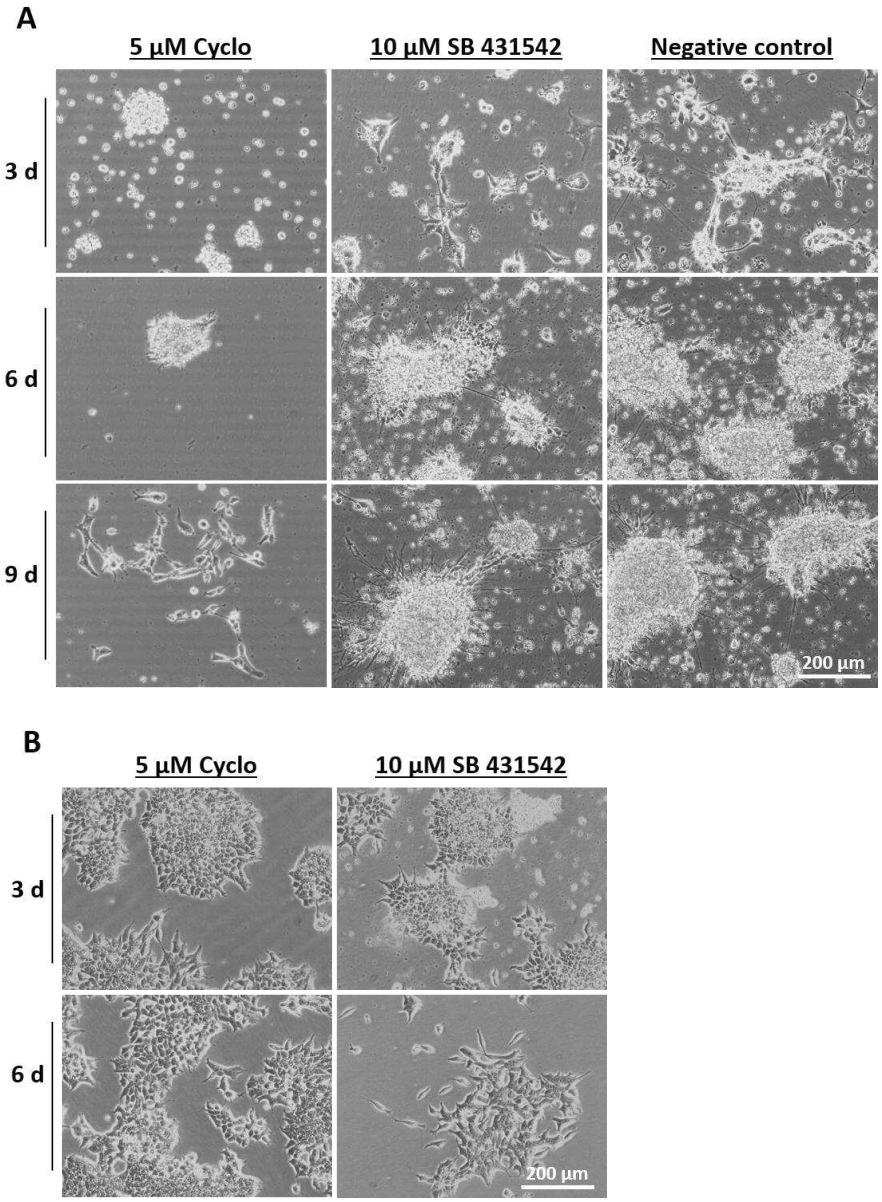

Figure 24: Effect of SMAD and Hh inhibition on neural induction by SD method. P19 cells were treated with 10 µM of the SMAD inhibitor SB431542 and 5 µM of the Hh inhibitor cyclopamine, supplemented to **(A)** SD medium and **(B)** growth medium. Scale bar, 200 µm.

Furthermore, the influence of three inhibitors was analysed that are known to have a promoting effect on neuronal differentiation. XAV939, is a tankyrase inhibitor that downregulates Wnt/β-catenin signalling. XAV939 was reported to enhance neuronal differentiation of ESC (Song *et al.,* 2018). DMH1 (dorsomorphin homolog 1), is a selective activin receptor-like kinase 2 (ALK2) inhibitor that has been used for inhibition of the bone morphogenetic protein (BMP). This molecule is able to induce neuronal differentiation of hiPSC (Neely *et al.,* 2012). DAPT is a γ-secretase inhibitor and indirectly inhibits Notch signalling. DAPT is implemented to promote cardiac as well as neuronal differentiation (Crawford *et al.,* 2007; Liu *et al.,* 2014). DAPT supplementation is also included in the protocol of Nakayama *et al.* (2014) because it revealed to be essential for the neurite development under their established conditions. By application of the SD method, these three inhibitors showed neither a positive nor a negative effect on

neuronal induction. In summary, the solvent DMSO displayed a critical concentration of 0.1 % in SD medium. None of the signalling pathway inhibitors presented an enhancing effect on neuronal differentiation by implementation of the SD method. SB431542 (TGFβ inhibition) and cyclopamine (Hh inhibition) had a partially negative effect on neurogenesis.

3.1.9 The ROS level influenced the potential to induce neuronal differentiation

Several studies demonstrated that the intrinsic ROS level and therefore the regulation of oxidative stress response has a strong impact on the potential to differentiate to neuronal fate (Bell *et al.,* 2015; Hu *et al.,* 2017; Oswald *et al.,* 2018). Recently, it has been shown that lowering ROS levels by antioxidants has neuroprotective effects in neurons while delaying or inhibiting the neuronal differentiation process (Bell *et al.,* 2015; Chiarotto *et al.,* 2014, Shaban *et al.,* 2017; Velusamy *et al.,* 2017). In this study, the effect of an increased and decreased ROS level on neuronal differentiation of the P19 cells by implementation of the SD method was investigated. Initially, the ROS level was attenuated by supplementation of the antioxidants tiron (1,2-dihydroxybenzene-3,5-disulfonate) and tempol (4-Hydroxy-2,2,6,6-tetramethylpiperidine-1-oxyl). Tiron, a vitamin E analogue, acts as a direct hydroxyl radical and superoxide scavenger (Krishna *et al.,* 1992). Lately, an upregulation of the Nrf2 pathway by tiron was reported (Khaled *et al.,* 2020; Mohamed *et al.,* 2020). Tempol, a nitroxide that, like tiron, functions as superoxide scavenger, is characterised by neuroprotective properties (Chiarotto *et al.,* 2014). The antioxidants tiron and tempol were mixed in SD medium and freshly added every day. The effect of both antioxidants seemed to be equal but in a different dose-dependent manner (tiron presented a stronger effect at the same concentration). In high concentrations (≥ 1 mM), cells just round up and die within hours. Also, treatment with a concentration of 500 µM caused reduced cell sizes, resulting in degeneration of all cells within 48 h. By decreasing the concentration to 50 µM tempol and 100 µM tiron, the shape and cell size appeared to be affected (Fig. 25). The size of cells was reduced and cells presented a round or unipolar morphology after 24 h of treatment. The proliferation of the cells until the third day was not affected by the antioxidants but the switch to a neuronal phenotype totally failed and cells started to degenerate completely. In lower concentrations (10 µM tempol and 50 µM tiron), a significant difference to negative control was observed from the fifth day of differentiation. In this concentration range, the neuronal differentiation event was not prevented by antioxidant exposure, but the cluster size decreased due to a reduced number of cells that survived the differentiation process. Furthermore, the branching pattern appeared strongly attenuated.

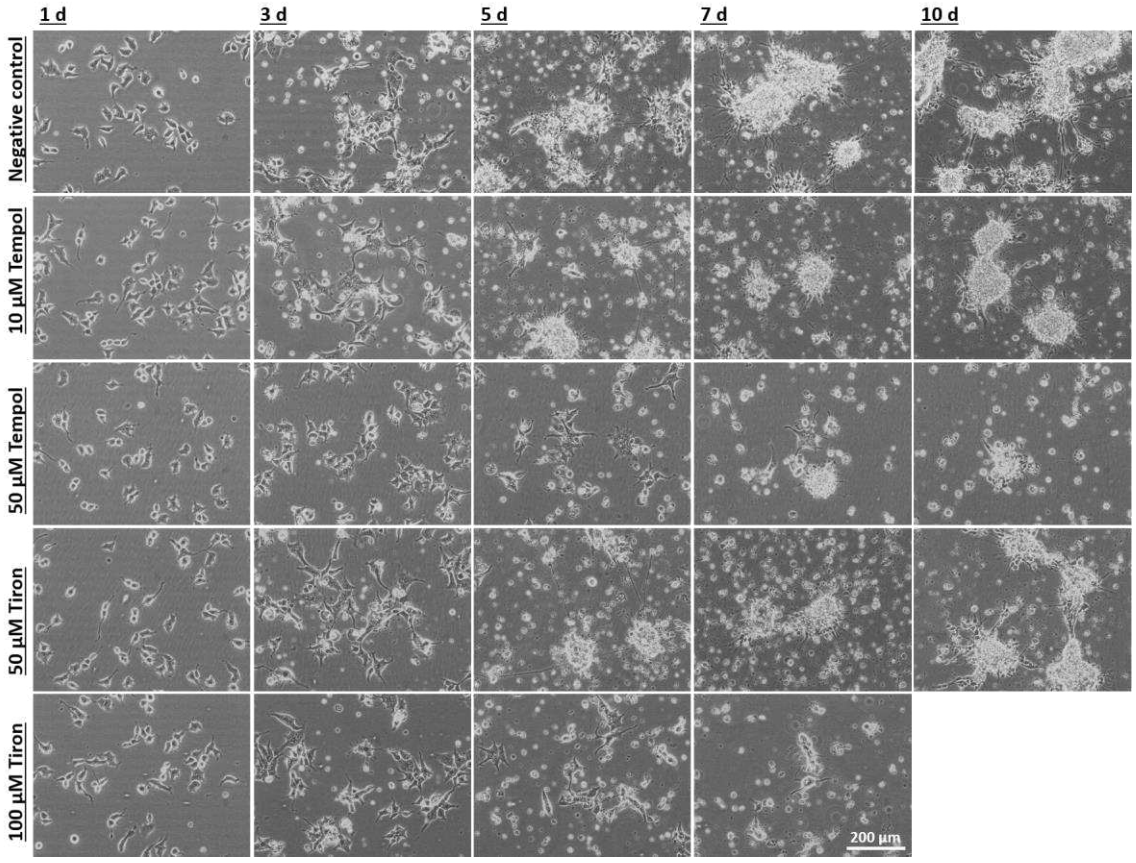

Figure 25: Influence of antioxidants on neuronal differentiation of P19 cells treated by SD method. SD medium was supplemented with the antioxidants tiron (50-100 µM) or tempol (10-50 µM) and changed on a daily base. Scale bar, 200 µm.

A crosscheck with P19 cells in the undifferentiated state showed that survival and proliferation of these pluripotent cells was also diminished by a high antioxidant concentration (Fig. 26). Altogether, high antioxidant concentrations affected cell survival of undifferentiated as well as P19 cells that are treated by the SD method. Neuronal differentiation appeared to be impaired by antioxidant exposure in a dose-dependent manner.

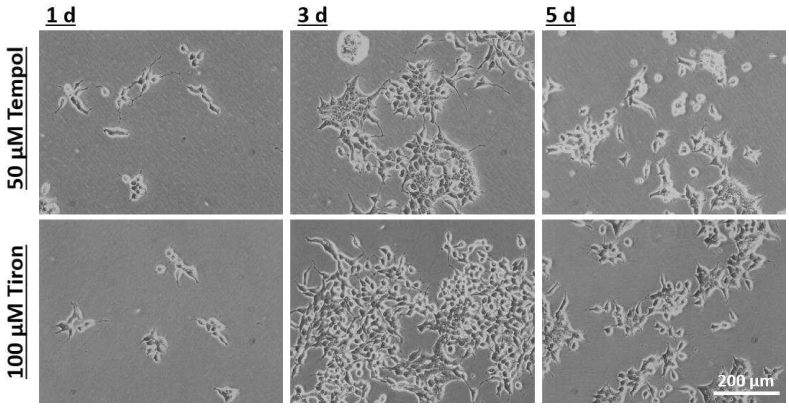

Figure 26: Influence of antioxidants on the proliferation of undifferentiated P19 cells. Growth medium was supplemented with 100 µM tiron or 50 µM tempol. The growth medium, supplemented with these antioxidants, was daily changed and cells were passaged at day four. Scale bar, 200 µm.

Furthermore, the influence of an increased ROS level was investigated by the generation of a *Nrf2* knockout mutant. NRF2 is a transcription factor that regulates oxidative stress defence and drug detoxification (He *et al.,* 2020). A *Nrf2* knockdown in hESC was reported to promote spontaneous neuronal differentiation (Hu *et al.,* 2017). This fits to the observation that *Nrf2* expression is constantly decreased during neuronal differentiation process (Olguín-Albuerne and Morán, 2018). In this study, a *Nrf2* knockout was implemented in P19 cells by usage of the CRISPR/Cas9-System. Deletion of three sequences of the *Nrf2* gene were achieved. Initially, success was controlled by sequencing. For each deletion, approximately 500 bp surrounding the targeted gRNA sequences were amplified and subsequently sequenced. Six picked clones were analysed by sequencing but none of them showed complete deletion of all three gRNA sequences. Subsequently, four of the most promising candidates were analysed by immunoblotting to prove whether *Nrf2* expression was inhibited (Fig. 27 B). The signal, detected with the usage of NRF2 antibodies was quite weak in WT. But no signal was detected for the two knockout mutants C3 and C4. Despite the similarities at the expression level, the sequencing results of clone 3 and 4 showed a completely different pattern (Fig. 27 A). While only several base pairs got deleted or replaced in the gRNA3 sequence of clone 4, this sequence in clone 3 was not affected. However, with the addition that the gRNA1 sequence was completely deleted and gRNA2 was partially eliminated in clone 3. The differences in the results of sequencing and immunoblotting highlighted the significance of knockout verification on protein and DNA level as well as the analysis of more than one verified clone. In conjunction with the sequencing results, it was assumed that the expression of the transcription factor was supressed in both clones or that NRF2 was dysfunctional and degraded.

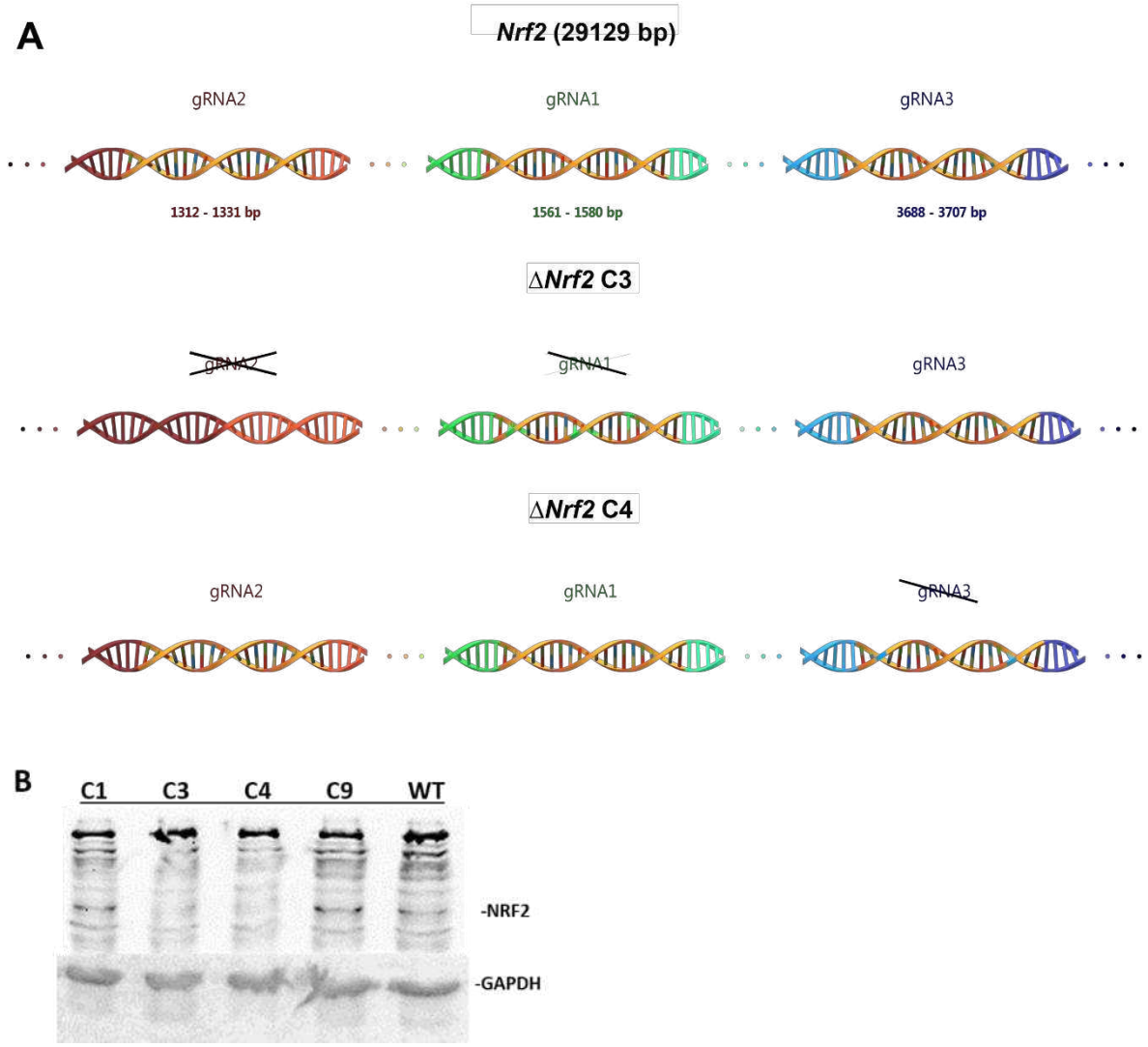

Figure 27: Verification of P19 *Nrf2* knockout mutant. A *Nrf2* knockout was implemented by deletion of three gRNA sequences within the *Nrf2* gene by usage of the CRISPR/Cas9-System. **A:** Verification of several picked clones of the Δ*Nrf2* knockout mutant on DNA level was implemented by amplification and sequencing of approximately 500 bp around the gRNA sequences. The complete gRNA1 sequence was deleted and several single bp were affected in gRNA2, for clone 3. Clone 4 showed only deletions of several bp in gRNA3. **B:** Immunoblotting with NRF2-antibodies was implemented to verify both clones (C3 and C4) on protein level by loss of the signal. Detection of GAPDH was used as loading control.

Initially, both verified *Nrf2* knockout mutants were culture in growth medium. The morphological phenotype of the knockout mutant displayed no significant differences to WT cells under these circumstances (Fig. 28 A). No evidence of spontaneous neuronal differentiation of the *Nrf2* knockout (KO) mutant was noted. In contrast to this observation, the influence of the *Nrf2* KO on neuronal differentiation by usage of the SD method clearly was pronounced (Fig. 28 B). Remarkably, the analysed mutants showed an inconsistent neuronal development that differs in both cases significantly from WT. While proliferation of the progenitor cells appeared to be reduced for C3, it was shown to be enhanced in C4. Both investigated clones did not lose their ability to switch to neuronal fate even if cell survival during differentiation process was promoted or attenuated through the knockout of *Nrf2*. In contrast to this observation, the survival of

mature neurons seemed to be negatively affected in both cases, as first signs of neurodegeneration appeared already after two weeks.

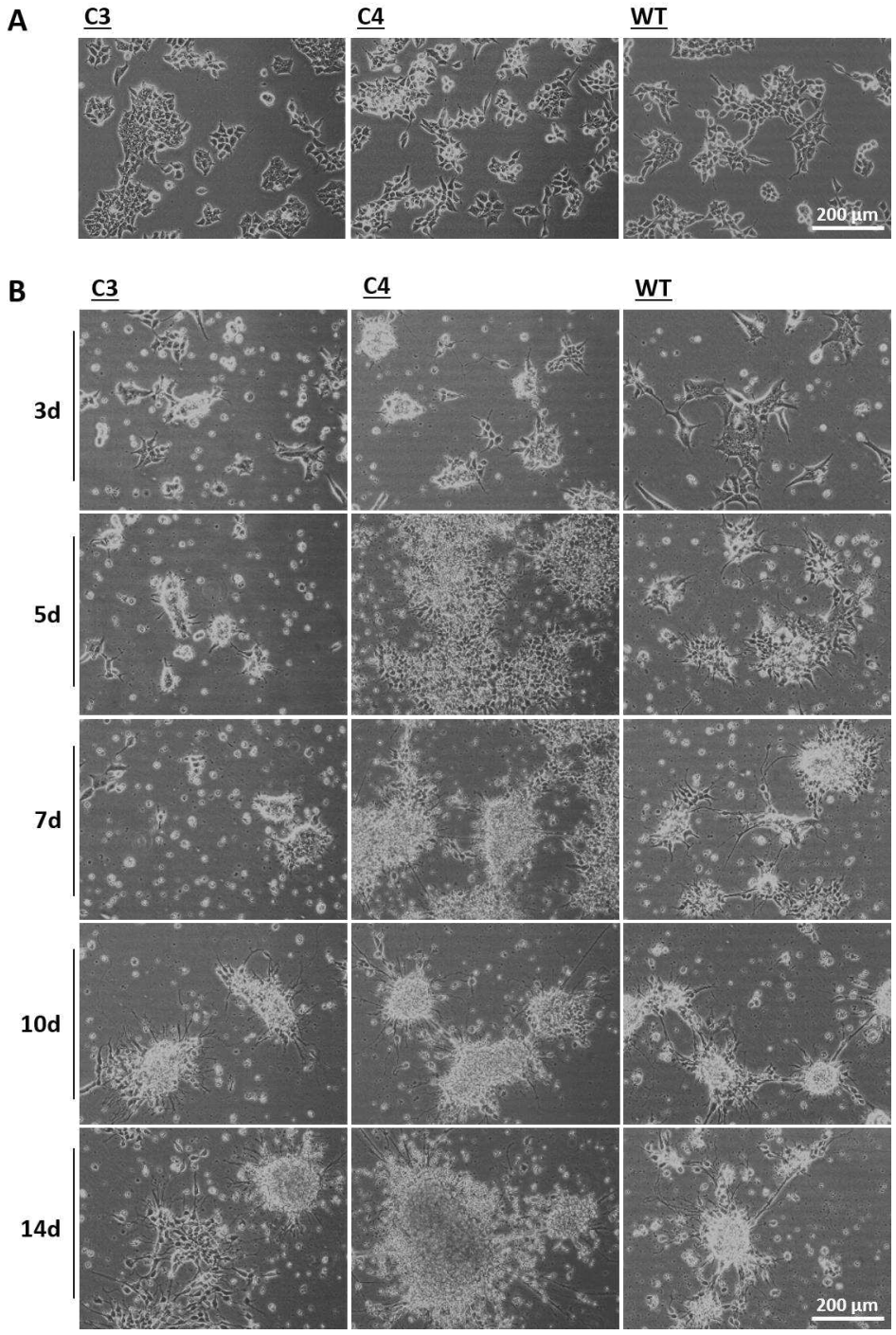

Figure 28: Neuronal induction in the generated Δ*Nrf2* knockout mutant. Two verified clones of the generated Δ*Nrf2* knockdown mutant (C3 and C4) were analysed in comparison to wildtype (WT) P19 cells. **A:** Cells were cultured in growth medium. **B:** Neuronal differentiation was induced by treatment with the SD protocol. Scale bar, 200 µM

Overall, these observations suggest that neuronal differentiation of P19 cells using the SD method, as well as survival of mature neurons, was dependent on ROS level. Supplementation of high antioxidant concentrations resulted in reduced cell survival

and prevented induction of neuronal differentiation while potential and branching growth was attenuated in lower dose. *Nrf2* knockdown was found to have no negative effect on neuronal induction but to affect survival during the process as well as in mature neurons. Spontaneous neuronal differentiation in growth medium was not observed for the mutant. Verification on DNA and protein level as well as the investigation of more than one clone appeared to be highly recommended since the behaviour of these clones was highly variable. Beside the well-known issue with off-targets, further unwanted events were recently revealed that result in deletion of large DNA sequences besides the targeted fragments (Adikusuma *et al.,* 2018). This might explain the differences in characteristics of the analysed clones.

3.2 Neuronal differentiation of mESC by implementation of the SD method

Induction of neuronal differentiation by the SD method revealed to be highly efficient in P19 embryonal carcinoma cells. To prove whether a successful neuronal induction by this method was limited on this carcinoma cell line or neuronal fate decision was caused by a common mechanism, the SD method was applied on mouse ESC.

3.2.1 Neuronal differentiation of mESC was induced in an improved SD medium

Compared to P19 cells, pluripotent ESC require higher media standards. The same was observed for neuronal differentiation using the SD method. The ESC were not able to proliferate and started to fully degenerate in SD medium within two days. It was figured out that survival of the ESC was dependent on distinct supplements that were then included in the used growth medium. β-mercaptoethanol, bovine serum albumin (BSA) and non-essential amino acids (NEAA) were additionally supplemented to SD medium. β-mercaptoethanol is a reducing agent that displays a slight toxic effect. Thus, β-mercaptoethanol has to be combined with BSA to buffer this effect (Chen *et al.* 2011). NEAA likewise demonstrated a positive effect on cell survival. Furthermore, these cells demonstrated a high preference to rhVTN over PLL or any other coating substrate. In addition, an increased DMEM/F12+ (including the N2 supplement) ratio in SD medium revealed to be necessary. Due to the limited ESC resources in this work, the perfect ratio of these two media connections was not examined. To ensure survival of the ESC, a high ratio of eight parts DMEM/F12+ to two parts EBSS was chosen. In any case, treatment with the adapted SD medium was shown to induce neuronal differentiation in ESC quite efficiently (Fig. 29; supplemental movie S4).

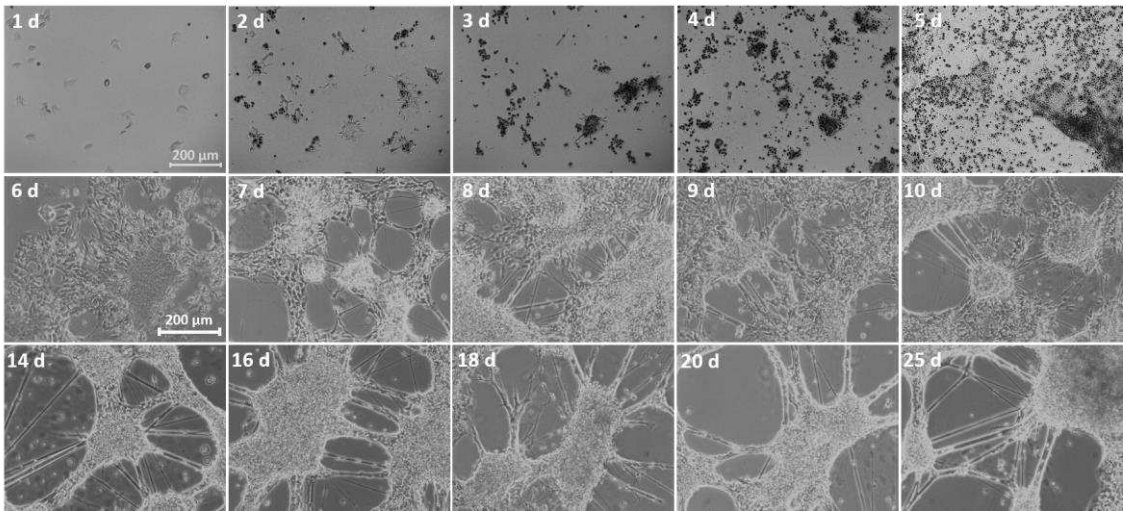

Figure 29: Pluripotent mESC differentiate to neurons by implementation of the SD method. mESC were differentiated on rhVTN coated culture dishes with an adapted SD medium. Imaging by confocal microscopy (10x objective) over the first 5 days with the Zeiss Observer Z1 microscope was followed by usage of the Nikon ECLIPSE TS 100 microscope until day 25. Imaging started 24 h after cell seeding (1 d). Scale bar, 200 µm.

ESCs, treated with the SD method, showed morphologically the same course as observed for P19 cells. This means the appearance of cluster formations and cell polarisation accompanied by a high degeneration level followed by neural rosette stage and the generation of neuronal networks with strong branching pattern. Furthermore, like for ECC, the ESC-derived neurons appeared to be stable for at least 25 days after induction. Size and shape of the generated cell cluster varied slightly compared to the mainly round arranged cluster formations of the carcinoma cells. In the ESC-derived neuronal culture, partially patches with morphologically distinct cells beneath the neurons were detected. A lack of purity in this neuronal culture was probably attributed to a high DMEM/F12+ level, because P19 cells were showing a quite comparable effect under this condition (chapter 4.1.2). Recording of the neuronal differentiation process in ESC showed further deviations from the observations of P19 cells. In some cases, individual cells appeared that differed in size and behaviour. These cells exhibited a much larger cells size and a cell shape reminiscent of astrocytes and revealed to be very mobile, switching between neuronal cell cluster. Another effect restricted to ESC-derived neuronal cultures was the creation of cavities probably beneath the cell clusters in a few instances (see movie S4). The volume of the cavity extended until it finally collapsed, and the process started again. Function or reason of this unexpected observation remained unclear. In conclusion, the SD protocol had to be slightly adapted on the demands of ESC to ensure cell survival during the differentiation process. Decreased purity of the culture is probably caused by the high DMEM/F12+ ratio and has to be adjusted for ESC in future. Anyway, ESC treated by SD method presented morphologically the same development of a neuronal phenotype as observed in P19 cells. Accordingly, neuronal induction by SD method without the requirement of RA supplementation or EB formation, demonstrated to be also highly efficient in ESC. Thus, this approach most likely reflects not a unique effect of the ECC line P19 but rather a general mechanism in pluripotent cells.

3.2.2 Immunofluorescence staining of neuronal marker in mESC-derived neurons

To verify the identity of ESC-derived neurons, pro-neuronal molecular markers were detected by immunofluorescence staining after application of the SD method over two weeks (Fig. 30). Analysis included the same markers as the one used for P19-derived cells (chapter 3.1.5). The markers NeuroD, Neurogenin2, ASCL1, Nestin and acetylated α-tubulin were expressed in ESC-derived neurons. Majority of the ESC ended up in neuronal fate. In some cases, however, patches of thin cell layers were observed in the background which were hardly detectable by this approach (see Fig. 30 A: NeuroD; 10x objective). These cells displayed a divergent morphology and arrangement compared to native as well as neuronal differentiated cells in this culture. Astrocytes were detected sporadically by GFAP at the edge of some neuronal cluster formations. This confirmed the observation that cells with a phenotype reminiscent of astrocytes occasionally appeared in this culture (chapter 3.2.1). Like mentioned above, the generation of non-neuron cells was probably caused by a high DMEM/F12+ level in the used SD medium for ESC.

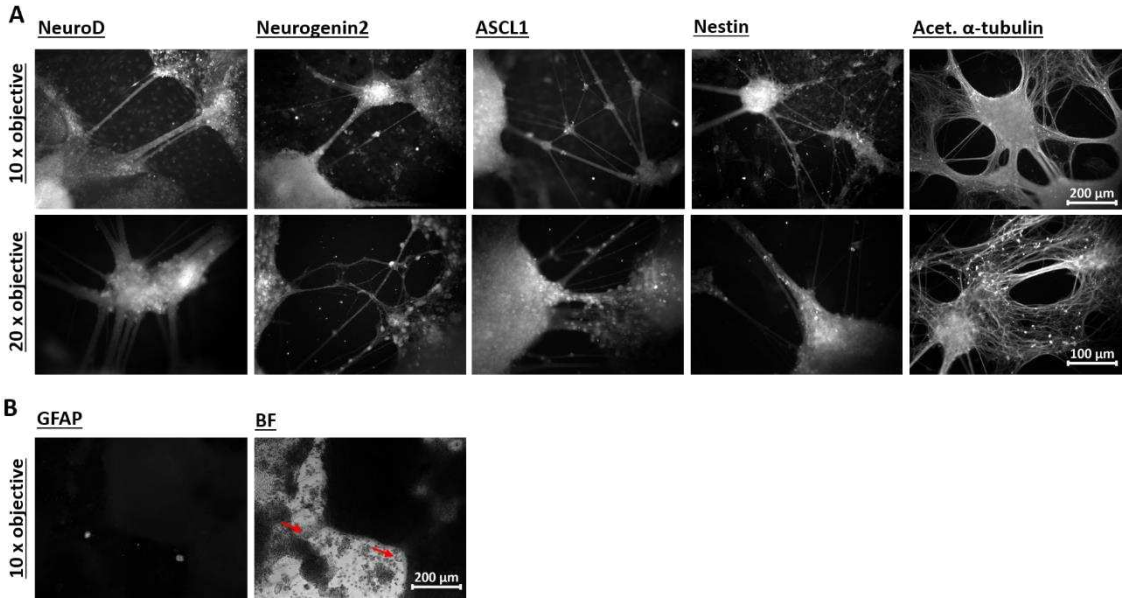

Figure 30: Immunofluorescence staining of ESC-derived neurons. A: The expressed neuronal markers NeuroD, Neurogenin2, ASCL1, Nestin, and acetylated α-tubulin were stained and imaged (10x and 20x objective). Scale bar, 100-200 µm. **B:** GFAP is an astrocyte marker. Comparison to brightfield (BF) view (40x objective) shows that astrocytes were sporadically detected. Scale bar, 50 µm.

The staining of neuronal expressed proteins strengthens the perception from morphological development of a neuronal culture derived from ESC. Therefore, the mechanism of neuronal induction by implementation of the SD method could besides the ECC line P19 also be verified in ESC. Consequently, the hypothesis that the SD method covers a common mechanism of neuronal induction in pluripotent cells appeared more likely.

3.3 Cell death in neuronal development

In mammalian development, about half of the postmitotic neurons and mitotic neuronal precursor cells die (Buss *et al.,* 2006; Kuan *et al.,* 2000; Oppenheim, 1991; Sadoul,1998). The neuronal cell death is thereby restricted in time and to distinct sites in the developing CNS (Kuan *et al.,* 2000). In this study, neuronal differentiation process, induced *in vitro*, was also shaped by a high degeneration level, independent on the applied differentiation protocol. By usage of the SD differentiation protocol, developed in this work, a high degeneration level was observed, especially between the third to sixth day. SD medium had to be changed every 24 hours to prevent degeneration of the whole culture. Thereby, the main part of cell debris was removed. In brain, cell debris, generated through an injury, is cleared by microglial cells to prevent the induction of secondary neuronal cell death (Herzog *et al.,* 2019; Nimmerjahn *et al.,* 2005). No glial cells were detected by usage of the SD method. Therefore, it would be possible that produced cell debris could promote cell death of the remaining cells. The mechanism behind and which type of cell death these cells underwent was investigated in several experimental procedures to get a closer insight into the influence on neuronal differentiation process.

3.3.1 Deposit on neuronal cluster was identified as dead cells

Neuronal differentiation of P19 cells using the SD method resulted in a period of high degeneration level. During the first 48 hours, the culture remained stable due to a low degree of degeneration. Subsequently, cell death appeared to be highly induced, resulting in accumulating cell debris. Despite daily medium change, accumulated dead cells and cell debris in the differentiation medium could only be partially removed. Visually, it looked like the dead cells were deposited on the neuronal clusters. This assumption was reinforced by the observation that the deposition became significantly condensed on clusters in the middle of dish, where cells debris tended to accumulate. By aging of neuronal cultures, clusters increased in size through fusion of several ones, while the dense layer on top of this formations expanded vertically. The deposits began to appear yellowish in places and became darker over time. After it had settled, it could not be dissolved even by digestion with trypsin. To verify the assumption that dead cells deposit on top of remaining neuronal cluster formations, a neuronal culture was treated with trypan blue (Fig. 31). Trypan blue labels dead cells exclusively.

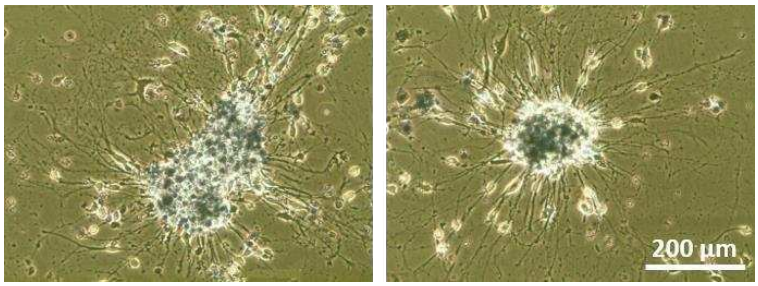

Figure 31: Trypan blue staining of neuronal cluster formations. A two-week-old neuronal culture, derived from P19 cells by application of the SD method, was treated with trypan blue. After the excess dye was washed out, dead cells that had taken up the blue dye were imaged. Scale bar, 200 µm.

The result clearly showed high amounts of death cells that have settled on neuronal cluster formations (Fig. 31). Cause or function of this occurrence remained obscure. In further experiments was investigated which form of cell death these cells underwent and the influence on neuronal differentiation process.

3.3.2 Monitoring of apoptotic and necrotic cell death in neuronal development

After demonstrating that dead cells were deposited on neuronal clusters, the form of cell death that these cells underwent was analysed. To discriminate between apoptotic and necrotic cell death and healthy cells, living cultures were stained at distinct time points of the neuronal differentiation protocol, from cell polarisation and cluster formation at the third day, over development to mature neurons, organised in neuronal networks, and finally to aged neurons 28 days after induction (Fig. 32). Whereas it should be noted, that necrotic as well as cells in a late apoptosis state were labelled by the green dye (7-AAD) because in both cases the loss of plasma membrane integrity allows the nucleus to be labelled. As previously noted during this work, the degeneration level increases abruptly on day three of SD protocol. The signal of apoptotic/necrotic cells at the third day was broadly distributed, with significant accumulation at clustered neuronal progenitors. Over time, the signal clearly concentrated on areas with vital cells. Monitoring the number of cells that underwent apoptotic or necrotic cell death showed a continuous increase over time while also the number of vital cells increased by proliferation. The denser and larger clusters appeared at age, the darker they appeared in the brightfield image and the larger the apoptotic/necrotic core became. Merging of the detected apoptotic and necrotic signals showed a complete match.

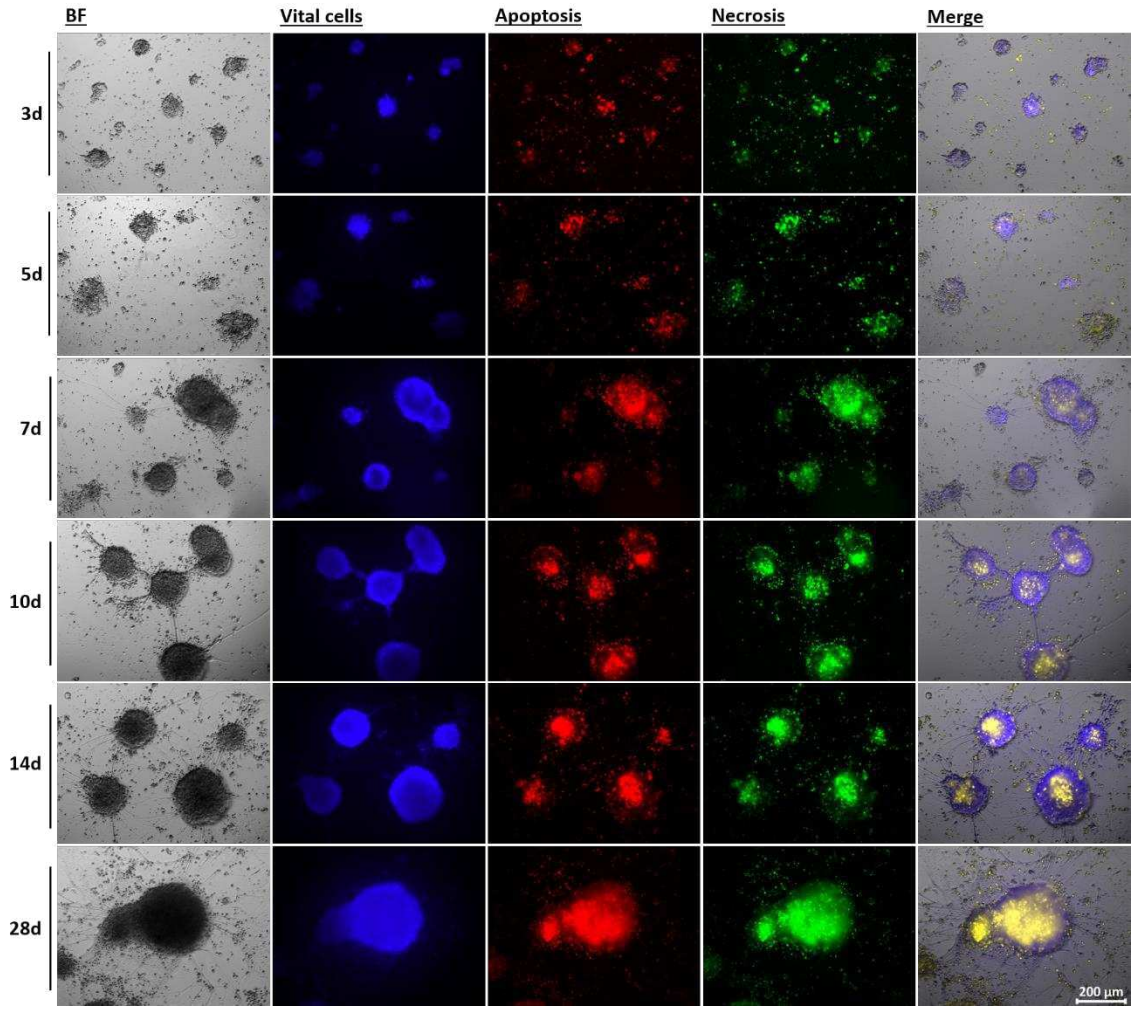

Figure 32: Apoptotic and necrotic cell death during neuronal differentiation. P19 cells were differentiated by applying the SD protocol. The increase in vital cells (blue) compared with cells that underwent apoptotic (red) or necrotic (green) cell death at several differentiation points was observed. The brightfield (BF) and fluorescence imaging was finally merged. The Cells were stained by usage of the Apoptosis/Necrosis Detection Kit (ab176750). Scale bar, 200 µm.

The clusters of healthy progenitor cells and neurons got tightly covered by an increasing layer of dead cells that deposit on these clusters. The complete overlap of the signals of apoptotic and necrotic cells indicated that necrosis was probably detected as an endpoint state of apoptotic cells that could not be removed. *In vivo* apoptotic bodies would be phagocytosed to clear the environment and prevent an inflammation (D'Arcy, 2019). Pure neuronal *in vitro* cultures are not able to free themselves from the cell debris. However, why cell debris accumulate and settle on neuronal clusters and how this influences the neurons, has remained relatively unnoticed in the field until now. Besides the detection of an increased level of apoptotic cells during the neuronal differentiation process, was furthermore the influence of the interplay between apoptosis and autophagy analysed (chapter 3.4.4 and 3.4.5).

3.3.3 Autophagy detection by LC3 immunofluorescence staining

The microtubule-associated protein 1A/1B-light chain 3 (MAP-LC3α/β), hereafter referred as LC3, is essential for autophagy and associated to the autophagosome membranes (Tanida *et al.,* 2008). Immunofluorescence staining was implemented to monitor autophagy by tracing LC3β in neuronal development (SD method). Signals from neuronal progenitor cells (3d) to mature neurons (14 d) were detected. At the beginning, the signal was quite moderate, slightly increasing from day seven onward (Fig. 33).

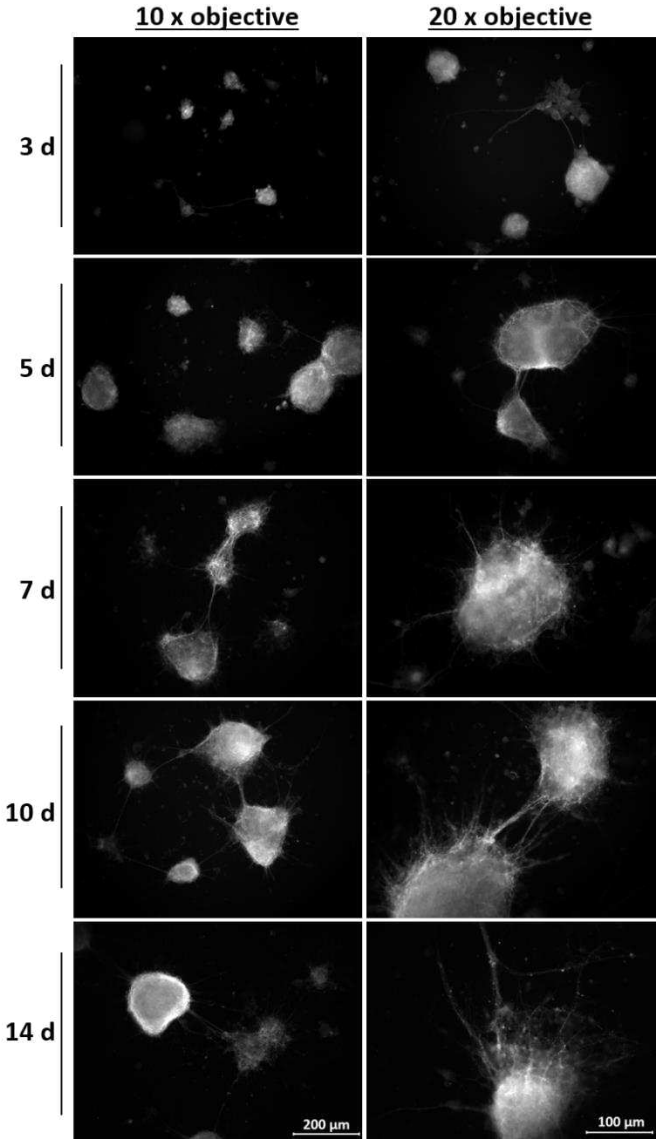

Figure 33: Immunofluorescence staining of LC3. Neuronal differentiation of P19 cells was implemented by the SD method. LC3β was detected by immunofluorescence staining in 3-14 day old neuronal cultures. Scale bar, 100-200 µm.

Interestingly, an inhomogeneous spread of the signal inside the clusters was detected. This was particularly visible at the fifth and seventh day, where the signal ran through the clusters like a knotted string of pearls. Strong signals were partially detected in the junctions. This reflects probably the transport of the autophagosomes from the distal axon towards the cell body (Ariosa and Klionsky, 2016). It could be possible that the

increase in signal strength was due to an accumulation of axons and dendrites within neuronal cluster formations. Signal strength appeared to increase only because of increasing cluster size. Monitoring of autophagy levels indicated a moderate increase over time but no sudden or tremendous changes during neuronal development. This result showed no significant increase at the stage of the highest degeneration level (3-6 d of the SD protocol), leading to the suggestion that apoptotic death may be predominantly responsible for the degeneration of cells in the differentiation process. In contrast to the observation that the autophagy level increases during neuronal differentiation (Zeng and Zhou, 2008), no significant alterations of the LC3 level were determined by this approach. But the LC3 level could be quantified in a further experimental procedure. Additionally, the impact of alterations of the autophagy level during neuronal differentiation was analysed in further studies.

3.4 Impact of altered autophagy levels on neuronal development

Several evidences suggest that autophagy plays a crucial role in neuronal development by regulating signalling pathways that are involved in the switch from pluripotent cells to neurons (Ban *et al.,* 2013; Fimia *et al.,* 2007). Some studies have reported that autophagy is upregulated during the initial period of neuronal differentiation and that its suppression, as well as further enhancement by mTOR inhibition, impairs it (Morgado *et al.,* 2015; Zeng and Zhou, 2008). In this study, the impact on neuronal differentiation of P19 cells by the SD method was proven with several autophagy inhibitors, enhancers and the generation and analysis of knockout mutants that lack the expression of autophagy relevant genes.

3.4.1 Treatment with autophagy inhibitors during early neuronal differentiation

P19 cells were treated with five different autophagy inhibitors during neuronal differentiation by SD protocol. 3-methyladenine (3-MA) inhibits the class I and III PI3K in different temporal pattern, while inhibition is limited of class I PI3K by treatment with LY294002 (Wu *et al.,* 2010). Akt1 is downstream of PI3K and is inhibited by A-674563, while it was reported that it also supresses the cyclin-dependent kinase 2 (CDK2) (Chorner and Moorehead, 2018). Chloroquine inhibits the autophagic flux by decreasing autophagosome-lysosome fusion (Mauthe *et al.,* 2018). STF-62247 accumulates in lysosomes and is a potent blocker of late stages of autophagy (Bouhamdani *et al.,* 2019). In this study, appropriate inhibitor concentrations were initially titrated. The inhibitors were supplemented over the whole experimental unit of two weeks (here not shown). In this case, it terminated in a complete degeneration of all cells after 10-14 days. This observation was independent of the chosen inhibitor. By limiting the inhibitor treatment on day two to four, the evoked phenotype during differentiation was still present, while early degeneration could be prevented. Treatment with any of the chosen autophagy inhibitors during early differentiation caused prematurely generation of neurites after already three days of the differentiation protocol that was followed by an axonal overgrowth, distinctly visible at day five (Fig. 34). But despite this large number of branches produced early, the neurites presented a lack of strength and organisation. After seven days, it came to an equalization to the negative control, in both cases, with

and without further inhibitor treatment after day five. Thenceforth, the generated neuronal networks were not significantly affected by the autophagy inhibition, while later on, all neurons degenerated by continuous inhibitor treatment.

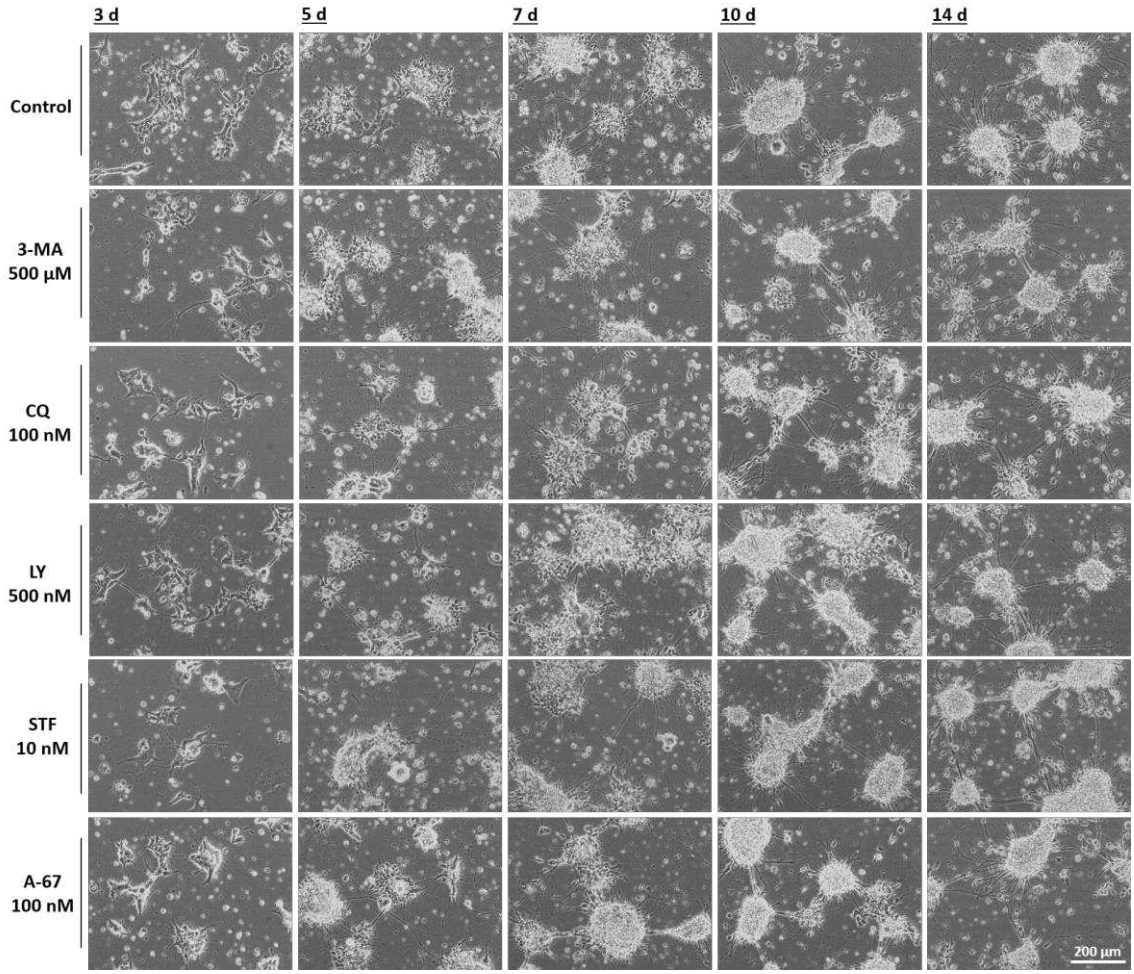

Figure 34: Autophagy inhibitor treatment during neuronal differentiation. P19 cells were differentiated by implementation of the SD protocol. Except for the control, the autophagy inhibitors 3-methyladenine (3-MA), chloroquine (CQ), LY294002 (LY), A-674563 (A-67), and STF-62247 (STF) were supplemented over three days (2-4 d). Scale bar, 200 µm.

In summary, no morphological differences were detected during the first two days of the differentiation protocol (w/ or w/o inhibitor), while an enhanced branching pattern was observed between the third and fifth day, until the phenotype of the control was nearly restored after seven days (w/ or w/o inhibitor). Therefore, neuronal differentiation was not impaired by autophagy inhibition and resulted in a period of an unorganised axonal overgrowth. The survival of mature neurons appeared to be strongly affected by autophagy inhibition. Hence, continuous inhibitor treatment resulted in early neuronal degeneration.

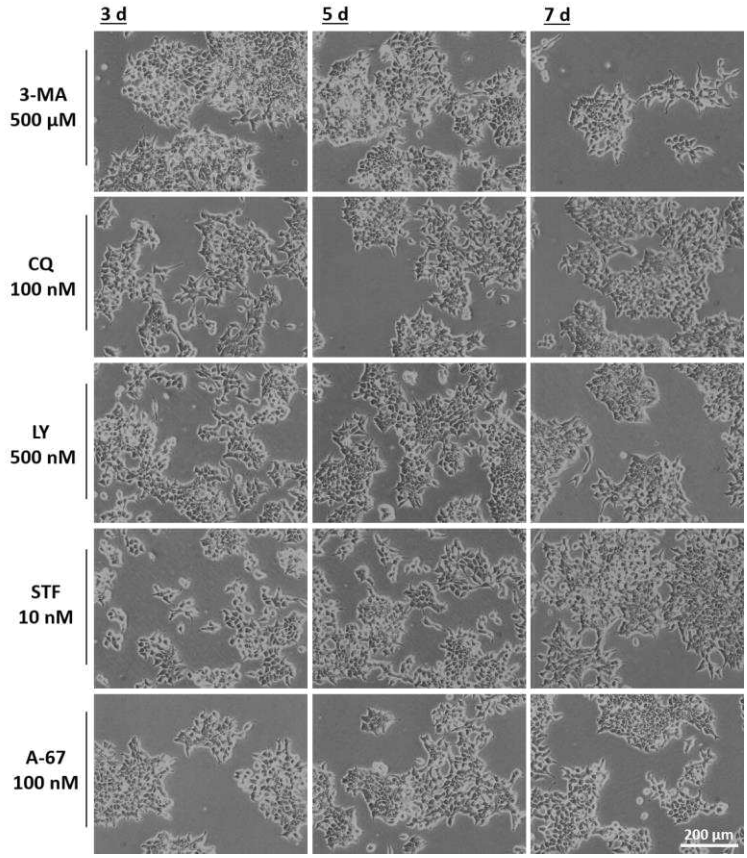

Figure 35: The effect of autophagy inhibitors on native P19 cells. Native P19 cells were grown in growth medium supplemented with the autophagy inhibitors 3-methyladenine (3-MA), chloroquine (CQ), LY294002 (LY), A-674563 (A-67), and STF-62247 (STF) over seven days. Cells were subdivided in between. Scale bar, 200 µm.

As usual, the chosen inhibitor concentration was used to prove whether it presents an effect on native P19 cells (Fig. 35). Cells were treated with the autophagy inhibitors over a whole week, while cells were subdivided in between. The cell morphology was not affected and beside a slightly increased degeneration level, no significant effect was detected.

3.4.2 Analysis of autophagy gene CRISPR knockout mutants

Another approach to investigate influence of autophagy inhibition in neurogenesis was the deletion of the autophagy genes *p62*, *Becl1*, *Atg7*, and *Atg9a* by usage of the CRISPR/Cas9 system. The cell morphology of the generated deletion mutants showed no significant differences compared to WT P19 cells (Fig. 36 A). For each gene knockout, several clones were picked and subsequently analysed on DNA and protein level for verification. For that reason, fragments with a size of about 500 bp that covers the targeted deletion sequence, were amplified and sequenced. The sequencing showed quite mixed results (Fig. 36 C).

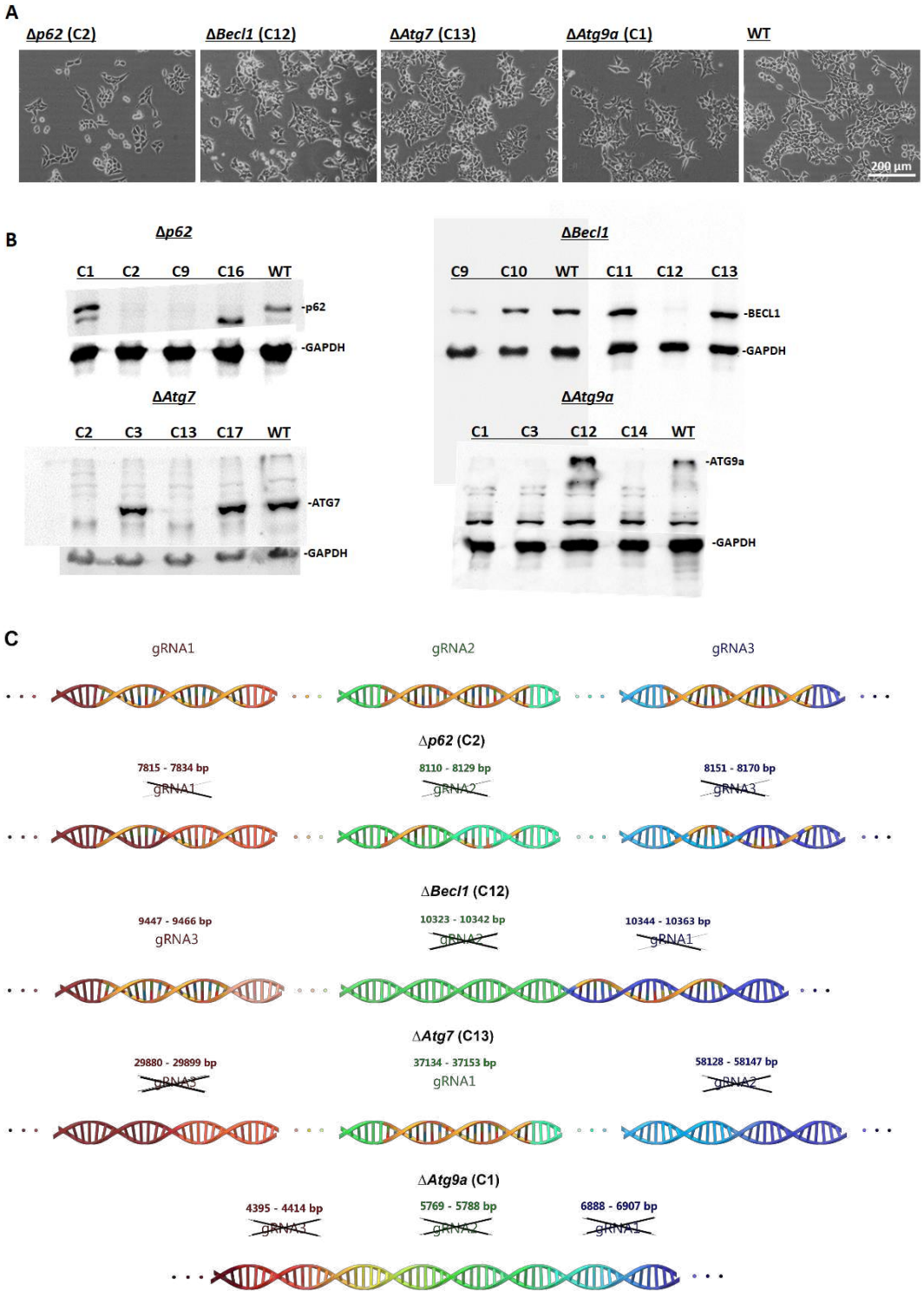

Figure 36: Verification of the generated autophagy gene CRISPR knockout mutants. For each gene knockout was one clone picked for further analysis that was verified by immunoblotting and sequencing *(Δp62* C2; Δ*Becl1* C12; Δ*Atg7* C13; Δ*Atg9a* C1). **A:** The selected mutants and the wildtype (WT) P19 cells were cultivated in growth medium without any significant differences in the expression of the phenotypes. Scale bar, 200 µm. **B:** Several knockout mutants were analysed by immunoblotting. GAPDH was used as loading control. **C:** The sequencing results of the selected mutants were depictured. The unicoloured areas described the adjacent sequence while the gRNA sequences were multicoloured illustrated.

It has to be noted that in none of all analysed clones, all three targeted gRNA sequences were sharply deleted like predicted. In some clones, one or two of the three gRNA sequences and sometimes even the regions around or between two targeted areas got deleted. In some cases, only some bases within these sequences were missing or replaced. The clones that revealed as the most promising were investigated by immunoblotting to preclude expression of an intact version of the targeted proteins (Fig. 36 B). Remarkably, clones with an identical DNA profile showed partially different profiles by immunoblotting and not always the most promising candidate from sequencing was verified on protein level. It clearly showed that a verification of CRISPR knockout mutants on protein level is crucial. For each gene knockout, the phenotype of three verified clones were analysed in native state and through the neuronal differentiation process. Because there was no significant difference between clones of a gene knockout mutant, one clone was selected in each case to compare morphology with WT cells (Fig. 37).

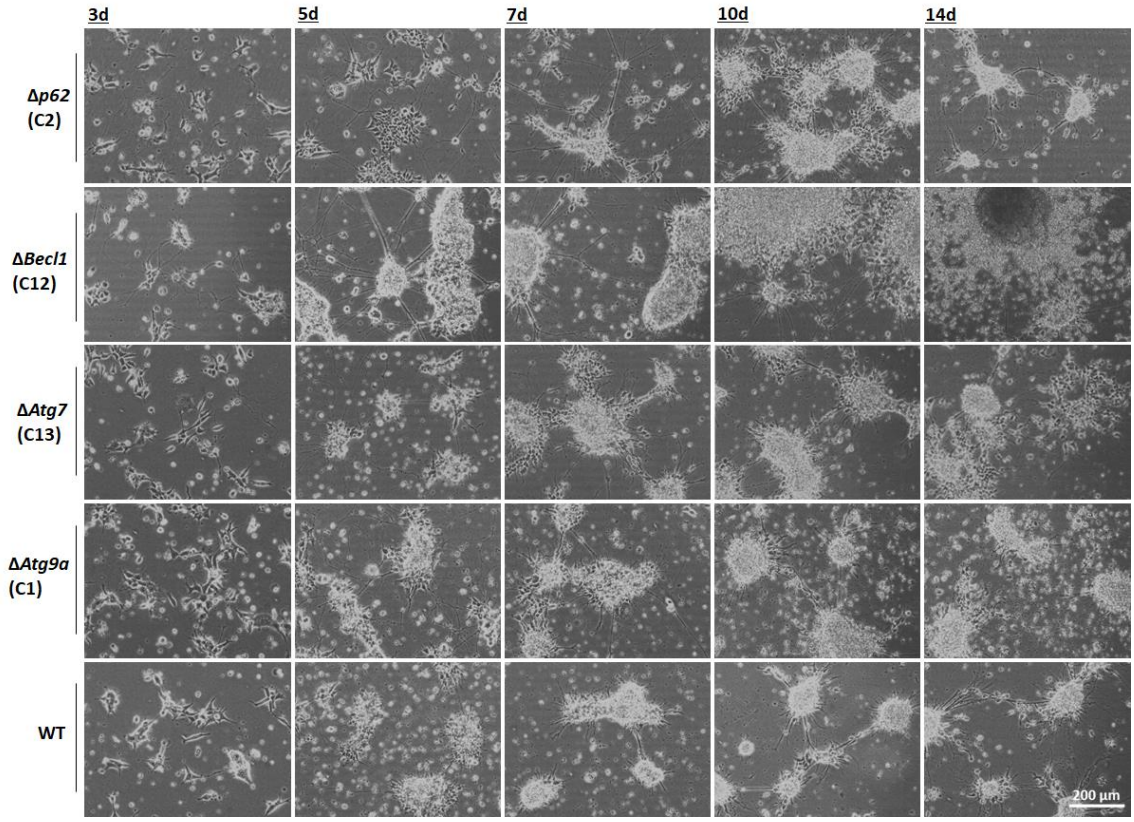

Figure 37: Neuronal differentiation of the generated autophagy gene CRISPR knockout mutants. The verified P19 knockout mutants Δ*p62* C2, Δ*Becl1* C12, Δ*Atg7* C13, Δ*Atg9a* C1, and wildtype (WT) cells were differentiated to neurons by implementation of the SD protocol. The knockout mutants showed an enhanced axonal branching after five days and early degeneration evidence after 10 days. Scale bar, 200 µm.

All autophagy genes knockout mutants (Δ*p62*, Δ*Becl1*, Δ*Atg7*, and Δ*Atg9a*) manifested a similar phenotype compared to WT that were treated with autophagy inhibitors over the whole differentiation process (see chapter 4.4.1). Prematurely branching started already after three days and led to the generation of a neuronal network within five days with a highly increased number of axons for this time point. At day seven of SD protocol,

it came to an alignment of the phenotypes of deletion mutants and WT. But while WT cells manifested a neuronal network, clusters of the knockout mutants started to lose their integrity and showed first signs of degeneration after ten days, followed by an early neuronal death caused by the lack of autophagy.

In conclusion, suppression of autophagy by inhibitors or by depletion of autophagy genes did not prevent neruonal differentiation. This observation fits to the recent reports that autophagy negatively regulates early axon growth by degradation of cytoskeletal components (Ban *et al.,* 2013; Chen *et al.,* 2013). Therefore, the loss of autophagy caused growth of longer axons but the accumulation of dysfunctional organelles and protein aggregates was probably leading to oxidative damage and finally to apoptotic cascades (Komatsu *et al.,* 2006; Maday, 2016). In contrast, the results in this study contradict with the report that suppression of autophagy impaired neuronal differentiation, while the process was delayed by knocking down *Becl1* (Zeng and Zhou). To get a deeper insight, further analysis of the impact of altered autophagy levels was realized by proteome analysis.

3.4.3 Treatment with autophagy enhancers during early neuronal differentiation

Autophagy was enhanced by inhibiting mTOR with drugs such as rapamycin or torin2 (Rubinsztein *et al.,* 2007). Low concentrations of rapamycin (0.5–100 nM) target mTORC1, while higher concentrations (0.2–20 µM) also inhibit mTORC2 (Foster and Toschi, 2009). Consequently, concentrations in both ranges were analysed (50 nM and 500 nM). Torin2 is a selective and very potent mTORC1 inhibitor and with an 800-fold less selectivity, it also inhibits PI3K (Liu *et al.,* 2011). Additionally, it was reported to inhibit proteins of the phosphatidylinositol-3 kinase–like kinase (PIKK) family (Liu *et al.,* 2013). As with autophagy inhibitors, autophagy enhancers were supplemented both throughout the differentiation process and during a limited period (day two to four), presenting the same phenotype in both cases. Treatment with both chosen rapamycin concentrations (50 nM and 500 nM) or high concentrations of 5-20 nM torin2 negatively affected survival during neuronal differentiation of P19 cells (Fig. 38). The impact of both inhibitors in this concentration range was quite similar. Evidence of induction of neuronal differentiation were observed but these cells barely survived the differentiation process and completely degenerated after cells passed the first week of the differentiation protocol (Fig. 38). Even limitation of inhibitor treatment on day two to four could not prevent an early cell death. After three days of treatment with 500 nM rapamycin, only strongly polarised single cells were left while at least some small clusters were generated by lower rapamycin doses. If mTORC2 was supressed by higher rapamycin concentrations under these conditions remained elusive. Remarkably, the impact of torin2 in a low concentration of 0.5 nM was more comparable to the effect of the autophagy inhibitors. Derived neurons under this circumstance showed an enhanced axonal outgrowth at day five, followed by an early degeneration evidence.

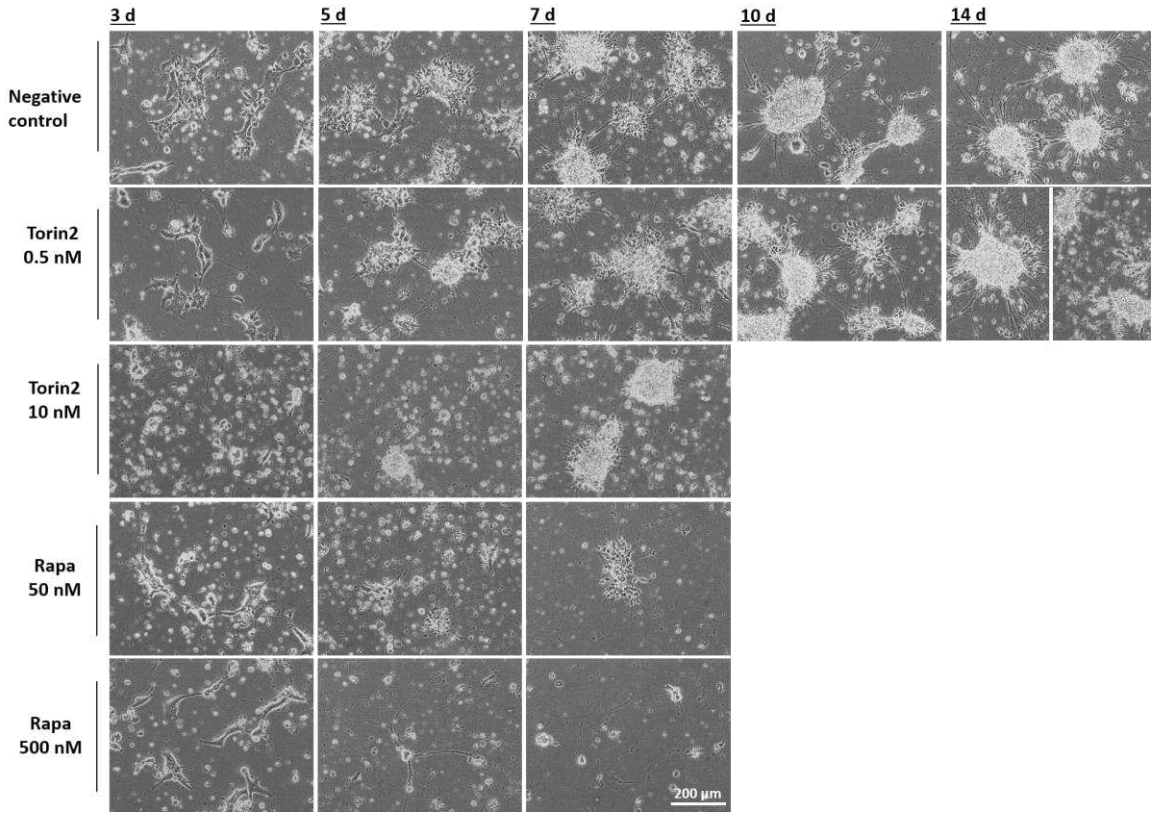

Figure 38: Autophagy enhancer treatment during neuronal differentiation. P19 cells were differentiated by application of the SD protocol. Except for negative control, the autophagy enhancers rapamycin (50 and 500 nM) and torin2 (0.5 and 10 nM) were supplemented over three days (2-4 d). Scale bar, 200 µm.

As always, the influence of these inhibitors on native cells was proven (Fig. 39). Rapamycin and torin2 slightly increased the degeneration level of undifferentiated cells but was not preventing the maintenance of a growing culture.

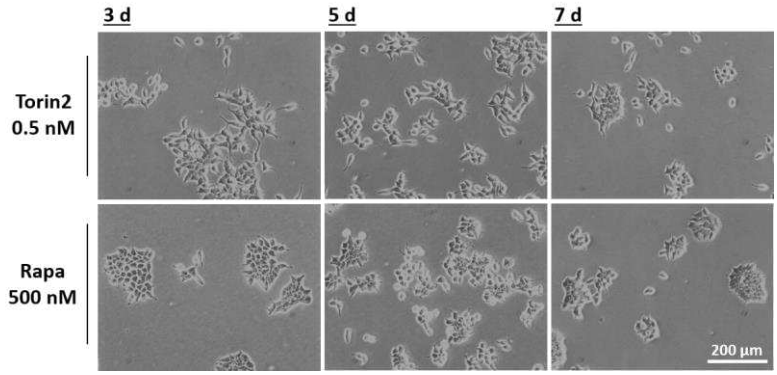

Figure 39: The effect of autophagy enhancers on native P19 cells. Native P19 cells were cultured in growth medium supplemented with the autophagy enhancers rapamycin and torin2 over seven days. Cells were subdivided in between. Scale bar, 200 µm.

Beforehand, it was reported that mTOR signalling is downregulated through the neuronal differentiation process and that further downregulation in N2a cells impairs neuronal differentiation (Zeng and Zhou, 2008). In contrast, the autophagy enhancer seemed not to prevent the induction of neuronal differentiation of P19 cells in this experiment, while it negatively affected survival of cells that underwent neuronal cell

fate decision. Other reports claimed that activation of the autophagy pathway with rapamycin results in shorter neurites (Ban *et al.,* 2013; Chen *et al.,* 2013). This could be confirmed for the generated cluster formations under inhibitor treatment but there were also single cells with long neurites detected.

3.4.4 Analysis of a *BirC6* CRISPR knockout mutant

In addition to the mTOR inhibitors rapamycin and Torin2, another approach was taken to increase autophagy levels. BIRC6 negatively regulates autophagy. Therefore, depletion of *BirC6* is supposed to rise the autophagy activity by increasing the level of cytosolic LC3β-I (Jia and Bonifacino, 2019). A *BirC6* knockout was generated using the CRISPR/Cas9 System. The *BirC6* deletion was verified on DNA level by sequencing and on protein level by immunoblotting (Fig. 40). The clones 3 and 5 (C3 and C5), were confirmed through a lack of BIRC6 detection by immunoblotting, while presenting totally different sequencing results. In C5, the sequences of gRNA1 and gRNA3 were completely deleted, while for C3 only some base in the gRNA1 sequence were missing. Proliferation in growth medium appeared to be reduced for both clones. While C3 displayed a divergent cell morphology with increased cell size and partially multipolar shape, C5 presented like WT a more bipolar shape. On the other hand, the cell arrangement of C5 showed a lack of cohesion.

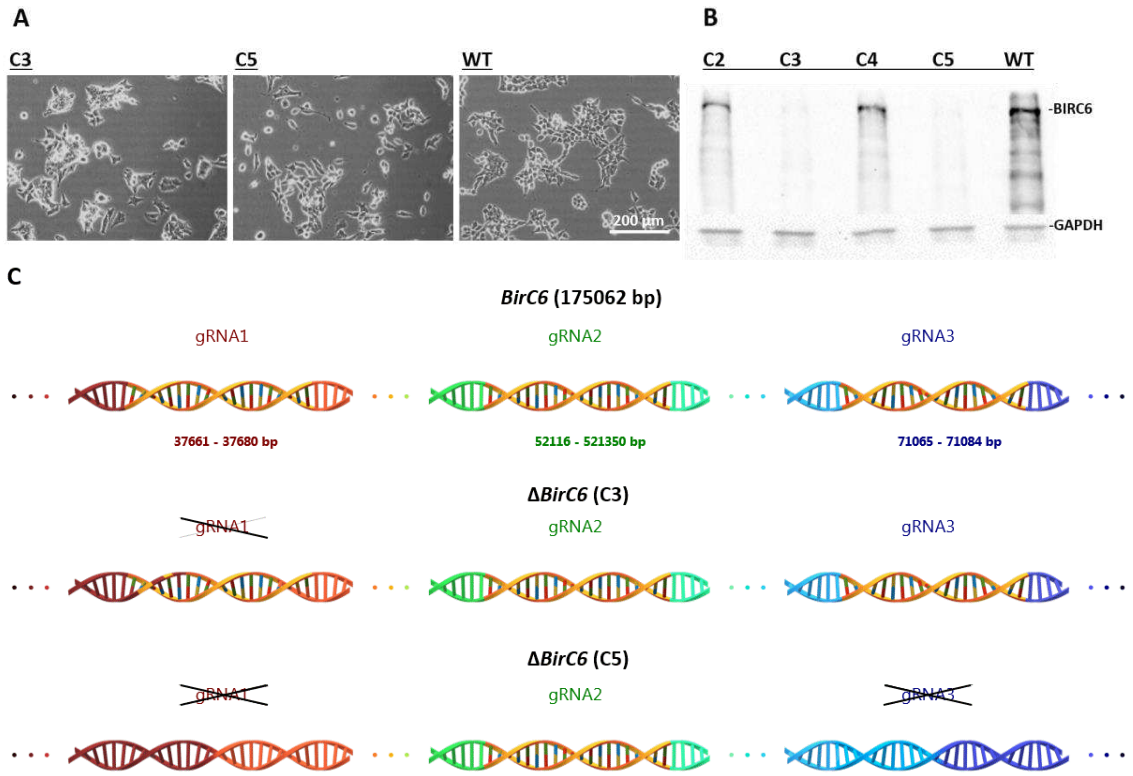

Figure 40: Verification of the generated *BirC6* CRISPR knockout mutant. Two clones of the Δ*BirC6* mutant (C3 and C5) that were picked for further analysis were verified by immunoblotting and sequencing. **A:** The selected Δ*BirC6* clones and P19 WT cells were cultivated in growth medium. The phenotype of the mutants appeared affected, and the proliferation rate significantly reduced. Scale bar, 200 µm. **B:** The knockout in C3 and C5 was verified by immunoblotting of several Δ*BirC6* clones. GAPDH was used as loading control. **C:** The sequencing results of the two selected mutants are depicted. The unicoloured areas described the adjacent sequence while the gRNA sequences were multicoloured.

Furthermore, both analysed clones shared common features as well as varieties when treated by SD protocol. Compared to WT, the neuronal differentiation process was diminished and retarded (Fig. 41). Δ*BirC6* clone 3 generated cell clusters that were characterised by multitude pseudopodia. Phenotype and cell number did not notably change over the first six days of protocol. Suddenly, cells appeared polarised and generated partially big cluster with hints to rosette-like formations, while cells appeared loosely arranged in other parts of the dish. C5 presented an earlier switch to a polarised cell morphology, characterised by an increased degeneration level that resulted in a strong accumulation of cell debris. Besides occasional formation of cell clusters with lost integrity, hardly any neurites were detected in both clones and especially not in clone 3.

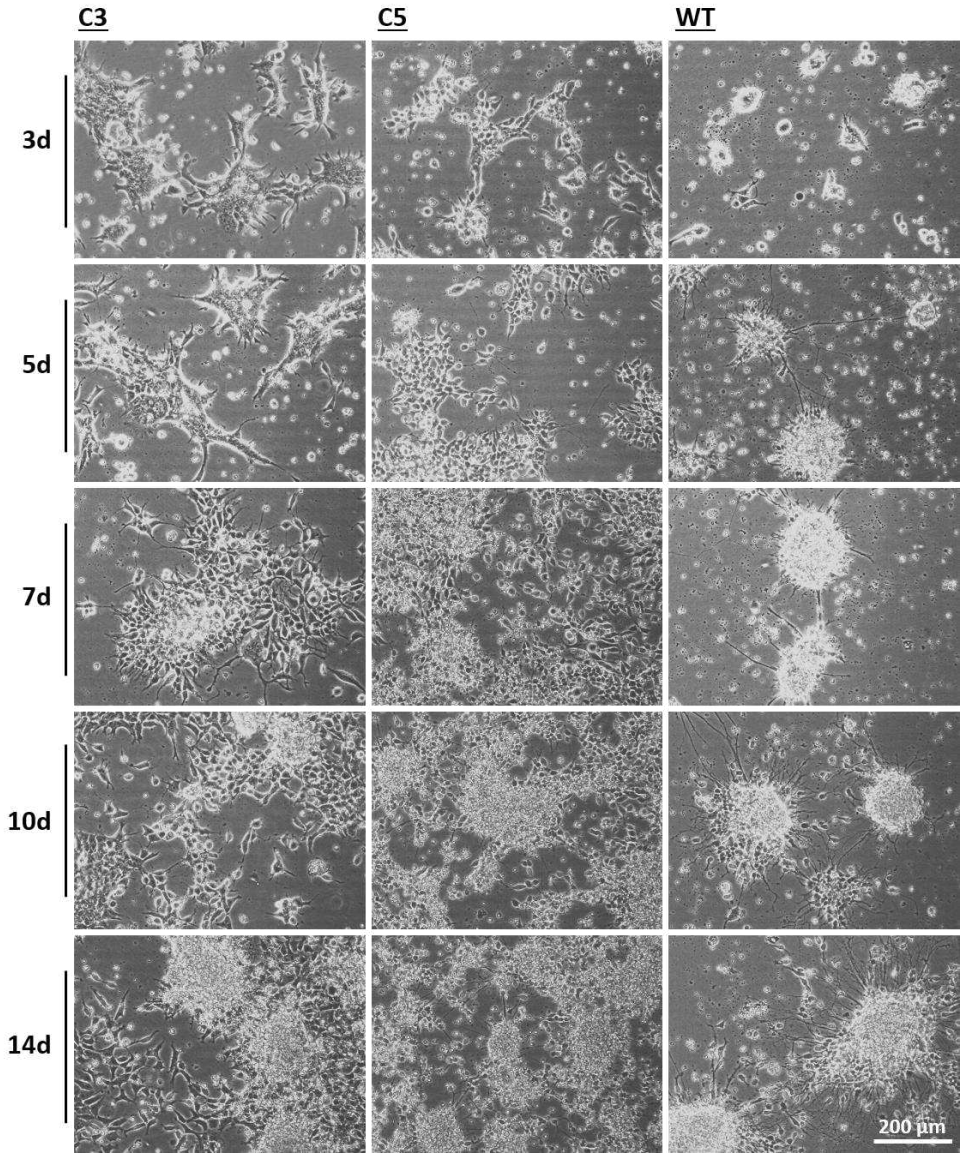

Figure 41: Neuronal differentiation of the generated *BirC6* CRISPR knockout mutant. The verified P19 *BirC6* knockout mutant clones 3, 5, and wildtype (WT) cells were treated with the SD protocol. While neuronal differentiation was induced in the WT cells, it failed for both analysed clones. Scale bar, 200 µm.

In summary, autophagy induction through rapamycin ended up in early cell degeneration but could not prevent the neuronal differentiation event, while *BirC6* deletion resulted in a strongly reduced potential or at least to a deficiency of axonal outgrowth. A deeper insight in cell fate decision and the influence of altered autophagy on molecular level, was provided by mass spectrometry analysis of the generated knockout mutant as well as the inhibitor treated wildtype.

3.4.5 Proteome analysis of early neuronal differentiation with altered autophagy level

Up to this point, the influence of altered autophagy levels on cell morphology has been extensively studied. To provide an insight on the molecular level and to search for a connection between neuronal autophagy and signalling pathways, known to be involved in the differentiation process, the proteome of P19 cells was analysed. Since the effect of an altered autophagy level through the differentiation process revealed to be morphologically the strongest at the fifth day, WT cells as well as the knockout mutants Δ*Becl1* and Δ*BirC6* in native state, and after five days treatment with the SD differentiation protocol, were examined. Each condition was analysed in biological triplicates. The samples had to be divided on two mass spectrometry runs. For a comparative purpose, WT cells (*Becl1*/*BirC6*_WT_CTRL/ND) were included in both runs. To compare the effect of the knockouts with the influence of inhibitor treatment, 3-MA or rapamycin (Rap) was supplemented to WT cell cultures on day two to four of the SD protocol. All conditions studied are listed below and all conditions where cells were treated with the neuronal differentiation protocol are highlighted in red:

1st run	**2nd run**	
*Becl1*_**WT**_CTRL	*BirC6*_**WT**_CTRL	CTRL= control (native cells)
*Becl1*_**WT**_ND	*BirC6*_**WT**_ND	ND= neuronal differentiation
*Becl1*_**WT**_3MA	*BirC6*_**WT**_Rap	(5th day of SD protocol)
*Becl1*_**KO**_CTRL	*BirC6*_**KO**_CTRL	WT= wildtype
*Becl1*_**KO**_ND	*BirC6*_**KO**_ND	KO= knockout mutant (Δ*Becl1*, Δ*BirC6*)

In each run, about 6000 proteins were quantified, while 5508 of the quantified proteins were detected in all samples. Between the conditions, still 5260 proteins provided an ANOVA sigificance. Analysis of the proteome data demonstrated a high similarity of the profiles between the three biological replicates of each condition, illustrated in a heatmap and a principal component analysis (PCA) (Fig. 42 A,B). It is also clearly detected that the induction of neuronal differentiation by the SD method resulted in a shift of the expression pattern, while the profile of the Δ*BirC6* mutant distinctly differed from the others, especially when treated by SD protocol. This confirmed the previous observation that the Δ*BirC6* cells in growth and SD medium exhibited a different cell morphology and neuronal induction failed in contrast to the other tested conditions. The proteome of the Δ*BirC6* mutant treated by the SD protocol significantly differed from the other native and neuronal differentiated cells. This suggested the derivation to a different cell fate. The profile of the Δ*Becl1* mutant in native state and after neuronal induction also differed from WT, while the influence of the inhibitor rapamycin and 3-MA appeared less pronounced, well demonstrated in the PCA (Fig. 42 B). In contrast to the Δ*BirC6* mutant, the Δ*Becl1* mutant derived neurons demonstrated a pattern that was closer to WT.

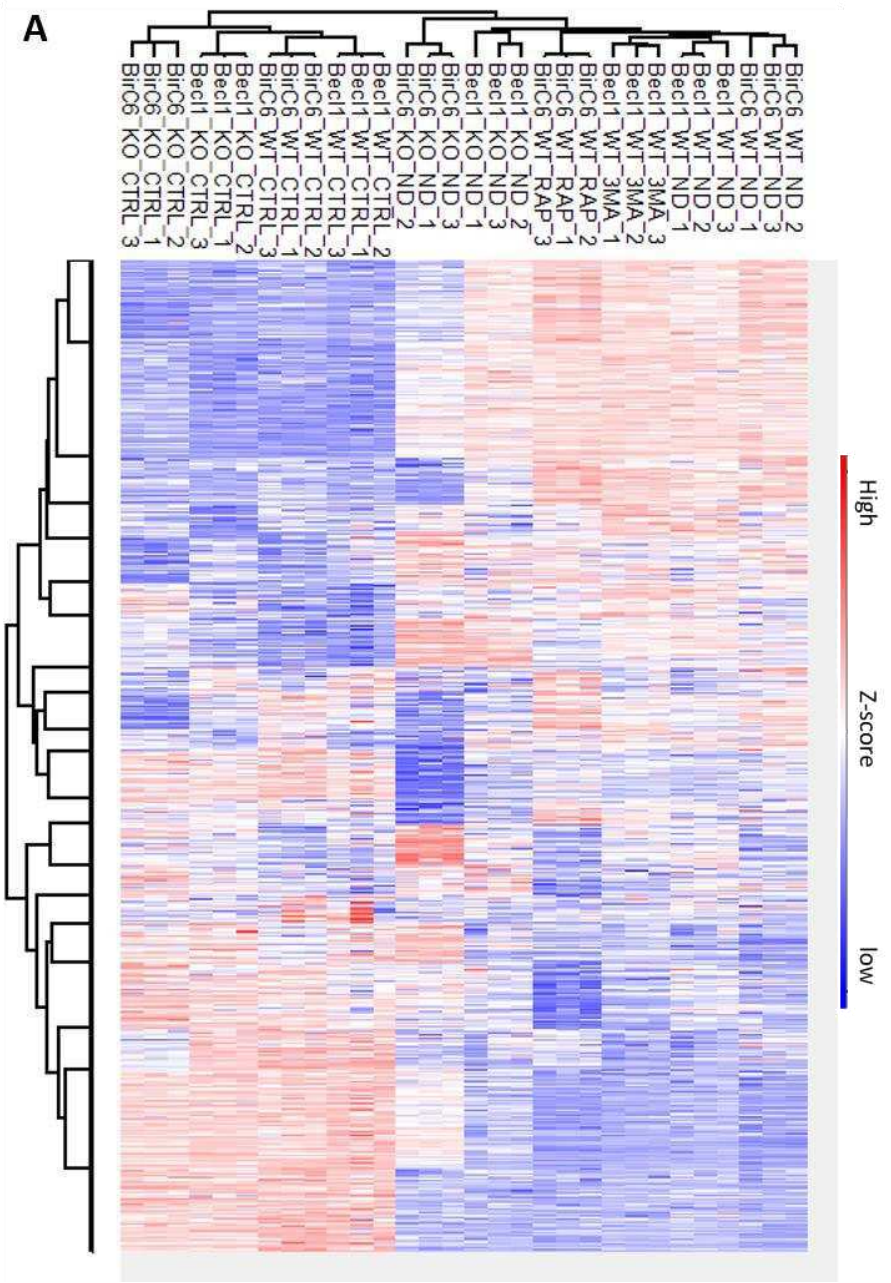
A
BirC6_KO_CTRL_3
BirC6_KO_CTRL_1
BirC6_KO_CTRL_2
Becl1_KO_CTRL_3
Becl1_KO_CTRL_1
Becl1_KO_CTRL_2
BirC6_WT_CTRL_3
BirC6_WT_CTRL_2
BirC6_WT_CTRL_1
Becl1_WT_CTRL_3
Becl1_WT_CTRL_1
Becl1_WT_CTRL_2
BirC6_KO_ND_2
BirC6_KO_ND_3
BirC6_KO_ND_1
Becl1_KO_ND_1
Becl1_KO_ND_3
Becl1_KO_ND_2
BirC6_WT_RAP_3
BirC6_WT_RAP_2
BirC6_WT_RAP_1
Becl1_WT_3MA_1
Becl1_WT_3MA_2
Becl1_WT_3MA_3
Becl1_WT_ND_2
Becl1_WT_ND_3
Becl1_WT_ND_1
BirC6_WT_ND_1
BirC6_WT_ND_3
BirC6_WT_ND_2
High
Z-score
low

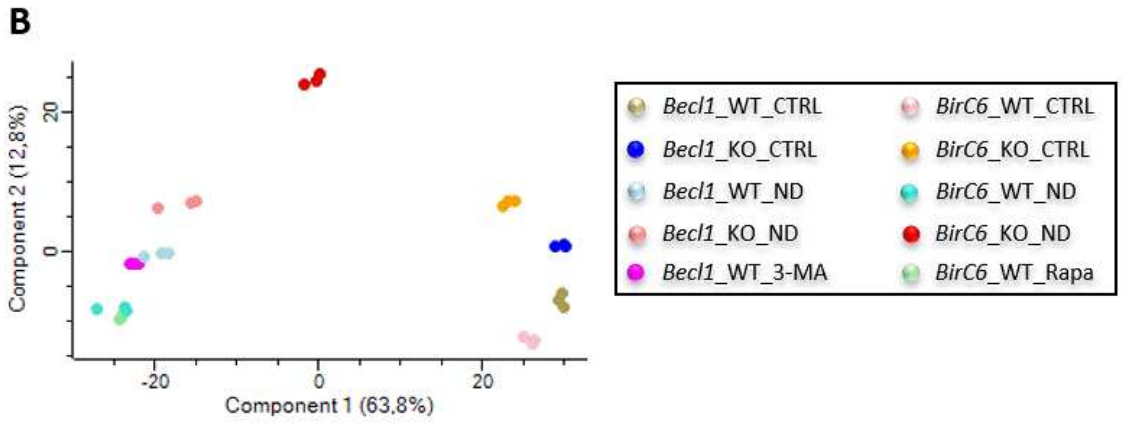
B
Component 2 (12,8%)
20
0
-20
0
20
Component 1 (63,8%)
Becl1_WT_CTRL
Becl1_KO_CTRL
Becl1_WT_ND
Becl1_KO_ND
Becl1_WT_3-MA
BirC6_WT_CTRL
BirC6_KO_CTRL
BirC6_WT_ND
BirC6_KO_ND
BirC6_WT_Rapa

C

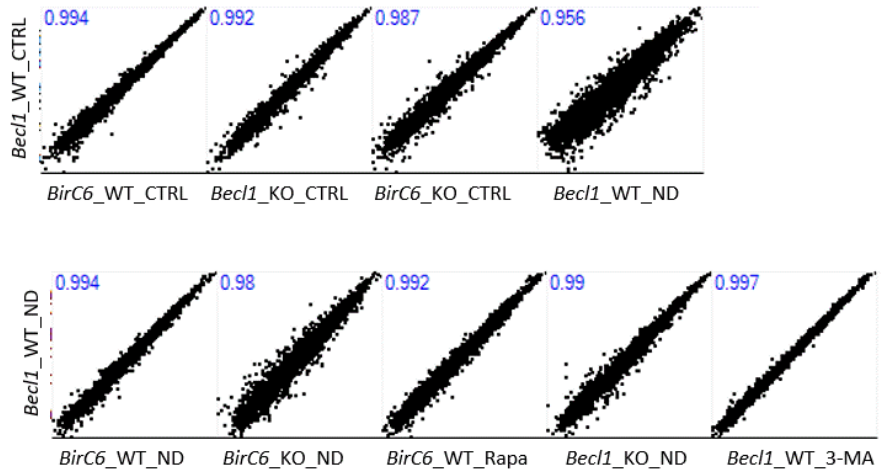

Figure 42: Comparative overview of the proteomic profiles. The expression pattern of P19 wildtype (WT), Δ*Becl1* and Δ*BirC6* mutant (KO) in native state (CTRL) or after 5 days treatment by SD protocol (ND) was illustrated. Additionally, WT was treated by the inhibitor 3-MA and rapamycin (Rapa) during neuronal differentiation. **A:** Data were z-score transformed to generate a heatmap of all quantified proteins, illustrated for each replicate. **B:** Principal component analysis with two of three main component groups. Similarities in the relative expression pattern of proteins in this component groups presented a clear distinction between native cells (CTRL), neuronal differentiated (ND), and the SD treated Δ*BirC6* mutant cells (*BirC6*_KO_ND). **C:** Multi scatter plot analysis of average groups of the triplicates. Profiles were labeled with the Pearson correlation (blue). In the first row, WT cells were compared with the other undifferentiated cultures and the neuronal WT differentiation profile was analysed. Below, neuronal differentiated WT cells were compared to the other differentiated cultures.

Average groups that were based on the median of the triplicates were generated for the multi scatter plot analysis (SPA) and the investigation of specific protein groups by usage of heatmaps. The SPA provided an overview about the similarities in the expression patterns under the given conditions, while the declared Pearson correlation (PC) supplied an indication about the consensus of the proteomes (Fig. 42 C). The WT of the first sample run in native state (*Becl1*_WT_CTRL) was compared with the WT of the second run (*BirC6*_WT_CTRL) and the knockout mutants in native state (*Becl1*_KO_CTRL, *BirC6*_KO_CTRL). With a PC of 0.994, the WT samples of both runs showed the greatest consensus in the expression profile, while the similarity was significantly reduced in comparison with the Δ*BirC6* mutant (PC = 0.987). With a correlation of 0.956, the deviation from WT cells in native to differentiated state was the largest. In addition, the differentiated WT cells were compared with all other conditions in which the cells were treated with the SD protocol. It was presented that the deviation caused by 3-MA treatment was quite low (PC = 0.997), while the SD treated Δ*BirC6* cells stands out due to the largest deviation (PC = 0.98). Several proteins of interest that showed a significant variation, were pooled from the data, and grouped in heatmaps (Fig. 43). The expression of thousands of proteins was affected through neuronal differentiation and alterations of the autophagy level by knockouts or inhibitor treatment. It was tried to select proteins that were implemented in the neuronal differentiation process and dependent on autophagy level. The study of crosstalk between autophagy and other signalling

pathways through the neuronal differentiation process was achieved. The first protein group included the NSC marker NES, SOX2, and LIN28a as well as the neuronal markers CAMSAP3, KLC1, DCX, MAP2, and TUBB3. Expression of these markers was recently reported to be upregulated during differentiation of hiPSC (Lindhout *et al,* 2020; Varderidou-Minasian *et al.,* 2020). In all cases, except for the Δ*BirC6* mutant, induction through SD treatment caused an increase in the expression level of all these markers. An effect from the *Becl1* knockout or the inhibitors 3-MA or rapamycin appeared less pronounced. This result confirmed the suggestion that knockout of *BirC6* was the only condition tested that prevented neuronal differentiation. The expression profile of the selected axon markers BASP1, GAP43, KIF5c, and NCAM1 revealed an increase through neuronal induction, like reported before by Lindhout *et al*. (2020). In comparison to the other samples, expression of NCAM1 was significantly lower in the native state and increased stronger during differentiation of the Δ*Becl1* mutant. Expression of these axonal markers was shown to be upregulated for the Δ*BirC6* mutant after induction of differentiation, nevertheless the protein level appeared slightly reduced compared to the successfully neuronal differentiated probes. ARPC2 and ARPC4 are subunits of the actin related protein 2/3 (ARP 2/3) and were identified as potential effectors of NCAM1 (Frese *et al.,* 2017). In contrast to the other axon markers, these subunits appeared to be slightly downregulated through neuronal induction of WT cultures. Expression of ARPC2 and ARPC4 in both knockout mutants, in native state and especially after treatment by the SD method, revealed to be higher.

The regulation of autophagy was illustrated by the expression profile of several proteins involved in this process, such as MAP1LC3α and MAP1LC3β. Both isoforms revealed to be upregulated through neuronal induction in WT and Δ*Becl1* cells. In contrast, the Δ*BirC6* mutant demonstrated in undifferentiated control conditions already a higher LC3 level. The ATG7 and ATG12 level was shown to increase through treatment by the SD method, even for the non-neuronal Δ*BirC6* cells. The ATG12 amount appeared significantly reduced through the *Becl1* knockout, while ATG7 demonstrated to be not affected. The expression profile of ATG16l1 was shown to be less unambiguous with the highest expression level of the SD treated Δ*BirC6* mutant. The regulation of GABARAP appeared quite volatile between the condition. Also, from ATG4b and ATG3 was no significant gradation between the conditions detected (not shown here). AMBRA and p62 (SQSTM1) presented to be significantly downregulated, five days after neuronal induction. Certainly, this was not the case for p62 in the Δ*Becl1* mutant, while rapamycin treatment leaded to an even lower p62 level. BECL1 was not detected in the second but in the first sample run. Therefore, the knockout in the Δ*Becl1* mutant could be clearly verified (Fig. 43-lowest row).

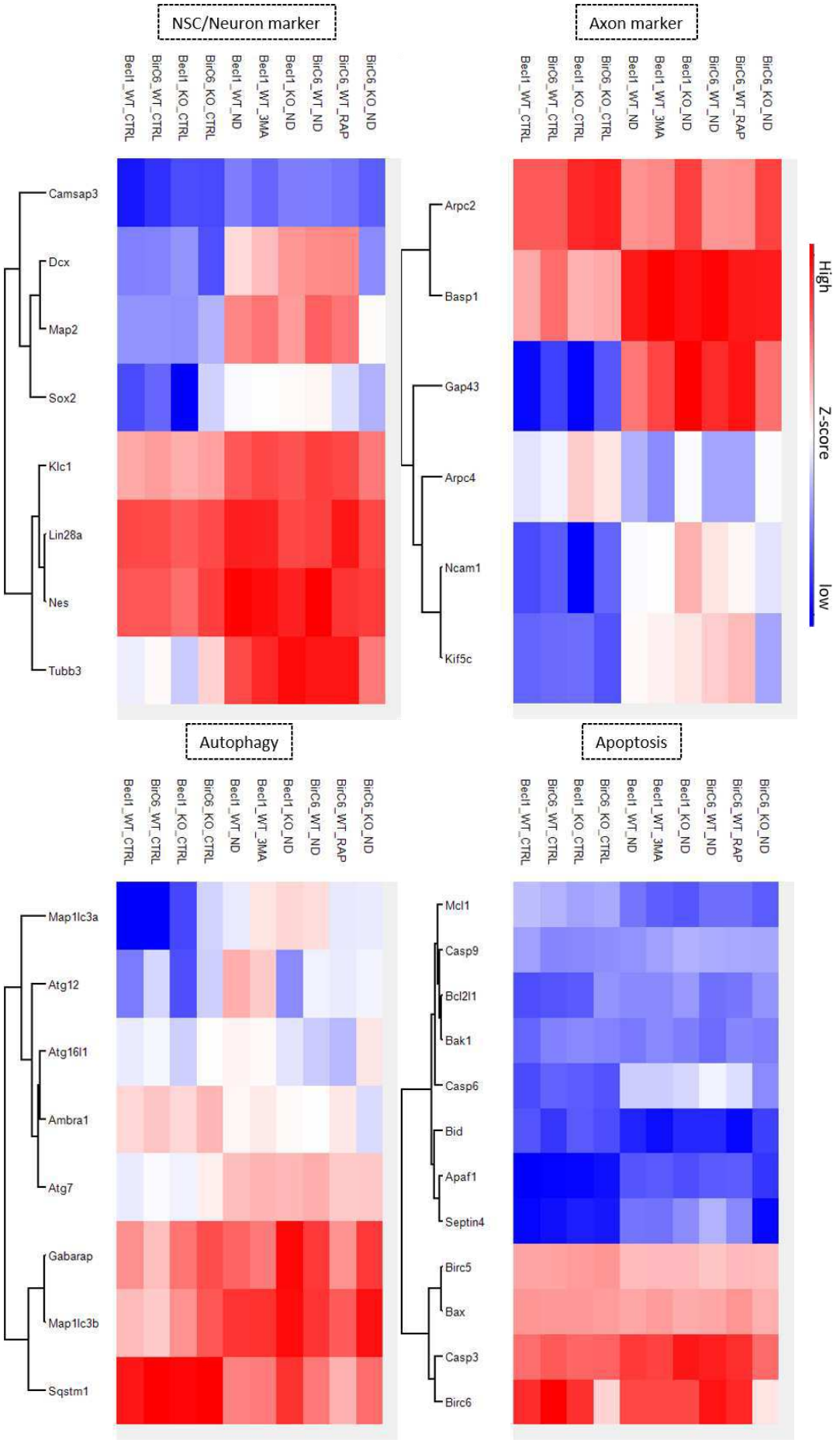
NSC/Neuron marker
Axon marker
Autophagy
Apoptosis
Becl1_WT_CTRL
BirC6_WT_CTRL
Becl1_KO_CTRL
BirC6_KO_CTRL
Becl1_WT_ND
Becl1_WT_3MA
Becl1_KO_ND
BirC6_WT_ND
BirC6_WT_RAP
BirC6_KO_ND
Camsap3
Dcx
Map2
Sox2
Klc1
Lin28a
Nes
Tubb3
Arpc2
Basp1
Gap43
Arpc4
Ncam1
Kif5c
High
Z-score
low
Map1lc3a
Atg12
Atg16l1
Ambra1
Atg7
Gabarap
Map1lc3b
Sqstm1
Mcl1
Casp9
Bcl2l1
Bak1
Casp6
Bid
Apaf1
Septin4
Birc5
Bax
Casp3
Birc6

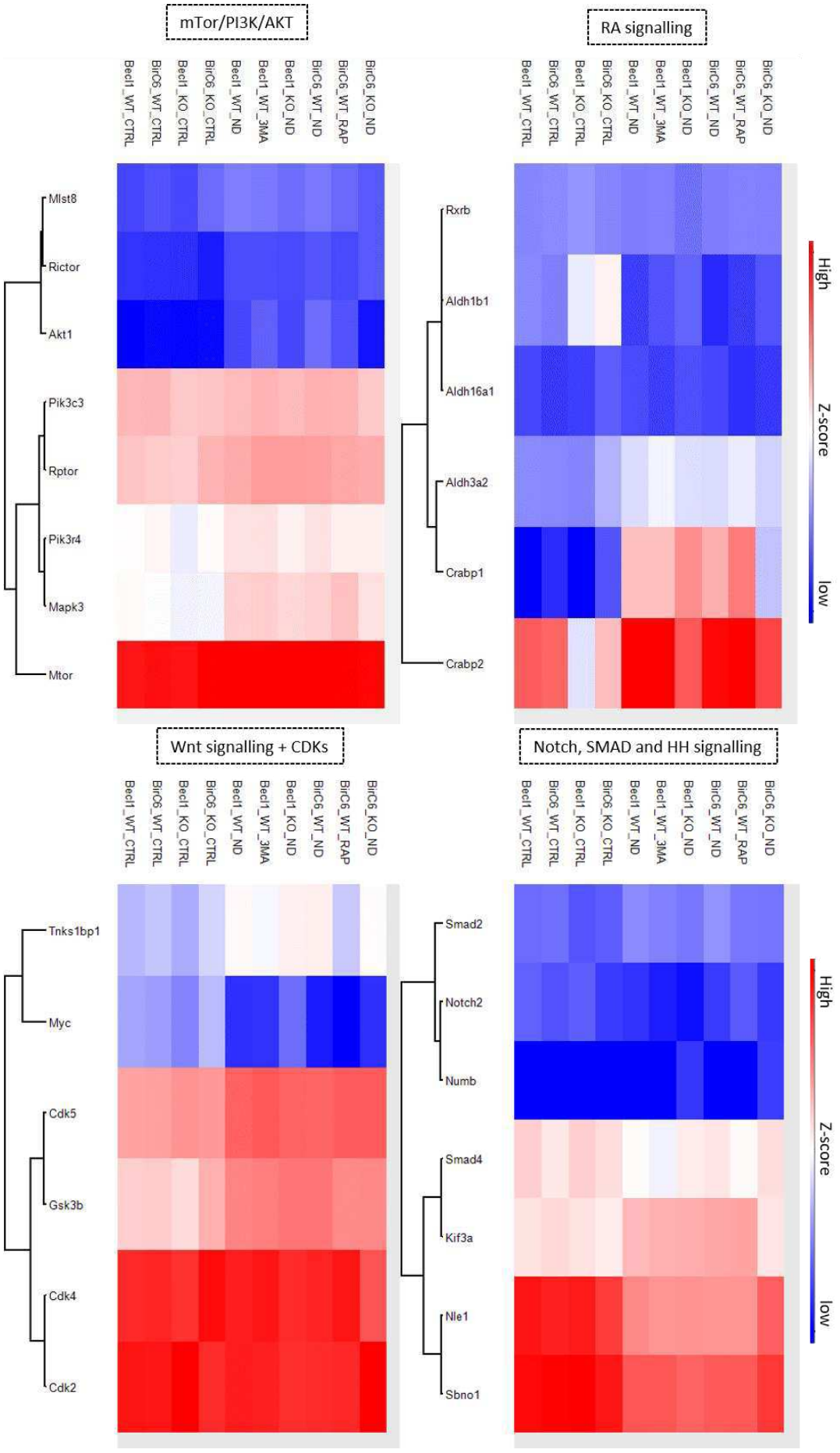
mTor/PI3K/AKT
RA signalling
Wnt signalling + CDKs
Notch, SMAD and HH signalling
Becl1_WT_CTRL
Birc6_WT_CTRL
Becl1_KO_CTRL
Birc6_KO_CTRL
Becl1_WT_ND
Becl1_WT_3MA
Becl1_KO_ND
Birc6_WT_ND
Birc6_WT_RAP
Birc6_KO_ND
Mlst8
Rictor
Akt1
Pik3c3
Rptor
Pik3r4
Mapk3
Mtor
Rxrb
Aldh1b1
Aldh16a1
Aldh3a2
Crabp1
Crabp2
Tnks1bp1
Myc
Cdk5
Gsk3b
Cdk4
Cdk2
Smad2
Notch2
Numb
Smad4
Kif3a
Nle1
Sbno1
High
Z-score
low

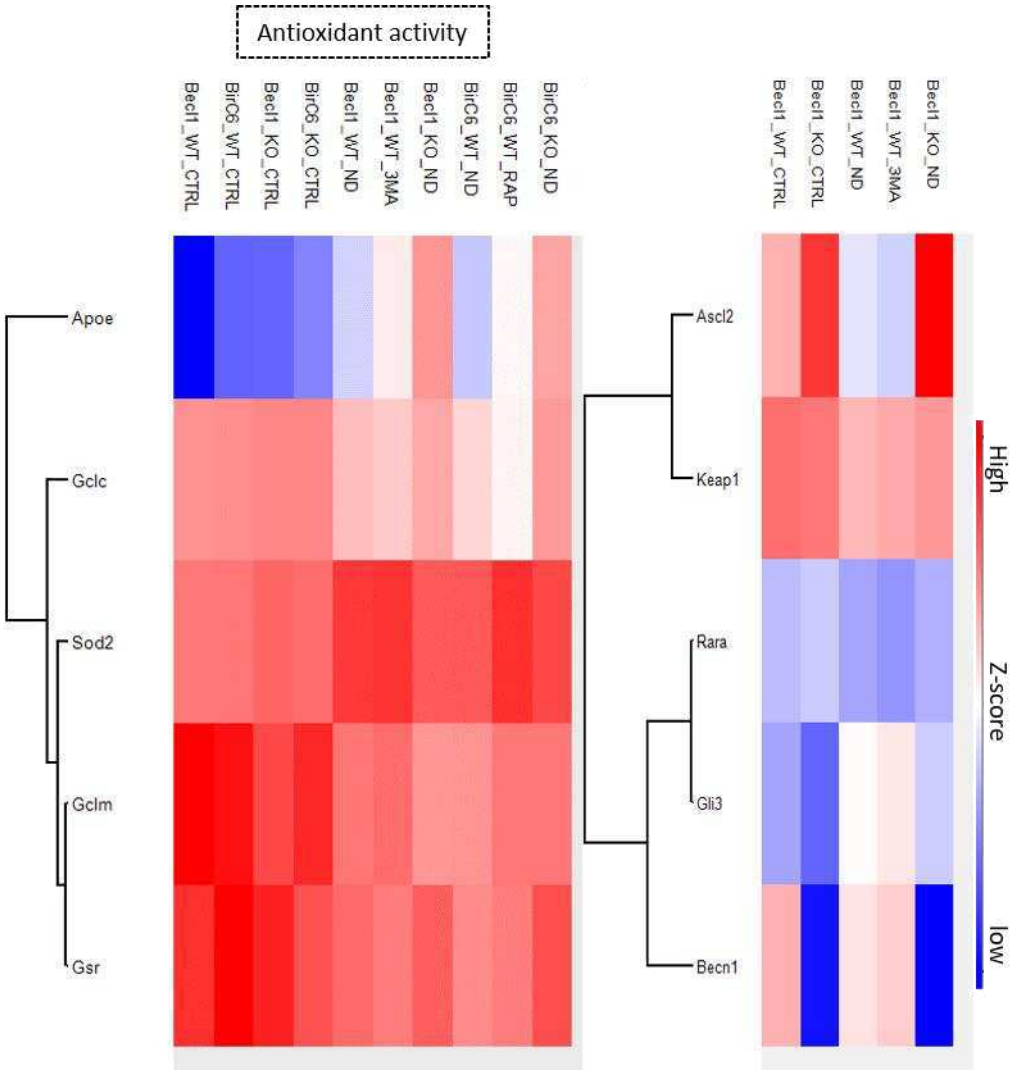

Figure 43: Profiling of the expression pattern of distinct protein groups. The expression pattern of P19 wildtype (WT), Δ*Becl1* and Δ*BirC6* mutant (KO) in native state (CTRL) or after 5 days treatment by SD protocol (ND) was illustrated. Additionally, WT was treated by the inhibitor 3-MA and rapamycin (Rapa) during neuronal differentiation. Data was z-score transformed and triplicates were fused to average groups, based on the median. Several proteins of interest that showed significant variations, were pooled from the data, and grouped in heatmaps, characterised by their topic.

Apoptosis was examined, among others, by investigation of the caspases 3, 6, and 9. While the regulation of CASP9 emerged as less apparent, except for the Δ*BirC6* mutant, the CASP3 and CASP6 level was clearly upregulated through neuronal differentiation. The same tendency was shown for SEPTIN4 and APAF1. The BIRC5 protein level was shown to be slightly decrease in all SD method treated samples, while illustrating the BIRC6 profile distinctly verified the *BirC6* knockout. For the pro-apoptotic Bcl-2 family proteins BAX and BAK1 was no clear differences between the conditions detected. The pro-apoptotic BH3-only protein BID as well as the anti-apoptotic MCL-1 presented to be downregulated in the developing neurons. While the pro-apoptotic BCL2L1 was slightly upregulated by neuronal induction, it was already shown to be increased in the Δ*BirC6* mutant.

Remarkably, all selected elements of the mTOR/PI3K/AKT signalling pathway displayed only a week shift in the expression profile. Some protein levels presented to be slightly increased through differentiation but a clear statement regarding the different conditions could not be provided for most of the pooled proteins of this category. Even the regulation of mTOR by rapamycin or any other condition was not detectable by this approach. AKT1, RICTOR, mLST8, PIK3R4, and MAPK3 (ERK1) demonstrated a slight increase in the protein level through differentiation. Investigation of the involvement of RA signalling proved to be more accessible. RARs (RARα/β/γ) were not detected in the second sample run, while RARα could be analysed in the first run (Fig. 43-lowest row). Here, RARα level was shown to be slightly decreased through neuronal differentiation of the WT (+/- 3-MA) but not in Δ*Becl1* cells. RXRβ could be detected under all conditions but did not show strong variations except for a slightly increased level in the native condition and a reduced level after neuronal induction of the Δ*Becl1* mutant. The RALDHs ALDH1B1, ALDH16A1, and ALDH3A2 were examined. ALDH3A2 was significantly upregulated through neuronal differentiation, while the opposite effect was observed for ALDH1B1. Additionally, significant higher ALDH1B1 levels in both knockout mutants in undifferentiated state were presented. In contrast, ALDH16A1 varied only insignificantly between conditions. It should be noted that of the three RALDHs analysed, ALDH1B1 is so far the only form known to metabolize all-trans-retinaldehyde (Jackson *et al.,* 2014). The cellular RA binding proteins CRABP1 and CRABP2 were both upregulated in the derived neuronal precursor cells while both knockout mutants revealed a reduced CRABP2 level. Overall, cellular RA binding proteins that mediate cellular RA transport presented to be upregulated after neuronal induction, while the expression of the RA synthesising enzyme ALDH1B1 and RARα was downregulated.

The cyclin-dependent kinases CDK2, CDK4, and CDK5 were pooled while only CDK5 evoked to be upregulated through treatment by SD method. MYC, a direct target of the Wnt pathway, was shown to be downregulated through differentiation, while the Wnt promoting tankyrase binding protein TNKS1BP1, and the glycogen synthase kinase GSK3β, that gets inhibited by Wnt signalling, demonstrated to be upregulated. Factors that are involved in the Notch pathway like SBNO1, NLE1, and NOTCH2 were downregulated through neuronal induction while NUMB, a Notch inhibitor stayed mostly unaffected, besides a little decrease in the differentiated knockout mutants. The SMAD proteins SMAD2 and SMAD4, revealed an opposing regulation through neuronal induction. The kinesin family members KIF3a was reported to regulate ciliogenesis in response to Hh signalling (Hoang-Minh *et al.,* 2016) and presented to be upregulated in neuronal cultures but not in SD treated Δ*BirC6* cells. The zinc finger protein GLI3 could be captured only in the first sample run (Fig. 43 -last row). GLI3, an effector of Hh signalling, was upregulated through neuronal differentiation of the WT (+/- 3-MA) and the Δ*Becl1* mutant. Compared to WT, the Gli3 level in pluripotent and differentiated Δ*Becl1* cells was reduced.

Finally, the antioxidant activity through the differentiation process was analysed. The apolipoprotein E (APOE) and superoxide dismutase 2 (SOD2) showed increased protein levels, after neuronal differentiation was induced. The glutamate cysteine ligase

catalytic (GCLc) or modifier (GCLm) protein and the glutathione reductase (GSR) demonstrated an opposing effect. KEAP1 could be only detected in the first sample run and presented to be downregulated through neuronal induction. Remarkably, ASCL2, a transcription factor that highly promotes neuronal differentiation, revealed to be downregulated after neuronal induction of the WT. In contrast, the ASCL2 concentration remained in native and differentiated state on high levels in the Δ*Becl1* mutant.

In summary, most of the morphological observations in this study were confirmed by proteomic analysis at the quantitative level. Neuronal differentiation of WT and Δ*Becl1* cells was verified by an increased expression of neuronal markers. The influence of the inhibitor rapamycin and 3-MA appeared very subtle in the profile of all as well as the selected proteins for analysis. Like assumed from morphology, data suggested that the Δ*BirC6* mutant was not able to differentiate into neurons under the given conditions but also highly differed from the phenotype of undifferentiated WT cells. The expression profile of the Δ*BirC6* mutant deviated for many of the examined proteins. But the regulation of several protein levels revealed to be affected by the *Becl1* knockout as well. Neuronal differentiation by SD method presented to impact various signalling pathways such as Notch, Wnt, Hh, mTOR/PI3K/AKT, RA signalling and the antioxidant activity, autophagy, and apoptosis in different ways. It has been shown that the regulation of protein levels after neuronal induction is dependent on autophagy for proteins such as NCAM1, ASCL2, MYC, GLI3, and APOE.

4. Discussion

4.1 A novel one-step approach to efficiently induce neuronal differentiation

In recent years, several neuronal differentiation protocols developed that circumvent the requirement of EB formation under serum-deprivation and simplified medium conditions (Morii *et al.,* 2020; Nakayama *et al*., 2014; Pauly *et al.,* 2018; Yamazoe *et al.,* 2006). In this study, a novel approach to induce neuronal differentiation *in vitro* was developed and established. Like for several other novel protocols, neither the formation of free-floating aggregates nor supplementation of serum was implemented. Circumvention of EB formation by the establishment of a serum-free monolayer culture was shown to shortens the length of the neuralization process considerably (Azari and Reynolds, 2020). Commonly, induction in this system can be implemented by co-cultures with stromal cells (Kawasaki *et al.,* 2000; Vazin *et al.,* 2008) or supplementation of several effectors that induce or enhance neuronal fate decision, while the list of supplemented factors is sometimes quite long (e.g. see protocols listed in Compagnucci *et al.,* 2014; Nakayama *et al.,* 2014). In contrast to the so far developed neuronal differentiation protocols, no co-culture or supplementation of growth factors or known inducers were necessary to generate a reliable, homogenic and pure neuronal culture in this study. Therefore, this method provides several advantages such as the possibility to generate stable pure neuronal cultures by a fast, simple, and highly reproducible one-step induction under defined medium conditions with a minimum of exogen effectors. The treatment with a simple, nutrition-poor medium mixture that is based on a dilution of DMEM/F12+N2 medium, proved to be sufficient to efficiently induce neuronal differentiation. A neuronal network was generated within one week and the cultures were shown to stay stable at least for three weeks. The life span of the generated neurons was significantly longer than for example in the protocol of Nakayama *et al.* (2014).

The self-developed SD method was established by using the murine embryonal carcinoma cell line P19 and could be transferred to murine ESC. The protocol had to be slightly adapted on the special demands of ESC to ensure cell survival during the differentiation process. In further studies, the dilution factor of the DMEM/F12+N2 medium has to be adjusted to optimize culture conditions and consequently increase the purity of the neuronal culture to a maximum. The applicability of this method could cover a common mechanism of neuronal induction in pluripotent cells and thus could be transferable to all pluripotent cell sources and neuronal progenitor cells. Neurons generated by applying the SD method showed a morphologically distinct phenotype and the formation of neuronal rosettes. Neural rosettes, also observed by *in vitro* differentiation of hESCs, are reminiscent of secondary neurulation during neural tube formation (Fedorova *et al.*, 2019). This study revealed a characteristic acetylated α-tubulin cytoskeleton arrangement of rosette formations (Curchoe *et al.,* 2013). The molecular process of this formation is barely understood but it was discovered that cells which are arranged in neural rosettes have the potential to differentiate into distinct region-specific neurons and glial cells (Harding *et al.,* 2014; Li *et al.,* 2011). Definition of

the neuronal subtype generated in this study is still pending, but expression of neuronal markers was detected by immunofluorescence staining and mass spectrometry analysis. The pro-neural markers Nestin, NeuroD, Neurogenin2, ASCL1 were highly expressed in two-week-old neuronal cultures, derived from P19 cells and ESC. The astrocyte marker GFAP was only detected for ESC, probably due to an insufficient dilution of DMEM/F12+N2 with the salt solution. Proteome analysis of P19 cells treated for five days with the SD method presented an upregulation of the NSC marker NES, SOX2, and LIN28a as well as the neuron marker CAMSAP3, KLC1, DCX, MAP2, and TUBB3, confirming the neuronal cell fate decision. Recently, it was reported that the expression of these markers is also upregulated during differentiation of hiPSC (Lindhout *et al.,* 2020; Varderidou-Minasian *et al.,* 2020). ASCL2, a transcription factor that reduces proliferation and highly promotes neuronal differentiation (Liu *et al.,* 2019), revealed to be downregulated after neuronal induction in the present study. The reason for the unexpected downregulation remained unclear, but as discussed later, ASCL2 levels showed autophagy dependence.

In agreement with the morphological identified outgrowth, the level of the axon markers BASP1, GAP43, KIF5c, and NCAM1 were increased. Furthermore, functionality of the synapses of the P19-derived neurons was shown by detection of calcium activity. The morphological development can be easily observed in the supplemental movies. Thereby, innumerable particles were observed that got continuously absorbed and released by the neuronal clusters. These are presumably extracellular vesicles like microvesicles, apoptotic blebs or exosomes, released by cells into the extracellular space (Caruso Bavisotto *et al.,* 2019). Several *in vitro* studies demonstrated an inter-neuronal communication by released exosomes, retaken by other neurons to provide an activity-dependent synaptic growth (Korkut *et al.,* 2013). However, identification and function of the particles observed in this setting, remained unclear. Axonal ablation in the generated neuronal cultures demonstrated a strong tension of the connections within the generated neuronal networks. Regrowth started immediately after axonal ablation, revealing a strong regeneration potential under the given conditions. The molecular mechanism that regulates axonal regrowth is not completely understood yet (Qian and Zhou, 2020; Yaniv *et al.,* 2012). But P19 cells were shown to be a suitable model to study axonal regeneration with a minimum of external influences. In total, the established SD method proved to be a useful tool to investigate the molecular background of neuronal differentiation as well as for high throughput screenings. Application of this method provides a fast, simple, and highly reproducible approach to efficiently induce neuronal differentiation, supplying a pure and stable culture of active neurons. The method is characterised by defined and steady medium conditions that makes the investigation of specific cell requirements during differentiation accessible. Since the method could be transferred from the ECC to the ESC, there is the possibility that this is a generally valid mechanism.

4.2 Neuronal differentiation is induced by a metabolically defined environment

At the time the SD protocol was developed, it was suspected that starvation conditions might cause neuronal induction. This assumption was based on the previous reports that

fasting induces or enhances neurogenesis *in vivo* (Gomes *et al*., 2016; Lee *et al.,* 2002). In a pure salt solution (EBSS), cells died within 24 h. Therefore, a strong dilution of DMEM/F12+N2 with EBSS was implemented that resulted in a nutrition-poor environment. DMEM with the nutrient mixture F12 is a widely used basal medium that is declared to support the growth of many different mammalian cells such as glial cells, fibroblasts, human endothelial cells, and rat fibroblasts. It is implemented in several protocols that describe neuronal induction under serum deprivation (e.g. Bibel *et al.,* 2007; Nakayama *et al.,* 2014; Pacherník *et al.,* 2005). The N2 supplement is based on Bottenstein's prominent N1-formulation, developed to maintain neuroblastoma cells in culture (Bottenstein and Sato, 1979). Defined as nutrition mixture, N2 is provided to ensure survival of neuroblastomas and post-mitotic neurons in primary cultures and is used to replace serum in DMEM(/F12) or Neurobasal medium. The provider claims that the N2 supplement selectively supports the growth of neuronal cells. In this study, the F12 nutritional mixture and the N2 supplement were shown to support the survival of neuronal differentiated cells. Supplementation of N2 revealed to be essential for the induction of neuronal fate or to ensure survival of neuronal precursor cells. Morphologically, neuronal differentiation was identified in undiluted DMEM/F12+N2 medium, but proliferating cells overgrew the culture within five days, eventually leading to culture degeneration. Whether this was caused by a high proliferation rate of neuronal progenitor cells or other cell types could not be clearly defined morphologically due to the high cell density. This is consistent with the phenotype of P19 cells in undiluted DMEM/F12+N2 observed in this study. Therefore, the suggestion that the cells likely differentiate to a neuroectodermal fate by forming proliferating progenitor cells in pure DMEM/F12+N2 strengthened. In this study, the phenotype of mature post-mitotic neurons, arising within a week, was elicited only when the medium was heavily diluted with a salt solution. Previously, P19 cells were reported to express neuroectodermal and no endodermal marker genes under comparable conditions, although no neurites were identified (Pacherník *et al.,* 2005). Anyway, strong dilution of the DMEM/F12+N2 medium (1:9) and therefore a strong nutrition decrease appeared to be essential to diminish proliferation and to simultaneously increase the ratio of post-mitotic neurons, resulting in a homogeneous neuronal culture.

Examination of individual components of N2 supplementation did not lead to the identification of an actual inducer. Insulin showed the strongest effect on lifespan extension, but in the absence of the components transferrin, putrescine, and progesterone, it was not sufficient to induce neuronal differentiation or to ensure the survival of neuronal differentiated cells. Only the mixture of all N2 components (except selenite) provided the necessary medium conditions to ensure survival of the differentiating cells. Overall, the observation of variations in SD medium composition strongly suggests that only cells that have undergone neuroectodermal fate decision can survive under the created conditions, resulting in a pure neuronal culture. Serum deprivation and strong dilution of DMEM/F12+N2 medium caused a nutrient-poor environment in which the influence of growth factors and inducers was minimized. Referring to the proposed default neuronal fate, initiated in the absence of extrinsic signals (Lenka and Ramasamy, 2007; Smukler *et al.,* 2006; Tropepe *et al.,* 2001), the

method could provide a feasible protocol for the neuronal default model. Whether such a default neural mechanism exist and how this is implemented across a broad spectrum of cell source, is currently addressed in several studies and still controversely discussed (Smukler *et al.,* 2006; Stern, 2006; Marchal *et al.,* 2009; Muñoz-Sanjuán and Brivanlou, 2002; Vallier *et al.,* 2006).

Recent studies reported that ESC, grown at low density and in the absence of exogenous factors or feeder layers, either die or attain neural identity as indicated by expression of the neural marker Nestin (Smukler *et al.,* 2006; Tropepe *et al.,* 2001). This default cell fate is presumably achieved by eliminating extracellular inhibitors of neuroectodermal fate and suppressing cell-cell signalling through limited cell density (Lenka and Ramasamy, 2007). But cells die after 24 hours under these minimal conditions (Smukler *et al.,* 2006; Tropepe *et al.,* 2001). Consistent with my observations, was recently reported that P19 cells survive and differentiate in serum-free DMEM/F12 medium containing transferrin, insulin, and selenite (Pacherník *et al.,* 2005). According to these reports, it was hypothesized that the SD medium, developed in this study, creates a metabolically defined environment that is free of extrinsic signals that prevent neuronal fate decision. In wildtype cells, these conditions allowed only the expression of a neuronal phenotype and ensured survival of most of the generated neurons over a long period. It is suggested that the metabolic composition of the medium only ensures the survival of neuronally differentiated cells and thus forces the cells to undergo neuronal differentiation.

Neuronal induction through inhibition of mesoderm and endoderm promoting signals, such as Wnts, Nodal, BMPs, and Notch signalling offers an opportunity to enhance or induce neuronal fate decision *in vitro* (Azari and Reynolds, 2020; Crawford and Roelink, 2007; Levine and Brivanlou, 2007). It was assumed that inducers of these signalling pathways were not present under the established medium conditions in this study. Therefore, my results suggest that the absence of mesoderm and endoderm promoting signals makes the addition of the corresponding inhibitors unnecessary. In summary, SD medium provides metabolically defined and steady conditions with a minimum of extrinsic factor that selectively promote the survival of neurons. While no actual inducer was detected, specific cell requirements of neuronally differentiated cells in SD medium were found to be covered and to drive the switch from pluripotent carcinoma cells to neurons.

4.3 The neuronal default mechanism is dependent on RA signalling

RA plays an essential role in cell signalling during embryogenesis and efficiently induces neuronal differentiation *in vitro* in a concentration dependent manner (Bain *et al.,* 1996; Blumberg, 1997; Okada *et al.,* 2004; Ross *et al.,* 2000). This morphogen promotes neuroectodermal and represses mesodermal gene expression (Bain *et al.,* 1996; Boudjelal *et al.,* 1997). EB formation as well as the supplementation of RA was shown to be essential to induce efficient neural differentiation of pluripotent cells in serum-containing cultures (Bain *et al.,* 1995, 1996; Jones-Villeneuve *et al.,* 1982; Glaser and Brüstle, 2005; Rohwedel *et al.,* 1999). In monolayer cultures treated with medium that

contains serum and RA, cells differentiate to endoderm like cells (Jones-Villeneuve *et al.,* 1982; Mummery *et al.,* 1990, Rochette-Egly and Chambon, 2001; Pacherník *et al.,* 2005). A recent study has shown that RA supplementation to monolayer cultures induces the expression of neuroectodermal and endodermal marker genes in P19 cells, irrespective of the presence or absence of serum in the medium (Pacherník *et al.,* 2005). In contrast, in serum- and RA-free medium only the expression of neuroectodermal marker was induced, while neurite outgrowth appeared diminished (Pacherník *et al.,* 2005). Anyway, according to the declared formulations of the SD medium components, the medium was expected to be free of RA or any precursor like retinol or carotenoids. RA is reported to be rapidly degraded, resulting in a short half-life of about one hour (Pennimpede *et al.,* 2010). Therefore, no cellular RA content was expected during neuronal differentiation. Nevertheless, Engberg *et al.* (2010) claimed that RA signalling is required to suppress spontaneous mesendodermal development in serum-free, adherent monocultures. We cannot exclude that the neuronal default mechanism in the absence of extrinsic signals observed in my study is guided by subnanomolar concentrations of RA or precursors from residual serum components, caused by a culturing in serum-containing medium prior to the experiments (Engberg *et al.,* 2010).

Here, the P19 cells were cultured in medium with 10 % FBS prior to the neuronal induction in serum-free SD medium. The composition of each batch of FBS is in fact extremely variable but it is assumed that the retinol concentration is roughly about 30 nM in medium containing 10 % FBS (Arigony *et al.,* 2013; Bryan *et al.,* 2011). To proof or disproof the RA dependency in the neuronal differentiation process by application of the SD method, RA signalling was challenged by several approaches. First, RA synthesis was blocked by DEAB, a competitive, reversible inhibitor antagonist that acts as substrate of several retinaldehyde dehydrogenases and irreversibly inhibits the RALDHs ALDH1A2, ALDH2 and ALDH7A1 (Begemann *et al.,* 2004; Morgan *et al.,* 2015). Blocking RA synthesis by DEAB resulted in a strong reduction of the cell number that survived the differentiation process but did not prevent neuronal induction. Therefore, the increased cell degeneration could result from a toxic effect of DEAB. In undifferentiated cells, toxicity was observed from a higher concentration range, possibly buffered by serum in the growth medium. The proteome analysis captured the RALDHs ALDH1B1, ALDH16A1, and ALDH3A2. ALDH3A2, primarily involved in the oxidation of medium- and long-chain aliphatic and aromatic aldehydes (Vasiliou and Nebert, 2005), was significantly upregulated through neuronal differentiation. Interestingly, ALDH1B1, which metabolizes nitroglycerin and all-trans-retinaldehyde (Jackson *et al.,* 2014), was decreased by neuronal induction. ALDH16A1, that revealed no regelation, was recently discovered and the function is still unknown (Vasiliou and Nebert, 2005).

In contrast, the protein level of both cellular RA binding proteins (CRABP1 and CRABP2) appeared increased after neuronal induction with the SD medium. CRABP1 was also reported to be involved in the non-canonical, cytoplasmic RA signalling (Persaud *et al.,* 2013). This pathway is RAR-independent and includes the RA-mediated activation of the extracellular signal-regulated kinase 1/2 (ERK1/2) that results in the disruption of pluripotency and proliferation, was shown to be essential for early neural differentiation

(Gupta *et al.,* 2008; Li *et al.,* 2006; Orford and Scadden, 2008; Persaud *et al.,* 2013; Wei, 2013). In addition to CRABP1, MAPK3 (ERK1) levels also showed an increase, indicating the involvement of non-canonical RA signalling in the neuronal differentiation process when the SD method was used. Moreover, a further non-canonical and the canonical RA signalling exist that involve RARs (Rhinn and Dollé, 2012; Wei, 2013). The RAC65 mutant is characterised by a truncated RARα and probably a further mutation that caused a downregulation of the CRABP gene through RA treatment (Jones-Villeneuve *et al.,* 1982; Malý and Dráber, 1992; Pratt *et al.,* 1990). This mutant displayed no effect on the potential to induce neuronal differentiation by application of the SD method.

The neuronal differentiation protocol of Nakayama *et al.* (2014) was also shown to function independently of RARα in this study. In their protocol, in addition to several enhancers that promote neuronal differentiation, RA is added as an actual inducer. Interestingly, application of this protocol showed that both, P19 WT and the RAC65 mutant cells, could differentiate into neurons in the absence of RA, but axonal growth and cell cluster integrity were significantly impaired. The fact that the phenotype of both WT and RAC65 mutant cells was equally rescued by RA supplementation under this condition suggests that RA promotes the differentiation process in a RARα-independent manner. Alternatively, it is conceivable that the truncated RARα in the RAC65 mutant was functionally substituted by the subtypes RARβ and RARγ (Koide *et al.,* 2001; Mark *et al.,* 1999; Taneja *et al.,* 1995). Consequently, the RAC65 mutant was proved not to be RA resistant in serum-free monolayer cultures. In contrast, by application of the conventional differentiation protocol (McBurney *et al.,* 1988), the RAC65 mutant cells were incapable to differentiate and kept the undifferentiated phenotype, as predicted (Jones-Villeneuve *et al.,* 1982; Pratt *et al.,* 1990). This observation might be explained by the influence of serum on the neuronal differentiation potency of RA (Magalingam *et al.,* 2020).

It has been reported that under serum deprivation and without RA in the medium, a concentration of 1 nM RA or more (residual from previous medium) is sufficient to induce neuronal differentiation (Engberg *et al.,* 2010; Pacherník *et al.,* 2005). In contrast, when RA is supplemented to EB in standard serum-containing media, a concentration of 50-500 nM RA is necessary for neuronal induction (Bain *et al.,* 1994). Under these conditions, a RA concentration of 10 nM or lower was reported to result in a myogenic cell fate (Edward and McBurney, 1983, Rohwedel *et al.,* 1999). In any case, 500 nM RA was added for both methods that were used for comparative purposes in this study (McBurney *et al.,* 1988; Nakayama *et al.,* 2014). It was assumed that the RA concentration would be significantly higher through supplementation of serum in the conventional protocol. However, it was probably not sufficient to compensate for the inhibitory effect of the serum and the truncated RARα at the same time. Therefore, a high RA concentration is likely required to supress the complex signalling from serum factors that supress the neuroectodermal fate. This hypothesis was reinforced by the observation that DMSO had a negative influence on neuronal differentiation by implementation of the SD method in a concentration-dependent manner. Indeed, exposure to 1 % DMSO is commonly used for induction of mesodermal differentiation

in P19 cells, and DMSO is also applied as RA solvent in neuronal differentiation protocols (Jasmin *et al.,* 2010; McBurney *et al.,* 1982). A high RA level combined with the treatment of 1 % DMSO was reported to prevent mesodermal differentiation, while a low RA level enhances skeletal myogenesis (Kennedy *et al.,* 2009; Pratt *et al.,* 1998). The SD protocol did not include RA supplementation, resulting in the expectation that the RA level was not exceeding the subnanomolar range. Consequently, the negative effect of DMSO on axonal growth and the neural rosette formation was likely caused by a low cellular RA level that was insufficient to supress the mesodermal promoting signal from DMSO concentrations higher than 0.1 %. The possibility that neuronal induction by implementation of the SD method is dependent on a low physiological RA level, was confirmed by application of the pan-RAR antagonist BMS493 that silenced the activity of all RAR subtypes. BMS493 prevented neuronal induction, resulting in a fast degeneration of all cells in the SD medium. This observation was in agreement with the report that suppression of all RAR subtypes in a serum- and RA-free culture blocks neuroectodermal differentiation of mESC (Engberg *et al.,* 2010). A simultaneous knockout of all RAR subtypes was reported to completely repress transcriptional response to RA (Laursen and Gudas, 2018). Indeed, knockdown of RARγ in ESC has been shown to be sufficient to suppress neuronal differentiation (Al Tanoury *et al.,* 2014). Whereas it was reported that RA-induced neuronal differentiation in P19 cell aggregates resulted in a rapid increase of RARα and RARβ mRNA, RARγ appeared to be strongly repressed (Bain *et al.,* 1994; Jonk *et al.,* 1992). In Addition, in P19 monolayer cultures, the maximal RARα level appeared to be even higher (Bain *et al.,* 1994). In this study, the opposing effect was detected. By proteome analysis, only RARα and RXRβ were detected. While RXRβ demonstrated no significant regulation, RARα was slightly decreased through neuronal induction by application of the SD method. These findings together with the observation that neuronal differentiation was independent of RARα only in serum-free medium, indicate that the complexity of the serum is critical for RA signalling. A deeper insight into the regulation of different RAR subtypes in dependence on serum addition is therefore of greatest interest.

To sum up, the present work reinforces the thesis of Engberg *et al.* (2010) that neuronal induction in serum-free monolayer cultures is dependent on little amounts of residual RA or precursor. RA signalling through neuronal induction by SD method suggests being regulated by RARβ or RARγ, since (i) RARα was slightly downregulated after induction, (ii) the truncated receptor had no influence on the induction efficiency in serum-free monolayer cultures, and (iii) a pan-RAR inhibitor supressed neuronal differentiation. Although no RA or precursor was present in SD medium, cellular RA-binding proteins that mediate cellular RA transport and are involved in non-canonical RA signalling were shown to be upregulated after neuronal induction. In contrast, the RA-synthesizing enzyme ALDH1B1 and RARα were downregulated after replacement of growth with SD medium, probably because of the decrease in retinoid concentration. This study suggests that supplementation of high RA concentrations is only required to supress signals from supplemented components like serum or DMSO (> 0.1 %). Since these components are not included in the SD medium, neuronal induction is probably driven by subnanomolar RA concentrations in an environment that is free of disruptive

inhibitors. The present study confirmed that canonical and non-canonical RA signalling is involved and crucial for neuronal induction.

4.4 Regulation of signalling pathways involved in cell fate decision

The patterning of the neural tube during embryogenesis and the differentiation toward distinct neural subtypes is primarily mediated by RA, BMP, Hh, Wnt and FGF signalling (Kudoh *et al.,* 2002; Lara-Ramírez *et al.,* 2013; Le Dreau and Marti, 2012). Inhibition of mesoderm and endoderm-promoting signals, such as Wnts (via Dkk1), Nodal (via cerberus and lefty), BMPs (via chordin, noggin, and follistatin), and Notch (via DAPT) offers an opportunity to enhance or induce neuronal fate decision *in vitro* (Azari and Reynolds, 2020; Crawford and Roelink, 2007; Levine and Brivanlou, 2007). In the developed SD differentiation medium, the content of growth factors and inducers was reduced to a minimum. The regulation of several signalling pathways in neuronal cell fate decision by application of the established method was accessed by inhibitor supplementation through the differentiation process and proteome analysis before and five days after neuronal induction.

Several studies have suggested that the neuronal default mechanism is a consequence of a lack of BMP signalling, preventing formation of neural tissue (Levine and Brivanlou, 2007; Muñoz-Sanjuán and Brivanlou, 2002). SMAD proteins are responsible for the intracellular transduction of signals from growth factors of the TGF-β superfamily, such as Activin, Nodal and BMP (Chen and Meng, 2004). In this study, the influence of the SMAD inhibitor SB431542 (ALK4, ALK5 and ALK7 inhibitor) and DMH1 (ALK2 inhibitor) on neuronal induction by implementation of the SD method was tested. Recently, it was shown that both inhibitors are appropriate to induce or promote neuronal differentiation *in vitro* (Kim *et al.,* 2010; Neely *et al.,* 2012; Pauly *et al.,* 2018). ALK2, ALK3, and ALK6 function as BMP receptor (Miyazawa *et al.,* 2002). In the established SD method, supplementation of the ALK2 inhibitor revealed no enhancing effect. The activin receptor-like kinases ALK4, ALK5, and ALK7 are activated by activin and nodal signal, stimulating SMAD2/3 in turn (Miyazawa *et al.,* 2002). In this study, the SMAD2/3 inhibitor SB431542 had a negative effect that occurred exclusively during the early differentiation process. Accordingly, proteome analysis demonstrated a slight increase of SMAD2 during early differentiation. These findings reinforced the suggestion that BMP inhibition is required only as a late step during neural induction (Linker and Stern, 2004). The inhibitory effect of SB431542 on early neuronal differentiation under the given conditions might also be caused by an evoked inhibition of RA response, recently observed in mESC (Du *et al.,* 2014). While the proteins SMAD1, SMAD5, and SMAD8 that are characterised as substrates for BMP-activated receptors (Miyazawa *et al.,* 2002) were not captured by the proteome analysis, a slight downregulation of the SMAD4 level after neuronal induction was shown. SMAD4 is a key player and forms complexes with activated SMAD proteins to enter the nucleus and regulate expression of target genes (Chen and Meng, 2004). Additionally, SMAD4 was reported to control CDK4 expression (Ueberham *et al.,* 2012). However, the protein level of CDK4 revealed no regulation through neuronal induction in this study. Several groups reported a tight correlation between inhibition of CDK activity and neuronal differentiation, showing for example

that overexpression of CDK4 delays neurogenesis and inhibition of CDK2 and/or CDK4 expressions induces neuronal differentiation in neural stem cells (Lange *et al.*, 2009; Lim and Kaldis, 2012). Surprisingly, CDK2 and CDK4 revealed a high expression level without significant regulation mediated by neuronal induction. Hence, it was hypothesised that downregulation of these cell cycle regulators occurs later when neuronal progenitor cells stop proliferation. CDK5 demonstrated a distinctly increased protein level after five days treatment by the SD method. CDK5 activity is found almost exclusively in postmitotic neurons and was reported to be essential for cell cycle arrest to facilitate neuronal differentiation (Cicero and Herrup, 2005).

The glycogen synthase kinase GSK3β antagonizes the canonical Wnt pathway and therefore plays a central role in the neuronal differentiation process (Valvezan and Klein, 2012). In this study, the increase of GSK3β after neuronal induction by application of the SD method suggests a repression of the Wnt signalling pathway. Further downregulation of the Wnt signalling by supplementation of the tankyrase inhibitor XAV939, that is supposed to downregulate Wnt/β-catenin signalling, thereby enhancing neuronal differentiation of ESC (Song *et al.,* 2018), presented no effect on P19 differentiation in this study. While tankyrase promotes Wnt signalling, the tankyrase binding protein TNKS1BP1 was reported to have several functions such as regulation of the actin cytoskeleton rearrangement (Ohishi *et al.,* 2017; Zou *et al.,* 2015). This might explain that TNKS1BP1 was upregulated after neuronal induction while the GSK3β level indicate a repression of Wnt signalling. Accordingly, MYC, a direct target of the Wnt pathway (He *et al.,* 1998), was downregulated during early differentiation in this study. MYC was reported to be critical for the maintenance of ES cell self-renewal and an upregulation in P19 cells was shown to promote cell proliferation (Varlakhanova *et al.,* 2010; Zhang *et al.,* 2012).

A previous study revealed that MYC promotes neuronal differentiation in the neural tube caused by an increased cell division of neuronal precursors and the inhibition of Notch signalling (Zinin *et al.,* 2014). The Notch signalling pathway was shown to promote glial differentiation while it supresses neuronal differentiation (Artavanis-Tsakonas *et al.,* 1999; Lutolf *et al.,* 2002). Accordingly, on protein level, several members of the Notch pathway, were downregulated during early neuronal differentiation in this study. This includes the strawberry notch homolog 1 (SBNO1) that was reported to play an important role during development of the vertebrate CNS (Takano *et al.,* 2010), the protein Notchless (NLE) that depending on the context, either negatively or positively regulates the Notch pathway (Cormier *et al.,* 2006; Royet *et al.,* 1998), and the Notch receptor NOTCH2 that was reported to inhibit differentiation of *cerebellar granule* neuron precursors by maintaining proliferation (Solecki *et al.,* 2001). Numb, an inhibitor that antagonizes Notch signalling, promotes cell cycle arrest and neuronal differentiation (Li *et al.,* 2003; Spana *et al.,*1996). However, NUMB, stayed mostly unaffected in this study. DAPT is a γ-secretase inhibitor and indirectly an inhibitor of Notch signalling and promotes cardiac as well as neuronal differentiation (Crawford *et al.,* 2007; Liu *et al.,* 2014). DAPT supplementation is also included in the protocol of

Nakayama *et al.* (2014) but had no effect on the neuronal differentiation by usage of the established SD medium.

A significant upregulation of two factors KIF3a and GLI3, involved in Hh signalling, were identified in the proteome analysis. The kinesin family member KIF3a was reported to regulate ciliogenesis in response to Hh signalling (Hoang-Minh *et al.,* 2016). The activity of GLI3, a zinc finger protein that acts as an effector of Hh signalling, is regulated through the primary cilium and thereby mediates cell cycle exit and the initiation of cortical neurogenesis (Hasenpusch-Theil *et al.,* 2018; Wilson *et al.,* 2012). But GLI3 has a dual function as transcriptional activator and repressor of the Hh pathway, depending on the form (Matissek and Elsawa, 2020; Sasaki *et al.,* 1999). The requirement of Hh signalling during early neuronal differentiation under the established conditions was elucidated by usage of the inhibitor cyclopamine. Inhibition of the Hh signalling pathway was reported to prevent the response to RA treatment and results in the arrest at the primitive ectoderm stage (Maye *et al.,* 2004). Accordingly, the ability to induce neuronal differentiation by the SD method appeared to be abolished through cyclopamine supplementation.

Overall, the established SD method was shown to regulate multiple effectors that mediate signalling pathways affecting neuronal differentiation. While SMAD and BMP inhibition revealed mixed results, Wnt and Notch signalling were downregulated in the early neuronal differentiation. Further inhibition of Wnt, Notch or BMP by supplementation of inhibitors that were applied in several protocols to promote differentiation, revealed to have no effect on the differentiation by application of the SD method. Since these signalling pathways were already downregulated without the addition of effectors, these inhibitors appeared to be redundant for the established method. In turn, proteome analysis suggests an activation of the Hh pathway. The requirement for activated Hh signalling was confirmed in this study by the suppressive effect of an Hh inhibitor on neuronal induction. The present results showed that the regulation was independent of exogenous factors except possible residual RA. The regulation of diverse signalling pathways, required for neuronal differentiation, suggests that no exogenous factors are necessary to mediate the switch from a pluripotent cell to a neuron.

4.5 Antioxidant defence and ROS signalling mediate the switch to neurons

ROS are involved in cell signalling and act as second messengers involved in the regulation of various cellular processes such as proliferation and cell survival (Bae *et al.,* 2009). The ROS level revealed to be critical for redox sensitive signalling pathways that mediate early neuronal development (Hu *et al.,* 2017). Here, the effect of decreasing ROS levels by antioxidant treatment and increasing ROS levels by knocking down NRF2 in P19 cells during neuronal differentiation was tested using the established SD method.

Previously was reported that a decrease of the ROS level by antioxidants have neuroprotective effects in neurons, but the neuronal differentiation process is retarded or inhibited (Bell *et al.,* 2015; Chiarotto *et al.,* 2014, Shaban *et al.,* 2017; Velusamy *et al.,* 2017). Also, it is known that pathways, important for dendritic and synaptic

development, are enhanced by mild ROS exposure (Budnik *et al.,* 2011; Rharass *et al.,* 2014; Rosso *et al.,* 2005). Moreover, excessive oxidative stress can lead to synapse overgrowth (Milton *et al.,* 2011). Here, a decreased ROS level through treatment with the antioxidants tiron and trolox appeared to impair neuronal differentiation in a dose-dependent manner. High antioxidant concentrations resulted in a reduced cell survival and prevented the induction of neuronal differentiation while differentiation potential and axonal growth was attenuated in lower dose. Thus, as expected, the absence of mild ROS exposure from antioxidant treatment negatively affects axonal growth to differentiation process.

In turn, to investigate an increased ROS level, a P19 *Nrf2* knockdown mutant was generated. NRF2 is a transcription factor that controls the expression of several antioxidant and detoxifying genes (Bell *et al.,* 2015). It was suggested that a steady decrease of NRF2 expression, provides a more flexible redox environment to mediate redox-sensitive signalling pathways during neuronal differentiation (Bell *et al.,* 2015; Olguín-Albuerne and Morán, 2018). For hESC, it has also been reported that knockdown of *Nrf2* promotes exit from the stem cell state and spontaneous neuronal differentiation (Hu *et al.,* 2017). However, spontaneous neuronal differentiation in the growth medium was not observed in the P19 *Nrf2* knockout mutants generated. Knockout of the *Nrf2* gene showed no effect on neuronal induction potential, but it should be noted that one of the verified knockout mutants showed delayed differentiation with reduced cell survival, whereas the other clone showed an increased proliferation rate. However, common to both clones was that the drastic reduction in antioxidant defence by *Nrf2* knockout likely led to high oxidative stress resulting in premature cell death.

Previous studies have observed that autophagy is involved in the regulation of ROS levels during neuronal development, for example, through mitophagy and the inactivation of NRF2 (Boya *et al.,* 2018; Jang *et al.,* 2016). Therefore, the level of several NRF2-ARE-controlled proteins and, KEAP1 und p62, the two effectors of NRF2, was investigated by mass spectrometry analysis in WT and Δ*Becl1* mutant cells. The protein level of the studied enzymes, involved in antioxidant defence and known to be regulated by NRF2-ARE, showed a various regulation through neuronal induction. The apolipoprotein E (APOE) and the superoxide dismutase 2 (SOD2) showed an increased protein level after neuronal induction. The APOE expression level was reported to reflect the degree of cellular differentiation during neural induction and to be highest at the earliest stage of neuronal differentiation, followed by dramatical decrease as the cells become more differentiated (Lee *et al.,* 2020). In previous studies, it was shown that the APOE ε4 allele plays an important role in antioxidant status (Miyata and Smith, 1996; Zappasodi *et al.,* 2008). The APOE4 isoform is also suspected interfere with the autophagic process (Parcon et al., 2018). However, the isoform could not be determined in the proteome analysis. A special requirement of SOD2 for early neural specification in mESC was described (Bhaskar *et al.,* 2020). Accordingly, the highest SOD2 level was detected in the CNS during early neuronal development in mice (Yon *et al.,* 2011). An increased SOD2 level during this developmental state could also be confirmed for P19 cells in my work. The glutamate cysteine ligase catalytic (GCLc) or modifier (GCLm) protein and the

glutathione reductase (GSR) demonstrated an opposite effect and were downregulated during early neuronal differentiation. The glutamate cysteine ligase, composed of GCLc and GCLm, is the rate limiting enzyme in the synthesis of glutathione, an important endogenous antioxidant (Mani *et al.,* 2013). Transcriptional regulation of GSR by NRF2 was also found to be critical for modulating the glutathione redox state (Harvey *et al.,* 2009). Surprisingly, the Δ*Becl1* and the Δ*BirC6* mutant demonstrated some common regulations of these enzymes that differ to WT cells. The antioxidant APOE, GCLc, and GSR appeared to be more increased in both differentiated mutants compared to WT. In the Δ*Becl1*, enhanced antioxidant defence through upregulation of these enzymes could compensate for the blocked regulatory function of autophagy, whereas no explanation was found for the Δ*BirC6*.

NRF2 itself presented a low concentration by immunoblotting and was not captured by proteome analysis. The assumption that the NRF2 level became restricted through neuronal induction was reinforced by the observation that the p62 protein level appeared to be reduced. Besides the function as cargo receptor for autophagic degradation of ubiquitinated targets, p62 is reported to be upregulated in response to oxidative stress (Mathew *et al.,* 2009; Zaffagnini and Martens, 2016). The promotor of p62 contains an ARE and therefore its expression is also induced by NRF2 (Jain *et al.,* 2010). p62 itself stimulates the NRF2 activity by binding to the NRF2 inhibitor KEAP1, resulting in an autophagic degradation of the repressor, creating a feedback-loop in the KEAP1/NRF2-pathway (Jain *et al.,* 2010). Accordingly, p62 and KEAP1 levels were downregulated in P19 WT cells during early neuronal differentiation, also suggesting an accompanied downregulation of NRF2. While the p62 got reduced after neuronal induction in WT was this not the case for the Δ*Becl1* mutant, while it experienced an even stronger downregulation caused by rapamycin treatment. This indicated a tight control of p62 by autophagy, likely indirectly by limiting the NRF2 concentration.

Altogether, ROS are known to be critical in the mediation of autophagy, apoptosis and diverse pathways that are involved in the switch from pluripotent, proliferating cells to postmitotic neurons. In this study, lowering ROS levels by antioxidant treatment attenuated axonal growth and the potential to induce neuronal differentiation, whereas increasing ROS levels by knocking down NRF2 negatively affected the survival of mature neurons. KEAP and p62, involved in the NRF2-pathway feedback-loop, were downregulated after neuronal induction, likely accompanied by a NRF2 restriction. NRF2 regulated enzymes demonstrated a varied regulation triggered by neuronal induction. The analysed glutathione modifying enzymes GCLc, GCLm, and GSR were downregulated, and SOD2 as well as APOE were upregulated during early neuronal differentiation. The differential regulation of different NRF2-controlled enzymes leads to the assumption that they have different importance in the weak intrinsic antioxidant defence that ensures tight regulation of redox-sensitive signalling pathways during early neuronal differentiation. Moreover, downregulation of p62, APOE, GCLc, and GSR after neuronal induction appeared to be dependent on autophagy levels.

4.6 Autophagy in the regulation of neurogenesis and early axonal growth

The mTOR/PI3K/AKT survival pathway is critical for the regulation of autophagy. mTOR is a downstream component of PI3K/AKT and ERK1/2 signalling (Switon *et al.,* 2017). PI3K/AKT signalling stimulates activity of the autophagy inhibitor mTORC1 that functions as a sensor of cellular nutrient level and is suppressed in the absence of growth factors, resulting in the activation of autophagy (Bar-Peled and Sabatini, 2014). Regulation of the PI3K/AKT pathway, and thus regulation of autophagy during neuronal differentiation, yielded conflicting results (Lopez-Carballo *et al.,* 2002; Magalingam *et al.,* 2020; Morgado *et al.,* 2015; Zeng and Zhou, 2008). The controversial findings of previous studies regarding the regulation of autophagy during neuronal differentiation could be explained by a time-dependent control. This assumption was reinforced by the observation that RA-induced neuronal differentiation of F9 cells follows a biphasic regulation of the PI3K/AKT pathway, with early activation followed by inhibition (Bastien *et al.,* 2006). The mTOR/AKT/PI3K signalling pathway is a key player of autophagy and of neuronal development (Sánchez-Alegría *et al.,* 2018). Therefore, manipulation of autophagy regulation was performed by interfering with this pathway or by direct targeting of autophagy related proteins. Remarkably, autophagy inhibition with 3-MA, LY294002, A-674563, chloroquine, or STF-62247 as well as the knockout of *Becl1*, *p62*, *Atg7*, or *Atg9a* that address autophagy at different stages, demonstrated to cause a similar morphological phenotype during the neuronal differentiation process. Since the disruption of the autophagic process at each level showed the same effect during neuronal differentiation, this strongly suggests that the phenotype is caused by a lack of autophagy and is not an effect of individual links in the process associated with further cellular functions.

Inhibition of autophagy caused an axonal overgrowth during early neuronal differentiation and premature cell death of mature neurons. Although, it was originally reported that disruption of autophagy impairs neuronal differentiation and causes axonal retraction (Zeng and Zhou, 2008). However, consistent with the results of this study, it was observed in later studies that depletion of ATG7 in murine neurons causes the growth of longer axons, whereas activation of the autophagy pathway with rapamycin results in shorter neurites (Ban *et al.,* 2013; Chen *et al.,* 2013). Accordingly, the mTOR inhibitors rapamycin and torin2 showed the opposite effect to the autophagy inhibitors and caused a shortening of neurite length. Autophagosomes generated at the tips of actively elongating axons contain membrane and cytoskeletal components (Hollenbeck and Bray, 1987; Maday *et al.,* 2012). Induction of autophagy results in degradation of cytoskeletal components and consequently to an inhibition of neurite outgrowth (Chen *et al.,* 2013; Stavoe *et al.,* 2016).

The expression profile of the selected axon markers BASP1, GAP43, KIF5c, and NCAM1 showed an increase after neuronal induction in this study, as previously reported for iPSC by Lindhout *et al.* (2020). ARPC2 and ARPC4 are subunits of the actin related protein 2/3 (ARP 2/3), that was suggested to be required at various stages of development in the nervous system and is essential for the formation of lamellipodia and filopodia, axon guidance, and growth cone motility (Chou and Wang, 2016; Korobova and Svitkina,

2008). The subunits of the ARP 2/3 complex were identified as potential effectors of NCAM1 (Frese *et al.,* 2017). However, in contrast to NCAM1 and the other axon markers studied, the subunits ARPC2 and ARPC4 showed reduced protein levels after neuronal induction in WT cells but not in the knockout mutants Δ*Becl1* and Δ*BirC6*. In contrast, the significantly higher NCAM1 level was restricted to the neuronal differentiated *Becl1* knockout mutant. The neural cell adhesion molecule 1 (NCAM1) is one of the most abundant neuronal adhesion proteins and promotes the actin filament growth at the dendritic growth cone where the protein is highly enriched during the early neuronal development (Frese *et al.,* 2017; Sharma *et al.,* 2015). During later neuronal differentiation, NCAM1 was found diffusely distributed over the dendritic plasma membrane (Frese *et al.,* 2017). These findings, together with the observations in this study, suggest that downregulation of NCAM1 levels is mediated by autophagy, possibly even by direct degradation. Increased NCAM1 levels resulting from the lack of autophagy could cause axonal overgrowth during early differentiation that likely disappears with the redistribution of NCAM1 from the growth cone to the cell soma and would consequently explain why the effect of axonal overgrowth in the Δ*Becl1* mutant is limited to early neuronal development.

Besides the function of mTOR/PI3K/AKT in the regulation of autophagy, it was reported that PI3K facilitates microtubule-dependent membrane transport for neuronal growth cone guidance (Akiyama and Kamiguchi, 2010). However, since axonal overgrowth occurred regardless of whether autophagy was inhibited via the PI3K complex or by directly addressing ATGs, it is more likely that the phenotype is directly influenced by autophagy level. By proteome analysis, mTOR/PI3K/AKT signalling was in part enhanced during early neuronal differentiation in SD medium. mTOR and mLST8 are both parts of the mTORC1 and mTORC2 complex. While mTOR revealed no significant regulation in the analysed conditions, the mLST8 scaffolding component slightly increased after neuronal induction was initiated. Recently, it was suggested that this protein is only critical for mTORC2 assembly and function, while being dispensable for mTORC1 (Hwang *et al.,* 2019). Even though the regulatory associated protein of mTOR-mTORC1 (RAPTOR/RPTOR) demonstrated a higher protein level than the rapamycin-insensitive companion of mTOR-mTORC2 (RICTOR), both levels showed an upregulation by SD treatment.

mTORC2 activates AKT which in turn phosphorylates a variety of substrates that are involved in processes such as cell survival, growth, and proliferation (Cheng *et al.,* 2013). While AKT1 is essential in the CNS, it is not clear whether it inhibits or promotes neuronal differentiation and mediates Notch-regulated neuronal differentiation (Bang *et al.,* 2001; Cheng *et al.,* 2013; Vojtek *et al.,* 2003). In this study, AKT1 was increased in the early neuronal differentiation. The regulation of PIK3C3 (VPS34) and PIK3R4 (VSP15) is less clear pronounced but a slight increased protein level in the differentiated P19 WT cells was observed. PIK3C3 and PIK3R4 are both components of an autophagy specific complex which is required for the initiation of autophagy (Itakura *et al.,* 2008). The protein level of MAPK (ERK1) also demonstrated an increase through neuronal induction by implementation of the SD method. The MAPK-ERK1/2 signalling pathway regulates a

broad variety of cellular processes and promotes early neuronal differentiation in murine ESCs by the release from the self-renewal program (Kosaka *et al.,* 2006; Kunath *et al.,* 2007; Li *et al.,* 2006). ERK1/2 is activated through non-canonical RA signalling mediated phosphorylation and the ERK1/2 signalling is suspected to be involved in the induction of neuronal differentiation by oxidative stress (Gupta *et al.,* 2008; Hu *et al.,* 2017; Persaud *et al.,* 2013).

Besides the regulation of autophagy by the mTOR/PI3K/AKT signalling pathway, the level of proteins that are directly involved in the autophagic degradation was analysed. An upregulation of *Atg9a*, *Atg7*, *Becl1*, *Ambra1* expression and the LC3-II/LC3-I ratio was described during neurogenesis of olfactory bulb derived NSCs and in the mouse cerebral cortex during the initial period of neuronal differentiation (Lv *et al.,* 2014; Morgado *et al.,* 2015, Vázquez *et al.,* 2012). In this study, autophagy was expected to be upregulated under established conditions because autophagy is known to be upregulated under nutrient-rich conditions and during neuronal differentiation, and here both conditions are present simultaneously. Indeed, LC3 (α/β), ATG7, ATG12 were upregulated indicating an increased autophagy level. In turn, the activating molecule in Becl1 regulated autophagy protein 1 (AMBRA1), BECL1 itself, and p62 (SQSTM1) presented a reduced protein level during early neuronal differentiation. This is possibly due to their dual cellular function. ATG5, ATG12, AMBRA1 and BECL1 are important factors that mediates the crosstalk between autophagy and apoptosis (Booth *et al.,* 2014; Sun, 2016). Besides the function as autophagic cargo receptor, p62 is known to be involved in the response to oxidative stress (Mathew *et al.,* 2009; Zaffagnini and Martens, 2016). In the Δ*Becl1* mutant, upregulation of ATG12 failed due to blockage of autophagy. Additionally, the Wnt target MYC was not regulated through neuronal induction. This suggest that regulation or direct degradation of MYC was dependent on autophagy or that Wnt signalling was not downregulated in contrast to WT. The levels of GLI3, an effector of HH signalling, and ASCL2, a transcription factor that reduces proliferation and strongly promotes neuronal differentiation (Liu *et al.,* 2019), were affected in the Δ*Becl1* mutant under both conditions analysed, suggesting that a basal autophagy level is required to regulate their expression. However, while GLI3 exhibits a reduced level, ASCL2 level is significantly increased in the Δ*Becl1* mutant in both conditions compared to the WT.

In a previous study, depletion of *BirC6* showed to enhance autophagy in non-neuronal cells as well as in neurons (Jia and Bonifacino, 2019). BIRC6 functions as Ub-conjugating enzyme (E2/E3) that negatively regulate autophagy. It is involved in mono-ubiquitination of LC3β, marking it for degradation by the proteasome. Hence, knockout of *BirC6* demonstrated to facilitate the clearance of protein aggregates by increasing the level of cytosolic LC3β-I (Jia and Bonifacino, 2019). In addition to the regulative function in autophagy, BIRC6 has an anti-apoptotic function and is required for the control of the final stages of cytokinesis (Lamers *et al.,* 2012; Pohl and Jentsch, 2008). But multiple binding partners and different functional domains of BIRC6 suggest a multifunctionality of this protein (Bartke *et al.,* 2004; Pohl and Jentsch, 2008). In this study, the phenotype of the *BirC6* knockout mutant was completely different from that of the rapamycin

treated WT during neuronal induction. Therefore, it was hypothesized that the lack of ability of the Δ*BirC6* mutant to promote neuronal differentiate under the given conditions was caused either by a greater increase in autophagic flux than mediated by rapamycin treatment or by the absence of other BIRC6 function. The Δ*BirC6* mutant showed significant differences in morphology and protein profile in growth and SD medium compared to the WT. Even though the morphology and the absence of the neuronal marker indicated that neuronal differentiation had failed, the mutant also showed a shift in expression profile caused by the switch to SD medium. Therefore, it was hypothesized that the Δ*BirC6* mutant differentiates, but in which direction remains unclear.

Although the expression profile does not indicate neuronal differentiation and barely any neurites could be detected, an increase of axon markers NCAM1, BASP1, and GAP43 was determined in SD medium. But it has to be noted that both KIF5c and KIF3c that were confirmed to be enriched in the neurons, were not upregulated in *BirC6* knockout mutant. The kinesin superfamily (KIF) mediate cargo transport along microtubules. KIF5c is enriched in neuronal cells to mediate the transport to nerve terminals while KIF3a regulate ciliogenesis in response to Hh signalling (Hirokawa *et al.,* 2010; Hoang-Minh *et al.,* 2016). In contrast, the culture treated with rapamycin induced by neuronal induction showed the strongest KIF5c increase, highlighting the different cell fates under the two conditions. The regulation of factors involved in the execution of apoptosis presented to be less pronounced for the Δ*BirC6* mutant in SD medium (further discussed below). In addition, the factors NLE and SBNO1 showed no downregulation in the mutant, suggesting that downregulation of the Notch signalling pathway, which is important for neuronal differentiation, was absent.

In a few cases, the Δ*Becl1* and the Δ*BirC6* share common regulations that differ from WT. Before neuronal induction was applied, the RA synthesizing enzyme ALDH1B1 was increased while CRABP2 was decreased in both mutants compared to WT. Furthermore, no regulation of CRABP2 in the Δ*BirC6* mutant was detected, while it appeared to be upregulated in all other conditions through neuronal induction. Additionally, the antioxidant APOE, GCLc, and GSR appeared to be stronger increased in both differentiated mutants in SD medium. Underlying mechanisms that caused the shared behaviour of both mutants to effect RA signalling and the antioxidant defence remain unclear. In neurons, pharmacological mTOR inhibition by rapamycin or torin1 revealed to be insufficient to upregulate autophagy (Maday and Holzbaur, 2016). Therefore, the response to rapamycin at day five of the differentiation protocol may already be reduced at the molecular level and explains the weak effect on the expression profile. From the investigated proteins only NOTCH2, TNKSBP1B1, and p62/SQSTM1 presented a significantly varied regulation compared to untreated WT cells. The effect of 3-MA treatment demonstrated to be even less pronounced on the proteome profile.

In summary, autophagy blocked by different approaches resulted in the same phenotype during differentiation, indicating that this effect is caused by a lack of autophagy in general. The controversially discussed role of autophagy was clearly solved for the conditions in this study. Autophagy inhibition did not impair neuronal

differentiation and causes independently on the application axonal overgrowth during early neuronal differentiation and premature cell death of mature neurons, while the mTOR inhibitors rapamycin and torin2 that enhance autophagy demonstrated the opposing effect and caused a shortens of the neurite length. Because of a highly increased NCAM1 level in the Δ*Becl1* mutant, is assumed that the limitation of NCAM1 prevents axonal overgrowth and is dependent on autophagy. Thus, a lack of autophagy could cause axonal overgrowth during early differentiation that disappears probably with the redistribution of NCAM1 from the growth cone to cell soma and would consequently explain why the effect in the Δ*Becl1* mutant is limited on early neuronal development. Moreover, the regulation of ASCL2, MYC, and GLI3 and some factors involved in the antioxidant defence and RA signalling revealed to be affected by the *Becl1* knockout. Nevertheless, successful neuronal differentiation of the Δ*Becl1* mutant could be clearly verified morphologically, by an increase of neuronal and axonal markers and a similar signalling pathway regulation as shown for differentiating WT cells, such as the necessary Notch downregulation. Therefore, the present data suggest that autophagy is upregulated but not essential for neuronal differentiation but is crucial for axonal development and the survival of mature neurons. The *BirC6* knockout mutant strongly deviate in morphology and protein profile from WT as well as Δ*Becl1* mutant cells, even if they showed some regulations in common. Neuronal marker revealed to stay downregulated also the different regulation of signalling pathways indicated a non-neuronal cell fate. Furthermore, neither the PI3K/AKT survival pathway nor pro-apoptotic factors or KIF proteins revealed an upregulation through induction of differentiation in these cells. Moreover, the downregulation of the Notch pathway, crucial for neuronal differentiation, failed. If the differences between the *BirC6* knockout mutant and the WT treated with rapamycin are explained by the multifunctionality of BIRC6 is pending. It is likely that the Δ*BirC6* phenotype was caused by a higher effectiveness to increase the autophagic flux or the loss of another function of this protein.

4.7 A decreased threshold to induce apoptosis during early neuronal differentiation

It was reported that half of the produced neurons are degraded by neuronal death during development of the nervous system (Oppenheim, 1991). Neuronal progenitors and neurons are selectively eliminated by apoptosis (Nijhawan *et al.,* 2000; Opferman and Korsmeyer, 2003). To ensure long-term survival of neurons in the mature nervous system, the threshold required to induce apoptosis becomes elevated during neuronal differentiation and maturation (Polster *et al.,* 2003). Application of the established SD method demonstrated a period of high cell death during early neuronal differentiation (3-6 d of the SD protocol). This subsequently led to an accumulation of cellular debris. *In vivo*, apoptotic bodies would be phagocytosed to clean the environment and prevent inflammation (D'Arcy, 2019; Elmore, 2007). Pure neuronal *in vitro* cultures are not able to free themselves from the cell debris. It was observed that if the cellular debris was not removed daily by media exchange during this period, this resulted in degeneration of the remaining cells in the culture. It was hypothesized that apoptotic bodies release their cellular components if not removed, inducing secondary necrosis (Kurosaka *et al.,*

2003; Savill and Fadok, 2000). In this study, it was shown that it is impossible to completely remove cell debris by media exchange. Tracking the cells through the differentiation process showed that cell debris was deposited on the neuronal clusters generated and increased in size during aging. This assumption was confirmed by staining the layer of (late) apoptotic/necrotic cells that increased simultaneously to cluster size of healthy neurons during neuronal development. Morphologically, the derived neural clusters by using the SD method did not differ from generated neural clusters by other protocols such as the method of Nakayama *et al.* (2014). Nevertheless, this observation and the underlying mechanism have not been addressed previously. Also in this study, the function and effect on the underlying neurons remains unclear.

The assessment that decreased or increased autophagy levels had a drastic effect on neurite development but not on differentiation potential, and that the amount of dying cells did not differ when autophagy was blocked, suggests that autophagic cell death was not involved during neuronal differentiation. The early cell death of mature neurons with blocked autophagy was probably caused by an accumulation of dysfunctional proteins during aging. In turn, an increased autophagy level triggered by rapamycin or torin2 treatment resulted in fewer cells surviving the differentiation process. Under these conditions, massive autophagy could have led to an autophagic cell death or to an enhanced apoptosis level induced through the crosstalk of autophagy and apoptosis. However, the proteomic profile shows that neither treatment with 3-MA, rapamycin, nor *Becl1* knockout leads to a massive increase in autophagy or exhibits drastic abnormalities in the regulation of apoptotic proteins.

Between autophagy and apoptosis exists an extensive crosstalk because both pathways share some common signals and regulatory components that mediate the molecular switch between both processes (Maiuri *et al.,* 2007; Wu *et al.,* 2014). A previous study showed that AKT inhibition induces autophagy and apoptosis, while induction is limited on autophagy by direct mTOR inhibition (Muilenburg *et al.,* 2014). Therefore, while mTOR signalling is restricted to the control of autophagy, PI3K/AKT regulates autophagy and apoptosis in divergent signalling pathways (Muilenburg *et al.,* 2014). Besides PI3K/AKT signalling, the MEK/ERK survival pathway was also recently reported to be involved in the restriction of the apoptotic pathway in neurons (Hollville *et al.,* 2019). The analysed proteome profile indicated an increased PI3K/AKT and MAPK/ERK signalling after neuronal induction of the treated and untreated WT cells and the Δ*Becl1* mutant. Nevertheless, detection of several important factors involved in autophagy and apoptosis, suggest an upregulation of both processes during early neuronal differentiation under the given conditions.

It is assumed that the molar ratio between pro-apoptotic and anti-apoptotic proteins gives information about the responsiveness to apoptotic signals (Raisova *et al.,* 2001). In this study, the proteome profile of the P19 cells after five days treatment with the SD method was analysed. During this early differentiation step, neurons just derived from neuronal precursor cells and further differentiated to mature postmitotic neurons during the following days. The protein profile of the WT and Δ*Becl1* mutant cells suggests an increased potential to induce apoptosis during early neuronal

differentiation. Pro-apoptotic proteins such as the CASP3, CASP6, APAF1, and SEPT4 were shown to be upregulated, while simultaneously anti-apoptotic proteins such as MCL-1, BIRC5, BECL1 and AMBRA1 were downregulated. AMBRA1-BECL1 interactions promote autophagy, while it is supressed by AMBRA1-BCL-2 and BECL1-BCL-2 or BECL1-BCL-xL interaction (Kang *et al.,* 2011; Ravikumar *et al.,* 2009; Sun, 2016). Besides the suppression of autophagy initiation through binding with the anti-apoptotic proteins of the Bcl-2- family, BECl1 is reported to be cleaved by the caspase-3-, 7- and 8, generating N- and C-terminal fragments that lose the ability to induce autophagy. The C-terminal fragment translocate to mitochondria, where it sensitizes cells to apoptotic signals (Djavaheri-Mergny *et al.,* 2010). In contrast to the other anti-apoptotic proteins detected, BCL2L1 (BCL-X) was as upregulated. BCL2L1 was reported to have a critical role during neuronal development and to promote neuronal survival (Harder *et al.,* 2012; Nakamura *et al.,* 2016). To prevent cell death in neurons, this anti-apoptotic protein inhibits BAX activation (Harder *et al.,* 2012). Anyway, protein levels of the pro-apoptotic Bcl-2 family proteins BAX and BAK1 were unaffected by neuronal induction, whereas the BAX level generally appeared significantly higher than BAK1 level. While neuronal progenitor cells still express BAK, an alternatively spliced form of BAK (N-BAK) is only present in post-mitotic neurons (Deckwerth *et al.,* 1996). A pro-apoptotic or neuroprotective function of this form is still controversial (Fannjiang *et al.,* 2003; Sun *et al.,* 2001; Uo *et al.,* 2005). The level of the pro-apoptotic Bcl2-family protein BAX decrease in the brain postnatally but is maintained at low levels (Krajewska *et al.,* 2002; Vekrellis *et al.,* 1997). Thus, regulation of these factors might be observed in a later neuronal differentiation state than analysed in this study.

The upregulation of several proteins with pro-apoptotic functions observed in this study is probably restricted to early neuronal differentiation. Expression of several caspases, including CASP3, and pro-apoptotic Bcl-2 or BH3-only family members were reported to be downregulated in mature neurons to reduce the responsiveness to apoptotic signals (Hollville *et al.,* 2019; Kumar *et al.,* 1992). But during early neuronal differentiation, CASP3 was reported to have a non-apoptotic function as a regulatory molecule in neurogenesis and synaptic activity, facilitating neurogenesis of neuronal progenitors (D'Amelio *et al.,* 2010). The level of APAF-1, the main scaffold protein of the apoptosome complex was reported to decreases during neuronal differentiation until expression is completely shut down in mature neurons (Wright *et al.,* 2007; Yakovlev *et al.,* 2001). In contrast to this finding, an increased APAF1 level was observed in this study after the switch from the pluripotent cells to early neurons, probably decreasing later during differentiation. SEPT4 is an inhibitor of apoptosis protein (IAP) antagonist that binds to IAPs, therefore presenting a pro-apoptotic function (Larisch *et al.,* 2000).

Due to the upregulation of the IAP antagonist SEPT4, the baculoviral IAP repeat containing (BirC) proteins BIRC5 showed a slight downregulation after neuronal induction. BIRC5 (Survivin) and BIRC6 (Bruce) suppress apoptosis through the inactivation of caspases and pro-apoptotic proteins through binding and/or cleavage or ubiquitin-dependent degradation (Low *et al.,* 2013; Lamers *et al.,* 2011; Verhagen *et al.,* 2001). In addition to their anti-apoptotic function, BIRC5 and BIRC6 are also involved in

the regulation of autophagy. BIRC5 negatively modulates the protein stability of ATG7 and physically binds to ATG12-ATG5 (Lin *et al.,* 2020). BIRC6 is involved in mono-ubiquitination of LC3β in cooperation with UBA6, marking it for degradation by the proteasome. Thus, knockout of *BirC6* has been shown to facilitate clearance of protein aggregates by increasing the level of cytosolic LC3β-I (Jia and Bonifacino, 2019). Unlike other cells, autophagy in neurons is not induced by either starvation or pharmacological mTOR inhibition with rapamycin or torin1 (Ariosa and Klionsky, 2016; Maday and Holzbaur, 2016). But recently, it has been reported that depletion of BIRC6 or UBA6 enhances autophagy in both non-neuronal cells and neurons (Jia and Bonifacino, 2019). From the proteomic profile, no clear conclusion could be drawn about the effect of the *BirC6* knockout on autophagic flux. For the analysed proteins involved in apoptosis execution or prevention, a clear separation of the Δ*BirC6* mutant from the wild type was shown. The ΔBirC6 cells revealed no (up)regulation of the pro-apoptotic CASP3, CASP6, APAF1, and SEPT4 in SD medium, while the anti-apoptotic proteins MCL-1, BIRC5, and AMBRA1 were downregulated simultaneous to WT cells. Thus, this suggests a decreased responsiveness to apoptotic signals in the Δ*BirC6* mutant compared to WT and Δ*Becl1* cells in SD medium. It is conceivable that increased levels of pro-apoptotic proteins are related to the neuronal differentiation that failed in this mutant. Anti-apoptotic BCL2L1 (BCL-X) was shown to be upregulated in the Δ*BirC6* mutant in both analysed conditions. Therefore, BCL-X was a potential candidate to compensate for the loss of anti-apoptotic BIRC6 function, regardless of media conditions. Furthermore, no regulation of the PI3K/AKT or MAPK/ERK signalling by detection of AKT1, PIK3C3, PIK3R4, and MAPK3 was discovered by the switch of the Δ*BirC6* mutant from growth to SD medium. Consequently, the shift in the proteome profile of the Δ*BirC6* mutant cells regarding the survival pathways was less pronounced.

Overall, early neuronal differentiation was characterized by a period of highly increased cell death due to apoptosis rather than autophagic cell death. It was shown that blocked autophagy only had an impact on the survival of mature neurons since dysfunctional proteins probably accumulated in the cell. In differentiating P19 WT and Δ*Becl1* mutant cells, an increased level of several pro-apoptotic proteins was detected. In contrast, except for the anti-apoptotic BCL-X, other anti-apoptotic proteins were downregulated after neuronal differentiation was induced. This highly suggests an increased responsiveness to apoptotic signals during early neuronal differentiation. It has been hypothesized that the increased BCL-X level and associated upregulation of PI3K/AKT and MAPK/ERK pathway limits apoptotic signalling and protects cells from cell death during early neuronal differentiation. Hence, the proteome profile indicated a tight regulation of cell death that was adjusted through neuronal differentiation with a decreased threshold to induce apoptosis. To ensure long-term survival of neurons in the mature nervous system, the apoptotic pathway becomes increasingly restricted during neuronal differentiation and maturation (Kole *et al.,* 2013). This probably occurs from the seventh day of the SD protocol, when the period of high cell death is rapidly terminated, and neuronal networks begin to establish. In contrast to WT and Δ*Becl1* cells, the Δ*BirC6* mutant failed to differentiate to neurons and revealed neither an upregulation of the PI3K/AKT or MAPK/ERK signalling nor of pro-apoptotic proteins.

However, the downregulation of the anti-apoptotic proteins studied occurred simultaneously to the neuronally differentiated WT cells. Only the anti-apoptotic BCL-X was upregulated in the Δ*BirC6* mutant, suggesting a potential candidate that compensate for the loss of the anti-apoptotic BIRC6 function. The differences in the regulation of apoptotic factors in WT and Δ*Becl1* compared to Δ*BirC6* when switching from growth to SD medium were attributed to the different cell fate decisions.

4.8 Future perspective

As this study covers a wide range of topics, it also offers many opportunities to follow up on and deepen individual topics. The proteomic data alone promise many more insights into the regulation of, for example, the cytoskeleton or other processes involved in the differentiation process. Also, the proteins identified to be involved in the regulation during neuronal differentiation, partially evoked to be controlled by autophagy, provides a rich source to augment the understanding of specific molecular mechanisms involved in neurodevelopment and offers a good starting point for future analysis. Since the proteomic data in this study cover only a snapshot in the early neuronal differentiation and the regulation of several pathways is known to be critical dependent on different time periods during neuronal differentiation, it would be interesting to expand the proteomic data to more time points.

The cell fate of the *BirC6* knockout mutant and the influence on autophagy has to be addressed in further analysis to understand the deviating phenotype of the mutant. In addition, a comparative analysis of the proteome profile of the generated *p62* or *Nrf2* knockdown mutants under varied autophagy levels as well as several knockdowns in combination could shed more light on the ROS mediated autophagy during neuronal development. Since NCAM1 was identified as potential candidate that causes axonal overgrowth in cells with blocked autophagy, this has to be further proven. It could be implemented for example by a simultaneous BECL1 and NCAM1 knockout. If depletion of NCAM1 rescues the phenotype of the Δ*Becl1* mutant, this would confirm the assumption that NCAM1 degradation is dependent on autophagy to prevent axonal overgrowth. Furthermore, definition of the generated neuronal subtype and the neurotransmitter phenotype is pending. Thereby, investigation of functionality of synapses in autophagy mutant cells would be of interest.

This study also confirmed that RA signalling is involved in the differentiation process even if no RA was supplemented in the established SD method. Determination of the exact cellular content of RA or precursors during the differentiation process is still pending. Furthermore, it would be interesting to find out whether the addition of different RA concentrations to the SD medium has an influence on differentiation, life span of neurons, or regeneration capacity of ablated axons. Additionally, a dependence on RARβ or RARγ in neuronal differentiation was suggested exclusively for serum-free monolayer cultures in this study. A deeper insight into regulation of different RAR subtypes in dependence of serum addition in monolayer cultures is therefore of greatest interest.

The establishment of a general protocol to allow comparability of different studies is still pending. Whether the SD method is transferable to any cell source remains to be verified. In this case, the SD method would provide a general approach to generate pure neuronal cultures under conditions that make investigations of specific cell requirements during differentiation accessible. In addition, the SD method provides a viable approach for applications such as the study of therapeutic and high throughput screenings. So far, the method has already been applied for the analysis of active substances in the group of Prof. Dr. Stefan Knapp (under revision in *J Med Chem*).

5. References

Abu-Abed S, Dollé P, Metzger D, Beckett B, Chambon P, Petkovich M (2001) The retinoic acid-metabolizing enzyme, CYP26A1, is essential for normal hindbrain patterning, vertebral identity, and development of posterior structures. *Gen Dev* **15:** 226–240

Adikusuma F, Piltz S, Corbett MA, Turvey M, McColl SR, Helbig KJ, Beard MR, Hughes J, Pomerantz RT, Thomas PQ (2018) Large deletions induced by Cas9 cleavage. *Nature* **560:** E8–E9

Adler S, Pellizzer C, Paparella M, Hartung T, Bremer S (2006) The effects of solvents on embryonic stem cell differentiation. *Toxicol In Vitro* **20:** 265-271

Akiyama H, Kamiguchi H (2010) Phosphatidylinositol 3-kinase facilitates microtubule-dependent membrane transport for neuronal growth cone guidance. *J Biol Chem* 285: 41740-41748

Al Tanoury Z, Gaouar S, Piskunov A, Ye T, Urban S, Jost B, Keime C, Davidson I, Dierich A, Rochette-Egly C (2014) Phosphorylation of the retinoic acid receptor RARγ2 is crucial for the neuronal differentiation of mouse embryonic stem cells. *J Cell Sci* **127:** 2095-2105

Albalat R (2009) The retinoic acid machinery in invertebrates: ancestral elements and vertebrate innovations. *Mol Cell Endocrinol* **313:** 23–35

Alers S, Löffler AS, Wesselborg S, Stork B (2012) Role of AMPK-mTOR-Ulk1/2 in the regulation of autophagy: cross talk, shortcuts, and feedbacks. *Mol Cell Biol* **32:** 2-11

Altimus CM, Marlin BJ, Charalambakis NE, Colón-Rodríguez A, Glover EJ, Izbicki P, Johnson A, Lourenco MV, Makinson RA, McQuail J, Obeso I, Padilla-Coreano N, Wells MF (2020) The Next 50 Years of Neuroscience. *J Neurosci* **40:** 101-106

Anderson DJ (1993) Cell fate determination in the peripheral nervous system: the sympathoadrenal progenitor. *J Neurobiol* **24:** 185–198

Andrews PW, Damjanov I, Simon D, Banting GS, Carlin C, Dracopoli NC, Føgh J (1984) Pluripotent embryonal carcinoma clones derived from the human teratocarcinoma cell line Tera-2. Differentiation *in vivo* and *in vitro*. *Lab Invest* **50:** 147–162

Arigony AL, de Oliveira IM, Machado M, Bordin DL, Bergter L, Prá D, Henriques JA (2013) The influence of micronutrients in cell culture: a reflection on viability and genomic stability. *Biomed Res Int* **2013:** 597282

Ariosa AR, Klionsky DJ (2016) Autophagy core machinery: overcoming spatial barriers in neurons. *J Mol Med* **94:** 1217-1227

Artavanis-Tsakonas S, Rand MD, Lake RJ (1999) Notch signaling: cell fate control and signal integration in development. *Science* **284:** 770–776

Aulehla A, Pourquie O (2010) Signaling gradients during paraxial mesoderm development. *Cold Spring Harb Perspect Bio* **2:** a000869

Axe EL, Walker SA, Manifava M, Chandra P, Roderick HL, Habermann A, Griffiths G, Ktistakis NT (2008) Autophagosome formation from membrane compartments enriched in phosphatidylinositol 3-phosphate and dynamically connected to the endoplasmic reticulum. *J Cell Biol* **182:** 685-701

Azari H and Reynolds BA (2016) *In Vitro* Models for Neurogenesis. *Cold Spring Harb Perspect Biol* **8:** a021279

Baas PW, Slaughter T, Brown A, Black MM (1991) Microtubule dynamics in axons and dendrites. *J Neurosci Res* **30:** 134–153

Bae YS, Oh H, Rhee SG, Yoo YD (2011) Regulation of reactive oxygen species generation in cell signaling. *Mol Cells* **32:** 491-509

Bain G, Ray WJ, Yao M, Gottlieb DI (1994) From embryonal carcinoma cells to neurons: The P19 pathway. *Bioessays* **16:** 343-348

Bain G, Ray WJ, Yao M, Gottlieb DI (1996) Retinoic acid promotes neural and represses mesodermal gene expression in mouse embryonic stem cells in culture. *Biochem Biophys Res Commun* **223:** 691-694

Bak LK, Schousboe A, Waagepetersen HS (2006) The glutamate/GABA-glutamine cycle: aspects of transport, neurotransmitter homeostasis and ammonia transfer. *J Neurochem* **98:** 641-653

Ban BK, Jun MH, Ryu HH, Jang DJ, Ahmad ST, Lee JA (2013) Autophagy negatively regulates early axon growth in cortical neurons. *Mol Cell Biol* **33:** 3907-3919

Bang OS, Park EK, Yang SI, Lee SR, Franke TF, Kang SS (2001) Overexpression of Akt inhibits NGF-induced growth arrest and neuronal differentiation of PC12 cells. *J Cell Sci* **114:** 81–88

Bar- Peled L, Sabatini Dm (2014) Regulation of mTORC1 by amino acids. *Trends Cell Biol* **24:** 400–406

Bastien J, Plassat JL, Payrastre B, Rochette-Egly C (2006) The phosphoinositide 3-kinase/Akt pathway is essential for the retinoic acid-induced differentiation of F9 cells. *Oncogene* **25:** 2040-2047

Beck CW, Christen B, Slack JM (2003) Molecular pathways needed for regeneration of spinal cord and muscle in a vertebrate. *Dev Cell* **5:** 429-39

Begemann G, Marx M, Mebus K, Meyer A, Bastmeyer M (2004) Beyond the neckless phenotype: influence of reduced retinoic acid signaling on motor neuron development in the zebrafish hindbrain. *Dev Biol* **271:** 119-29

Bell KF, Al-Mubarak B, Martel MA, McKay S, Wheelan N, Hasel P, Márkus NM, Baxter P, Deighton RF, Serio A, Bilican B, Chowdhry S, Meakin PJ, Ashford ML, Wyllie DJ, Scannevin RH, Chandran S, Hayes JD, Hardingham GE (2015) Neuronal development is promoted by weakened intrinsic antioxidant defences due to epigenetic repression of Nrf2. *Nat Commun* **6:** 7066

Bhaskar S, Sheshadri P, Joseph JP, Potdar C, Prasanna J, Kumar A (2020) Mitochondrial Superoxide Dismutase Specifies Early Neural Commitment by Modulating Mitochondrial Dynamics. *iScience* **23:** 101564

Bhatlekar S, Fields JZ, Boman BM (2018) Role of HOX Genes in Stem Cell Differentiation and Cancer. *Stem Cells Int* **2018:** 3569493

Bibel M, Richter J, Lacroix E, Barde YA (2007) Generation of a defined and uniform population of CNS progenitors and neurons from mouse embryonic stem cells. *Nat Protoc* **2:** 1034-1043

Biswas SC, Greene LA (2002) Nerve growth factor (NGF) down-regulates the Bcl-2 homology 3 (BH3) domain-only protein Bim and suppresses its proapoptotic activity by phosphorylation. *J Biol Chem* **277:** 49511–49516

Bittinger F, Gonzalez-Garcia JL, Klein CL, Brochhausen C, Offner F, Kirkpatrick CJ (1998) Production of superoxide by human malignant melanoma cells. *Melanoma Res* **8:** 381–387

Blumberg B (1997) An essential role for retinoid signaling in anteroposterior neural specification and neuronal differentiation. *Semin Cell Dev Biol* **8:** 417-428

Booth LA, Tavallai S, Hamed HA, Cruickshanks N, Dent P (2014) The role of cell signalling in the crosstalk between autophagy and apoptosis. *Cell Signal* **26:** 549-555

Bottenstein JE, Sato GH (1979) Growth of a rat neuroblastoma cell line in serum-free supplemented medium. *Proc Natl Acad Sci* **76:** 514-517

Boudjelal M, Taneja R, Matsubara S, Bouillet P, Dolle P, Chambon P (1997) Overexpression of Stra13, a novel retinoic acid-inducible gene of the basic helix-loop-helix family, inhibits mesodermal and promotes neuronal differentiation of P19 cells. *Genes Dev* **11:** 2052–2065

Bouhamdani N, Comeau D, Cormier K, Turcotte S (2019) STF-62247 accumulates in lysosomes and blocks late stages of autophagy to selectively target von Hippel-Lindau-inactivated cells. *Am J Physiol Cell Physiol* **316:** 605-620

Bouhon IA, Kato H, Chandran S, Allen ND (2005) Neural differentiation of mouse embryonic stem cells in chemically defined medium. *Brain Res Bull* **68:** 62–75

Boya P, Codogno P, Rodriguez-Muela N (2018) Autophagy in stem cells: repair, remodelling and metabolic reprogramming. *Development* **145:** 146506

Bradl M, Lassmann H (2010) Oligodendrocytes: biology and pathology. *Acta Neuropathol* **119:** 37-53

Breitenfeld T, Jurasic MJ, Breitenfeld D (2014) Hippocrates: the forefather of neurology. *Neurol Sci* **35:** 1349-1352

Brenner D, Mak TW (2009) Mitochondrial cell death effectors. *Curr Opin Cell Biol* **21:** 871–877

Brewer GJ, Torricelli JR, Evege EK, Price PJ (1993) Optimized survival of hippocampal neurons in B27-supplemented neurobasal, a new serum-free medium combination. *J Neurosci Res* **35:** 567–576

Bryan N, Andrews KD, Loughran MJ, Rhodes NP, Hunt JA (2011) Elucidating the contribution of the elemental composition of fetal calf serum to antigenic expression of primary human umbilical-vein endothelial cells in vitro. *Biosci Rep* **31:** 199-210

Budnik V, Salinas PC (2011) Wnt signaling during synaptic development and plasticity. *Curr Opin Neurobiol* **21:** 151–159

Buss RR, Gould TW, Ma J, Vinsant S, Prevette D, Winseck A, Toops KA, Hammarback JA, Smith TL, Oppenheim RW (2006) Neuromuscular development in the absence of programmed cell death: phenotypic alteration of motoneurons and muscle. *J Neurosci* **26:** 13413–13427

Busskamp V, Lewis NE, Guye P, Ng AHM, Shipman SL, Byrne SM, Sanjana NE, Murn J, Li Y, Li S, Stadler M, Weiss R, Church GM (2014). Rapid neurogenesis through transcriptional activation in human stem cells. *Mol Syst Biol* **10:** 760

Butt AM, Fern RF, Matute C (2014) Neurotransmitter signaling in white matter. *Glia* **62:** 1762-1779

Cai AQ, Radtke K, Linville A, Lander AD, Nie Q, Schilling TF (2012) Cellular retinoic acid binding proteins are essential for hindbrain patterning and signal robustness in zebrafish. *Development* **139:** 2150–2155

Cai C, Grabel L (2007) Directing the differentiation of embryonic stem cells to neural stem cells. *Dev Dyn* **236:** 3255–3266

Canzoniero LM, Sensi SL, Turetsky DM, Finley MF, Choi DW, Huettner JE (1996) Glutamate receptor-mediated calcium entry in neurons derived from P19 embryonalcarcinoma cells. *J Neurosci Res* **45:** 226–236

Cardozo MJ, Mysiak KS, Becker T, Becker CG (2017) Reduce, reuse, recycle - Developmental signals in spinal cord regeneration. *Dev Biol* **432:** 53-62

Caruso Bavisotto C, Scalia F, Marino Gammazza A, Carlisi D, Bucchieri F, Conway de Macario E, Macario AJL, Cappello F, Campanella C (2019) Extracellular vesicle-mediated

cell-cell communication in the nervous system: focus on neurological diseases. *Int J Mol Sci* **20:** 434

Casares-Crespo L, Calatayud-Baselga I, García-Corzo L, Mira H (2018) On the Role of Basal Autophagy in Adult Neural Stem Cells and Neurogenesis. *Front Cell Neurosci* **12:** 339

Castro DS, Martynoga B, Parras C, Ramesh V, Pacary E, Johnston C, Drechsel D, Lebel-Potter M, Garcia LG, Hunt C, et al. (2011) A novel function of the proneural factor Ascl1 in progenitor proliferation identified by genome-wide characterization of its targets. *Genes Dev* **25:** 930–945

Caviness VSJ, Takahashi T, Nowakowski RS (1995) Numbers, time and neocortical neurogenesis: a general developmental and evolutionary model. *Trends Neurosci* **18:** 379-383

Cayuso J, Ulloa F, Cox B, Briscoe J, Martí E (2006) The Sonic hedgehog pathway independently controls the patterning, proliferation and survival of neuroepithelial cells by regulating Gli activity. *Development* **133:** 517-528

Cazillis M, Rasika S, Mani S, Gressens P, Leliévre V (2006) In vitro induction of neural differentiation of embryonic stem (ES) cells closely mimics molecular mechanisms of embryonic brain development. *Pediatric Res* **59:** 48-53

Chambers SM, Fasano CA, Papapetrou EP, Tomishima M, Sadelain M, Studer L (2009) Highly efficient neural conversion of human ES and iPS cells by dual inhibition of SMAD signaling. *Nat Biotechnol* **27:** 275-280

Chambon P (1996) A decade of molecular biology of retinoic acid receptors. *FASEB J* **10:** 940–954

Chawla A, Repa JJ, Evans RM, Mangelsdorf DJ (2001) Nuclear receptors and lipid physiology: opening the X-files. *Science* **294:** 1866-18187

Chen CW, Liu CS, Chiu IM, Shen SC, Pan HC, Lee KH, Lin SZ, Su HL (2010) The signals of FGFs on the neurogenesis of embryonic stem cells. *J Biomed Sci* **17:** 33

Chen G, Gulbranson DR, Hou Z, Bolin JM, Ruotti V, Probasco MD, Smuga-Otto K, Howden SE, Diol NR, Propson NE, Wagner R, Lee GO, Antosiewicz-Bourget J, Teng JMC, Thomson JA (2011) Chemically defined conditions for human iPS cell derivation and culture. *Nat Methods* **8:** 424–429

Chen JX, Sun YJ, Wang P, Long DX, Li W, Li L, Wu YJ (2013) Induction of autophagy by TOCP in differentiated human neuroblastoma cells lead to degradation of cytoskeletal components and inhibition of neurite outgrowth. *Toxicology* **310:** 92-97

Chen N, Napoli JL (2008) All-trans-retinoic acid stimulates translation and induces spine formation in hippocampal neurons through a membrane-associated RARalpha. *FASEB J* **22:** 236–245

Chen Y, Klionsky DJ (2011) The regulation of autophagy - unanswered questions. *J Cell Sci* **124:** 161-170

Chen YG, Meng AM (2004) Negative regulation of TGF-β signaling in development. *Cell Research* **14:** 441-449

Cheng XT, Zhou B, Lin MY, Cai Q, Sheng ZH (2015) Axonal autophagosomes recruit dynein for retrograde transport through fusion with late endosomes. *J Cell Biol* **209:** 377–386

Cheng YC, Hsieh FY, Chiang MC, Scotting PJ, Shih HY, Lin SJ, Wu HL, Lee HT (2013) Akt1 mediates neuronal differentiation in zebrafish via a reciprocal interaction with notch signaling. *PLoS One* **8:** e54262

Chenn A, McConnell SK (1995) Cleavage orientation and the asymmetric inheritance of Notch1 immunoreactivity in mammalian neurogenesis. *Cell* **82:** 631-641

Chiarotto GB, Drummond L, Cavarretto G, Bombeiro AL, Rodrigues de Oliveira AL (2014) Neuroprotective effect of tempol (4 hydroxy-tempo) on neuronal death induced by sciatic nerve transection in neonatal rats. *Brain Res Bulletin* **106:** 1-8

Chin MH, Mason MJ, Xie W, Volinia S, Singer M, Peterson C, Ambartsumyan G, Aimiuwu O, Richter L, Zhang J, et al. (2009) Induced pluripotent stem cells and embryonic stem cells are distinguished by gene expression signatures. *Cell Stem Cell* **5:** 111-123

Chipuk JE, Moldoveanu T, Llambi F, Parsons MJ, Green DR (2010) The BCL-2 family reunion. *Mol Cell* **37:** 299-310

Chorner PM, Moorehead RA (2018) A-674563, a putative AKT1 inhibitor that also suppresses CDK2 activity, inhibits human NSCLC cell growth more effectively than the pan-AKT inhibitor, MK-2206. *PLoS One* **13:** e0193344

Chou FS, Wang PS (2016) The Arp2/3 complex is essential at multiple stages of neural development. *Neurogenesis* **3:** e1261653

Chuang JH, Tung LC, Lin Y (2015) Neural differentiation from embryonic stem cells in vitro: An overview of the signaling pathways. *World J Stem Cells* **7:** 437-447

Cicchini M, Karantza V, Xia B (2015) Molecular pathways: autophagy in cancer-a matter of timing and context. *Clin Cancer Res* **21:** 498-504

Cicero S, Herrup K (2005) Cyclin-dependent kinase 5 is essential for neuronal cell cycle arrest and differentiation. *J Neurosci* **25:** 9658-9668

Clagett-Dame M, DeLuca HF (2002) The role of vitamin A in mammalian reproduction and embryonic development. *Annu Rev Nutr* **22:** 347-381

Cohen MA, Itsykson P, Reubinoff BE (2010) The role of FGF-signaling in early neural specification of human embryonic stem cells. *Dev Biol* **340:** 450-458

Compagnucci C, Nizzardo M, Corti S, Zanni G, Bertini E (2014) In vitro neurogenesis: Development and functional implications of iPSC technology. *Cell Mol Life Sci* **71:** 1623–1639

Cong L, Ran FA, Cox D, Lin S, Barretto R, Habib N, Hsu PD, Wu X, Jiang W, Marraffini LA, Zhang F (2013) Multiplex genome engineering using CRISPR/Cas systems. *Science* **339:** 819–823

Cooper KF (2018) Till death do us part: The marriage of autophagy and apoptosis. *Oxidative Med Cell Longev* **2018:** 4701275

Cormier S, Le Bras S, Souilhol C, Vandormael-Pournin S, Durand B, Babinet C, Baldacci P, Cohen-Tannoudji M (2006) The murine ortholog of notchless, a direct regulator of the notch pathway in Drosophila melanogaster, is essential for survival of inner cell mass cells. *Mol Cell Biol* **26:** 3541-3549

Cory S, Adams JM (2002) The Bcl2 family: regulators of the cellular life-or-death switch. *Nat Rev Cancer* **2:** 647-656

Crawford TQ, Roelink H (2007) The notch response inhibitor DAPT enhances neuronal differentiation in embryonic stem cell-derived embryoid bodies independently of sonic hedgehog signaling. *Dev Dyn* **236:** 886–892

Cuervo AM (2008) Autophagy and aging: keeping that old broom working. *Trends Genet* **24:** 604-612

Cunningham T J, Duester G (2015) Mechanisms of retinoic acid signalling and its roles in organ and limb development. *Natur Rev Mol Cell Biol* **16:** 110-123

Curchoe CL, Russo J, Terskikh AV (2012) hESC derived neuro-epithelial rosettes recapitulate early mammalian neurulation events; an *in vitro* model. *Stem Cell Res* **8:** 239-246

D'Ambrosio DN, Clugston RD, Blaner WS (2011) Vitamin A metabolism: an update. *Nutrients* **3:** 63–103

D'Arcy MS (2019) Cell death: a review of the major forms of apoptosis, necrosis and autophagy. *Cell Biol Int* **43:** 582-592

Datta PK (2013) Murine teratocarcinoma-derived neuronal cultures. *Methods Mol Biol* **1078:** 35–44

Davis AA, Temple S (1994) A self-renewing multipotential stem cell in embryonic rat cerebral cortex. *Nature* **372:** 263-266

Dawud RA, Schreiber K, Schomburg D, Adjaye J (2012) Human Embryonic Stem Cells and Embryonal Carcinoma Cells Have Overlapping and Distinct Metabolic Signatures. *PLoS One* **7:** e39896

de Bilbao F, Guarin E, Nef P, Vallet P, Giannakopoulos P, Dubois-Dauphin M (1999) Postnatal distribution of cpp32/caspase 3 mRNA in the mouse central nervous system: an *in situ* hybridization study. *J Comp Neurol* **409:** 339–357

Debnath J, Baehrecke EH, Kroemer G (2005) Does autophagy contribute to cell death? *Autophagy* **1:** 66–74

Deckwerth TL, Elliott JL, Knudson CM, Johnson EM, Snider WD & Korsmeyer SJ (1996) BAX is required for neuronal death after trophic factor deprivation and during development. *Neuron* **17:** 401–411

Denton D, Xu T, Kumar S (2015) Autophagy as a pro-death pathway. *Immunol Cell Biol* **93:** 35-42

Deschamps J, van Nes J (2005) Developmental regulation of the Hox genes during axial morphogenesis in the mouse. *Development* **132:** 2931-2942

Dickson DW (2004) Apoptotic mechanisms in Alzheimer neurofibrillary degeneration: cause or effect? *J Clin Invest* **114:** 23–27

Diez del Corral R, Olivera-Martinez I, Goriely A, Gale E, Maden M, Storey K (2003) Opposing FGF and retinoid pathways control ventral neural pattern, neuronal differentiation, and segmentation during body axis extension. *Neuron* **40:** 65–79

Diez del Corral R, Storey KG (2004) Opposing FGF and retinoid pathways: a signalling switch that controls differentiation and patterning onset in the extending vertebrate body axis. *Bioessays* **26:** 857-69

Dikic I, Elazar Z (2018) Mechanism and medical implications of mammalian autophagy. *Nat Rev Mol Cell Biol* **19:** 349-364

Djavaheri-Mergny M, Maiuri MC, Kroemer G (2010) Cross talk between apoptosis and autophagy by caspase-mediated cleavage of Beclin 1. *Oncogene* **29:** 1717–1719

Dollé P (2009) Developmental expression of retinoic acid receptors (RARs). *Nucl Recept Signal* **7:** e006

Dorey K, Amaya E (2010) FGF signalling: diverse roles during early vertebrate embryogenesis. *Development* **137:** 3731–3742

Dringen R, Pfeiffer B, Hamprecht B (1999) Synthesis of the antioxidant glutathione in neurons: supply by astrocytes of CysGly as precursor for neuronal glutathione. *J Neurosci* **19:** 562–569

Du J, Wu Y, Ai Z, Shi X, Chen L, Guo Z (2014) Mechanism of SB431542 in inhibiting mouse embryonic stem cell differentiation. *Cell Signal* **26:** 2107-16

Duester G (1996) Involvement of alcohol dehydrogenase, short-chain dehydrogenase/reductase, aldehyde dehydrogenase, and cytochrome P450 in the

control of retinoid signaling by activation of retinoic acid synthesis. *Biochemistry* **35:** 12221–12227

Duester G (2017) Retinoic acid's reproducible future. *Science* **358:** 15

Edinger AL, Thompson CB (2004) Death by design: apoptosis, necrosis and autophagy. *Curr Opin Cell Biol* **16:** 663–669

Edward MK, McBurney MW (1983) The concentration of retinoic acid determines the differentiated cell types formed by a teratocarcinoma cell line. *Dev Biol* **98:** 187-191

Eiraku M, Watanabe K, Matsuo-Takasaki M, Kawada M, Yonemura S, Matsumura M, Wataya T, Nishiyama A, Muguruma K, Sasai Y (2008) Self-organized formation of polarized cortical tissues from ESCs and its active manipulation by extrinsic signals. *Cell Stem Cell* **3:** 519–532

Element AR (2004) An important role of Nrf2-ARE pathway in the cellular defense mechanism. *Internat J Biochem Mol Biol* **37:** 139–143

Elkabetz Y and Studer L (2008) Human ESC-derived neural rosettes and neural stem cell progression. *Cold Spring Harb Symp Quant Biol* **73:** 377-387

Ellenbroek B and Youn J (2016) Rodent models in neuroscience research: is it a rat race? *Dis Model Mech* **9**: 1079–1087

Elmore S (2007) Apoptosis: a review of programmed cell death. *Toxicol Pathol* **35:** 495–516

Engberg N, Kahn M, Petersen DR, Hansson M, Serup P (2010) Retinoic acid synthesis promotes development of neural progenitors from mouse embryonic stem cells by suppressing endogenous, Wnt-dependent Nodal signaling. *Stem cells* **28:** 1498–1509

Evans MJ, Kaufman MH (1981) Establishment in culture of pluripotential cells from mouse embryos. *Nature* **292:** 154–156

Fannjiang Y, Kim CH, Huganir RL, Zou S, Lindsten T, Thompson CB, Mito T, Traystman RJ, Larsen T, Griffin DE *et al.* (2003) BAK alters neuronal excitability and can switch from anti- to pro-death function during postnatal development. *Dev Cell* **4:** 575–585

Fedorova V, Vanova T, Elrefae L, Pospisil J, Petrasova M, Kolajova V, Hudacova Z, Baniariova J, Barak M, Peskova L, *et al.* (2019) Differentiation of neural rosettes from human pluripotent stem cells in vitro is sequentially regulated on a molecular level and accomplished by the mechanism reminiscent of secondary neurulation. *Stem Cell Res* **40:** 101563

Fex G, Albertsson PA, Hansson B (1979) Interaction between prealbumin and retinol-binding protein studied by affinity chromatography, gel filtration and two-phase partition. *Europ J Biochem* **99:** 353–360

Fimia GM, Stoykova A, Romagnoli A, Giunta L, Di Bartolomeo S, Nardacci R, Corazzari M, Fuoco C, Ucar A, Schwartz P, Gruss P, Piacentini M, Chowdhury K, Cecconi F (2007) Ambra1 regulates autophagy and development of the nervous system. *Nature* **447:** 1121-1125

Finegan KG, Wang X, Lee EJ, Robinson AC, Tournier C (2009) Regulation of neuronal survival by the extracellular signal-regulated protein kinase 5. *Cell Death Differ* **16:** 674–683

Finley MFA, Devata S, Huettner JE (1999) BMP-4 inhibits neural differentiation in murine embryonic stem cells. *J Neurobiol* **40:** 271–287

Fishell G, Heintz N (2013) The Neuron Identity Problem: Form Meets Function. *Neuron* **80:** 602-612

Fogarty LC, Flemmer RT, Geizer BA, Licursi M, Karunanithy A, Opferman JT, Hirasawa K, Vanderluit JL (2019) Mcl-1 and Bcl-xL are essential for survival of the developing nervous system. *Cell Death Differ* **26:** 1501–1515

Fortin A, Cregan SP, MacLaurin JG, Kushwaha N, Hickman ES, Thompson CS, Hakim A, Albert PR, Cecconi F, Helin K *et al.* (2001) APAF1 is a key transcriptional target for p53 in the regulation of neuronal cell death. *J Cell Biol* **155:** 207–216

Foster DA, Toschi A (2009) Targeting mTOR with rapamycin: One dose does not fit all. *Cell Cycle* **8:** 1026–1029

Fraichard A, Chassande O, Bilbaut G, Dehay C, Savatier P, Samarut J (1995). *In vitro* differentiation of embryonic stem cells into glial cells and functional neurons. *J Cell Sci* **108:** 3181–3188

Freeman BA, Crapo JD (1982) Biology of disease: free radicals and tissue injury. *Lab Invest* **47:** 412-426

Frese CK, Mikhaylova M, Stucchi R, Gautier V, Liu Q, Mohammed S, Heck AJR, Altelaar AFM, Hoogenraad CC (2017) Quantitative Map of Proteome Dynamics during Neuronal Differentiation. *Cell Rep* **18:** 1527-1542

Fricker M, Tolkovsky AM, Borutaite V, Coleman M, Brown GC (2018) Neuronal Cell Death. *Physiol Rev* **98:** 813-880

Galderisi U, Jori FP, Giordano A (2003) Cell cycle regulation and neural differentiation. *Oncogene* **22:** 5208–5219

Gao C, Cao W, Bao L, Zuo W, Xie G, Cai T, Fu W, Zhang J, Wu W, Zhang X, Chen YG (2010) Autophagy negatively regulates Wnt signalling by promoting Dishevelled degradation. *Nat Cell Biol* **12:** 781-790

Germain N, Banda E, Grabel L (2010) Embryonic stem cell neurogenesis and neural specification. *J Cell Biochem* **111:** 535-542

Germain P, Iyer J, Zechel C, Gronemeyer H (2002) Co-regulator recruitment and the mechanism of retinoic acid receptor synergy. *Nature* **415:** 187-192

Ghosh AS, Wang B, Pozniak CD, Chen M, Watts RJ, Lewcock JW (2011) DLK induces developmental neuronal degeneration via selective regulation of proapoptotic JNK activity. *J Cell Biol* **194:** 751–764

Ghyselinck NB, Duester G (2019) Retinoic acid signaling pathways. *Development* **146:** 167502

Glaser T, Brüstle O (2005) Retinoic acid induction of ES-cell-derived neurons: the radial glia connection. *Trends Neurosci* **28:** 397–400

Goings GE, Kozlowski DA, Szele FG. 2006. Differential activation of microglia in neurogenic versus non-neurogenic regions of the forebrain. *Glia* **54:** 329–342

Golstein P, Kroemer G (2007) Cell death by necrosis: towards a molecular definition. *Trends Biochem Sci* **32:** 37–43

Gomes LC, Odedra D, Dikic I, Pohl C (2016) Autophagy and modular restructuring of metabolism control germline tumor differentiation and proliferation in *C. elegans. Autophagy* **12:** 529-546

Gonzalez C, Armijo E, Bravo-Alegria J, Becerra-Calixto A, Mays CE, Soto C (2018) Modeling amyloid beta and tau pathology in human cerebral organoids. *Mol Psychiatry* **23:** 2363–2374

Gordon J, Amini S, White MK (2013) General overview of neuronal cell culture. *Methods Mol Biol* **1078:** 1–8

Gossler A (1992) Early embryonic development of animals. Hennig W, Nover L, and Scheer U eds, Berlin, New York: Springer-Verlag

Gouti M, Gavalas A (2008) Hoxb1 controls cell fate specification and proliferative capacity of neural stem and progenitor cells. *Stem Cells* **26:** 1985–1997

Gowrishankar S, Yuan P, Wu Y, Schrag M, Paradise S, Grutzendler J, De Camilli P, Ferguson SM (2015) Massive accumulation of luminal protease-deficient axonal lysosomes at Alzheimer's disease amyloid plaques. *Proc Natl Acad Sci U S A* **112:** 3699-3708

Gozuacik D, Kimchi A (2004) Autophagy as a cell death and tumorsuppressor mechanism. *Oncogene* **23:** 2891–2906

Granger AJ, Mulder N, Saunders A, Sabatini BL (2016) Cotransmission of acetylcholine and GABA. *Neuropharmacology* **100:** 40-46

Guerrero P, Perez-Carrasco R, Zagorski M, Page D, Kicheva A, Briscoe J, Page KM (2019) Neuronal differentiation influences progenitor arrangement in the vertebrate neuroepithelium. *Development* **146:** 176297

Gupta P, Ho PC, Huq MM, Ha SG, Park SW, Khan AA, Tsai NP, Wei LN (2008) Retinoic acid-stimulated sequential phosphorylation, PML recruitment, and SUMOylation of nuclear receptor TR2 to suppress Oct4 expression. *Proc Natl Acad Sci U S A* **105:** 11424–11429

Habas A, Hahn J, Wang X, Margeta M (2013) Neuronal activity regulates astrocytic Nrf2 signaling. *Proc Natl Acad Sci USA* **110:** 18291–18296

Hacker G (2000) The morphology of apoptosis. *Cell Tissue Res* **301:** 5–17

Halliwell B (1996) Antioxidants in human health and disease. *An Rev Nutri* **16:** 33–50

Happo L, Strasser A, Cory S (2012) BH3-only proteins in apoptosis at a glance. *J Cell Sci* **125:** 1081–1087

Hara T, Nakamura K, Matsui M, Yamamoto A, Nakahara Y, Suzuki-Migishima R, Yokoyama M, Mishima K, Saito I, Okano H, Mizushima N (2006) Suppression of basal autophagy in neural cells causes neurodegenerative disease in mice. *Nature* **441:** 885-889

Harder JM, Ding Q, Fernandes KA, Cherry JD, Gan L, Libby RT (2012) BCL2L1 (BCL-X) promotes survival of adult and developing retinal ganglion cells. *Mol Cell Neurosci* **51:** 53-59

Harding MJ, McGraw HF, Nechiporuk A (2014) The roles and regulation of multicellular rosette structures during morphogenesis. *Dev Camb Engl* **141:** 2549-2558

Harris CA, Johnson EM Jr (2001) BH3-only Bcl-2 family members are coordinately regulated by the JNK pathway and require Bax to induce apoptosis in neurons. *J Biol Chem* **276:** 37754–37760

Harrison RG, Greenman MJ, Mall FP, Jackson CM (1907) Observations on the living developing nerve fibre. *Proc Soc Exp Biol* **1:** 116-128

Harvey CJ, Thimmulappa RK, Singh A, Blake DJ, Ling G, Wakabayashi N, Fujii J, Myers A, Biswal S (2009) Nrf2-regulated glutathione recycling independent of biosynthesis is critical for cell survival during oxidative stress. *Free Radic Biol Med* **46:** 443-453

Hasenpusch-Theil K, West S, Kelman A, Kozic Z, Horrocks S, McMahon AP, Price DJ, Mason JO, Theil T (2018) Gli3 controls the onset of cortical neurogenesis by regulating the radial glial cell cycle through Cdk6 expression. *Development* **145:** dev163147

He F, Ru X, Wen T (2020) NRF2, a transcription factor for stress response and beyond. *Internat J Mol Sci* **21:** 4777

He TC, Sparks AB, Rago C, Hermeking H, Zawel L, da Costa LT, Morin PJ, Vogelstein B, Kinzler KW (1998) Identification of c-MYC as a target of the APC pathway. *Science* **281:** 1509-1512

Hegarty SV, O'Keeffe GW, Sullivan AM (2013) BMP-Smad 1/5/8 signalling in the development of the nervous system. *Prog Neurobiol* **109:** 28–41

Herculano-Houzel S, Dos Santos SE (2018) You Do Not Mess with the Glia. *Neuroglia* **1:** 193-219

Hernandez D, Torres CA, Setlik W, Cebrian C, Mosharov EV, Tang G, Cheng HC, Kholodilov N, Yarygina O, Burke RE, Gershon M, Sulzer D (2012) Regulation of presynaptic neurotransmission by macroautophagy. *Neuron* **74:** 277–284

Herrup K, Yang Y (2007) Cell cycle regulation in the postmitotic neuron: oxymoron or new biology? *Nat Rev Neurosci* **8:** 368–378

Herzog C, Garcia LP, Keatinge M, Greenald D, Moritz C, Peri F, Herrgen L (2019) Rapid clearance of cellular debris by microglia limits secondary neuronal cell death after brain injury *in vivo*. *Development* **146:** 174698

Hirokawa N, Niwa S, Tanaka Y (2010) Molecular motors in neurons: transport mechanisms and roles in brain function, development, and disease. *Neuron* **68:** 610-638

Hoang-Minh LB, Deleyrolle LP, Siebzehnrubl D, Ugartemendia G, Futch H, Griffith B, Breunig JJ, De Leon G, Mitchell DA, Semple-Rowland S, Reynolds BA, Sarkisian MR (2016) Disruption of KIF3A in patient-derived glioblastoma cells: effects on ciliogenesis, hedgehog sensitivity, and tumorigenesis. *Oncotarget* **7:** 7029-7043

Hodge R, Bakken T, Miller J, Smith K, Barkan E, Graybuck L, Close J, Long B, Johansen N, Penn O, et al. (2019) Conserved cell types with divergent features in human versus mouse cortex. *Nature* **573:** 61–68

Hollenbeck PJ, Bray D (1987) Rapidly transported organelles containing membrane and cytoskeletal components: their relation to axonal growth. *J Cell Biol* **105:** 2827-2835

Hollville E, Romero SE, Deshmukh M (2019) Apoptotic cell death regulation in neurons. *FEBS J* **286:** 3276-3298

Hosokawa N, Hara T, Kaizuka T, Kishi C, Takamura A, Miura Y, Iemura S, Natsume T, Takehana K, Yamada N, Guan JL, Oshiro N, Mizushima N (2009) Nutrient-dependent mTORC1 association with the ULK1-Atg13-FIP200 complex required for autophagy. *Mol Biol Cell* **20:** 1981-1991

Hou W, Han J, Lu C, Goldstein LA, Rabinowich H (2010) Autophagic degradation of active caspase-8: a crosstalk mechanism between autophagy and apoptosis. *Autophagy* **6:** 891–900

Hu Q, Khanna P, Ee Wong BS, Lin Heng ZS, Subhramanyam CS, Thanga LZ, Sing Tan SW, Baeg GH (2017) Oxidative stress promotes exit from the stem cell state and spontaneous neuronal differentiation. *Oncotarget* **9:** 4223-4238

Huang HS, Redmond TM, Kubish GM, Gupta S, Thompson RC, Turner DL, Uhler MD (2015) Transcriptional regulatory events initiated by Ascl1 and Neurog2 during neuronal differentiation of P19 embryonic carcinoma cells. *J Mol Neurosci* **55:** 684-705

Hwang Y, Kim LC, Song W, Edwards DN, Cook RS, Chen J (2019) Disruption of the scaffolding function of mLST8 selectively inhibits mTORC2 assembly and function and suppresses mTORC2-dependent tumor growth in vivo. *Cancer Res* **79:** 3178-3184

Imai K, Hao F, Fujita N, Tsuji Y, Oe Y, Araki Y, Hamasaki M, Noda T, Yoshimori T (2016) Atg9A trafficking through the recycling endosomes is required for autophagosome formation. *J Cell Sci* **129:** 3781-3791

Ishii T, Itoh K, Takahashi S, Sato H, Yanagawa T, Katoh Y, Bannai S, Yamamoto M (2000) Transcription factor Nrf2 coordinately regulates a group of oxidative stress-inducible genes in macrophages. *J Biol Chem* **275:** 16023-16029

Itakura E, Kishi C, Inoue K, Mizushima N (2008) Beclin 1 forms two distinct phosphatidylinositol 3-kinase complexes with mammalian Atg14 and UVRAG. *Mol Biol Cell* **19:** 5360-5372

Itakura E, Mizushima N (2010) Characterization of autophagosome formation site by a hierarchical analysis of mammalian Atg proteins. *Autophagy* **6:** 764–776

Itoh K, Wakabayashi N, Katoh Y, Ishii T, Igarashi K, Engel JD, Yamamoto M (1999) Keap1 represses nuclear activation of antioxidant responsive elements by Nrf2 through binding to the amino-terminal Neh2 domain. *Genes Dev* **13:** 76–86

Jacinto E, Loewith R, Schmidt A, Lin S, Rüegg MA, Hall A, Hall MN (2004) Mammalian TOR complex 2 controls the actin cytoskeleton and is rapamycin insensitive. *Nat Cell Biol* **6:** 1122-1128

Jackson BC, Reigan P, Miller B, Thompson DC, Vasiliou V (2015) Human ALDH1B1 polymorphisms may affect the metabolism of acetaldehyde and all-trans retinaldehyde--*in vitro* studies and computational modeling. *Pharm Res* **32:** 1648-1662

Jacob SW, Herschler R (1986) Pharmacology of DMSO. *Cryobiology* **1:** 14–27

Jain A, Lamark T, Sjøttem E, Larsen KB, Awuh JA, Øvervatn A, McMahon M, Hayes JD, Johansen T (2010) p62/SQSTM1 is a target gene for transcription factor NRF2 and creates a positive feedback loop by inducing antioxidant response element-driven gene transcription. *J Biol Chem* **285:** 22576-22591

Janesick A, Abbey R, Chung C, Liu S, Taketani M, Blumberg B (2013) ERF and ETV3L are retinoic acid-inducible repressors required for primary neurogenesis. *Development* **140:** 3095–3106

Janesick A, Wu SC, Blumberg B (2015) Retinoic acid signaling and neuronal differentiation. *Cell Mol Life Sci* **72:** 1559–1576

Jang J, Wang Y, Kim HS, Lalli MA, Kosik KS (2014) Nrf2, a regulator of the proteasome, controls self-renewal and pluripotency in human embryonic stem cells. *Stem Cells* **32:** 2616-2625

Jasmin, Spray DC, Campos de Carvalho AC, Mendez-Otero R (2010) Chemical induction of cardiac differentiation in p19 embryonal carcinoma stem cells. *Stem Cells Dev* **19:** 403-412

Jia R, Bonifacino JS (2019) Negative regulation of autophagy by UBA6-BIRC6-mediated ubiquitination of LC3. *Elife* **8:** e50034

Jimenez AJ, Dominguez-Pinos MD, Guerra MM, Fernandez-Llebrez P, Perez-Figares JM (2014) Structure and function of the ependymal barrier and diseases associated with ependyma disruption. *Tissue Barriers* **2:** e28426

Jimenez-Sanchez M, Menzies FM, Chang YY, Simecek N, Neufeld TP, Rubinsztein DC (2012) The Hedgehog signalling pathway regulates autophagy. *Nat Commun* **3:** 1200

Jinek M, Chylinski K, Fonfara I, Hauer M, Doudna JA, Charpentier E (2012) A programmable dual-RNA–guided DNA endonuclease in adaptive bacterial immunity. *Science* **337:** 816–821

Jones-Villeneuve EMW, McBurney MW, Rogers KA, Kalinins VU (1982) Retinoic acid induces embryonal carcinoma cells to differentiate into neurons and glial cells. *J Cell Biol* **94:** 253-262

Jonk, LJ, de Jonge ME, Kruyt FA, Mummery CL, van der Saag PT, Kruijer W (1992) Aggregation and cell cycle dependent retinoic acid receptor mRNA expression in P19 embryonal carcinoma cells. *Mech Dev* **36:** 165-172

Jung CH, Jun CB, Ro SH, Kim YM, Otto NM, Cao J, Kundu M, Kim DH (2009) ULK-Atg13-FIP200 complexes mediate mTOR signaling to the autophagy machinery. *Mol Biol Cell* **20:** 1992-2003

Kadoshima T, Sakaguchi H, Nakano T, Soen M, Ando S, Eiraku M, Sasai Y (2013) Self-organization of axial polarity, inside-out layer pattern, and species-specific progenitor dynamics in human ES cell-derived neocortex. *Proc Natl Acad Sci USA* **110:** 20284–20289

Kamada H, Nito C, Endo H & Chan PH (2007) Bad as a converging signaling molecule between survival PI3-K/Akt and death JNK in neurons after transient focal cerebral ischemia in rats. *J Cereb Blood Flow Metab* **27:** 521–533

Kang R, Zeh HJ, Lotze MT, Tang D (2011) The Beclin 1 network regulates autophagy and apoptosis. *Cell Death Differ* **18:** 571-580

Karzbrun E, Reiner O (2019) Brain organoids: a bottom-up approach for studying human neurodevelopment. *Bioengineering* **6:** 1-9

Kashyap V, Laursen KB, Brenet F, Viale AJ, Scandura JM, Gudas LJ (2013) RARγ is essential for retinoic acid induced chromatin remodeling and transcriptional activation in embryonic stem cells. *J Cell Sci* **126:** 999–1008

Kastner P, Krust A, Mendelsohn C, Garnier JM, Zelent A, Leroy P, Staub A, Chambon P (1990) Murine isoforms of retinoic acid receptor gamma with specific patterns of expression. *Proc Natl Acad Sci U S A* **87:** 2700-2704

Kastner P, Mark M, Ghyselinck N, Krezel W, Dupe V, Grondona JM, Chambon P (1997) Genetic evidence that the retinoid signal is transduced by heterodimeric RXR/RAR functional units during mouse development. *Development* **124:** 313–326

Kawaguchi R, Yu J, Honda J, Hu J, Whitelegge J, Ping P, Wiita P, Bok D, Sun H (2007) A membrane receptor for retinol binding protein mediates cellular uptake of vitamin A. *Science* **315:** 820–825

Kawasaki H, Mizuseki K, Nishikawa S, Kaneko S, Kuwana Y, Nakanishi S, Nishikawa SI, Sasai Y (2000) Induction of midbrain dopaminergic neurons from ES cells by stromal cell-derived inducing activity. *Neuron* **28:** 31–40

Kazyken D, Magnuson B, Bodur C, Acosta-Jaquez HA, Zhang D, Tong X, Barnes TM, Steinl GK, Patterson NE, Altheim CH *et al.* (2019) AMPK directly activates mTORC2 to promote cell survival during acute energetic stress. *Sci Signaling* **12:** 3249

Keller R, Shih J, Sater AK, Moreno C (1992) Planar induction of convergence and extension of the neural plate by the organizer of Xenopus. *Dev Dyn* **193:** 218–234

Kelly GM, Gatie MI (2017) Mechanisms regulating stemness and differentiation in embryonal carcinoma cells. *Stem Cells Int* **2017:** 3684178-98

Kennedy KA, Porter T, Mehta V, Ryan SD, Price F, Peshdary V, Karamboulas C, Savage J, Drysdale TA, Li SC, et al. (2009) Retinoic acid enhances skeletal muscle progenitor formation and bypasses inhibition by bone morphogenetic protein 4 but not dominant negative β-catenin. *BMC Biol* **7:** 67

Kerr JF, Wyllie AH, Currie AR (1972) Apoptosis: a basic biological phenomenon with wide-ranging implications in tissue kinetics. *Br J Cancer* **26:** 239–257

Kettenmann H, Ransom BR (2005) The Concept of Neuroglia: A Historical Perspective. *Oxford: Oxford University Press*

Khaled S, Makled MN, Nader MA (2020) Tiron protects against nicotine-induced lung and liver injury through antioxidant and anti-inflammatory actions in rats in vivo. *Life Sci* **260:** 118426

Kilpatrick TJ, Richards L J, Bartlett PF (1995) The regulation of neural precursor cells within the mammalian brain. *Mol Cell Neurosci* **6:** 2-15

Kim JH, Lee SY, Oh SY, Han SI, Park HG, Yoo M, Kang HS (2004) Methyl jasmonate induces apoptosis through induction of Bax/Bcl- XS and activation of caspase-3 via ROS production in A549 cells. *Oncol Rep* **12:** 1233–1238

King KL, Cidlowski JA (1998) Cell cycle regulation and apoptosis. *Annu Rev Physiol* **60:** 601–617

Kiyono K, Suzuki HI, Matsuyama H, Morishita Y, Komuro A, Kano MR, Sugimoto K, Miyazono K (2009) Autophagy is activated by TGF-beta and potentiates TGF-beta-mediated growth inhibition in human hepatocellular carcinoma cells. *Cancer Res* **69:** 8844-8852

Klappacher GW, Lunyak VV, Sykes DB, Sawka-Verhelle D, Sage J, Brard G, Ngo SD, Gangadharan D, Jacks T, Kamps MP, et al (2002) An induced Ets repressor complex regulates growth arrest during terminal macrophage differentiation. *Cell* **109:** 169–180

Klionsky DJ, Schulman BA (2014) Dynamic regulation of macroautophagy by distinctive ubiquitin-like proteins. *Nat Struct Molecular Biol* **21:** 336–345

Kobayashi C Suda T (2012) Regulation of reactive oxygen species in stem cells and cancer stem cells. *J Cell Physiol* **227:** 421–430

Koide T, Downes M, Chandraratna RA, Blumberg B, Umesono K (2001) Active repression of RAR signaling is required for head formation. *Genes Dev* **15:** 2111-2121

Kole AJ, Annis RP & Deshmukh M (2013) Mature neurons: equipped for survival. *Cell Death Dis* **4:** e689

Komatsu M, Waguri S, Chiba T, Murata S, Iwata J, Tanida I, Ueno T, Koike M, Uchiyama Y, Kominami E, Tanaka K (2006) Loss of autophagy in the central nervous system causes neurodegeneration in mice. *Nature* **441:** 880-884

Korkut C, Li Y, Koles K, Brewer C, Ashley J, Yoshihara M, Budnik V (2013) Regulation of postsynaptic retrograde signaling by presynaptic exosome release. *Neuron* **77:** 1039–1046

Korobova F, Svitkina T (2008) Arp2/3 complex is important for filopodia formation, growth cone motility, and neuritogenesis in neuronal cells. *Mol Biol Cell* **19:** 1561-1574

Kosaka N, Kodama M, Sasaki H, Yamamoto Y, Takeshita F, Takahama Y, Sakamoto H, Kato T, Terada M Ochiya T (2006) FGF-4 regulates neural progenitor cell proliferation and neuronal differentiation. *FASEB J* **20:** 1484-1485

Krajewska M, Mai JK, Zapata JM, Ashwell KW, Schendel SL, Reed JC, Krajewski S (2002) Dynamics of expression of apoptosis-regulatory proteins Bid, Bcl-2, Bcl-X, Bax and Bak during development of murine nervous system. *Cell Death Differ* **9:** 145–157

Krishna CM, Liebmann JE, Kaufman D, DeGraff W, Hahn SM, McMurry T, Mitchell JB, Russo A (1992) The catecholic metal sequestering agent 1,2-dihydroxybenzene-3,5-disulfonate confers protection against oxidative cell damage. *Arch Biochem Biophys* **294:** 98-106

Kuan CY, Roth KA, Flavell RA, Rakic P (2000) Mechanisms of programmed cell death in the developing brain. *Trends Neurosci* **23:** 291-297

Kudoh T, Wilson SW, Dawid IB (2002) Distinct roles for Fgf, Wnt and retinoic acid in posteriorizing the neural ectoderm. *Development* **129**: 4335–4346

Kuff EL, Fewell JW (1980) Induction of neural-like cells and acetylcholinesterase activity in cultures of F9 teratocarcinoma treated with retinoic acid and dibutyryl cyclic adenosine monophosphate. *Dev Biol* **77:** 103–115

Kumar S, Tomooka Y, Noda M (1992) Identification of a set of genes with developmentally down-regulated expression in the mouse brain. *Biochem Biophys Res Commun* **185:** 1155–1161

Kunath T, Saba-El-Leil MK, Almousailleakh M, Wray J, Meloche S, Smith A (2007) FGF stimulation of the Erk1/2 signalling cascade triggers transition of pluripotent embryonic stem cells from self-renewal to lineage commitment. *Development* **134:** 2895-2902

Kurosaka K, Takahashi M, Watanabe N, Kobayashi Y (2003) Silent clean-up of very early apoptotic cells by macrophages. *J Immunol* **171:** 4672–4679

Labbadia J, Morimoto RI (2014) Proteostasis and longevity: when does aging really begin? *F1000 PrimeRep* **6:** 7

Lalevée S, Anno YN, Chatagnon A, Samarut E, Poch O, Laudet V, Benoit G, Lecompte O, Rochette-Egly C (2011) Genome-wide in silico identification of new conserved and functional retinoic acid receptor response elements (direct repeats separated by 5 bp). *J Biol Chem* **286:** 33322–33334

Lamers F, Schild L, Koster J, Speleman F, Øra I, Westerhout EM, van Sluis P, Versteeg R, Caron HN, Molenaar JJ (2012) Identification of BIRC6 as a novel intervention target for neuroblastoma therapy. *BMC Cancer* **12:** 285

Lamers F, van der Ploeg I, Schild L, Ebus ME, Koster J, Hansen BR, Koch T, Versteeg R, Caron HN, Molenaar JJ (2011) Knockdown of survivin (BIRC5) causes apoptosis in neuroblastoma via mitotic catastrophe. *Endocr Relat Cancer* **18:** 657-668

Lancaster MA, Renner M, Martin CA, Wenzel D, Bicknell LS, Hurles ME, Homfray T, Penninger JM, Jackson AP, Knoblich JA (2013) Cerebral organoids model human brain development and microcephaly. *Nature* **501:** 373–379

Lange C, Huttner WB, Calegari F (2009) Cdk4/cyclinD1 overexpression in neural stem cells shortens G1, delays neurogenesis, and promotes the generation and expansion of basal progenitors. *Cell Stem Cell* **5:** 320-331

Lara-Ramírez R, Zieger E, Schubert M (2013) Retinoic acid signaling in spinal cord development. *Int J Biochem Cell Biol* **45:** 1302-1313

Larisch S, Yi Y, Lotan R, Kerner H, Eimerl S, Tony Parks W, Gottfried Y, Birkey Reffey S, de Caestecker MP, Danielpour D, et al. (2000). A novel mitochondrial septin-like protein, ARTS, mediates apoptosis dependent on its P-loop motif. *Nat Cell Biol* **2:** 915-921

Laursen KB, Gudas LJ (2018) Combinatorial knockout of RARα, RARβ, and RARγ completely abrogates transcriptional responses to retinoic acid in murine embryonic stem cells. *J Biol Chem* **293:** 11891-11900

Laursen KB, Wong PM, Gudas LJ (2012) Epigenetic regulation by RARα maintains ligand-independent transcriptional activity. *Nucleic Acids Res* **40:** 102-115

Le Belle JE, Orozco NM, Paucar AA, Saxe JP, Mottahedeh J, Pyle AD, Wu H, Kornblum HI (2011) Proliferative neural stem cells have high endogenous ROS levels that regulate selfrenewal and neurogenesis in a PI3K/Akt-dependant manner. *Cell Stem Cell* **8:** 59–71

Le Dreau G, Marti E (2012) Dorsal-ventral patterning of the neural tube: a tale of three signals. *Dev Neurobiol* **72:** 1471–1481

Le Dreau G, Marti E (2013) The multiple activities of BMPs during spinal cord development. *Cell Mol Life Sci* **70:** 4293–4305

Leahy A, Xiong JW, Kuhnert F, Stuhlmann H (1999) Use of developmental marker genes to define temporal and spatial patterns of differentiation during embryoid body formation. *J Exp Zool* **284:** 67–81

Lee H, Nowosiad P, Dutan Polit LM, Price J, Srivastava DP, Thuret S (2020) Apolipoprotein E expression pattern in human induced pluripotent stem cells during in vitro neural induction. *F1000Res* **9:** 353

Lee J, Seroogy KB, Mattson MP (2002) Dietary restriction enhances neurotrophin expression and neurogenesis in the hippocampus of adult mice. *J Neurochem* **80:** 539-547

Lee S, Sato Y, Nixon RA (2011) Lysosomal proteolysis inhibition selectively disrupts axonal transport of degradative organelles and causes an Alzheimer's-like axonal dystrophy. *J Neurosci* **31:** 7817-7830

Lenka N, Ramasamy SK (2007) Neural induction from ES cells portrays default commitment but instructive maturation. *PLoS One* **2:** e1349

Levine AJ, Brivanlou AH (2007) Proposal of a model of mammalian neural induction. *Dev Biol* **308:** 247–256

Levine B, Klionsky DJ (2004) Development by self-digestion: molecular mechanisms and biological functions of autophagy. *Dev Cell* **6:** 463-477

Li HS, Wang D, Shen Q, Schonemann MD, Gorski JA, Jones KR, Temple S, Jan LY, Jan YN (2003) Inactivation of Numb and Numblike in embryonic dorsal forebrain impairs neurogenesis and disrupts cortical morphogenesis. *Neuron* **40:** 1105-1118

Li S, Yu W, Kishikawa H, Hu G (2010) Angiogenin prevents serum withdrawal-induced apoptosis of P19 embryonal carcinoma cells. *FEBS J* **277:** 3575-3587

Li W, Sun W, Zhang Y, Wei W, Ambasudhan R, Xia P, Talantova, M, Lin T, Kim X, Wang X, Kim WR, Lipton SA, Zhang K, Ding S (2011) Rapid induction and long-term self-renewal of primitive neural precursors from human embryonic stem cells by small molecule inhibitors. *Proc Natl Acad Sci* **108:** 8299-8304

Li Z, Theus MH, Wei L (2006) Role of ERK 1/2 signaling in neuronal differentiation of cultured embryonic stem cells. *Dev Growth Differ* **48:** 513-523

Lim S, Kaldis P (2012) Loss of Cdk2 and Cdk4 induces a switch from proliferation to differentiation in neural stem cells. *Stem Cells* **30:** 1509-1520

Lin P, Kusano K, Zhang Q, Felder CC, Geiger PM, Mahan LC (1996) GABAA receptors modulate early spontaneous excitatory activity in differentiating P19 neurons. *J Neurochem* **66:** 233–242

Lin TY, Chan HH, Chen SH, Sarvagalla S, Chen PS, Coumar MS, Cheng SM, Chang YC, Lin CH, Leung E, Cheung CHA (2020) BIRC5/Survivin is a novel ATG12-ATG5 conjugate interactor and an autophagy-induced DNA damage suppressor in human cancer and mouse embryonic fibroblast cells. *Autophagy* **16:** 1296-1313

Lindhout FW, Kooistra R, Portegies S, Herstel LJ, Stucchi R, Snoek BL, Altelaar AM, MacGillavry HD, Wierenga CJ, Hoogenraad CC (2020) Quantitative mapping of transcriptome and proteome dynamics during polarization of human iPSC-derived neurons. *Elife* **9:** e58124

Linker C, Stern CD (2004) Neural induction requires BMP inhibition only as a late step, and involves signals other than FGF and Wnt antagonists. *Development* **131:** 5671-5681

Lipinski MM, Zheng B, Lu T, Yan Z, Py BF, Ng A, Xavier RJ, Li C, Yankner BA, Scherzer CR, Yuan J (2010) Genome-wide analysis reveals mechanisms modulating autophagy in normal brain aging and in Alzheimer's disease. *Proc Natl Acad Sci U S A* **107:** 14164-14169

Liu K, Ding L, Li Y, Yang H, Zhao C, Lei Y, Han S, Tao W, Miao D, Steller H, Welsh MJ, Liu L (2014) Neuronal necrosis is regulated by a conserved chromatin-modifying cascade. *Proc Natl Acad Sci U S A* **111:** 13960-13965

Liu Q, Lü L, Sun H, Zhang J, Ma W, Zhang T (2018) Effect of serum on the differentiation of neural stem cells. *Chinese J reparat reconstruc surg* **32:** 223-227

Liu Q, Wang J, Kang SA, Thoreen CC, Hur W, Ahmed T, Sabatini DM, Gray NS (2011) Discovery of 9-(6-aminopyridin-3-yl)-1-(3-(trifluoromethyl)phenyl)benzo[h][1,6] naphthyridin-2(1H)-one (Torin2) as a potent, selective, and orally available mammalian target of rapamycin (mTOR) inhibitor for treatment of cancer. *J Med Chem* **54:** 1473-1480

Liu Q, Xu C, Kirubakaran S, Zhang X, Hur W, Liu Y, Kwiatkowski NP, Wang J, Westover KD, Gao P, *et al.* (2013) Characterization of Torin2, an ATP-competitive inhibitor of mTOR, ATM, and ATR. *Cancer Res* **73:** 2574-2586

Liu Y, Kern JT, Walker JR, Johnson JA, Schultz PG, Luesch H (2007) A genomic screen for activators of the antioxidant response element. *Proc Natl Acad Sci* **104:** 5205–5210

Liu Y, Li P, Liu K, He Q, Han S, Sun X, Li T, Shen L (2014) Timely inhibition of Notch signaling by DAPT promotes cardiac differentiation of murine pluripotent stem cells. *PLoS One* **9:** e109588

Liu Z, Wang X, Jiang K, Ji X, Zhang YA, Chen Z (2019) TNFα-induced up-regulation of Ascl2 affects the differentiation and proliferation of neural stem cells. *Aging Dis* **10:** 1207-1220

Lockshin RA, Zakeri Z (2004) Apoptosis, autophagy, and more. *Int J Biochem Cell Biol* **36:** 2405–2419

Locksley RM, Killeen N, Lenardo MJ (2001) The TNF and TNF receptor superfamilies: integrating mammalian biology. *Cell* **104:** 487-501

López-Carballo G, Moreno L, Masiá S, Pérez P, Barettino D (2002) Activation of the phosphatidylinositol 3-kinase/Akt signaling pathway by retinoic acid is required for neural differentiation of SH-SY5Y human neuroblastoma cells. *J Biol Chem* **277:** 25297-25304

Low CG, Luk IS, Lin D, Fazli L, Yang K, Xu Y, Gleave M, Gout PW, Wang Y (2013) BIRC6 protein, an inhibitor of apoptosis: role in survival of human prostate cancer cells. *PLoS One* **8:** e55837

Lu HE, Yang YC, Chen SM, Su HL, Huang PC, Tsai MS, Wang TH, Tseng CP, Hwang SM (2013) Modeling neurogenesis impairment in Down syndrome with induced pluripotent stem cells from Trisomy 21 amniotic fluid cells. *Exp Cell Res* **319:** 498–505

Luo S, Rubinsztein DC (2010) Apoptosis blocks Beclin 1-dependent autophagosome synthesis: an effect rescued by Bcl-xL. *Cell Death Differ* **17:** 268–277

Lutolf S, Radtke F, Aguet M, Suter U, Taylor V (2002) Notch1 is required for neuronal and glial differentiation in the cerebellum. *Development* **129:** 373–385

Lv X, Jiang H, Li B, Liang Q, Wang S, Zhao Q, Jiao J (2014) The crucial role of Atg5 in cortical neurogenesis during early brain development. *Sci Rep* **4:** 6010

M D'Amelio, V Cavallucci, F Cecconi (2010) Neuronal caspase-3 signaling: not only cell death. *Cell Death Differ* **17:** 1104–1114

Ma Q (2013) Role of nrf2 in oxidative stress and toxicity. *Annu Rev Pharmacol Toxicol* **53:** 401-426

Maconochie M, Nonchev S, Morrison A, Krumlauf R (1996) Paralogous Hox genes: function and regulation. *Annu Rev Genet* **30:** 529-556

MacPherson PA, Jones S, Pawson PA, Marshall KC, McBurney MW (1997) P19 cells differentiate into glutamatergic and glutamate responsive neurons in vitro. *Neurosci* **80:** 487–499

MacPherson PA, McBurney MW (1995) P19 embryonal carcinoma cells: A source of cultured neurons amenable to genetic manipulation. *Sci methods* **7:** 238-252

Maday S (2016) Mechanisms of neuronal homeostasis: Autophagy in the axon. *Brain Res* **1649:** 143-150

Maday S, Holzbaur EL (2014) Autophagosome biogenesis in primary neurons follows an ordered and spatially regulated pathway. *Dev Cell* **30:** 71–85

Maday S, Holzbaur EL (2016) Compartment-specific regulation of autophagy in primary neurons. *J Neuroscience* **36:** 5933-5945

Maday S, Wallace KE, Holzbaur EL (2012) Autophagosomes initiate distally and mature during transport toward the cell soma in primary neurons. *J Cell Biol* **196:** 407-417

Maden M (2007) Retinoic acid in the development, regeneration and maintenance of the nervous system. *Nat Rev Neurosci* **8:** 755–765

Maden M, Hind M (2003) Retinoic acid, a regeneration-inducing molecule. *Dev Dyn* **226:** 237–244

Madhusudanan P, Reade S, Shankarappa SA (2017) Neuroglia as targets for drug delivery systems: A review. *Nanomed: NBM* **13:** 667-679

Magalingam KB, Radhakrishnan AK, Somanath SD, Md S, Haleagrahara N (2020) Influence of serum concentration in retinoic acid and phorbol ester induced differentiation of SH-SY5Y human neuroblastoma cell line. *Mol Biol Rep* **47:** 8775-8788

Magnuson DS, Morassutti DJ, Staines WA, McBurney MW, Marshall KC (1995) *In vivo* electrophysiological maturation of neurons derived from a multipotent precursor (embryonal carcinoma) cell line. *Brain Res Dev* **84:** 130–141

Maiuri MC, Criollo A, Tasdemir E, Vicencio JM, Tajeddine N, Hickman JA, Geneste O, Kroemer G (2007) BH3-only proteins and BH3 mimetics induce autophagy by competitively disrupting the interaction between Beclin 1 and Bcl-2/Bcl-X(L). *Autophagy* **3:** 374-376

Maiuri MC, Zalckvar E, Kimchi A, Kroemer G (2007) Self-eating and self-killing: crosstalk between autophagy and apoptosis. *Nat Rev Mol Cell Biol* **8:** 741-752

Mali P, Yang L, Esvelt KM, Aach J, Guell M, DiCarlo JE, Norville JE, Church GM (2013) RNA-guided human genome engineering via Cas9. *Science* **339**: 823–826

Malý P, Dráber P (1992) Retinoic acid-induced changes in differentiation-defective embryonal carcinoma RAC65 cells. *FEBS Lett* **311:** 102-106

Mani M, Khaghani S, Gol Mohammadi T, Zamani Z, Azadmanesh K, Meshkani R, Pasalar P, Mostafavi E (2013) Activation of Nrf2-antioxidant response element mediated glutamate cysteine ligase expression in hepatoma cell line by homocysteine. *Hepat Mon* **13:** e8394

Marchal L, Luxardi G, Thomé V, Kodjabachian L (2009) BMP inhibition initiates neural induction via FGF signaling and Zic genes. *Proc Natl Acad Sci USA* **106:** 17437-17442

Marchetto MC, Yeo GW, Kainohana O, Marsala M, Gage FH, Muotri AR (2009) Transcriptional signature and memory retention of human-induced pluripotent stem cells. *PLoS One* **4:** e7076

Marikawa Y, Tamashiro DAA, Fujita TC, Alarcón VB (2009) Aggregated P19 mouse embryonal carcinoma cells as a simple *in vitro* model to study the molecular regulations of mesoderm formation and axial elongation morphogenesis. *Genesis* **47:** 93–106

Marino G, Niso-Santano M, Baehrecke EH, Kroemer G (2014). Selfconsumption: the interplay of autophagy and apoptosis. *Nat Rev Mol Cell Biol* **15:** 81-94

Mark M, Ghyselinck NB, Chambon P (2009) Function of retinoic acid receptors duringembryonic development. *Nucl Recep Signal* **7:** e002

Mark M, Ghyselinck NB, Wendling O, Dupe V, Mascrez B, Kastner P, Chambon P (1999) A genetic dissection of the retinoid signalling pathway in the mouse. *Proc Nutr Soc* **58:** 609–613

Marklund M, Sjodal M, Beehler BC, Jessell TM, Edlund T, Gunhaga L (2004) Retinoic acid signalling specifies intermediate character in the developing telencephalon. *Development* **131:** 4323-4332

Marlétaz F, Holland LZ, Laudet V, Schubert M (2006) Retinoic acid signaling and the evolution of chordates. *Int J Biol Sci* **2:** 38-47

Martin V, Herrera F, Garcia-Santos G, Antolin I, Rodriguez-Blanco J, Rodriguez C (2007) Signaling pathways involved in antioxidant control of glioma cell proliferation. *Free Radic Biol Med* **42:** 1715–1722

Martinez-Ceballos E, Gudas LJ (2008) Hoxa1 is required for the retinoic acid-induced differentiation of embryonic stem cells into neurons. *J Neurosci Res* **86:** 2809–2819

Martinvalet D, Zhu P, Lieberman J (2005) Granzyme A induces caspase-independent mitochondrial damage, a required first step for apoptosis. *Immunity* **22:** 355–370

Mathew R, Karp CM, Beaudoin B, Vuong N, Chen G, Chen HY, Bray K, Reddy A, Bhanot G, Gelinas C, Dipaola RS, Karantza-Wadsworth V, White E (2009) Autophagy suppresses tumorigenesis through elimination of p62. *Cell* **137:** 1062-1075

Matissek SJ, Elsawa SF (2020) GLI3: a mediator of genetic diseases, development and cancer. *Cell Commun Signal* **18:** 54

Mauthe M, Orhon I, Rocchi C, Zhou X, Luhr M, Hijlkema KJ, Coppes RP, Engedal N, Mari M, Reggiori F (2018) Chloroquine inhibits autophagic flux by decreasing autophagosome-lysosome fusion. *Autophagy* **14:** 1435-1455

Maves L, Kimmel CB (2005) Dynamic and sequential patterning of the zebrafish posterior hindbrain by retinoic acid. *Dev Biol* **285:** 593-605

Maye P, Becker S, Siemen H, Thorne J, Byrd N, Carpentino J Grabel L (2004) Hedgehog signaling is required for the differentiation of ES cells into neurectoderm. *Dev Biol* **265:** 276-290

McBurney MW (1993) P19 embryonal carcinoma cells. *Int J Dev Biol* **37:** 135-140

McBurney MW, Jones-Villeneuve EMW, Edwards M, Anderson P (1982) Controlled differentiation of teratocarcinoma cells in culture. *Nature* **299:** 165-167

McBurney MW, Rogers BJ (1982) Isolation of male embryonal carcinoma cells and their chromosome replication patterns. *Dev Biol* **89:** 503–508

Meldrum BS (2000) Glutamate as a Neurotransmitter in the Brain: Review of Physiology and Pathology. *J Nutrition* **130:** 1007–1015

Melino G, Thiele CJ, Knight RA, Piacentini M (1997) Retinoids and the control of growth death decisions in human neuroblastoma cell lines. *J Neurooncol* **31:** 65–83

Mendoza-Parra MA, Walia M, Sankar M, Gronemeyer H (2011) Dissecting the retinoid-induced differentiation of F9 embryonal stem cells by integrative genomics. *Mol Syst Biol* **7:** 538

Merry DE, Veis DJ, Hickey WF & Korsmeyer SJ (1994) Bcl-2 protein expression is widespread in the developing nervous-system and retained in the adult Pns. *Development* **120:** 301–311

Mic FA, Molotkov A, Benbrook DM, Duester G (2003) Retinoid activation of retinoic acid receptor but not retinoid X receptor is sufficient to rescue lethal defect in retinoic acid synthesis. *Proc Natl Acad Sci USA* **100:** 7135-7140

Milton JD, Jarett HE, Gowers K, Chalak S, Briggs L, Robinson IM, Sweeney ST (2011) Oxidative stress induces overgrowth of the Drosophila neuromuscular junction. *Proc Natl Acad Sci USA* **108:** 17521–17526

Miyata M, Smith JD (1996) Apolipoprotein E allele-specific antioxidant activity and effects on cytotoxicity by oxidative insults and beta-amyloid peptides. *Nat Genet* **14:** 55–61

Miyazawa K, Shinozaki M, Hara T, Furuya T, Miyazono K (2002) Two major Smad pathways in TGF-beta superfamily signalling. *Genes Cells* **7:** 1191-204

Mizushima N, Levine B (2010) Autophagy in mammalian development and differentiation. *Nat Cell Biol* **12:** 823-830

Mizushima N, Levine B, Cuervo AM, Klionsky DJ (2008) Autophagy fights disease through cellular self-digestion. *Nature* **451:** 1069–1075

Mohamed, SA, El-Kashef, DH, Nader, MA (2020) Tiron alleviates MPTP-induced Parkinsonism in mice via activation of Keap-1/Nrf2 pathway. *J Biochem Mol Toxicol* **2020:** e22685

Molotkova N, Molotkov A, Sirbu IO, Duester G (2005) Requirement of mesodermal retinoic acid generated by Raldh2 for posterior neural transformation. *Mech Dev* **122:** 145-155

Monticone M, Taherian R, Stigliani S, Carra E, Monteghirfo S, Longo L, Daga A, Dono M, Zupo S, Giaretti W, Castagnola P (2014) NAC, tiron and trolox impair survival of cell cultures containing glioblastoma tumorigenic initiating cells by inhibition of cell cycle progression. *PLoS One* **9:** e90085

Monzo HJ, Park TIH, Montgomery JM, Faull RLM, Dragunow M, Curtis MA (2012) A method for generating high-yield enriched neuronal cultures from P19 embryonal carcinoma cells. *J Neurosci Methods* **204:** 87-103

Morassutti DJ, Staines WA, Magnuson DS, Marshall KC, McBurney MW (1994) Murine embryonal carcinoma-derived neurons survive and mature following transplantation into adult rat striatum. Neurosci **58:** 753–763

Morgado AL, Xavier JM, Dionísio PA, Ribeiro MF, Dias RB, Sebastião AM, Solá S, Rodrigues CM (2015) MicroRNA-34a Modulates Neural Stem Cell Differentiation by Regulating Expression of Synaptic and Autophagic Proteins. *Mol Neurobiol* **51:** 1168-1183

Morgan CA, Parajuli B, Buchman CD, Dria K, Hurley TD (2015) N,N-diethylaminobenzaldehyde (DEAB) as a substrate and mechanism-based inhibitor for human ALDH isoenzymes. *Chem Biol Interact* **234:** 18-28

Morii A, Katayama S, Inazu T (2020) Establishment of a simple method for inducing neuronal differentiation of P19 EC Cells without embryoid body formation and analysis of the role of histone deacetylase 8 activity in this differentiation. *Biol Pharm Bull* **43:** 1096–1103

Moutier E, Ye T, Choukrallah MA, Urban S, Osz J, Chatagnon A, Delacroix L, Langer D, Rochel N, Moras D *et al.* (2012) Retinoic acid receptors recognize the mouse genome through binding elements with diverse spacing and topology. J Biol Chem **287:** 26328-26341

Muilenburg D, Parsons C, Coates J, Virudachalam S, Bold RJ (2014) Role of autophagy in apoptotic regulation by Akt in pancreatic cancer. *Anticancer Res* **34:** 631-637

Mummery CL, Feyen A, Freund E, Shen S (1990) Characteristics of embryonic stem cell differentiation: a comparison with two embryonal carcinoma cell lines. *Cell Differ Dev* **30:** 195-206

Muñoz-Sanjuán I, Brivanlou AH (2002) Neural induction, the default model and embryonic stem cells. *Nat Rev Neurosci* **3:** 271-80

Murtomäki S, Virtanen I, Liesi P (1999) Neurofilament proteins are constitutively expressed in F9 teratocarcinoma cells. *Int J Dev Neurosci* **17:** 829-38

Nakamura A, Swahari V, Plestant C, Smith I, McCoy E, Smith S, Moy SS, Anton ES, Deshmukh M (2016) Bcl-xL Is Essential for the Survival and Function of Differentiated Neurons in the Cortex That Control Complex Behaviors. *J Neurosci* **36:** 5448-5461

Nakayama Y, Wada A, Inoue R, Terasawa K, Kimura I, Nakamura N, Kurosaka A (2014) A rapid and efficient method for neuronal induction of the P19 embryonic carcinoma cell line. *J Neurosci Methods* **227:** 100-106

Neely MD, Litt MJ, Tidball AM, Li GG, Aboud AA, Hopkins CR, Chamberlin R, Hong CC, Ess KC, Bowman AB (2012) DMH1, a highly selective small molecule BMP inhibitor promotes neurogenesis of hiPSCs: comparison of PAX6 and SOX1 expression during neural induction. *ACS Chem Neurosci* **3:** 482-491

Niederreither K, Abu-Abed S, Schuhbaur B, Petkovich M, Chambon P, Dollé P (2002) Genetic evidence that oxidative derivatives of retinoic acid are not involved in retinoid signaling during mouse development. *Nat Gen* **31:** 84–88

Niehrs C, Acebron SP (2012) Mitotic and mitogenic Wnt signalling. *EMBO J* **31:** 2705–2713

Nijhawan D, Honarpour N, Wang X (2000) Apoptosis in neural development and disease. *Annu Rev Neurosci* **23:** 73-87

Nimmerjahn A, Kirchhoff F, Helmchen F (2005) Resting microglial cells are highly dynamic surveillants of brain parenchyma in vivo. *Science* **308:** 1314-1318

Nishiyama J, Miura E, Mizushima N, Watanabe M, Yuzaki M (2007) Aberrant membranes and double-membrane structures accumulate in the axons of Atg5-null Purkinje cells before neuronal death. *Autophagy* **3:** 591–596

Novitch BG, Wichterle H, Jessell TM, Sockanathan S (2003) A requirement for retinoic acid-mediated transcriptional activation in ventral neural patterning and motor neuron specification. *Neuron* **40:** 81-95

Ohi Y, Qin H, Hong C, Blouin L, Polo JM, Guo T, Qi Z, Downey SL, Manos PD, Rossi DJ, *et al.* (2011) Incomplete DNA methylation underlies a transcriptional memory of somatic cells in human iPS cells. *Nature Cell Biol* **13:** 541-549

Ohishi T, Yoshida H, Katori M, Migita T, Muramatsu Y, Miyake M, Ishikawa Y, Saiura A, Iemura SI, Natsume T, Seimiya H (2017) Tankyrase-Binding Protein TNKS1BP1 Regulates Actin Cytoskeleton Rearrangement and Cancer Cell Invasion. *Cancer Res* **77:** 2328-2338

Okabe S, Forsberg-Nilsson K, Spiro AC, Segal M, McKay RD (1996) Development of neuronal precursor cells and functional postmitotic neurons from embryonic stem cells *in vitro*. *Mech Dev* **59:** 89–102

Okada Y, Shimazaki T, Sobue G, Okano H (2004) Retinoic-acid-concentration-dependent acquisition of neural cell identity during *in vitro* differentiation of mouse embryonic stem cells. *Dev Biol* **275:** 124-142

Olguín-Albuerne M, Morán J (2018) Redox signaling mechanisms in nervous system development. *Antioxid Redox Signal* **28:** 1603-1625

Olivera-Martinez I, Storey KG (2007) Wnt signals provide a timing mechanism for the FGF-retinoid differentiation switch during vertebrate body axis extension. *Development* **134:** 2125-2135

Opferman JT, Korsmeyer SJ (2003) Apoptosis in the development and maintenance of the immune system. *Nat Immunol* **4:** 410–415

Oppenheim RW (1991) Cell death during development of the nervous system. *Annu Rev Neurosci* **14:** 453–501

Oppenheim RW, Flavell RA, Vinsant S, Prevette D, Kuan CY, Rakic P (2001) Programmed cell death of developing mammalian neurons after genetic deletion of caspases. *J Neurosci* **21:** 4752–4760

Ordonez AN, Jessick VJ, Clayton CE, Ashley MD, Thompson SJ, Simon RP & Meller R (2010) Rapid ischemic tolerance induced by adenosine preconditioning results in Bcl-2 interacting mediator of cell death (Bim) degradation by the proteasome. *Int J Physiol Pathophysiol Pharmacol* **2:** 36–44

Orford KW, Scadden DT (2008) Deconstructing stem cell self-renewal: genetic insights into cell-cycle regulation. *Nat Rev Genet* **9:** 115-128

Oswald MCW, Garnham N, Sweeney ST, Landgraf M (2018) Regulation of neuronal development and function by ROS. *FEBS Lett* **592:** 679-691

Ozawa T (1995) Mechanism of somatic mitochondrial DNA mutations associated with age and diseases. *Biochim Biophys Acta* **1271:** 177–189

Pacherník J, Bryja V, Esner M, Kubala L, Dvorák P, Hampl A (2005) Neural differentiation of pluripotent mouse embryonal carcinoma cells by retinoic acid: inhibitory effect of serum. *Physiol Res* **54:** 115-122

Pankiv S, Clausen TH, Lamark T, Brech A, Bruun JA, Outzen H, Øvervatn A, Bjørkøy G, Johansen T (2007) p62/SQSTM1 binds directly to Atg8/LC3 to facilitate degradation of ubiquitinated protein aggregates by autophagy. *J Biol Chem* **282:** 24131-24145

Parcon PA, Balasubramaniam M, Ayyadevara S, Jones RA, Liu L, Shmookler Reis RJ, Barger SW, Mrak RE, Griffin WST (2018) Apolipoprotein E4 inhibits autophagy gene products through direct, specific binding to CLEAR motifs. *Alzheimers Dement* **14:** 230-242

Park IH, Arora N, Huo H, Maherali N, Ahfeldt T, Shimamura A, Lensch MW, Cowan C, Hochedlinger K, Daley GQ (2008) Disease-specific induced pluripotent stem cells. *Cell* **134:** 877–886

Parrado A, Despouy G, Kraïba R, Le Pogam C, Dupas S, Choquette M, Robledo M, Larghero J, Bui H, Le Gall I, et al. (2001) Retinoic acid receptor α1 variants, RARα1ΔB and RARα1ΔBC, define a new class of nuclear receptor isoforms, *Nucleic Acids Res* **29:** 4901–4908

Parzych KR, Klionsky DJ (2014) An overview of autophagy: morphology, mechanism, and regulation. *Antioxid Redox Signal* **20:** 460-473

Pattingre S, Tassa A, Qu X, Garuti R, Liang XH, Mizushima N, Packer M, Schneider MD, Levine B (2005) Bcl-2 antiapoptotic proteins inhibit Beclin 1-dependent autophagy. *Cell* **122:** 927-939

Pauly MG, Krajka V, Stengel F, Seibler P, Klein C, Capetian P (2018) Adherent vs. free-floating neural induction by dual SMAD inhibition for neurosphere cultures derived from human induced pluripotent stem cells. *Front Cell Dev Biol* **6:** 3

Pennimpede T, Cameron DA, MacLean GA, Li H, Abu-Abed S, Petkovich M (2010) The role of CYP26 enzymes in defining appropriate retinoic acid exposure during embryogenesis. *Birth Defects Res* **88:** 883-894

Pera MJ, Cooper S, Mills J, Parrington JM (1989) Isolation and characterization of a multipotent clone of human embryonal carcinoma cells. *Differentiation* **42:** 10–23

Pereira IM, Marote DA, Salgado AJ, Silva NA (2019) Filling the gap: neural stem cells as a promising therapy for spinal cord injury. *Pharmaceuticals* **12:** 65

Pérez Estrada C, Covacu R, Sankavaram SR, Svensson M, Brundin L (2014) Oxidative stress increases neurogenesis and oligodendrogenesis in adult neural progenitor cells. *Stem Cells Dev* **23:** 2311-2327

Persaud SD, Lin YW, Wu CY, Kagechika H, Wei L-N (2013) Cellular retinoic acid binding protein I mediates rapid non-canonical activation of ERK1/2 by all-trans retinoic acid. *Cell Signal* **25:** 19–25

Piacentini M, Evangelisti C, Mastroberardino PG, Nardacci R, Kroe-mer G (2003) Does prothymosin-alpha act as molecular switch between apoptosis and autophagy? *Cell Death Differ* **10:** 937–939

Pohl C, Jentsch S (2008) Final stages of cytokinesis and midbody ring formation are controlled by BRUCE. *Cell* **132:** 832-845

Polster BM, Robertson CL, Bucci CJ, Suzuki M, Fiskum G (2003) Postnatal brain development and neural cell differentiation modulate mitochondrial Bax and BH3 peptide-induced cytochrome c release. *Cell Death Differ* **10:** 365–370

Poon IK, Lucas CD, Rossi AG, Ravichandran KS (2014) Apoptotic cell clearance: basic biology and therapeutic potential. *Nat Rev Immunol* **14:** 166–180

Poon MM, Chen L (2008) Retinoic acid-gated sequence-specific translational control by RARalpha. *Proc Natl Acad Sci U S A* **105:** 20303–20308

Pozzi S, Rossetti S, Bistulfi G, Sacchi N (2006) RAR-mediated epigenetic control of the cytochrome P450 Cyp26a1 in embryocarcinoma cells. *Oncogene* **25:** 1400-1407

Pratt MA, Crippen C, Hubbard K, Menard M (1998) Deregulated expression of the retinoid X receptor alpha prevents muscle differentiation in P19 embryonal carcinoma cells. *Cell Growth Differ* **9:** 713-722

Pratt MA, Crippen CA, Ménard M (2000) Spontaneous retinoic acid receptor beta 2 expression during mesoderm differentiation of P19 murine embryonal carcinoma cells. *Differentiation* **65:** 271-279

Pratt MA, Kralova J, McBurney MW (1990) A dominant negative mutation of the alpha retinoic acid receptor gene in a retinoic acid-nonresponsive embryonal carcinoma cell. *Mol Cell Biol* **10:** 6445-6453

Price JC, Guan S, Burlingame A, Prusiner SB, Ghaemmaghami S (2010) Analysis of proteome dynamics in the mouse brain. *Proc Natl Acad Sci USA* **107:** 14508-14513

Putcha GV, Deshmukh M, Johnson EM Jr (2000) Inhibition of apoptotic signaling cascades causes loss of trophic factor dependence during neuronal maturation. *J Cell Biol* **149:** 1011–1018

Putcha GV, Le S, Frank S, Besirli CG, Clark K, Chu B, Alix S, Youle RJ, LaMarche A, Maroney AC, Johnson EM Jr (2003) JNK-mediated BIM phosphorylation potentiates BAX-dependent apoptosis. *Neuron* **38:** 899–914

Qian C, Zhou FQ (2020) Updates and challenges of axon regeneration in the mammalian central nervous system. *J Mol Cell Biol* **12:** 798–806

Qian X, Davis AA, Goderie SK, Temple S (1997) FGF2 concentration regulates the generation of neurons and glia from multipotent cortical stem cells. *Neuron* **18:** 81–93

Qian X, Shen Q, Goderie SK, He W, Capela A, Davis AA, Temple S (2000) Timing of CNS cell generation: a programmed sequence of neuron and glial cell production from isolated murine cortical stem cells. *Neuron* **28:** 69–80

Qu X, Zou Z, Sun Q, Luby-Phelps K, Cheng P, Hogan RN, Gilpin C, Levine B (2007) Autophagy gene-dependent clearance of apoptotic cells during embryonic development. *Cell* **128:** 931-946

Raisova M, Hossini AM, Eberle J, Riebeling C, Wieder T, Sturm I, Daniel PT, Orfanos CE, Geilen CC (2001) The Bax/Bcl-2 ratio determines the susceptibility of human melanoma cells to CD95/Fas-mediated apoptosis. *J Invest Dermatol* **117:** 333-340

Rakic P (1995) A small step for the cell, a giant leap for mankind: a hypothesis of neocortical expansion during evolution. *Trends Neurosci* **18:** 383-388

Ravikumar B, Futter M, Jahreiss L, Korolchuk VI, Lichtenberg M, Luo S, Massey DC, Menzies FM, Narayanan U, Renna M, *et al.* (2009) Mammalian macroautophagy at a glance. *J Cell Sci* **122:** 1707-1711

Resende RR, Majumder P, Gomes KN, Britto LRG, Ulrich H (2007) P19 embryonal carcinoma cells as in vitro model for studying purinergic receptor expression and modulation of N-methyl-D-aspartate-glutamate and acetylcholine receptors during neuronal development. *Neurosci* **146:** 1169–1181

Reynolds BA and Weiss S (1992) Generation of neurons and astrocytes from isolated cells of the adult mammalian central nervous system. *Science* **255:** 1707–1710

Reynolds JN, Prasad A, Gillespie LL, Paterno GD (1996) Developmental expression of functional GABAA receptors containing the gamma 2 subunit in neurons derived from embryonal carcinoma (P19) cells. *Brain Res Mol Brain Res* **35:** 11–18

Rharass T, Lemcke H, Lantow M, Kuznetsov SA, Weiss DG, Panáková D (2014) Ca2+-mediated mitochondrial reactive oxygen species metabolism augments Wnt/β-catenin pathway activation to facilitate cell differentiation. *J Biol Chem* **289:** 27937-27951

Rhinn M, Dollé P (2012) Retinoic acid signalling during development. *Development* **139:** 843-858

Roberts C (2020) Regulating Retinoic Acid Availability during Development and Regeneration: The Role of the CYP26 Enzymes. *J Dev Biol* **8:** 1-6

Robertson EJ (1987) Teratocarcinomas and embryonic stem cells: A practical approach. ed Robertson EJ, IRL Press, Washington DC

Robertson JA (2001) Human embryonic stem cell research: Ethical and legal issues. *Nat Rev Genet* **2:** 74–78

Rochette-Egly C, Chambon P (2001) F9 embryocarcinoma cells: a cell autonomous model to study the functional selectivity of RARs and RXRs in retinoid signaling. *Histol Histopathol* **16:** 909-922

Rochette-Egly C, Germain P (2009) Dynamic and combinatorial control of gene expression by nuclear retinoic acid receptors (RARs). *Nucl Recept Signal* **7:** e005

Rohwedel J, Guan K, Wobus AM (1999) Induction of cellular differentiation by retinoic acid *in vitro*. *Cells Tiss Org* **165:** 190–202

Rosenthal MD, Wishnow RM, Sato GH (1970) *In vitro* growth and differentiation of clonal populations of multipotent mouse cells derived from a transplantable testicular teratocarcinoma. *J Natl Cancer Inst* **44:** 1001-1014

Ross SA, McCaffery PJ, Drager UC, De Luca LM (2000) Retinoids in embryonal development. *Physiol Rev* **80:** 1021-1054

Rosso SB, Sussman D, Wynshaw-Boris A, Salinas PC (2005) Wnt signaling through Dishevelled, Rac and JNK regulates dendritic development. *Nat Neurosci* **8:** 34–42

Rubinsztein DC, Gestwicki JE, Murphy LO, Klionsky DJ (2007) Potential therapeutic applications of autophagy. *Nat Rev Drug Discov* **6:** 304-312

Rubinsztein DC, Marino G, Kroemer G (2011). Autophagy and aging. *Cell* **146:** 682-695

Sadoul R (1998) Bcl-2 family members in the development and degenerative pathologies of the nervous system. *Cell Death Differ* **5:** 805–815

Saelens X, Festjens N, Vande Walle L, van Gurp M, van Loo G, Vandenabeele P (2004) Toxic proteins released from mitochondria in cell death. *Oncogene* **23:** 2861-2874

Saleem S, Biswas SC (2017) Tribbles pseudokinase 3 induces both apoptosis and autophagy in amyloidbeta-induced neuronal death. *J Biol Chem* **292:** 2571–2585

Sánchez-Alegría K, Flores-León M, Avila-Muñoz E, Rodríguez-Corona N, Arias C (2018) PI3K signaling in neurons: A central node for the control of multiple functions. *Int J Mol Sci* **19:** 3725

Sanphui P, Biswas SC (2013) FoxO3a is activated and executes neuron death via Bim in response to beta-amyloid. *Cell Death Dis* **4:** e625

Sasaki H, Nishizaki Y, Hui C, Nakafuku M, Kondoh H (1999) Regulation of Gli2 and Gli3 activities by an amino-terminal repression domain: implication of Gli2 and Gli3 as primary mediators of Shh signaling. *Development* **126:** 3915-3924

Sathyamurthy A, Johnson KR, Matson KJE, Dobrott C I, Li L, Ryba AR, Bergman TB, Kelly MC, Kelley MW, Levine AJ (2018) Massively parallel single nucleus transcriptional profiling defines spinal cord neurons and their activity during behaviour. *Cell Rep* **22:** 2216-2225

Savill J, Fadok V (2000) Corpse clearance defines the meaning of cell death. *Nature* **407:** 784–788

Schuler M, Green DR (2001) Mechanisms of p53-dependent apoptosis. *Biochem Soc Trans* **29:** 684–688

Schwartz LM. Smith SW, Jones ME, Osborne BA (1993) Do all programmed cell deaths occur via apoptosis? *Proc Natl Acad Sci USA* **90:** 980–984

Semple BD, Blomgren K, Gimlin K, Ferriero DM, Noble-Haeusslein LJ (2013) Brain development in rodents and humans: Identifying benchmarks of maturation and vulnerability to injury across species. *Prog Neurobiol* **106-107:** 1-16

Sennerstama R, Strömberg JO (1984) A comparative study of the cell cycles of nullipotent and multipotent embryonal carcinoma cell lines during exponential growth *Develop Biol* **103:** 221-229

Shaban S, El-Husseny MWA, Abushouk AI, Salem AMA, Mamdouh M, Abdel-Daim MM (2017) Effects of antioxidant supplements on the survival and differentiation of stem cells. *Oxid Med Cell Longev* **2017:** 5032102

Shackelford RE, Kaufmann WK, Paules RS (2000) Oxidative stress and cell cycle checkpoint function. *Free Radic Biol Med* **28:** 1387–1404

Shahbazi MN (2020) Mechanisms of human embryo development: from cell fate to tissue shape and back. *Development* **147:** 190629

Shahbazi MN, Zernicka-Goetz M (2018) Deconstructing and reconstructing the mouse and human early embryo. *Nature Cell Biol* **20:** 878–887

Shahhoseini M, Taghizadeh Z, Hatami M, Baharvand H (2013) Retinoic acid dependent histone 3 demethylation of the clustered HOX genes during neural differentiation of human embryonic stem cells. *Biochem Cell Biol* **91:** 116-122

Shamas-Din A, Brahmbhatt H, Leber B, Andrews DW (2011) BH3-only proteins: orchestrators of apoptosis. *Biochim Biophys Acta* **1813:** 508–520

Sharma K, Schmitt S, Bergner CG, Tyanova S, Kannaiyan N, Manrique-Hoyos N, Kongi K, Cantuti L, Hanisch UK, Philips MA (2015) Cell type- and brain region-resolved mouse brain proteome. *Nat Neurosci* **18:** 1819-1831

Shehata M, Matsumura H, Okubo-Suzuki R, Ohkawa N, Inokuchi K (2012) Neuronal stimulation induces autophagy in hippocampal neurons that is involved in AMPA receptor degradation after chemical long-term depression. *J Neurosci* **32:** 10413–10422

Shih AY, Johnson DA, Wong G, Kraft AD, Jiang L, Erb H, Johnson JA, Murphy TH (2003). Coordinate regulation of glutathione biosynthesis and release by Nrf2-expressing glia potently protects neurons from oxidative stress. *J Neurosci* **23:** 3394–3406

Shimohama S, Fujimoto S, Sumida Y, Tanino H (1998) Differential expression of rat brain bcl-2 family proteins in development and aging. *Biochem Biophys Res Commun* **252:** 92–96

Shintani T, Klionsky DJ (2004) Autophagy in health and disease: a double-edged sword. *Science* **306:** 990–995

Sica A, Wang JM, Colotta F, Dejana E, Mantovani A, Oppenheim JJ, Larsen CG, Zachariae CO, Matsushima K (1990) Monocyte chemotactic and activating factor gene expression induced in endothelial cells by IL-1 and tumor necrosis factor. *J Immuno* **144:** 3034–3038

Simões-Costa M, Bronner ME (2013) Insights into neural crest development and evolution from genomic analysis. *Genome Res* **23:** 1069-1080

Sloan SA, Darmanis S, Huber N, Khan TA, Birey F, Caneda C, Reimer R, Quake SR, Barres BA, Pasca SP (2017) Human astrocyte maturation captured in 3D cerebral cortical spheroids derived from pluripotent stem cells. *Neuron* **95:** 779–790

Smith JL, Schoenwolf GC (1989) Notochordal induction of cell wedging in the chick neural plate and its role in neural tube formation. *J Exp Zool* **250:** 49–62

Smith JL, Schoenwolf GC (1997) Neurulation: Coming to closure. *Trends Neurosci* **11:** 510–517

Smukler SR, Runciman SB, Xu S, van der Kooy D (2006) Embryonic stem cells assume a primitive neural stem cell fate in the absence of extrinsic influences. J Cell Biol **172:** 79-90

Sofroniew MV, Vinters HV (2010) Astrocytes: biology and pathology. *Acta Neuropathol* **119:** 7–35

Solecki DJ, Liu XL, Tomoda T, Fang Y, Hatten ME (2001) Activated Notch2 signaling inhibits differentiation of cerebellar granule neuron precursors by maintaining proliferation. *Neuron* **31:** 557-568

Song Y, Lee S, Jho EH (2018) Enhancement of neuronal differentiation by using small molecules modulating Nodal/Smad, Wnt/β-catenin, and FGF signaling. *Biochem Biophys Res Commun* **503:** 352-358

Spana EP, Doe CQ (1996) Numb antagonizes Notch signaling to specify sibling neuron cell fates. *Neuron* **17:** 21-26

Sperandio S, de Belle I, Bredesen DE (2000) An alternative, non-apoptotic form of programmed cell death. *Proc Natl Acad Sci USA* **97:** 14376–14381

Stains WA, Utti DJM, Reuhl KR, Ally AI, McBurney MW (1994) Neurons derive from P19 embryonal carcinoma cells have varied morphologies and neurotransmitter. *Neurosci* **58:** 735-751

Stavoe AK, Hill SE, Hall DH, Colón-Ramos DA (2019) KIF1A/UNC-104 Transports ATG-9 to Regulate Neurodevelopment and Autophagy at Synapses. *Dev Cell* **38:** 171-85

Stern CD (2005) Neural induction: old problem, new findings, yet more questions. *Development* **132:** 2007-2021

Stern CD (2006) Neural induction: 10 years on since the 'default model'. *Curr Opin Cell Biol* **18:** 692-697

Stewart R, Christie VB, Przyborski SA (2003) Manipulation of human pluripotent embryonal carcinoma stem cells and the development of neural subtypes. *Stem Cells* **21:** 248-256

Strickland S, Mahdavi V (1978) The induction of differentiation in teratocarcinoma stem cells by retinoic acid. *Cell* **15:** 393-403

Strübing C, Ahnert-Hilger G, Shan J, Wiedenmann B, Hescheler J, Wobus AM (1995) Differentiation of pluripotent embryonic stem cells into the neuronal lineage *in vitro* gives rise to mature inhibitory and excitatory neurons. *Mech Dev* **53:** 275–287

Sun WL (2016) Ambra1 in autophagy and apoptosis: Implications for cell survival and chemotherapy resistance. *Oncol Lett* **12:** 367-374

Sun Y, Nadal-Vicens M, Misono S, Lin MZ, Zubiaga A, Hua X, Fan G, Greenber ME (2001) Neurogenin promotes neurogenesis and inhibits glial differentiation by independent mechanisms. *Cell* **104:** 365–376

Sun YF, Yu LY, Saarma M, Timmusk T, Arumae U (2001) Neuron-specific Bcl-2 homology 3 domain only splice variant of Bak is anti-apoptotic in neurons, but pro-apoptotic in non-neuronal cells. *J Biol Chem* **276:** 16240–16247

Surh YJ, Kundu JK, Li MH, Na HK, Cha YN (2009) Role of Nrf2-mediated heme oxygenase-1 upregulation in adaptive survival response to nitrosative stress. *Arch Pharm Res* **32:** 1163-1176

Suzuki YJ, Shults NV (2019) Antioxidant Regulation of Cell Reprogramming. *Antioxidants* **8:** 323

Swenson R (2006) Review of clinical and functional neuroscience. *Dartmouth Medical School*, Chapter 4

Swistowska AM, da Cruz AB, Han Y, Swistowski A, Liu Y, Shin S, Zhan M, Rao MS, Zeng X (2010) Stage-specific role for shh in dopaminergic differentiation of human embryonic stem cells induced by stromal cells. *Stem Cells Dev* **19:** 71-82

Switon K, Kotulska K, Janusz-Kaminska A, Zmorzynska J, Jaworski J (2017) Molecular neurobiology of mTOR. *Neuroscience* **341:** 112-153

Takano A, Zochi R, Hibi M, Terashima T, Katsuyama Y (2010) Expression of strawberry notch family genes during zebrafish embryogenesis. *Dev Dyn* **239:** 1789-1796

Tam PP, Loebel DA (2007) Gene function in mouse embryogenesis: get set for gastrulation. *Nat Rev Genet* **8:** 368-381

Taneja R, Bouillet P, Boylan JF, Gaub MP, Roy B, Gudas LJ, Chambon P (1995) Reexpression of retinoic acid receptor (RAR) gamma or overexpression of RAR alpha or RAR beta in RAR gamma-null F9 cells reveals a partial functional redundancy between the three RAR types. *Proc Natl Acad Sci USA* **92:** 7854–7858

Tanida I, Ueno T, Kominami E (2008) LC3 and Autophagy. *Methods Mol Biol* **445:** 77-88

Tatton WG, Chalmers-Redman R, Brown D, Tatton N (2003) Apoptosis in Parkinson's disease: signals for neuronal degradation. *Ann Neurol* **53:** 61–72

Taylor MK, Yeager K, Morrison SJ (2007) Physiological Notch signaling promotes gliogenesis in the developing peripheral and central nervous systems. *Development* **134:** 2435–2447

Taylor RC, Cullen SP & Martin SJ (2008) Apoptosis: controlled demolition at the cellular level. *Nat Rev Mol Cell Biol* **9:** 231–241

Tewari M, Pandey HS, Seth P (2017) Using Human Neural Stem Cells as a Model to Understand the “Science of Ashwagandha”. *Science of Ashwagandha: Preventive and Therapeutic Potentials (Eds.)* pp 319-344

Thompson S, Stern PL, Webb M, Walsh FS, Engstrom W, Evans EP, Shi WK, Hopkins B, Graham CF (1984) Cloned human teratoma cells differentiate into neuron-like cells and other cell types in retinoic acid. *J Cell Sci* **72:** 37–64

Trachootham D, Lu W, Ogasawara MA, Nilsa RD, Huang P (2008) Redox regulation of cell survival. *Antioxid Redox Signal* **10:** 1343-1374

Tropepe V, Hitoshi S, Sirard C, Mak TW, Rossant J, van der Kooy D (2001) Direct neural fate specification from embryonic stem cells: a primitive mammalian neural stem cell stage acquired through a default mechanism. *Neuron* **30:** 65-78

Trump BF, Berezesky IK, Chang SH, Phelps PC (1997) The pathways of cell death: oncosis, apoptosis, and necrosis. *Toxicol Pathol* **25:** 82–88

Tsunemoto R, Lee S, Szűcs A, Chubukov P, Sokolova I, Blanchard JW, Eade KT, Bruggemann J, Wu C, Torkamani A, Sanna PP, Baldwin KK (2018) Diverse reprogramming codes for neuronal identity. *Nature* **557:** 375-380

Tsunemoto RK, Eade KT, Blanchard JW, Baldwin KK (2015) Forward engineering neuronal diversity using direct reprogramming. *EMBO J* **34:** 1445-1455

Udolph G, Prokop A, Bossing T, Technau GM (1993) A common precursor for glia and neurons in the embryonic CNS of Drosophila gives rise to segment-specific lineage variants. *Development* **118:** 765-775

Ueberham U, Hilbrich I, Ueberham E, Rohn S, Glockner P, Dietrich K, Brückner MK, Arendt T (2012) Transcriptional control of cell cycle-dependent kinase 4 by Smad proteins-implications for Alzheimer's disease. *Neurobiol Aging* **33:** 2827-2840

Uo T, Kinoshita Y, Morrison RS (2005) Neurons exclusively express N-Bak, a BH3 domain-only Bak isoform that promotes neuronal apoptosis. *J Biol Chem* **280:** 9065–9073

Vaaga CE, Borisovska M, Westbrook GL (2014) Dual-transmitter neurons: functional implications of co-release and co-transmission. *Curr Opin Neurobiol* **0:** 25-32

Vallier L, Reynolds D, Pedersen RA (2004) Nodal inhibits differentiation of human embryonic stem cells along the neuroectodermal default pathway. *Dev Biol* **275:** 403-421

Valvezan AJ, Klein PS (2012) GSK-3 and Wnt Signaling in Neurogenesis and Bipolar Disorder. *Front Mol Neurosci* **5:** 1

van der Heydena MAG, Defizeb LHK (2003) Twenty-one years of P19 cells: what an embryonal carcinoma cell line taught us about cardiomyocyte differentiation. *Cardiovas Res* **58:** 292–302

Varderidou-Minasian S, Verheijen BM, Schätzle P, Hoogenraad CC, Pasterkamp RJ, Altelaar M (2020) Deciphering the Proteome Dynamics during Development of Neurons Derived from Induced Pluripotent Stem Cells. *J Proteome Res* **19:** 2391-2403

Varlakhanova NV, Cotterman RF, deVries WN, Morgan J, Donahue LR, Murray S, Knowles BB, Knoepfler PS (2010) Myc maintains embryonic stem cell pluripotency and self-renewal. *Differentiation* **80:** 9-19

Vasiliou V, Nebert DW (2005) Analysis and update of the human aldehyde dehydrogenase (ALDH) gene family. *Hum Genomics* **2:** 138-143

Vazin T, Chen J, Lee CT, Amable R, Freed WJ (2008) Assessment of stromal-derived inducing activity in the generation of dopaminergic neurons from human embryonic stem cells. *Stem Cells* **26:** 1517–1525

Vázquez P, Arroba AI, Cecconi F, de la Rosa EJ, Boya P, de Pablo F (2012) Atg5 and Ambra1 differentially modulate neurogenesis in neural stem cells. *Autophagy* **8:** 187-199

Vekrellis K, McCarthy MJ, Watson A, Whitfield J, Rubin LL, Ham J (1997) Bax promotes neuronal cell death and is downregulated during the development of the nervous system. *Development* **124:** 1239–1249

Velasco I, Salazar P, Giorgetti A, Ramos-Mejia V, Castano J,Romero-Moya D, Menendez P (2014) Generation of neurons from somatic cells of healthy individuals and neurological patients through induced pluripotency or direct conversion. *Stem Cells* **32:** 2811–2817

Velusamy T, Panneerselvam AS, Purushottam M, Anusuyadevi M, Pal PK, Jain S, Essa MM, Guillemin GJ, Kandasamy M (2017) Protective Effect of Antioxidants on Neuronal Dysfunction and Plasticity in Huntington's Disease. *Oxid Med Cell Long* **2017:** 3279061

Verani R, Cappuccio I, Spinsanti P, Gradini R, Caruso A, Magnotti MC, Motolese M, Nicoletti F, Melchiorri D (2007) Expression of the Wnt inhibitor Dickkopf-1 is required for the induction of neural markers in mouse embryonic stem cells differentiating in response to retinoic acid. *J Neurochem* **100:** 242-250

Verdi JM, Bashirullah A, Goldhawk DE, Kubu CJ, Jamali M, Meakin SO, Lipshitz HD (1999) Distinct human NUMB isoforms regulate differentiation vs. proliferation in the neuronal lineage. *Proc Natl Acad Sci USA* **96:** 10472–10476

Verhagen AM, Coulson EJ, Vaux DL (2001) Inhibitor of apoptosis proteins and their relatives: IAPs and other BIRPs. *Genome Biol* **2:** REVIEWS3009

Verma I, Seshagiri PB (2018) Directed differentiation of mouse P19 embryonal carcinoma cells to neural cells in a serum- and retinoic acid-free culture medium. *In Vitro Cell Devel Biol* **54:** 567–579

Vojtek AB, Taylor J, DeRuiter SL, Yu JY, Figueroa C, Kwok RP, Turner DL (2003) Akt regulates basic helix-loop-helix transcription factor-coactivator complex formation and activity during neuronal differentiation. *Mol Cell Biol* **23:** 4417–4427

Von Bartheld CS, Bahney J, Herculano-Houzel S (2016) The search for true numbers of neurons and glial cells in the human brain: A review of 150 years of cell counting. *J Comp Neurol* **524:** 3865–3895

Wang C, Xia C, Bian W, Liu L, Lin W, Chen YG, Ang SL, Jing N (2006) Cell aggregation induced FGF8 elevation is essential for P19 cell neural differentiation. *Mol Biol Cell* **17:** 3075–3084

Wang H, Liu K, Geng M, Gao P, Wu X, Hai Y, Li Y, Li Y, Luo L, Hayes JD, Wang XJ, Tang X (2013) RXRα inhibits the NRF2-ARE signaling pathway through a direct interaction with the Neh7 domain of NRF2. *Cancer Res* **73:** 3097-3108

Wang T, Martin S, Papadopulos A, Harper CB, Mavlyutov TA, Niranjan D, Glass NR, Cooper-White JJ, Sibarita JB, Choquet D, Davletov B, Meunier FA (2012) Control of autophagosome axonal retrograde flux by presynaptic activity unveiled using botulinum neurotoxin type a. *J Neurosci* **35:** 6179-6194

Wang X, Lou N, Xu Q, Tian GF, Peng WG, Han X, Kang J, Takano T, Nedergaard M (2006) Astrocytic Ca2+ signaling evoked by sensory stimulation *in vivo*. *Nat Neurosci* **9:** 816–823

Wang XT, Pei DS, Xu J, Guan QH, Sun YF, Liu XM, Zhang GY (2007) Opposing effects of Bad phosphorylation at two distinct sites by Akt1 and JNK1/2 on ischemic brain injury. *Cell Signal* **19:** 1844–1856

Wei D, Gao N, Li L, Zhu JX, Diao L, Huang J, Han QJ, Wang S, Xue H, Wang Q, Wu QF, Zhang X, Bao L (2017) α-tubulin acetylation restricts axon overbranching by dampening microtubule plus-end dynamics in neurons. *Cereb Cortex*, **28:** 1–15

Wei LN (2013) Non-canonical activity of retinoic acid in epigenetic control of embryonic stem cell. *Transcription* **4:** 158-161

White JA, Beckett-Jones B, Guo YD, Dilworth FJ, Bonasoro J, Jones G, Petkovich M (1997) cDNA cloning of human retinoic acid-metabolizing enzyme (hP450RAI) identifies a novel family of cytochromes P450. *J Biol Chem* **272:** 18538–18541

White JC, Highland M, Kaiser M, Clagett-Dame M (2000) Vitamin A deficiency results in the dose-dependent acquisition of anterior character and shortening of the caudal hindbrain of the rat embryo. *Dev Biol* **220:** 263-284

White JH, Fernandes I, Mader S, Yang XJ (2004) Corepressor recruitment by agonist-bound nuclear receptors. *Vitam Horm* **68:** 123–143

White RJ, Nie Q, Lander AD, Schilling TF (2007) Complex regulation of cyp26a1 creates a robust retinoic acid gradient in the zebrafish embryo. *PLoS Biol* **5:** e304

Wichterle H, Lieberam I, Porter JA, Jessell TM (2002) Directed differentiation of embryonic stem cells into motor neurons. *Cell* **110:** 385-397

Wilde JJ, Petersen JR, Niswander L (2014) Genetic, epigenetic, and environmental contributions to neural tube closure. *Annu Rev Genet* **48:** 583-611

Wiles MV, Johansson BM (1999) Embryonic stem cell development in a chemically defined medium. *Exp Cell Res* **247:** 241–248

Wilson JG, Roth CB, Warkany J (1953) An analysis of the syndrome of malformations induced by maternal vitamin A deficiency. Effects of restoration of vitamin A at various times during gestation. *Am J Anat* **92:** 189-217

Wilson L, Gale E, Chambers D, Maden M (2004) Retinoic acid and the control of dorsoventral patterning in the avian spinal cord. *Dev Biol* **269:** 433-446

Wilson SL, Wilson JP, Wang C, Wang B, McConnell SK (2012) Primary cilia and Gli3 activity regulate cerebral cortical size. *Dev Neurobiol* **72:** 1196-1212

Wright KM, Smith MI, Farrag L, Deshmukh M (2007) Chromatin modification of Apaf-1 restricts the apoptotic pathway in mature neurons. *J Cell Biol* **179:** 825–832

Wu H, Che X, Zheng Q, Wu A, Pan K, Shao A, Wu Q, Zhang J, Hong Y (2014) Caspases: A Molecular Switch Node in the Crosstalk between Autophagy and Apoptosis. *Int J Biol Sci* **10:** 1072-1083

Wu MY, Chow SN (2005) Derivation of germ cells from mouse embryonic stem cells. *J Formos Med Assoc* **104:** 697–706

Wu X, Fleming A, Ricketts T, Pavel M, Virgin H, Menzies FM, Rubinsztein DC (2016) Autophagy regulates Notch degradation and modulates stem cell development and neurogenesis. *Nat Commun* **7:** 10533

Wu YT, Tan HL, Shui G, Bauvy C, Huang Q, Wenk MR, Ong CN, Codogno P, Shen HM (2010) Dual role of 3-methyladenine in modulation of autophagy via different temporal patterns of inhibition on class I and III phosphoinositide 3-kinase. *J Biol Chem* **285:** 10850-10861

Xie Y, Zhou B, Lin MY, Wang S, Foust KD, Sheng ZH (2015) Endolysosomal deficits augment mitochondria pathology in spinal motor neurons of asymptomatic fALS mice. *Neuron* **87:** 355-370

Yakovlev AG, Ota K, Wang G, Movsesyan V, Bao WL, Yoshihara K, Faden AI (2001) Differential expression of apoptotic protease-activating factor-1 and caspase-3 genes and susceptibility to apoptosis during brain development and after traumatic brain injury. *J Neurosci* **21:** 7439–7446

Yamauchi K, Ishihara A (2009) Evolutionary changes to transthyretin: developmentally regulated and tissue-specific gene expression. *FEBS J* **276:** 5357–5366

Yamazoe H, Kobori M, Murakami Y, Yano K, Satoh M, Mizuseki K, Sasai Y, Iwata H (2006) One-step induction of neurons from mouse embryonic stem cells in serum-free media containing vitamin B12 and heparin. *Cell Transplant* **15:** 135-145

Yang J, Wu C, Stefanescu I, Horowitz A (2017) Analysis of retinoic acid-induced neural differentiation of mouse embryonic stem cells in two and three-dimensional embryoid bodies. *J Vis Exp* **122:** 55621

Yaniv SP, Issman-Zecharya N, Oren-Suissa M, Podbilewicz B, Schuldiner O (2012) Axon regrowth during development and regeneration following injury share molecular mechanisms. *Curr Biol* **22:** 1774-1782

Yin Z, Pascual C, Klionsky DJ (2016) Autophagy: machinery and regulation. *Microb Cell* **3:** 588-596

Ying QL, Stavridis M, Griffiths D, Li M, Smith A (2003) Conversion of embryonic stem cells into neuroectodermal precursors in adherent monoculture. *Nat Biotechnol* **21:** 183–186

Yon JM, Baek IJ, Lee BJ, Yun YW, Nam SY (2011) Dynamic expression of manganese superoxide dismutase during mouse embryonic organogenesis. *Int J Dev Biol* **55:** 327-334

Young AR, Chan EY, Hu XW, Köchl R, Crawshaw SG, High S, Hailey DW, Lippincott-Schwartz J, Tooze SA (2006) Starvation and ULK1-dependent cycling of mammalian Atg9 between the TGN and endosomes. *J Cell Sci* **119:** 3888-900

Yousefi S, Simon HU (2007) Apoptosis regulation by autophagy gene 5. *Crit Rev Oncol Hematol* **63:** 241-244

Yu J, Vodyanik MA, Smuga-Otto K, Antosiewicz-Bourget J, Frane JL, Tian S, Nie J, Jonsdottir GA, Ruotti V, Stewart R, Slukvin II, Thomson JA (2007) Induced pluripotent stem cell lines derived from human somatic cells. *Science* **318:** 1917-1920

Yu WH, Kumar A, Peterhoff C, Shapiro Kulnane L, Uchiyama Y, Lamb BT, Cuervo AM, Nixon RA (2004) Autophagic vacuoles are enriched in amyloid precursor protein-secretase activities: implications for beta-amyloid peptide over-production and localization in Alzheimer's disease. *Int J Biochem Cell Biol* **36:** 2531–2540

Yue Z (2007) Regulation of neuronal autophagy in axon: implication of autophagy in axonal function and dysfunction/degeneration. *Autophagy* **3:** 139-141

Zachari M, Ganley IG (2017) The mammalian ULK1 complex and autophagy initiation. *Essays Biochem* **61:** 585-596

Zaffagnini G, Martens S (2016) Mechanisms of selective autophagy. *J Mol Biol* **428:** 1714-1724

Zappasodi F, Salustri C, Babiloni C, Cassetta E, Del Percio C, Ercolani M, Rossini PM, Squitti R (2008) An observational study on the influence of the APOE-epsilon4 allele on the correlation between 'free' copper toxicosis and EEG activity in Alzheimer disease. *Brain Res* **1215:** 183-189

Zechner D, Fujita Y, Hulsken J, Muller T, Walther I, Taketo MM, Crenshaw EB, Birchmeier W, Birchmeier C (2003) beta-Catenin signals regulate cell growth and the balance between progenitor cell expansion and differentiation in the nervous system. *Dev Biol* **258:** 406–418

Zeisel A, Muñoz-Machado AB, Codeluppi S, Lönnerberg P, La Manno G, Juréus A, Marques S, Munguba H, He L, Betsholtz C et al. (2015) Cell types in the mouse cortex and hippocampus revealed by single-cell RNA-seq. *Science* **347:** 1138–1142

Zeiss CJ (2003) The apoptosis-necrosis continuum: insights from genetically altered mice. *Vet Pathol* **40:** 481–495

Zelent A, Mendelsohn C, Kastner P, Krust A, Garnier JM, Ruffenach F, Leroy P, Chambon P (1991) Differentially expressed isoforms of the mouse retinoic acid receptor beta generated by usage of two promoters and alternative splicing. *EMBO J* **10:** 71-81

Zeng H, Sanes JR Neuronal cell-type classification: challenges, opportunities and the path forward. *Nat Rev Neurosci* **18:** 530-546

Zeng M, Zhou JN (2008) Roles of autophagy and mTOR signaling in neuronal differentiation of mouse neuroblastoma cells. *Cell Signal* **20:** 659-665

Zhang J, Liu J, Liu L, McKeehan WL, Wang F (2012) The fibroblast growth factor signaling axis controls cardiac stem cell differentiation through regulating autophagy. *Autophagy* **8:** 690-691

Zhang S, Li Y, Wu Y, Shi K, Bing L, Hao J (2012) Wnt/β-catenin signaling pathway upregulates c-Myc expression to promote cell proliferation of P19 teratocarcinoma cells. *Anat Rec (Hoboken)* **295:** 2104-2113

Zhang SC, Wernig M, Duncan ID, Brüstle O, Thomson JA (2001) *In vitro* differentiation of transplantable neural precursors from human embryonic stem cells. *Nat Biotechnol* **19**: 1129–1133

Zhang T, Guo L, Yang Y (2020) Mammalian ATG9s drive the autophagosome formation by binding to LC3. *bioRxiv* **091637**

Zhang Y, Pak C, Han Y, Ahlenius H, Zhang Z, Chanda S, Marro S, Patzke C, Acuna C, Covy J, Xu W, Yang N, Danko T, Chen L, Wernig M, Südhof TC (2013) Rapid single-step induction of functional neurons from human pluripotent stem cells. *Neuron* **78:** 785–798

Zhou C, Ma K, Gao R, Mu C, Chen L, Liu Q, Luo Q, Feng D, Zhu Y, Chen Q (2017) Regulation of mATG9 trafficking by Src- and ULK1-mediated phosphorylation in basal and starvation-induced autophagy. *Cell Res* **27:** 184–201

Zinin N, Adameyko I, Wilhelm M, Fritz N, Uhlén P, Ernfors P, Henriksson MA (2014) MYC proteins promote neuronal differentiation by controlling the mode of progenitor cell division. *EMBO Rep* **15:** 383-391

Zou LH, Shang ZF, Tan W, Liu XD, Xu QZ, Song M, Wang Y, Guan H, Zhang SM, Yu L, Zhong CG, Zhou PK (2015) TNKS1BP1 functions in DNA double-strand break repair though facilitating DNA-PKcs autophosphorylation dependent on PARP-1. *Oncotarget* **6:** 7011-7022

6. List of figures

7. List of tables

8. Supplemental data

Movie S1: Neuronal differentiation of P19 cells (5x). P19 cell were neuronal differentiated by application of the SD method. Cells were traced over 14 d by imaging with a 5x objective. The movie was compiled with 100 frames per second (FPS).

Movie S2: Neuronal differentiation of P19 cells (10x). P19 cell were neuronal differentiated by application of the SD method. Cells were traced over 21 d by imaging with a 10x objective. The movie was compiled with 50 FPS.

Movie S3: Laser ablation in a P19 derived neuronal culture. P19 cell were neuronal differentiated by application of the SD method over 14 days before several connections between neuronal cluster formations were laser ablated. Axonal regrowth was traced by imaging with a 10x objective. The movie was compiled with 100 FPS.

Movie S4: Neuronal differentiation of ESC. mESC were neuronal differentiated by application of the SD method. Cells were traced over 14 d by imaging with a 10x objective. The movie was compiled with 50 FPS.

9. Abbreviations

ADH/RDH	Alcohol or retinol dehydrogenases
Apaf-1	Apoptotic protease-activating factor 1
ASC	Adult stem cells
Atg	Autophagy-related genes
BMP	Bone morphogenic proteins
°C	Degree Celsius
CDK	Cyclin-dependent kinase
CNS	Central nervous system
CRABP	Cellular retinoic acid binding protein
CRBP	Cellular retinol binding protein
CYP26	Cytochrome p450 subfamily 26
DMEM	Dulbecco's modified eagle medium
DMSO	Dimethyl sulfoxide
e.g.	For example (latin: *exempli gratia*)
EB	Embryoid body
EBSS	Earles balanced salt solution
ECC	Embryonal carcinoma cell
ERK	Extracellular signal-regulated kinase
ESC	Embryonal stem cell
F12	Ham's F-12 Nutrient Mixture
FBS	Fetal Bovine Serum
FGF	Fibroblast growth factors
FPS	Frames per second
FSC	Fetal stem cell
g	Gravitational constant
GABA	γ-aminobutyric acid
h	Hour
ICM	Inner cell mass

iPSC	Induced pluripotent stem cell
kDa	Kilo Dalton
Keap1	Kelch-like ECH-associated protein 1
m	Meter
M	Molar
MAP1LC3	Microtubule-associated protein 1A/1B-light chain 3
mESC/hESC	Mouse/human ESC
min	Minute
MOMP	Mitochondrial outer membrane permeabilization
mTOR	Mechanistic target of rapamycin
Nrf2(Nfe2l2)	Nuclear factor erythroid 2–related factor 2
NSC	Neural stem cell
PCR	Polymerase chain reaction
PI3K	Phosphoinositide 3-kinase
PLL	Poly-L-lysine
RA	Retinoic acid
RALDH	Retinaldehyde dehydrogenases
RAR	Retinoic acid receptor
RARE	Retinoic acid response element
RBP	Retinol binding protein
ROS	Reactive oxygen species
Rpm	Revolutions per minute
RT	Room temperature
RXR	Retinoid X receptor
s	Second
Shh	Sonic hedgehog
TGFβ	Transforming growth factor β
Wnt	Wingless-related integration site
WT	Wildtype

11. Declaration

I herewith declare that I have not previously participated in any doctoral examination procedure in a mathematics or natural science discipline.

Frankfurt am Main, 08/30/2021

I herewith declare that I have produced my doctoral dissertation on the topic of

Metabolically induced neuronal differentiation

independently and using only the tools indicated therein. In particular, all references borrowed from external sources are clearly acknowledged and identified.

I confirm that I have respected the principles of good scientific practice and have not made use of the services of any commercial agency in respect of my doctorate.

Frankfurt am Main, 08/30/2021